

**Assessment of relaxation pathways in isolated arteries
from the human uteroplacental unit**

by

Ana Caroline Dordea

A thesis submitted to
the Faculty of Medical Sciences, Newcastle University
in fulfilment of the requirements
for the degree of
Doctor of Philosophy



Newcastle University

September 2012

Abstract

The successful development of the human fetus during pregnancy depends on a tight regulation of the uteroplacental vasculature in order to allow sufficient provision of oxygen and nutrients from the mother to the placenta and fetus. To accomplish this, the fetoplacental circulation develops *de novo*, whilst the uterine vasculature undergoes dynamic remodelling. Such distinct features of these circulations suggest that regulation of their vascular function may differ. If so, then *in vitro* examination of these blood vessels may serve as a useful model for tissue-specific mechanisms of human vascular tone regulation. A reduction in intracellular Ca^{2+} ($[\text{Ca}^{2+}]_i$) in vascular smooth muscle cells leads to an increase of myosin light chain phosphatase (MLCP) activity, which induces myosin light chain dephosphorylation and vasodilation. Further molecular signal transduction mechanisms may serve to desensitise the myofilaments to changes in $[\text{Ca}^{2+}]_i$. There is surprisingly little information on the nature of desensitisation to Ca^{2+} in human myometrial (MA) and placental arteries (PA). Therefore, this study aimed to primarily assess Ca^{2+} -desensitisation mechanisms in MA and PA. Here, we showed (i) that the phenomenon of Ca^{2+} -desensitisation occurred in MA and PA. (ii) That it was promoted by the activation of protein kinase G (PKG) and dependent upon an active MLCP. (iii) That MA displayed greater PKG-mediated Ca^{2+} -desensitisation capabilities compared to PA. In addition, this sensitivity remained greater in MA and PA over the soluble guanylate cyclase/PKG axis, but was, surprisingly, reversed at the NO level. Moreover, these differences were not the result of differing expression levels of PKG and PKG-interacting proteins involved in the vasodilatory pathway, as these were similar between the two artery types. These results highlight a variation in vasodilatory responses between MA and PA, which may illustrate a difference in the regulation of vascular tone between the two circulations. Further investigation of the mechanisms involved may prove useful in the development of more tissue-specific therapies.

*To my parents,
Ioana and Marius,
Who make anything possible.*

Acknowledgments

This research would not have been possible without the support and invaluable advice of many people. First and foremost, I would like to thank my primary supervisor, Prof Michael Taggart for challenging my every thought and stimulating my interest on a daily basis. It is his constant support, encouragement and suggestions, which made this work successful. I would also like to thank my secondary supervisor, Prof Stephen Robson, for his encouragement and enthusiasm throughout the PhD.

Many thanks go to Newcastle University for providing financial means and laboratory facilities for this project, to the Research Midwives, theatre staff and patients of the Royal Victoria Infirmary for providing the myometrial and placental samples for this research study. Thank you to Dr Michèle Sweeney for her invaluable support, advice and patience in helping me develop the necessary micro-dissection and microscopy skills to achieve the dreaded mounting of small vessels. I would also like to acknowledge Julie Taggart for the joint collaboration on the assessment of protein expression by western blotting, reported in this thesis. My appreciation is also due to all lab and office colleagues: Joanna Sankar, Magdalena Karolczak-Bayatti, Ellen Hatch and Aiqing Chen for their advice. Thank you also to my partner, Chris Nicholson, for being kind, patient and understanding with me, particularly during the anxious write-up months. Warm thanks also go to Debbie and Stewart Nicholson for being so caring and generous from the moment I met them.

Finally and most importantly, I would like to make a special acknowledgment to my family. I am deeply and forever indebted to my parents, Ioana and Marius, for their love, support and encouragement and for giving me every opportunity in life. Thank you also to my brother, Matei, for being loving and a wonderful help throughout my studies in the United Kingdom and to his wife, Andrea, who joined our family in my last year of PhD.

Table of Contents

Thesis Title	i
Abstract	ii
Acknowledgments	iv
List of Figures	x
List of Tables	xiv
Abbreviations	xv
 Chapter 1	 1
Introduction	1
1.1. General overview	2
1.2. The physiological adaptations during human pregnancy	3
1.2.1. <i>Maternal changes in pregnancy</i>	3
1.2.2. <i>Embryonic and placental development</i>	6
1.3. Characterisation of the placental and uterine circulations	10
1.3.1. <i>De novo formation and characterisation of the placental circulation</i>	10
1.3.2. <i>Dynamic remodelling and characterisation of the uterine vasculature</i>	11
1.4. Signalling transduction mechanisms regulating vascular tone	15
1.4.1. <i>Blood vessel structure</i>	15
1.4.2. <i>Induction of contractile mechanisms in smooth muscles</i>	15
1.4.3. <i>Induction of relaxatory mechanisms in smooth muscles</i>	22
1.5. Mechanisms involved in tone regulation of human uterine and placental arteries	34
1.5.1. <i>Structural properties of myometrial and placental arteries</i>	34
1.5.2. <i>Functional characteristics of myometrial and placental arteries</i>	36
1.6. Aims of the present study	40

Chapter 2	41
Materials and Methods	41
2.1. Chemicals and Solutions	42
2.1.1. <i>General chemicals</i>	42
2.1.2. <i>General and controlled calcium (stock) solutions</i>	42
2.2. Human Tissue processing	46
2.2.1. <i>Placental and myometrial biopsies</i>	46
2.2.2. <i>Tissue microdissections</i>	49
2.3. The myograph system	52
2.3.1. <i>The mounting procedure</i>	52
2.3.2. <i>The normalisation procedure</i>	54
2.3.3. <i>Normalisation of the myometrial and placental arteries</i>	56
2.4. Quality assessment of human arteries	56
2.5. The permeabilisation procedure	58
2.5.1. <i>Preparation of Staphylococcus aureus α-toxin stock aliquots</i>	58
2.5.2. <i>Preparation of the α-toxin permeabilisation cocktail</i>	59
2.5.3. <i>The permeabilisation protocol</i>	60
2.6. Immuno-blotting	61
2.7. Analysis and Statistics	64
2.7.1. <i>Analysis</i>	64
2.7.2. <i>Statistics</i>	64
Chapter 3	65
Ca²⁺-sensitisation in human myometrial and placental arteries in the presence of G protein-coupled agonists	65
3.1. Introduction	66
3.2. Materials and Methods	68
3.2.1. <i>Experimental protocol</i>	68
3.2.2. <i>Analysis and Statistics</i>	68
3.3. High K ⁺ - and Ca ²⁺ -induced force production of human myometrial and placental arteries	71
3.4. Ca ²⁺ -induced force production of human myometrial and placental arteries over increasing Ca ²⁺ concentrations	75

3.5. Agonist-induced enhancement of Ca^{2+} -dependent constriction in human myometrial and placental arteries	79
3.5.1. <i>Assessment of agonist effects on Ca^{2+}-dependent constriction of human myometrial arteries</i>	79
3.5.2. <i>Assessment of agonist effects on Ca^{2+}-dependent constriction of human placental arteries</i>	84
3.6. Comparison of Ca^{2+} -dependent contractions between myometrial and placental arteries	90
3.7. Discussion	94
Chapter 4	100
Ca^{2+}-desensitisation in human myometrial and placental arteries	100
4.1. Introduction	101
4.2. Materials and methods	104
4.2.1. <i>Experimental protocol</i>	104
4.2.2. <i>Statistics</i>	105
4.3. Ca^{2+} -desensitisation in arteries pre-sensitised with G protein-coupled agonists	106
4.3.1. <i>Assessment of Ca^{2+}-desensitisation in U46619-induced Ca^{2+}-sensitised human myometrial and placental arteries</i>	106
4.3.2. <i>Ca^{2+}-desensitisation in human permeabilised myometrial and placental arteries pre-sensitised to Ca^{2+} with the G protein-coupled agonists, endothelin-1 or sphingosine-1-phosphate</i>	113
4.4. Assessment of protein kinase G-mediated Ca^{2+} -desensitisation in human arteries pre-constricted with pCa 4.5	118
4.5. Potential role of myosin light chain phosphatase (MLCP) in PKG-mediated relaxation of Ca^{2+} -constricted permeabilised arteries	122
4.6. Expression of PKG and putative PKG-interacting myofilament-associated proteins of human myometrial and placental arteries	126
4.6.1. <i>PKGIα protein levels in myometrial and placental arteries</i>	126
4.6.2. <i>HSP20 protein levels in human myometrial and placental arteries</i>	128
4.6.3. <i>Telokin protein levels in human myometrial and placental arteries</i>	130
4.6.4. <i>MYPT1 protein levels in human myometrial and placental arteries</i>	133
4.6.5. <i>CPI-17 protein levels in human myometrial and placental arteries</i>	134
4.7. Discussion	135

Chapter 5	142
Effect of endothelium-dependent and -independent vasodilators on intact human myometrial and placental arteries	142
5.1. Introduction	143
5.2. Materials and Methods	146
5.2.1. <i>Experimental Protocols</i>	<i>146</i>
5.2.2. <i>Statistics</i>	<i>147</i>
5.3. Assessing the effects of percentage oxygen saturation on endothelium-dependent and –independent relaxations of placental arteries	149
5.3.1. <i>Endothelium-dependent relaxation in placental arteries exposed to 20 % and 7 % oxygen</i>	<i>149</i>
5.3.2. <i>Endothelium-independent relaxations in placental arteries exposed to 20 % and 7 % oxygen</i>	<i>149</i>
5.4. Effects of endothelial-dependent agonists on pre-constricted human myometrial and placental arteries	151
5.5. Effects of YC-1 and SNP on pre-constricted human myometrial and placental arteries	154
5.5.1. <i>Assessment of YC-1-induced responses in KPSS-constricted myometrial and placental arteries</i>	<i>154</i>
5.5.2. <i>Assessment of SNP-induced responses in KPSS-constricted myometrial and placental arteries</i>	<i>158</i>
5.6. Discussion	162
Chapter 6	168
General Discussion.	168
Appendix A: Ethical approval forms	182
A.1 Myometrial ethical approval forms	182
A.2 Placental ethical approval forms	185
Appendix B: Consent forms	187
B.1 Myometrial consent forms	187
B.2 Placental consent forms	190

Appendix C: Patient Information Form	192
Appendix D: α-Toxin Export Licence	194
Appendix E: Presentations and Publications	197
E.1 Presentations and Awards	197
E.2 Publications (scientific and non-scientific)	197
E.3 Society Affiliations	198
References	199

List of Figures

Figure 1.1: Vascular changes during pregnancy.	5
Figure 1.2: Schematic diagram of tertiary chorionic villi.	9
Figure 1.3: Overview of the uterine vasculature in a uterus from a pregnant woman.	17
Figure 1.5: Mechanisms governing constriction and Ca^{2+} -sensitisation in vascular smooth muscles.	21
Figure 1.6: Schematic model of Protein Kinase G I.	26
Figure 1.7: PKGI-mediated relaxatory mechanisms in vascular smooth muscles.	28
Figure 1.8: PKGI-mediated Ca^{2+} -desensitisation mechanisms in vascular smooth muscles.	30
Figure 1.9: Electron micrographs of transverse sections of arterial walls from a myometrial (A) and placental artery (B).	35
Figure 2.1: Histogram of human myometrial consents July 2009 – July 2011.	47
Figure 2.2: Summary of myometrial biopsies obtained and used for <i>in vitro</i> functional studies.	48
Figure 2.3: Photograph of a placenta following delivery by elective Caesarean section.	50
Figure 2.4: Photograph of a myometrial biopsy.	51
Figure 2.5: Photograph of a myograph bath.	52
Figure 2.6: Schematic drawing of a vessel mounted on the myograph jaws.	53
Figure 2.7: Schematic diagram of the normalisation procedure on a human myometrial artery.	55
Figure 2.8: Constrictions to 60 mM KPSS in human myometrial (MA) and placental arteries (PA).	57
Figure 2.9: Raw tracing of the permeabilisation procedure in a human myometrial artery.	60
Figure 3.1: Original raw tracings of responses in (A) a myometrial and (B) a placental artery to 60 mM KPSS pre-permeabilisation and to pCa 4.5 post-permeabilisation.	72
Figure 3.2: Summary data of contractile responses to 60 mM KPSS (A) and pCa 4.5 (B) in myometrial and placental arteries.	74
Figure 3.3: Original raw tracings of responses in (A) a myometrial and (B) a placental permeabilised artery to increasing Ca^{2+} concentrations.	76

Figure 3.4: Summary data of contraction responses to increasing Ca^{2+} concentrations in myometrial (MA) and placental (PA) arteries.	78
Figure 3.5: Original raw tracings of agonist effects on Ca^{2+} -dependent force of four individual permeabilised myometrial arteries.	80
Figure 3.6: Summary force data in the presence of the G protein-coupled agonists, U46619, ET-1 and S1P, in permeabilised myometrial arteries.	82
Figure 3.7: Normalised force data in the presence of the G protein-coupled agonists, U46619, ET-1 and S1P, in permeabilised myometrial arteries.	83
Figure 3.8: Original raw tracings of agonist effects on Ca^{2+} -dependent force of four individual permeabilised placental arteries.	85
Figure 3.9: Summary of force production (kPa) in the presence of the G protein-coupled agonists, U46619, ET-1 and S1P, in permeabilised placental arteries.	87
Figure 3.10: Normalised force data in the presence of the G protein-coupled agonists, U46619, ET-1 and S1P, in permeabilised placental arteries.	89
Figure 3.11: Comparison of force production in the presence and absence of the three G protein-coupled agonists in permeabilised myometrial (MA) and placental (PA) arteries.	91
Figure 3.12: Comparison of normalised force data in the presence of three G protein-coupled agonists in permeabilised myometrial (MA) and placental (PA) arteries.	93
Figure 4.1: Effect of 10 μM 8-bromo-cGMP in two individual permeabilised myometrial arteries pre-sensitised with U46619.	107
Figure 4.2: Effect of 10 μM 8-bromo-cGMP in two individual permeabilised placental arteries pre-sensitised with U46619.	107
Figure 4.3: Summary data of responses induced by 10 μM 8-bromo-cGMP in human myometrial and placental arteries pre-sensitised to the thromboxane mimetic, U46619.	109
Figure 4.4: Summary data of responses induced by 1 μM and 0.1 μM 8-bromo-cGMP responses in human myometrial and placental arteries pre-sensitised to the thromboxane mimetic, U46619.	111
Figure 4.5: Summary data of 8-bromo-cGMP-induced responses in human myometrial and placental arteries pre-sensitised to the G protein-coupled agonist endothelin-1.	115

Figure 4.6: Summary data of 8-bromo-cGMP-induced responses in human myometrial and placental arteries pre-sensitised to the G protein-coupled agonist sphingosine-1-phosphate.	115
Figure 4.7: Original raw tracings of the relaxatory effects of 10 μ M 8-bromo-cGMP in two individual human myometrial arteries.	119
Figure 4.8: Original raw tracings of the relaxatory effect of 10 μ M 8-bromo-cGMP in two individual human placental arteries.	119
Figure 4.9: Summary data of 10 μ M 8-bromo-cGMP-induced responses in human myometrial and placental arteries.	121
Figure 4.10: Effect of the phosphatase inhibitor, calyculin A (1 μ M), on PKG-mediated relaxation of two human arteries at resting $[Ca^{2+}]$.	123
Figure 4.11: Summary data of 8-bromo-cGMP-induced responses in human myometrial and placental arteries in the presence of the phosphatase inhibitor, calyculin A.	125
Figure 4.12: PKGI α protein expression in human myometrial and placental arteries.	127
Figure 4.13: Quantified expression levels of PKGI α protein in human myometrial and placental arteries.	127
Figure 4.14: HSP20 protein expression in human myometrial and placental arteries.	129
Figure 4.15: Quantified expression levels of HSP20 protein in human myometrial and placental arteries.	129
Figure 4.16: Telokin protein expression in human myometrial and placental arteries.	131
Figure 4.17: Quantified expression levels of telokin protein in human myometrial and placental arteries.	131
Figure 4.18: MLCK protein expression in human myometrial and placental arteries.	132
Figure 4.19: Quantified expression levels of MLCK protein human myometrial and placental arteries.	132
Figure 4.20: MYPT1 protein expression in human myometrial and placental arteries.	133
Figure 4.21: Quantified levels of MYPT1 protein in human myometrial and placental arteries.	133
Figure 4.22: CPI-17 protein expression in human myometrial and placental arteries.	134
Figure 4.23: Quantified levels of CPI-17 protein in human myometrial and placental arteries.	134

Figure 5.1: Responses to 3×10^{-5} M YC-1 (A) and 10^{-5} M SNP (B) in intact human placental arteries at 20 % and 7 % oxygen.	150
Figure 5.2: Effect of 10^{-6} M bradykinin in an intact myometrial artery (A) and an intact placental artery (B) pre-constricted with 60 mM KPSS.	152
Figure 5.3: Effect of 10^{-5} M histamine in an intact myometrial artery (A) and an intact placental artery (B) pre-constricted with 60 mM KPSS.	152
Figure 5.4: Summary data of maximal responses induced by bradykinin and histamine in human myometrial and placental arteries pre-constricted with 60 mM KPSS.	153
Figure 5.5: Effect of YC-1 in three individual intact myometrial arteries constricted with 60 mM KPSS.	155
Figure 5.6: Effect of YC-1 in three individual intact placental arteries constricted with 60 mM KPSS.	155
Figure 5.7: Summary data of maximal responses induced by YC-1 in human myometrial and placental arteries pre-constricted with 60 mM KPSS.	157
Figure 5.8: Summary data of responses induced by 10^{-6} M YC-1 in human myometrial and placental arteries pre-constricted with 60 mM KPSS.	157
Figure 5.9: Effect of sodium nitroprusside in three individual intact myometrial arteries constricted with 60 mM KPSS.	159
Figure 5.10: Effect of sodium nitroprusside in three individual intact placental arteries constricted with 60 mM KPSS.	159
Figure 5.11: Summary data of responses induced by sodium nitroprusside in human myometrial and placental arteries pre-constricted with 60 mM KPSS.	161
Figure 5.12: Summary data of responses induced by 3×10^{-8} M sodium nitroprusside in human myometrial and placental arteries pre-constricted with 60 mM KPSS.	161
Figure 6.1: Potential mechanisms inducing PKG-mediated Ca^{2+} -desensitisation in human myometrial and placental arteries.	174

List of Tables

Table 1.1: Effect of receptor-coupled endothelium-dependent vasodilators on placental and maternal vasculatures.	37
Table 1.2: Effect of endothelium-independent vasodilators on placental and maternal vasculatures.	38
Table 2.1: Composition of general solutions.	43
Table 2.2: Compositions of the controlled calcium solutions G_1 , G_{10} and CaG.	44
Table 2.3: The G_{10} and CaG compositions of a range of pCa solutions.	45
Table 2.4: Demographic details of the participants used in this study.	49
Table 2.5: Summary of immuno-blotting conditions for PKGI α and PKG-interacting myofilament-associated proteins.	63
Table 4.1: Summary of maximal relaxations induced by 8-bromo-cGMP and time to reach half maximal relaxation in human permeabilised myometrial and placental arteries.	112
Table 4.2: Constrictions induced by submaximal $[Ca^{2+}]$ and the G protein-coupled agonists, U46619, endothelin-1 and sphingosine-1-phosphate in human placental and myometrial arteries.	117
Table 6.1: Concentrations of ions, vasodilators and vasoconstrictors in human maternal and fetal circulations.	171

Abbreviations

α -toxin	alpha toxin
μ M	micromolar
8-br-cGMP	8-bromo-cGMP
$[\text{Ca}^{2+}]$	concentration of free calcium ions
$[\text{Ca}^{2+}]_i$	intracellular concentration of free calcium ions
ACh	acetylcholine
ANGII	angiotensin II
ANOVA	analysis of variance
ATP	adenosine-5'-triphosphate
BK	bradykinin
BK _{Ca}	large conductance potassium channels
BSA	bovine serum albumin
Ca ²⁺	calcium
CaCl ₂	calcium chloride
CaM	calmodulin
CaMKII	calmodulin kinase II
cAMP	cyclic adenosine monophosphate
cGMP	cyclic guanosine monophosphate
CICR	calcium-induced calcium-release
cN	cyclic nucleotide(s)
CO	cardiac output
CO ₂	carbon dioxide
CPI-17	protein phosphatase 1 regulatory subunit 17A
DAG	diacylglycerol
ddH ₂ O	double-deionised water
DMSO	dimethyl sulfoxide
EC	endothelial cell(s)
ECL	enhanced chemiluminescence
EDHF	endothelium-derived hyperpolarising factor
EDTA	Ethylenediaminetetraacetic acid
ET-1	endothelin-1
eNOS	endothelial nitric oxide synthase
FGF	fibroblast growth factor(s)

GC	guanylate cyclase
GKIP(s)	cGMP-dependent protein kinase-interacting protein(s)
GTN	glyceryl trinitrate
GTP	guanosine-5'-triphosphate
GTP γ S	guanosine 5-O-(3-thiotriphosphate
HCl	hydrogen chloride
His	histamine
HSP20	heat shock protein 20
HSP27	heat shock protein 27
IEL	internal elastic lamina
IICR	inositol 1,4,5-trisphosphate-induced calcium-release
IP ₃	inositol 1,4,5-trisphosphate
K ⁺	potassium ions
K _{Ca}	calcium-activated potassium channels
KCl	potassium chloride
kDa	kilodalton
KH ₂ PO ₄	Monopotassium phosphate
KMs	potassium methanesulfonic acid
kPa	kilopascals
KPSS	high-potassium salt solution
LZ	leucine zipper
LZ ⁺	leucine zipper positive
LZ ⁻	leucine zipper negative
M	molar
MA	myometrial arteries
Mg ²⁺	magnesium ions
MgMs ₂	magnesium methanesulfonic acid
MgO	magnesium oxide
MgSO ₄	magnesium sulfate
MLC ₂₀	myosin light chain
MLCK	myosin light chain kinase
MLCP	myosin light chain phosphatase
mM	millimolar
mmHg	millimetres of mercury
mN	millinewtons

MOPS	3-(N-morpholino)propanesulfonic acid
Ms	methanesulfonic acid
MYPT1	myosin phosphatase targeting subunit 1
N ₂	nitrogen gas
Na ⁺	sodium ions
Na ₂ ATP	sodium adenosine-5'-triphosphate
NaCl	sodium chloride
Na ₂ CO ₃	sodium carbonate
Na ₂ CP	sodium creatinine
NaHCO ₃	sodium bicarbonate or sodium hydrogen carbonate
NaNO ₂	sodium nitrite
NaOH	sodium hydroxide
NIF	nifedipine
NKB	neurokinin B
nM	nanomolar
NO	nitric oxide
NOS	nitric oxide synthase
NP-40	tergitol-type nonyl phenoxyethoxylethanol
PA	placental arteries
pHSP20	phosphorylated heat shock protein 20
pHSP27	phosphorylated heat shock protein 27
PDE(s)	phosphodiesterase(s)
PGF _{2α}	Prostaglandin F _{2α}
PGE ₂	Prostaglandin E ₂
PIPES	piperazine-N,N'-bis(2-ethanesulfonic acid)
PKA	protein kinase A
PKC	protein kinase C
PKG	protein kinase G
PKGI	protein kinase G isoform I
PKGIα	protein kinase G isoform I alpha
PKGIβ	protein kinase G isoform I beta
PKGII	protein kinase G isoform II
PSS	physiological salt solution
PVDF	polyvinylidene difluoride
ROK	RhoA-kinase

ROK α	RhoA-kinase isoform alpha
RyR	ryanodine receptor(s)
S1P	sphingosine-1-phosphate
sGC	soluble guanylate cyclase
SEM	standard error of the mean
SM	smooth muscle(s)
SMC	smooth muscle cell(s)
SNAP	S-nitroso-N-acetyl-penicillamine
SNG	S-nitroso-glutathione
SNP	sodium nitroprusside
SR	sarcoplasmic reticulum
SVR	systemic vascular resistance
TC	time control
TCB	tissue collection buffer
VASP	vasodilator-stimulated phosphoprotein
VC	vehicle control
VEGF	vascular endothelial growth factor(s)
VER	verapamil
VSM	vascular smooth muscle(s)
VSMC	vascular smooth muscle cell(s)
WPI	world precision instruments

Chapter 1

Introduction

1.1. General overview

During pregnancy, a tightly regulated exchange must develop between the mother and growing fetus and be kept throughout the gestational 40 weeks. A fetus may be considered a foreign body with increasing demands for oxygen and nutrients allowing its full development. The dependence of the fetus on the mother requires the latter to undergo several dramatic adaptations to provide for these expectations. These include immune, renal, pulmonary and, perhaps most importantly, vascular and allow the recognition of the fetus and a maternal endurance of the pregnancy. The importance of adequate vascular adaptations is highlighted in the fact that the only available delivery route from mother to fetus is vascular. The placental and uterine circulations play a vital role in this contraption. They represent the highly regulated circuits through which the fetus receives oxygen and nutrients from, and exports waste products to, the mother. The mechanisms involved in regulating tone of these two vasculatures are therefore likely to be complicated and discreet. However, despite the essential role of the two circulations, our knowledge of the biological processes involved in their regulation is limited.

The placental vascular bed develops *de novo* into one of relatively low resistance (Boura, 1998) and the uterine circulation becomes extensively remodelled (Ramsey, 1981), all to accommodate the increasing demands of a growing fetus. However, in pregnancy complications, such as preeclampsia, fetal growth restriction (FGR) and preterm birth, *in vitro* resistance of maternal and/or placental circulations is increased and blood flow is compromised (Poston et al., 1995, Wilson et al., 2003, Wallis et al., 2008). The increased vascular resistance is thought to occur as a result of deficient remodelling of uterine spiral arteries, which are not transformed to low-resistance vessels, and hence restrict blood flow to the intervillous space and placental circulation (Khong et al., 1986) and, especially in preeclampsia, endothelial dysfunction within upstream uterine resistance arteries and/or placental arteries contributes to the pathology (McCarthy et al., 1993, Ashworth et al., 1997, Wareing and Baker, 2004). Indeed, aberrant endothelial function has been observed in small intact arteries dissected from a number of human vascular beds (placental, omental, myometrial) following functional assessments with endothelial-dependent vasodilators, such as bradykinin (McCarthy et al., 1993, Ashworth et al., 1997, Wareing and Baker, 2004).

The only effective management option for severe complications of this nature, where fetal and/or maternal health is at risk, is the preterm delivery of the infant. Deliveries occurring before the 37th week of gestation are considered preterm and in developed countries, such as the United Kingdom, account for around 6 - 8 % of all deliveries (Goldenberg et al., 2008). The care of preterm infants puts a great burden on the healthcare infrastructure, with costs estimated at 1 billion pounds per annum (Petrou et al., 2011). Infants born pre-term are at increased risk of both immediate adverse neonatal outcomes, such as haemorrhage, neonatal sepsis, bronchopulmonary dysplasia and long-term disabilities, such as respiratory problems, learning difficulties, social and behavioural problems (Anderson and Doyle, 2003, Wen et al., 2004, Iams et al., 2008, Saigal and Doyle, 2008, Zhang et al., 2011). Current therapies for placenta-mediated disease are very limited. With respect to preterm labour tocolytic interventions, such as β -agonists, L-type Ca^{2+} channel blockers, vasopressin/oxytocin receptor antagonists are ineffective; studies have failed to demonstrate benefits in terms of prevention of preterm birth or improvement in neonatal outcomes (Hollier, 2005, Lyndrup and Lamont, 2007). This, in part, reflects the fact that they act on vasculature as well as the myometrium.

Thus, it has never been more important to develop our understanding of the vascular mechanisms governing healthy pregnancies, in order to allow a better approach at developing more specific therapies.

1.2. The physiological adaptations during human pregnancy

The physiological adjustments that occur during pregnancy are specifically designed to promote an environment that supports fetal development and growth, whilst maintaining maternal wellbeing. Several major maternal adaptations are required during pregnancy in alliance with placental organogenesis and fetal development.

1.2.1. Maternal changes in pregnancy

1.2.1.1. Cardiovascular adaptations

Perhaps the most profound and essential maternal adaptations during pregnancy occur in the cardiovascular system. The uterine blood flow increases dramatically as the cardiac output (CO) rises from the 5th week of pregnancy, peaking around 32 weeks at

approximately 30 – 50 % above non-pregnant values (Figure 1.1) (Clark et al., 1989, Easterling et al., 1987, Robson et al., 1989). Preceding and enabling the increase of CO, the systemic vascular resistance (SVR) decreases during the first trimester of pregnancy and reaches a nadir at 14 - 24 weeks of gestation. Thereafter, SVR rises reaching pre-pregnancy values by term (Clark et al., 1989, Bosio et al., 1999). The fall in SVR is due to peripheral and renal arterial vasodilation in early pregnancy, thought to be mediated by progesterone and oestrogen and by vasodilators such as nitric oxide (NO) (Weiner et al., 1994). These mechanisms of remodelling will be further discussed in Section 1.3.2. With the increase in CO but a greater relative decrease in SVR (Phippard et al., 1986), blood pressure, which is the product of CO and SVR, falls by approximately 10 % by mid-pregnancy and then increases thereafter reaching or exceeding pre-pregnancy values by term (Clapp et al., 1988, Clapp and Capeless, 1997, Robson et al., 1989).

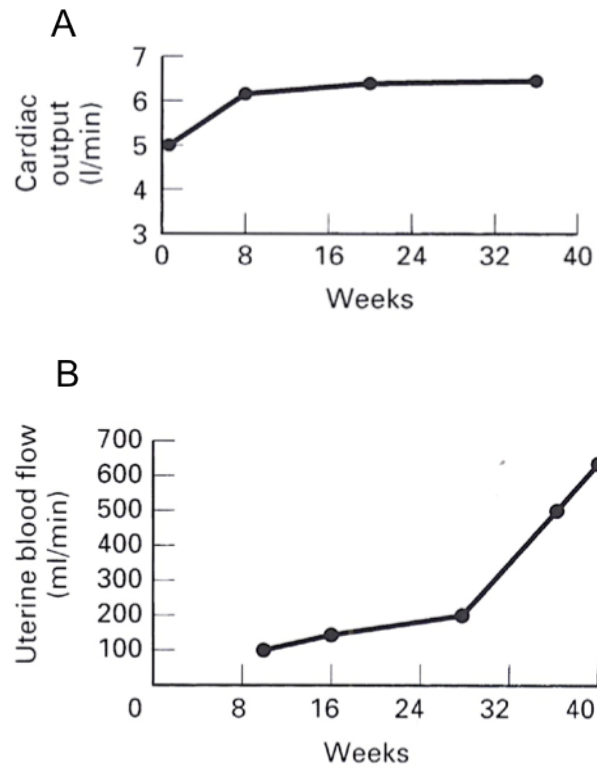


Figure 1.1: Vascular changes during pregnancy. Diagrams highlighting the changes in cardiac output (A) and uterine blood flow (B) during pregnancy. Adapted from (Turnbull, 2001).

1.2.1.2. Changes in the renal system

Both renal blood flow and glomerular filtration rate increase by 35 – 60 % during pregnancy, which increases the functional capacity of the kidneys (Davison and Hytten, 1975), allowing an increase in urea, creatinine and urate clearance (Higby et al., 1994). The activities of renin-angiotensin, aldosterone and progesterone are also increased, leading to an increase in water and sodium retention and a decreased plasma osmolarity (Davison et al., 1981, Lindheimer and Barron, 1998). Over-activation of renin-angiotensin by a low-sodium diet attenuated maternal artery remodelling, impairing adequate neonatal development in pregnant rat (St-Louis et al., 2006). Additionally, in preeclamptic women, over-expression of the angiotensin I receptor has been documented, potentially contributing to the hypertensive state of the pathology (Mandala and Osol, 2012).

1.2.2. Embryonic and placental development

1.2.2.1. Embryonic development

The first week of pregnancy results in implantation of the blastocyst, into the decidual endometrium, which is the inner-most layer of the uterine wall (Benirschke and Kaufmann, 1991, Pijnenborg, 1990). The blastocyst is composed of a fluid-filled cavity within a cell mass; the surface (outer) cells will become the trophoblast and give rise to the extra-embryonic structures, including the placenta; whilst the inner cell mass or embryoblast will form the embryo (Cross et al., 1994). By the 10th day post-fertilisation, the surface trophoblastic cells of the adhering blastocyst have differentiated into an inner cellular layer, the cytotrophoblast, and an outer syncytiotrophoblast (Boyd and Hamilton, 1966), which are important cell types for the establishment of placentation (Norwitz et al., 2001). During the second week, the embryoblast becomes flattened to form the embryonic disc. This structure then differentiates into three germinal tissues, an ectodermal layer, mesodermal layer and endodermal layer, in which a small fluid-filled cavity, the amniotic sac, forms (Gray, 1975, Elder, 2002). The dorsal ectoderm will develop into the entire nervous system, the skin and its appendages (hair and glands) and the other sensory organs, such as the eyes and ears. The intermediate mesoderm will form the supporting structures of the body – bones, joints, muscles, connective tissues – and the vascular and urogenital systems. Finally, the endoderm is

responsible for the gastro-intestinal tract and the remaining organs, such as the lungs and thyroid glands (Gray, 1975). During the third week of pregnancy, the secretion of human chorionic gonadotrophin by the syncytiotrophoblast of the early formed placenta stimulates the maternal ovaries to produce progesterone and oestrogen (Foidart et al., 1992). Thus, it is the control of the maternal reproductive system by the embryo, which sustains the pregnancy state and inhibits menstrual cycles for the remainder of gestation. By the time the embryo is one month old, all the major organs have developed and for the remainder of the pregnancy, these organs will mature and grow in size.

1.2.2.2. Placental Development

The human placenta is a haemochorial structure, which means that the maternal circulation comes into direct contact with the placental surface (chorion), but not with the fetoplacental circulation itself (Benirschke and Kaufmann, 1991, Gray, 1975). The placenta is the first of the fetal organs to form and its development is characterised by a particularly invasive behaviour, analogous to a locally invasive tumour (Foidart et al., 1992). It mediates implantation and establishes the interface for nutrient and gas exchange between maternal and fetal circulations. Additionally, it contributes to maternal recognition of pregnancy by altering the local hormonal and immune environment.

Placentation begins at the end of the first week post-fertilisation with the implantation of the blastocyst (Benirschke and Kaufmann, 2000). Columns of proliferating cytotrophoblasts penetrate and invade the decidual endometrium (Boving, 1959a). These then assume the extravillous trophoblastic lineage and invade by two distinct routes – interstitial and endovascular. Both contribute to the invasion and transformation of the distal branches of the maternal uterine circulation, also known as spiral arteries, thereby promoting increase in blood flow to the site of implantation (Kilman, 2000, Kilman, 1993, Pijnenborg, 1990, Kaufmann et al., 2003). By the end of the second week post-fertilisation, an early intervillous space exists formed from the coalescence of maternal vascular spaces derived from dilated uterine capillaries (Boving, 1959b, Dempsey, 1972).

The trophoblast lining the intervillous space develops forming a series of villous structures from primary to tertiary villi (at the end of the third week), ultimately

developing into the chorionic villus network (Dempsey, 1972, Demir et al., 1989). From the fourth week, the maternal ends of villous stems start to subdivide and side branches develop off the main villous trunk (Boving, 1959a). Each villous stem forms a complex network consisting of a single trunk attached by its base to the chorion, and from which arise distally, second and third degree branches, making up the cotyledon (Figure 1.2). Each new terminal villous branch passes through primary, secondary and tertiary villous development stages (Castellucci et al., 1990, Castellucci et al., 2000). Most importantly, these terminal villi have a high degree of capillarisation (Feneley and Burton, 1991), which enables adequate maternal-fetal exchange of nutrients, oxygen and waste products.

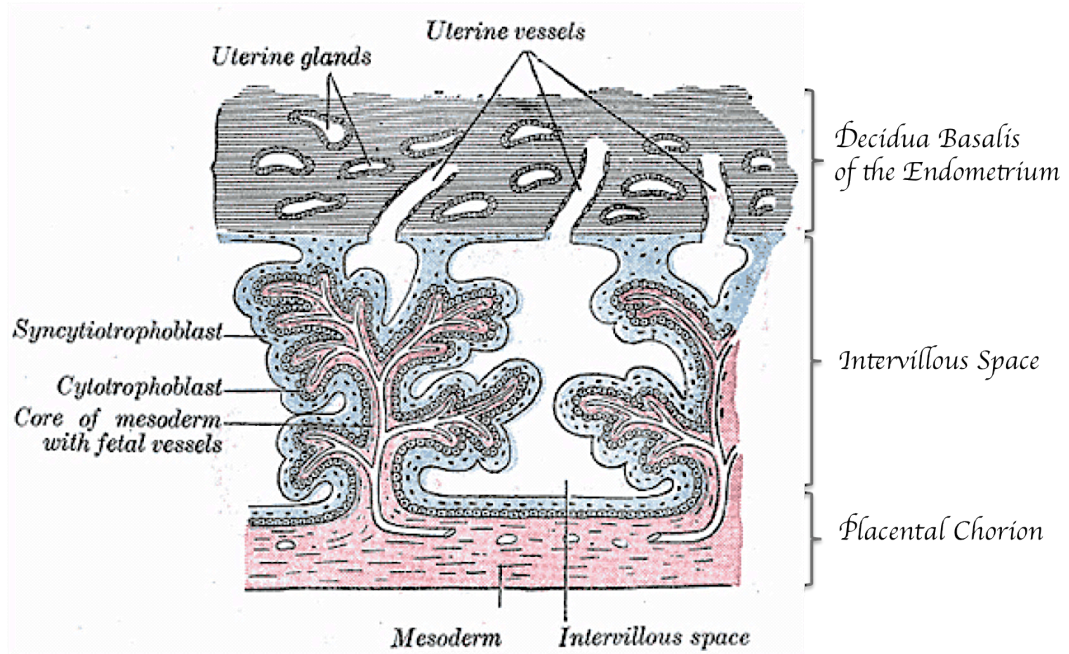


Figure 1.2: Schematic diagram of tertiary chorionic villi. The uterine vessels in the decidua represent spiral arteries, which, once remodelled following invasion of trophoblasts, display a rather non-contractile phenotype, due to the loss of their smooth muscle cells (see Section 1.3.2). Adapted from (Gray, 1975).

1.3. Characterisation of the placental and uterine circulations

In human pregnancy, the *de novo* formation of the placental circulation and the remodelling of the uterine vasculature both occur during the first 20 weeks; however these processes take place separately. The two vasculatures do not physically meet and remain separated by the intervillous space.

1.3.1. De novo formation and characterisation of the placental circulation

1.3.1.1. The development of the placental circulation by vasculogenesis and angiogenesis

The placental vasculature develops via two distinct processes, vasculogenesis, which is the formation of new blood vessels by *de novo* development of endothelial progenitor cells, and angiogenesis, which is the formation of new blood vessels from pre-existing ones (Kaufmann et al., 2004, Demir et al., 1989). The process of vasculogenesis involves (i) the production of haemangioblasts (the progenitors of hematopoietic cells) and angioblasts (the progenitors of endothelial cells), possibly induced by fibroblast growth factors, leading to the formation of primitive capillaries (Hanahan, 1997, Ribatti et al., 2002), (ii) the assembly of primordial vessels, a process, which is mediated by vascular endothelial growth factors (VEGF) (Demir et al., 2006) and (iii) the activation of VEGF receptors to induce the transition from vasculogenesis to angiogenesis (Demir et al., 2010).

Angiogenesis occurs through both sprouting and non-sprouting processes (Kaufmann et al., 2004). The former is characterised by the development of branches, with each branch passing through primary, secondary and tertiary villous development stages, as described in Section 1.2.2.2, until a primitive feto-placental circulation is established. The latter is the formation of capillary loops through elongation of existing capillaries (Demir et al., 2006). The formation of novel capillaries by vasculogenesis followed by the expansion of the villous vascular system by angiogenesis is thought to occur throughout gestation (Benirschke and Kaufmann, 2000).

1.3.1.2. Characterisation of the fetoplacental circulation

Studies on blood flow using Doppler ultrasound have described the placental vasculature as a “low-pressure circulatory system” (Rosenberg, 1998, Ferre, 2001, Kleiner-Assaf et al., 1999, Boura, 1998). Anatomically, the placental circulation is made up of three umbilical vessels (two arteries and a vein), vessels on the surface of the chorionic plate, vessels within the stem villi and vessels present in the terminal portions of the villus trees (Kaufmann, 1998). Arteries from the chorionic plate have the size characteristics of small arteries (less than 500 μm), which are thought to contribute to the resistance of peripheral vascular beds (Mulvany, 1987, Mulvany and Aalkjaer, 1990, Wareing et al., 2002). However, it remains unclear to what extent the chorionic plate and downstream stem villi vessels each contribute to vascular resistance in the placental vascular bed (MacLean et al., 1992, Wareing et al., 2002).

Small arteries (and arterioles) from the systemic vascular beds are controlled by the sympathetic and nervous systems, which contribute to the maintenance of basal tone (Mulvany and Aalkjaer, 1990, Mulvany and Korsgaard, 1983). However, evidence suggests that the placental (and umbilical) vasculature has no neuronal input (Reilly and Russell, 1977, Fox and Khong, 1990), suggesting that tone of the placental vessels is predominantly regulated by endocrine and paracrine factors (Boura, 1998, Poston et al., 1995).

1.3.2. Dynamic remodelling and characterisation of the uterine vasculature

1.3.2.1. Effects of remodelling on the uterine vasculature

As illustrated in Figure 1.3, the blood supply of the uterus is comprised of uterine radial arteries, which originate from a common arcuate (main) artery (Brosens et al., 1967). As radial arteries approach the inner myometrium and decidua, they become coiled (spiral arteries) (Brosens et al., 1967, Pijnenborg et al., 2006, Ramsey, 1981). During pregnancy, spiral arteries are transformed from high-resistance, low-flow vessels into dilated high flow, low resistance vessels (Osol and Mandala, 2009, Burton et al., 2009). These alterations occur as a result of loss of smooth muscle cell (SMC) and elastic lamina from the vessel wall (Pijnenborg et al., 2006, Pijnenborg et al., 1980). Breakdown of elastin within the internal elastic lamina (IEL) is crucial to allow expansion and abolish elastic recoil. The endothelium is temporarily replaced with a

trophoblast layer (restored later in pregnancy), which may account for the low oxygen tension in the fetal environment relative to maternal tissues (Huppertz and Peeters, 2005). This ‘plugging’ by the trophoblast layer may be necessary as fetal organ differentiation is highly vulnerable to free oxygen radicals (Burton et al., 2003, Burton et al., 1999). These perturbations in the arterial wall result in a two-fold increase in arterial diameter, which characterizes the outward hypertrophic vasodilatory process during arterial remodelling (Osol and Mandala, 2009) and allows for a ten-fold increase in the blood supply to the fetoplacental unit (Hyttén, 1985). This enlargement is usually accompanied by little or no thickening of the wall (Huppertz and Peeters, 2005, Osol and Mandala, 2009).

1.3.2.2. The purpose of myometrial (basal and radial) arteries.

While, spiral arteries are extensively remodelled and lose their SMC and elastic lamina, their vasoconstrictive/vasodilatory capacities are decreased. Although the basal and radial arteries supplying the myometrium do not undergo physical remodelling, they likely undergo vasodilatory adaptations to support the increase in blood flow throughout gestation. This vasodilatory process may be due both local factors associated with embryonic implantation and to systemic hormone changes, particularly elevated oestrogen and progesterone (Leiberman et al., 1993). Oestrogen may augment NO synthesis (Kim et al., 2008, van der Heijden et al., 2005); studies in rat uterine arteries have shown that endothelial NO synthase (eNOS) is upregulated during pregnancy, as eNOS ablation abrogated uterine vascular remodelling (Sladek et al., 1997). This supports a key role for NO as a primary mediator of human uterine vasodilation during pregnancy (Osol et al., 2009). In term pregnant rats, the equivalent of human remodelled spiral arteries did not constrict in response to intraluminal pressure elevation, possibly reflecting the loss of SMC in these arteries. Such observations were not made in non-pregnant rats (Gokina et al., 2003). Therefore, vascular tone in myometrial radial arteries may be a key determinant of overall vascular tone in the uterus (Gokina et al., 2003). The importance of myometrial (radial) arteries is further illustrated by the evidence that they have impaired endothelium-dependent vasorelaxatory responses in preeclampsia (Ashworth et al., 1997). This study has therefore used radial myometrial arteries (Figure 1.3).

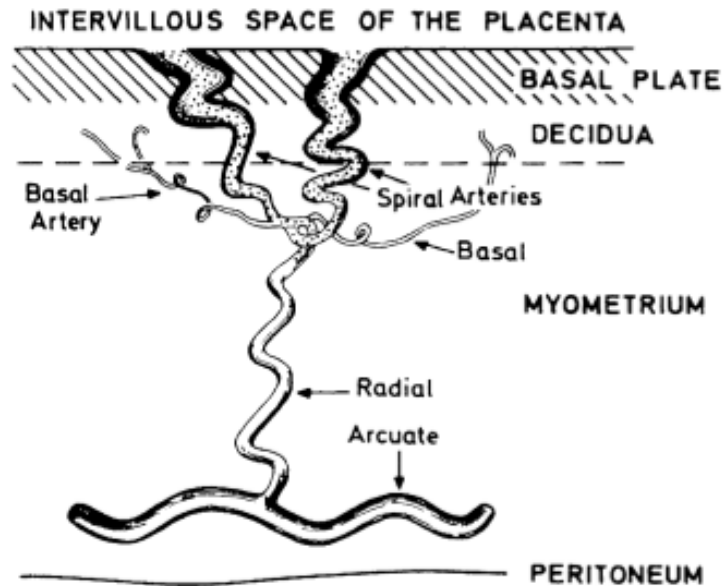


Figure 1.3: Overview of the uterine vasculature in a uterus from a pregnant woman. The radial arteries likely play a central role in the regulation of blood flow to the distal sites (such as spiral arteries/arterioles) and were the (myometrial) arteries used in this study (around 200 – 400 μm). Adapted from (Brosens et al., 1967, Pijnenborg et al., 2006).

Thus, during human pregnancy, the significant increase in CO is facilitated by a dynamic remodelling of the uterine vasculature, which along with a complex *de novo* formation of the placenta and placental circulation, accommodate the growing fetus and its nutritional demands. One might, now, wish to consider the contributions, which the maternal and placental circulations make to match fetal nutrient demand and maternal provision thereof. To do so, it is necessary to understand what mechanisms regulate the vasoreactivity of these two circulations and it is therefore worth considering what, in general terms, is known about constrictive and dilatory mechanisms regulating blood vessel tone of the vasculature.

1.4. Signalling transduction mechanisms regulating vascular tone

1.4.1. Blood vessel structure

Arteries are usually composed of three main layers; the intima is made up of endothelial cells (EC) and IEL, the media is predominantly SMC and the adventia, the outermost layer, is formed of collagen fibers and fibroblasts.

SMC contain a complex intracellular filamentous system consisting of cytoskeletal and contractile filaments. The cytoskeleton, which regulates cell shape and motility, is made up of three filamentous structures; actin thin filaments (~6 nm diameter), intermediate filaments (~10 nm diameter) and microtubules (~20-25 nm diameter) (Taggart and Morgan, 2007, Yu and Lopez Bernal, 1998). Thick myosin filaments and thin actin filaments make up the contractile filaments and their interaction governs the extent of the SM contraction. The principal determinant of contractile force is the level of free intracellular calcium ions ($[Ca^{2+}]_i$) with the rise and fall in $[Ca^{2+}]_i$ being the primary mechanism initiating constriction and relaxation, respectively (Somlyo and Himpens, 1989).

1.4.2. Induction of contractile mechanisms in smooth muscles

Contraction of SM is regulated by dynamic changes in $[Ca^{2+}]_i$ and, partly, by the sensitivity of the myofilaments to any activating Ca^{2+} in response to changes in the environment surrounding the SMC.

1.4.2.1. Ca^{2+} -dependent contractile mechanisms

Elevation in $[Ca^{2+}]_i$ results in the co-operative binding of Ca^{2+} to the calcium-binding protein calmodulin (CaM). Subsequent association of the regulatory Ca^{2+} -CaM complex with the catalytic subunit of the intracellular myosin light chain kinase (MLCK) activates it to cause phosphorylation of threonine and serine at positions 18 and 19, respectively, on the 20 kDa regulatory myosin light chain (MLC₂₀) of myosin II (Figure 1.4). This induces constriction of the myofilaments (Somlyo and Himpens, 1989). Calmodulin kinase II (CaMKII) also phosphorylates MLC₂₀ at Ser-19 but at a much slower rate (1/20 of the V_{max} of MLCK), which is unlikely to initiate contraction

(Edelman et al., 1990). A fall in $[Ca^{2+}]_i$ leads to a reduction in activity of MLCK allowing dephosphorylation of MLC_{20} by myosin light chain phosphatase (MLCP). This leads to deactivation of actomyosin ATPase resulting in relaxation (Somlyo and Somlyo, 1994).

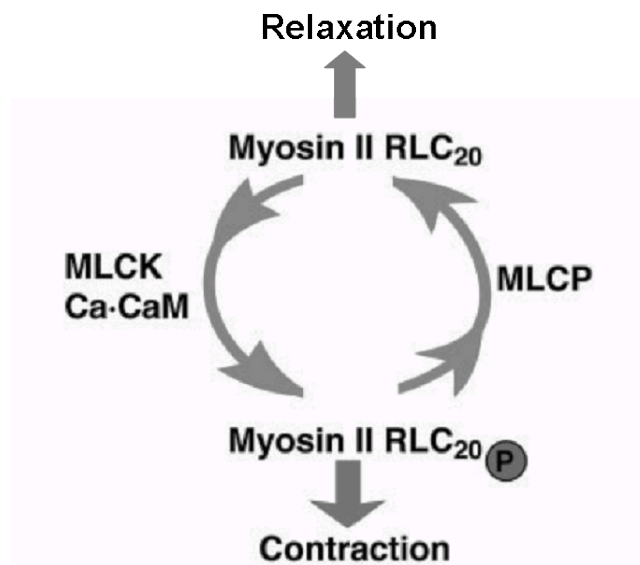


Figure 1.4: Overview of the regulation of contraction/relaxation balance. MCLK: myosin light chain kinase, Ca-CaM: Ca^{2+} -calmodulin, Myosin II RLC₂₀: myosin light chain, MLCP: myosin light chain phosphatase. Adapted from (Somlyo and Somlyo, 2003).

Andrew and Avril Somlyo, pioneers in SM research, introduced the concept of excitation-contraction coupling over fifty years ago to explain the principal mechanisms leading to increases in $[Ca^{2+}]_i$ and contraction of SMC. These mechanisms were termed as electromechanical and pharmacomechanical coupling (Somlyo and Somlyo, 1968).

Electromechanical coupling operates through changes in the membrane potential. Positive potentials open voltage-gated Ca^{2+} channels (mainly L-type), leading to Ca^{2+} influx, an increase in $[Ca^{2+}]_i$ and contraction. Membrane depolarization may be observed in both tonic and phasic SMC, however tonic SMC respond to excitatory stimuli resulting in delayed graded depolarisation through signal transduction mechanisms, whereas phasic SMC generate action potentials or electrical slow waves (Somlyo and Somlyo, 1968, Somlyo and Somlyo, 1994). Additional Ca^{2+} may be released through calcium-induced calcium-release (CICR) from the sarcoplasmic reticulum (SR) induced by increased $[Ca^{2+}]_i$ (Figure 1.5, see Page 19).

Pharmacomechanical coupling operates via multiple cellular signalling mechanisms, which can change the level of force production without necessarily changing the membrane potential. The major mechanisms of pharmacomechanical coupling occur following agonists, such as thromboxane A_2 , endothelin-1 (ET-1) or sphingosine-1-phosphate (S1P), binding to G protein-coupled receptors (Figure 1.5, Page 19). Ca^{2+} release from the principal intracellular Ca^{2+} store, sarcoplasmic reticulum (SR), may also occur via CICR (Ogawa, 1994, Zucchi et al., 1994) or via inositol 1,4,5-trisphosphate (IP_3)-induced Ca^{2+} -release (IICR) mechanisms (Somlyo and Somlyo, 1968, Somlyo et al., 1988, Somlyo and Somlyo, 1990). CICR, which arises following activation of ryanodine receptors (RyR), is likely activated by Ca^{2+} influx through L-type Ca^{2+} -channels, as was shown in guinea pig aorta and rat portal vein (Ito et al., 1991, Ganitkevich and Isenberg, 1992). IICR results from IP_3 binding to its receptors on SR. Activation of the membrane G protein-coupled receptors by agonists (thromboxane A_2 , ET-1 and/or S1P) induce the formation of IP_3 and diacylglycerol (DAG) by phospholipase C (Somlyo et al., 1988). Enhancement of IICR by Ca^{2+} has been shown below 300 nM; above this concentration, IICR was inhibited as a negative feedback (Iino, 1990, Iino and Endo, 1992).

Thus electromechanical and pharmacomechanical coupling likely work in synergy to regulate $[Ca^{2+}]_i$.

1.4.2.2. Ca^{2+} -sensitisation mechanisms

The regulation of contractile cellular mechanisms can be further modulated by Ca^{2+} sensitivity. The phenomenon of Ca^{2+} -sensitisation has been defined as an increase in force production induced by agonist G protein-coupled receptor stimulation at constant suprabasal $[\text{Ca}^{2+}]_i$ (Figure 1.5, Page 21) (Somlyo and Somlyo, 2003, Somlyo and Somlyo, 1992).

The mechanism of G protein-coupled receptor-mediated Ca^{2+} -sensitisation has been studied in several intact and permeabilised animal SM preparations. In intact porcine cardiac arteries, Ca^{2+} -sensitive fluorophores were used to compare steady-state force to steady-state Ca^{2+} levels. It was found that the force/ Ca^{2+} ratio was higher upon activation by agonists than by depolarization induced by high K^+ , indicating Ca^{2+} sensitizing potential and effect by agonists (Bradley and Morgan, 1987). Permeabilisation of arteries allowed for $[\text{Ca}^{2+}]_i$ to be clamped (with Ca^{2+} chelators) and controlled, thereby excluding the possibility of confounding effects due to the intracellular Ca^{2+} compartmentalisation and/or cytoplasmic Ca^{2+} gradients. α -Toxin permeabilised arteries seem to retain their G protein-coupled signalling pathways and receptor activity as activation of these receptors by agonist or guanosine 5-O-(3-thiotriphosphate) (GTP γ S) at constant, highly buffered $[\text{Ca}^{2+}]_i$ led to an increase in MLC_{20} phosphorylation and force (Kitazawa et al., 1989, Himpens et al., 1990, Nishimura et al., 1990). This was indicative of Ca^{2+} sensitisation via a G-protein coupled mechanism and was shown in both rat and rabbit mesenteric and pulmonary arteries (Kitazawa et al., 1989, Himpens et al., 1990, Nishimura et al., 1990). Different agonists have been shown to induce different maximal Ca^{2+} -sensitised force production (Hemmings et al., 2006, Wareing et al., 2005b). The mechanisms responsible have yet to be identified, but may result from variable coupling between agonists, G proteins and guanine nucleotide factors or the activation of distinct downstream intracellular effectors (Somlyo and Somlyo, 2003).

One mechanism proposed to explain changes in Ca^{2+} -sensitivity within SMC (vascular and non-vascular) relates to the fact that an increase in $[\text{Ca}^{2+}]_i$ may activate CaMKII, as a negative feedback, which would phosphorylate MLCK and decrease its activity (Tansey et al., 1994, Stull et al., 1990). Agonists may somehow abolish this feedback. However, studies in airways and vascular smooth muscles (VSM) negated this

possibility (Tang et al., 1992, Van Riper et al., 1995); they showed that increases in $[Ca^{2+}]_i$ increased MLCK phosphorylation regardless of the simulant. Somlyo and co-workers asserted the second and most likely mechanism, in which Ca^{2+} -sensitivity is induced by agonist-mediated MLCP inhibition (Kitazawa et al., 1991b, Somlyo and Somlyo, 1992). In addition, GTP γ S was thought to decrease Ca^{2+} -sensitivity of myofilaments by inhibiting MLCP (Kubota et al., 1992). Studies have shown that arachidonic acid enhanced Ca^{2+} -induced constrictions in α -toxin permeabilised chicken gizzard SM, resulting in both MLCP activity and MLC₂₀ dephosphorylation inhibition (Gong et al., 1992b, Gong et al., 1995).

The signal for Ca^{2+} -sensitisation was found to be communicated by the RhoA/ROK pathway. Studies in guinea-pig ileal SM and rat caudal arterial SM have shown that the serine/threonine Rho-kinase (ROK), activated by the GTP-bound form of RhoA (a small 20 kDa monomeric GTPase), induced phosphorylation of the regulatory subunit of MLCP inhibiting the catalytic phosphatase activity of MLCP and inducing contraction (Sward et al., 2000, Wilson et al., 2005a). The activity of MLCP may also be inhibited by the DAG-activated protein kinase C (PKC) (Jensen et al., 1996) or by CPI-17, a protein, which can be activated by phosphorylation by a variety of factors, such as PKC (Woodsome et al., 2001, Kitazawa et al., 2000) or ROK (MacDonald et al., 2001, Koyama et al., 2000). Inhibition of MLCP activity is, therefore, likely to be the prime mechanism of Ca^{2+} -sensitisation.

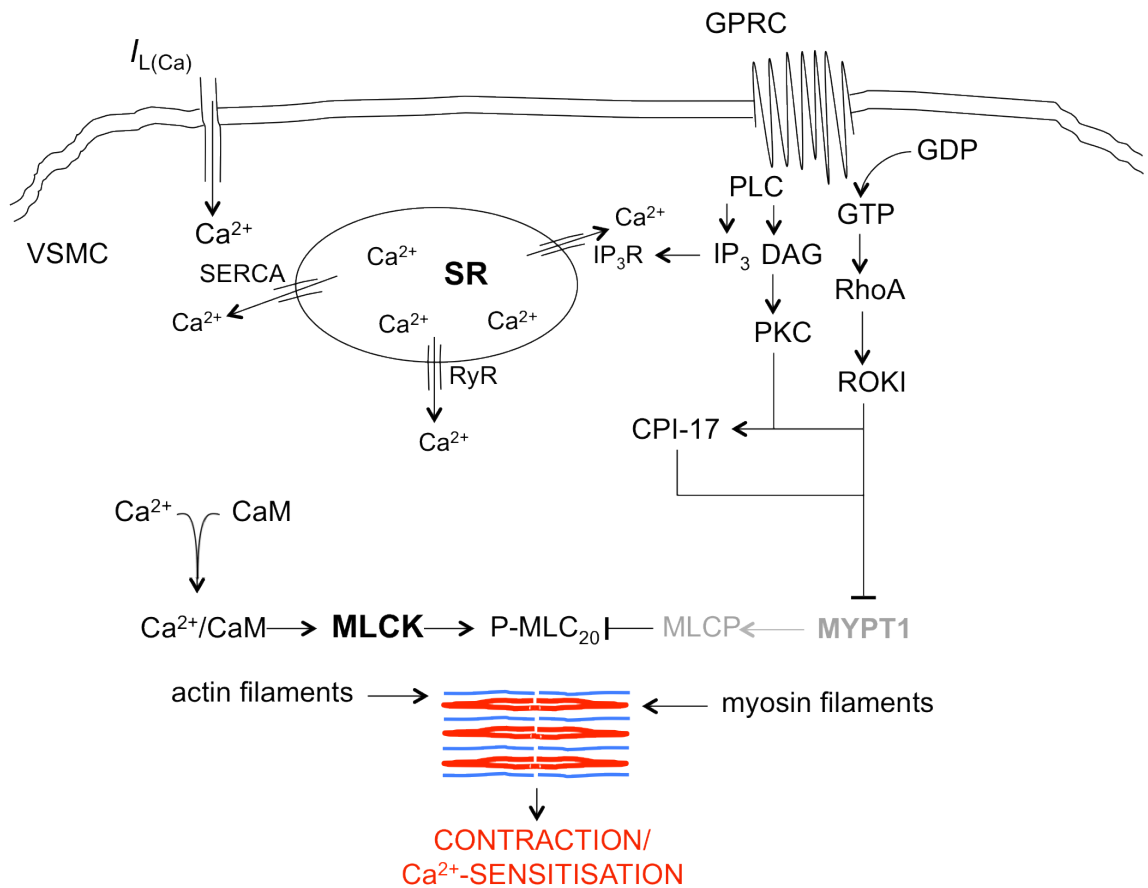


Figure 1.5: Mechanisms governing constriction and Ca^{2+} -sensitisation in vascular smooth muscles. $I_{L(\text{Ca})}$: L-type Ca^{2+} -channels, GPRC: G protein-coupled receptors VSMC: vascular smooth muscle cell, Ca^{2+} : calcium, CaM: calmodulin, SR: sarcoplasmic reticulum, SERCA: SR Ca^{2+} -ATPase pump, RyR: ryanodine receptor, IP_3 : inositol 1,4,5-triphosphate, IP_3R : IP_3 receptor, DAG: diacylglycerol, PLC: phospholipase C, PKC: protein kinase C, GDP: guanosine diphosphate, GTP: guanosine-5'-triphosphate, ROKI: RhoA kinase isoform I, MLCP: myosin light chain phosphatase, MYPT1: MLCP targeting subunit, MLCK: myosin light chain kinase, CaM: calmodulin, P-MLC₂₀: phosphorylated myosin light chains. Grey lines: inhibited signalling. Black arrows: stimulation. Black stop: inhibition.

1.4.3. Induction of relaxatory mechanisms in smooth muscles

Similarly to constriction, relaxation may be induced by two mechanisms. The first involves a dramatic decrease in $[Ca^{2+}]_i$, the second, experimentally at least, is observed without the prerequisite of reducing Ca^{2+} levels.

1.4.3.1. Mechanisms inducing vascular smooth muscle relaxation

Relaxation may be initiated through membrane repolarization resulting in reduction of $[Ca^{2+}]_i$ via closing of the voltage-gated-operated channels and removal of Ca^{2+} from cytoplasm via membrane pumps/channels and uptake by the SR (Somlyo and Somlyo, 1994). Studies in guinea-pig mesenteric veins have shown that the extent and rate of intracellular Ca^{2+} sequestration by the SR is sufficient to induce relaxation of SMC (Bond et al., 1984). ATP-dependent plasma membrane Ca^{2+} pumps and to a lesser extent Na^+/Ca^{2+} exchanger also contribute to the removal of the cytoplasmic Ca^{2+} (Karaki et al., 1997, Somlyo and Somlyo, 1994).

The tightly connected EC also act as regulators of the contractile system by producing vasodilators, which penetrate through the IEL to act on the underlying SMC to control their degree of contraction and relaxation.

Endothelium-derived relaxant mechanisms

The first pathway involves the endothelium-derived hyperpolarising factor (EDHF), which was first reported as a “new endogenous inhibitor from the vascular endothelium” in 1987 (Taylor and Weston, 1988). In fact, it rather defines an entity, than a single factor (Edwards et al., 2010). EDHF refers to a variety of signalling mechanisms involved in communications between the EC and VSMC. The classical EDHF pathway leads to an endothelial hyperpolarisation, followed by an increase in EC $[Ca^{2+}]_i$ and the activation of the Ca^{2+} -activated K^+ channels (K_{Ca}), large K_{Ca} (BK_{Ca}), intermediate K_{Ca} (IK_{Ca}), and small K_{Ca} (SK_{Ca}), which are located in the membrane caveolae and in EC extensions through the IEL (Edwards and Weston, 1998). The endothelial hyperpolarisation can then either be transmitted to the SMC via EC-SMC gap junctions, without the involvement of another factor, or the K^+ ions can escape through the activated K_{Ca} channels and activate endothelial Na^+/K^+ -ATPases to generate SMC hyperpolarisation and vasodilation (Edwards et al., 1998). The second major pathway

of relaxation is also endothelium-derived and involves Ca^{2+} -dependent release of endothelium-derived vasodilators, such as NO (Edwards et al., 2010).

Nitric Oxide

NO is synthesized by the catalytic action of a family of NO synthases (NOS). Endothelial cells contain endothelial NOS (eNOS). These synthases convert the precursor amino acid, L-arginine, to NO and L-citrulline (Ignarro, 1999, Ignarro, 2005). NO synthesis and release from EC is increased in response to mechanical shear stress from blood passing through the vessel and to release of vasodilators, such as acetylcholine or bradykinin (Ignarro et al., 1987, Furchgott and Zawadzki, 1980). NO then diffuses into the intercellular space and traverses the plasma membrane of nearby cells, such as SMC, where it acts as a signal for subsequent biological processes, including relaxation (Ignarro, 2005). NO induces changes in target proteins by binding to their tyrosines or cysteines or by forming complexes with the associated heme groups of proteins such as the guanylate cyclase (GC) (Ignarro, 1999). In SMC, NO at nanomolar levels binds tightly to a prosthetic heme of the β -subunit of GC, also known as soluble GC (sGC), and causes a 100- to 200-fold increase in its activity (Friebe and Koesling, 2003). The activation of sGC induces the production of cyclic guanosine monophosphate (cGMP), a cyclic nucleotide deriving from guanosine triphosphate (GTP), resulting in an elevation of intracellular cGMP and relaxation (Waldman and Murad, 1987). The elevation in cGMP primarily activates protein kinase G (PKG I), though cGMP-gated channels, cyclic nucleotide (cN) phosphodiesterases (PDEs) and PKG II are also thought to be important targets of cGMP actions (Warner et al., 1994, Wang et al., 2002, Burnett, 1995).

NO is the 'first messenger' in the NO/cGMP/PKG I signalling pathway. However, even if sufficient NO is generated by EC, an imbalance in the rates of cGMP production and/or degradation or abnormalities in sGC, PKG I or other mediators of the cGMP-mediated signalling pathway, may lead to vascular pathology. Endothelial dysfunction leading to aberrant production of NO has been found in patients with metabolic syndrome, hypertension, diabetes, erectile dysfunction and pregnancy complications, such as preeclampsia (Celermajer et al., 1993, Knock and Poston, 1996, Knock et al., 1997, Burnett, 2006).

Protein kinase G isoform I

PKGI monomers contain a regulatory domain, located on the N-terminal portion of the protein and a catalytic domain, present in the C-terminal portion; each contains multiple sub-domains providing specific functions (Francis et al., 2010). There are two PKGI isozymes, PKGI α and PKGI β , which are products of alternative splicing and differ by 100 amino acids in their N-terminal region (Francis and Corbin, 1994). The sequence divergence affects a variety of parameters, such as cGMP affinity, cN analogue selectivity, protein-substrate specificity, state of activation and subcellular localisation (Wolfe et al., 1989b, Ruth et al., 1997, Surks et al., 1999). cGMP binds to the PKG regulatory domain and increases its activity 3- to 10-fold (Wolfe et al., 1989a, Francis and Corbin, 1994). The more N-terminal cN-binding site in PKGI isozymes has a higher affinity for cGMP compared to the C-terminal (Reed et al., 1997) and PKI α displays around 10-fold greater affinity for cGMP than PKGI β (Wolfe et al., 1989a). cGMP analogues, such as 8-bromo-cGMP (8-br-cGMP), have been extensively used to investigate the biological effects elicited by PKGI α , as they traverse cell membranes freely and act directly on the target proteins (Francis et al., 1988, Poppe et al., 2008). Studies in Chinese hamster ovary cell lines have shown that PKGI α activation by 8-br-cGMP suppressed increases in $[Ca^{2+}]_i$ in response to thrombin receptor stimulation (Christensen and Mendelsohn, 2006).

The regulatory domain of PKGI is made up of a dimerization and cell-localisation sub-domain provided by an extended leucine-zipper motif, overlapping autoinhibitory and autophosphorylation sub-domains and two homologous cGMP-binding sites arranged in tandem (Figure 1.6). The catalytic domain contains an Mg^{2+} /ATP binding domain and a substrate-binding domain (Lincoln et al., 1977, Lincoln et al., 1978). The respective leucine/isoleucine-zipper motif at the N-terminus of each PKGI monomer provides for a high affinity homodimerisation (Richie-Jannetta et al., 2003). The leucine/isoleucine zipper of PKGI α is made up of five heptad repeats, which are stabilised by hydrophobic residues and an extensive network of hydrogen bonds (Sharma et al., 2008), whilst the leucine/isoleucine zipper of PKGI β contains eight heptad repeats involved in dimerization. This unique leucine zipper signature of PKGI isozymes regulate the interaction with cGMP-dependent protein kinase-interacting proteins (GKIPs), which localise PKG to certain cellular regions and also represent PKGI substrates (Surks et al., 1999). One such GKIP is the targeting subunit of MLCP, MYPT1, which has been

found to interact with PKGI via their respective leucine-zipper motifs targeting PKGI to the SMC myofilaments (Surks et al., 1999, Sharma et al., 2008, Lee et al., 2007).

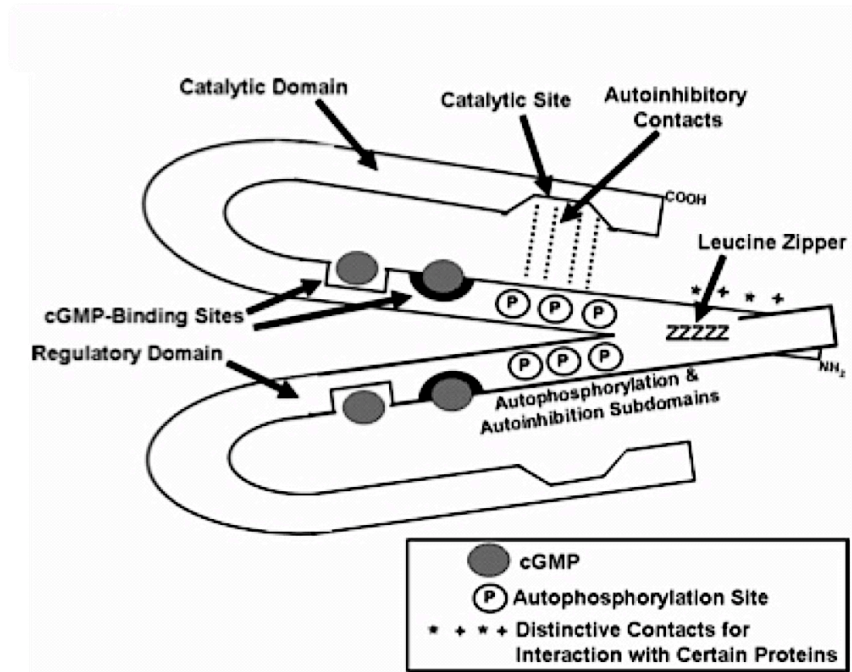


Figure 1.6: Schematic model of Protein Kinase G I. PKGI isoforms are homodimers, which are dimerised by an extended leucine/isoleucine zipper motif (ZZZZZ). These motifs provide for selective interaction (indicated by *+*+) with a variety of specific cellular proteins, including the targeting subunit of myosin light chain phosphatase, MYPT1. Multiple sites of autophosphorylation, as a negative feedback, are indicated by encircled P. The cGMP-binding sites are homologous, but the sites closest to the N-terminal domain present higher affinities for cGMP – these are indicated by heavy dark semi-circles. Adapted from (Francis et al., 2010).

Modulation of intracellular calcium

Numerous targets of PKGI are implicated in modulating $[Ca^{2+}]_i$. The NO/cGMP/PKGI signalling pathways generally promote increased sequestration and decreased release of calcium from intracellular stores as a result of phosphorylation of target proteins (Figure 1.7). PKGI phosphorylation of the G protein-activated phospholipase C β 2/ β 3 at Ser-26 and Ser-1105 leads to the inhibition of this enzyme, thereby decreasing the generation of IP $_3$ and calcium influx from the SR, causing relaxation in intact SM (Xia et al., 2001). Similarly, PKGI β phosphorylates the IP $_3$ -associated PKG substrate (IRAG) at Ser-696, which converts IRAG to an inhibitor of the IP $_3$ receptor activity, thereby blocking calcium release from the SR (Schlossmann et al., 2000). PKGI is also thought to phosphorylate and activate BK $_{Ca}$, thereby promoting channel opening, which results in loss of potassium, hyperpolarisation of the plasma membrane and ultimately decreased calcium influx through L-type Ca $^{2+}$ channels (White et al., 1993). Similarly, the PKG activator, cGMP, was found to be required for activation of Ca $^{2+}$ -activated Cl $^-$ -channels, now also known as cGMP-dependent Cl $^-$ -channels, and activation of these channels led to hyperpolarisation of rat mesenteric arteries plasma membrane and vasodilation (Matchkov, 2004). Further phosphorylation may occur on phospholamban at Ser-16, which would raise its inhibitory effect on the SR Ca $^{2+}$ /ATPase pump, increasing Ca $^{2+}$ sequestration (Schlossmann et al., 2000). Finally, PKGI may also increase GTPase activity of G $_{\alpha q}$ proteins and interfere with G protein-coupled receptor activation by agonists, such as thromboxane, thereby counteracting constriction of SM by pharmacomechanical coupling (Huang et al., 2007).

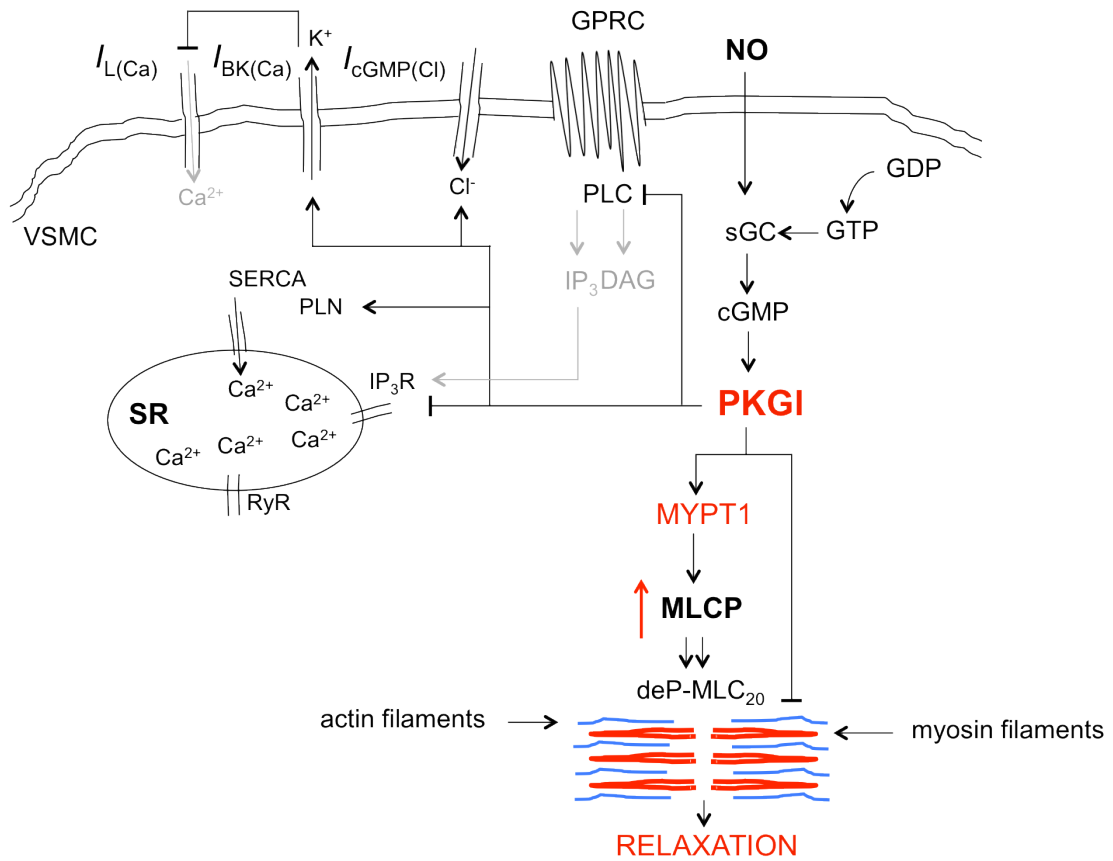


Figure 1.7: PKGI-mediated relaxatory mechanisms in vascular smooth muscles. $I_{L(Ca)}$: L-type Ca^{2+} -channel, $I_{BK(Ca)}$: large conductance Ca^{2+} -activated K^{+} -channel, $I_{cGMP(Cl)}$: cGMP-dependent Cl^{-} -channel, GPCR: G protein-coupled receptor, VSMC: vascular smooth muscle cell, Ca^{2+} : calcium, SR: sarcoplasmic reticulum, SERCA: SR Ca^{2+} -ATPase pump, RyR: ryanodine receptor, PLN: phospholamban, P-Ser16: phosphorylation at Serine 16, IP₃: inositol 1,4,5-triphosphate, IP₃R: IP₃ receptor, DAG: diacylglycerol, PLC: phospholipase C, MLCP: myosin light chain phosphatase, MYPT1: MLCP targeting subunit, MLCK: myosin light chain kinase, CaM: calmodulin, deP-MLC₂₀: dephosphorylated myosin light chains. Black arrows: stimulation. Grey lines: inhibited signalling. Red arrow: increase in activity.

1.4.3.2. Ca^{2+} -desensitisation mechanisms in smooth muscles

Ca^{2+} -desensitisation is defined by a decrease in MLC_{20} phosphorylation and a reduction in force production at constant $[Ca^{2+}]_i$ (Kitazawa and Somlyo, 1990). Conversely to Ca^{2+} -sensitisation occurring via MLCP inhibition, desensitisation is thought to take place primarily via increase in the MLCP activity rather than the inhibition of MLCK. Although the primary mechanism inducing relaxation in VSM has been shown to involve lowering $[Ca^{2+}]_i$, additional regulation of vascular tone may be achieved via desensitisation of the contractile machinery to the effects of Ca^{2+} (Figure 1.8).

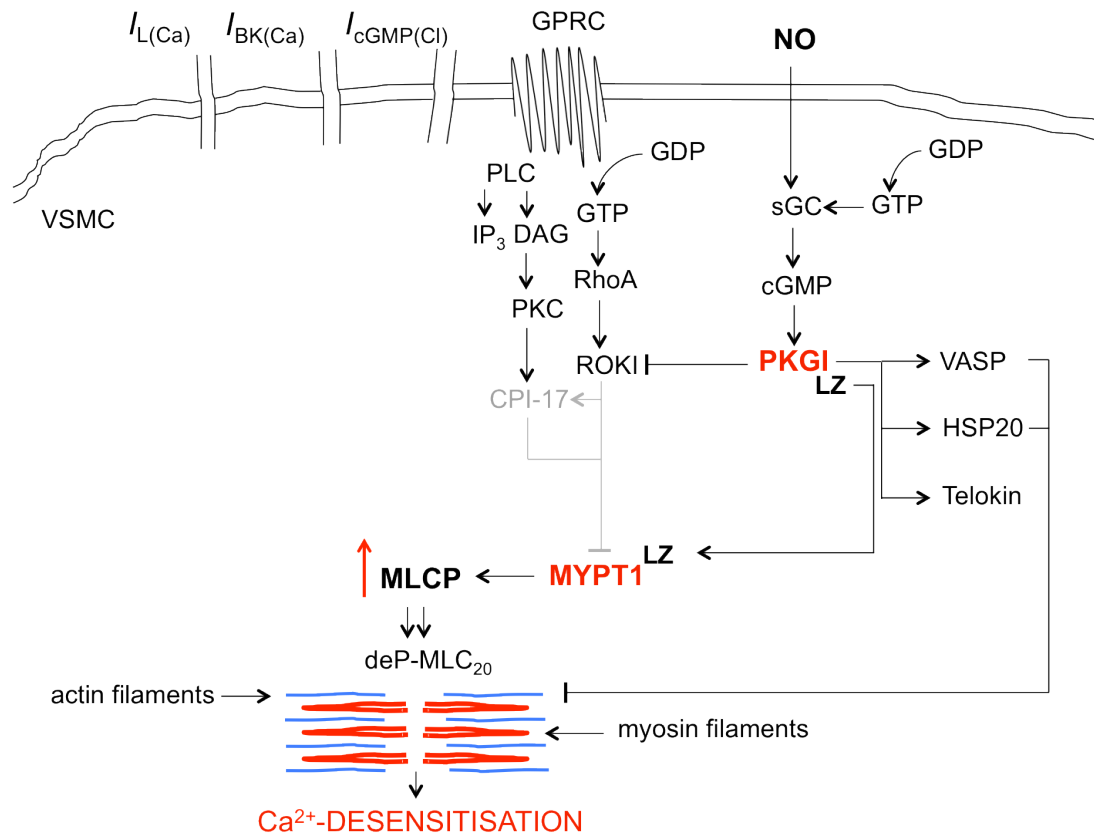


Figure 1.8: PKGI-mediated Ca^{2+} -desensitisation mechanisms in vascular smooth muscles.
 $I_{L(\text{Ca})}$: L-type Ca^{2+} -channel, $I_{BK(\text{Ca})}$: large conductance Ca^{2+} -activated K^{+} -channel, $I_{c\text{GMP}(\text{Cl})}$: cGMP-dependent Cl^{-} -channel, GPCR: G protein-coupled receptor, VSMC: vascular smooth muscle cell, Ca^{2+} : calcium, SR: sarcoplasmic reticulum, SERCA: SR Ca^{2+} -ATPase pump, RyR: ryanodine receptor, IP_3 : inositol 1,4,5-triphosphate, IP_3R : IP_3 receptor, DAG: diacylglycerol, PLC: phospholipase C, PKC: protein kinase C, GDP : guanosine diphosphate, GTP : guanosine-5'-triphosphate, ROKI: RhoA kinase isoform I, MLCP: myosin light chain phosphatase, MYPT1: MLCP targeting subunit, MLCK: myosin light chain kinase, CaM: calmodulin, deP-MLC₂₀: dephosphorylated myosin light chains. Black arrows: stimulation. Grey lines: inhibited signalling. Red arrow: increase in activity.

PKGI as a prime mediator in Ca^{2+} -desensitisation

cGMP-mediated Ca^{2+} desensitisation has been found to be mediated by both soluble and particulate (ie. membrane-bound) isoforms of PKGI. Production of cGMP by the sGC induces activation of soluble PKGI, which ultimately results in a decrease in the inhibitory state of MLCP activity via a variety of potential pathways, ultimately leading to relaxation of VSM.

The significant role of PKG as vasodilatory mediator was shown in studies in PKG α null mice. These mice displayed a hypertensive phenotype, which was reversed after transfection of PKGI α into their SM. Jejenum and aorta strips from these 'rescue' mice relaxed significantly and to a similar extent to 8-br-cGMP, compared with wild-type mice (Feil et al., 2002, Weber et al., 2007). As described previously, direct stimulation of MLCP may also occur via interaction between the LZ motifs of PKGI α and MYPT1. In chicken gizzard, loss of the LZ motifs on MYPT1 blocked 8-br-cGMP-induced dephosphorylation of MLC₂₀ and SM relaxation (Khatri et al., 2001). In addition, PKGI is thought to phosphorylate RhoA at Ser 188 (Sauzeau et al., 2000a), lifting ROK-induced phosphorylation of MYPT1, known to inhibit MLCP activity (Kitazawa et al., 2009, Sauzeau et al., 2000a, Gudi et al., 2002). Further PKG-mediated desensitisation to Ca^{2+} may occur via interaction with a number of other actinomyosin filament-interacting proteins discussed below.

Vasodilator-Stimulated Phosphoprotein

The actin binding protein, vasodilator-stimulated phosphoprotein (VASP), is another substrate of PKGI and known to inhibit actin polymerisation (Reinhard et al., 2001). This decreases actin and myosin filament interactions and thus induces SM relaxation. In addition, studies in rat and rabbit aortas have shown that prolonged exposure to nitroglycerin decreased phosphorylated VASP levels, whilst unphosphorylated VASP, sGC and PKGI levels remained unchanged and induced vasodilation (Oelze et al., 2000, Schulz et al., 2002, Mulsch et al., 2001, Schafer et al., 2003). This introduced VASP as a reliable marker for vascular vasodilatory activity via the NO-mediated cGMP/PKGI pathway and its effect on actin filaments.

Telokin

Phosphorylation of the 17 kDa SM specific telokin protein has also been found to mediate Ca^{2+} -desensitisation via PKA and PKG (activated following elevation of intracellular cAMP and cGMP, respectively) (Somlyo and Somlyo, 2003). Telokin is derived from the SM MLCK gene, shares identical COOH terminus with MLCK and is phosphorylated by PKGI (Ito et al., 1989, Wu et al., 1998). Depletion of endogenous telokin from permeabilised rabbit ileal SM was found to correlate with a loss of 8-br-cGMP-induced relaxation and was rescued by the addition of recombinant telokin and further enhanced by PKGI (Wu et al., 1996, Wu et al., 1998, Walker et al., 2001). It was also shown that telokin null mice displayed normal expression of MLCK but a marked decrease in MCLP activity and an increase in MLC₂₀ phosphorylation as compared to wild-type (WT) mice (Khromov et al., 2006). Finally, telokin was also shown to interact with inhibited MYPT1 to enhance MLCP activity and MYPT1 interaction with myosin filaments (Khromov et al., 2012), thus decreasing actinomyosin filament interactions. This highlights a role for telokin in Ca^{2+} -desensitisation of force and cGMP-induced relaxation in telokin-rich SM.

Heat-shock proteins

Another PKA/PKG target, identified in SM, is the small heat shock protein 20 (HSP20), which was found to regulate relaxation of SM via its interaction with actin, independently of MLC₂₀ dephosphorylation (Tyson et al., 2008b). HSP20 is abundantly expressed in smooth, skeletal and cardiac muscle and belongs to the small HSP (sHSP) family (Kato et al., 1994). Several studies have shown that phosphorylation of HSP20 (phospho-HSP20) occurs during cGMP-induced relaxation of pre-constricted swine carotid arteries (Rembold et al., 2000, Stulc et al., 1994) and that this is cAMP/cGMP-dependent in term human umbilical arteries (Bergh et al., 1995). Moreover, the application of a phospho-peptide HSP20 analogue (containing phospho-Serine 16) to permeabilised bovine carotid arteries has been shown to inhibit agonist-induced contraction, whilst an unphosphorylated peptide had no effect (Beall et al., 1999). A recent study has reported the presence of HSP20 in rat myometrium; mRNA and protein levels were highly expressed in early to mid-gestation and then decreased during late pregnancy and labour (Cross et al., 2007). Recent proteomics studies have identified the presence of phospho-HSP20 in human term labouring myometrium and co-immunoprecipitation studies have revealed a specific association of HSP20 with α -SM actin and HSP27, a key regulator of actin filament dynamics. These studies indicate that

phospho-HSP20 modulates cGMP-mediated relaxation in term myometrium via its interaction with actin (Tyson et al., 2008b).

1.4.3.3. Altered protein expression and tissue-specific differences in responsiveness to NO and/or PKG

The expression levels of the relaxatory proteins telokin, HSP20 and MYPT1 have been suggested to differ between SM types, which is thought to influence their vasodilatory capacities. Visceral SM are thought to be predominantly fast phasic, with rapid constrictions and relaxations, whilst vascular SM are thought to display a rather slow tonic phenotype (slow constrictions or relaxations) (Owens et al., 2004). However, within vascular SM, SMC may also exhibit a more phasic or tonic phenotype (Owens et al., 2004). Differences in expression levels of relaxatory proteins have been reported by comparing visceral with vascular SM or within vascular SM (portal vein with large arteries and veins) to highlight wide differences between phasic and tonic SM phenotypes. However, no studies have, to my knowledge, reported expression levels in human tissues or artery types, such as myometrial and placental small arteries, which may also display more phasic and tonic phenotypes.

Telokin has been suggested to be highly expressed in fast phasic SM with only small amounts in slow tonic SM (Choudhury et al., 2004). Studies in Ca^{2+} -constricted tonic femoral arteries have shown that telokin induced maximal relaxations of 30 %, whilst relaxations in phasic ileum muscle reached 90 % and telokin expression levels were four fold higher in the ileum compared to arteries (Choudhury et al., 2004). Conversely, phospho-HSP20 was shown to slow the relaxation time course in guinea pig phasic taenia cecum SM through decreased actin-myosin interactions, whilst no effects were observed in tonic skinned carotid arteries (Hashimoto et al., 2009). Meanwhile, MYPT1 LZ-positive isoforms have been identified predominantly in slow-tonic SM, whilst LZ-negative isoforms are thought to be expressed in higher levels in fast-phasic SM (Payne, 2004). The LZ-negative isoform is thought to result in a resistance to the calcium desensitising effects of cGMP (Khatri et al., 2001). However, a switch from LZ-positive to LZ-negative isoforms has been reported during neonatal development of the rat portal vein, turning a slow-tonic SM at birth into a fast-phasic SM following development (Payne et al., 2006). Thus, within vascular SM, slow-tonic phenotypes may develop into fast-phasic SM. These studies highlighted wide differences in protein expression and

functional responses between phasic and tonic SM; however they also stressed the difficulty in determining the phenotypic profile of a SM type wholly from expression levels and vasodilatory capacities, as they may shift to change phasic into tonic or tonic into phasic SM. The phenotypic differences existing between phasic and tonic SM may be more difficult to underline and compare in SM of small resistance arteries, such as myometrial and/or placental arteries.

1.5. Mechanisms involved in tone regulation of human uterine and placental arteries

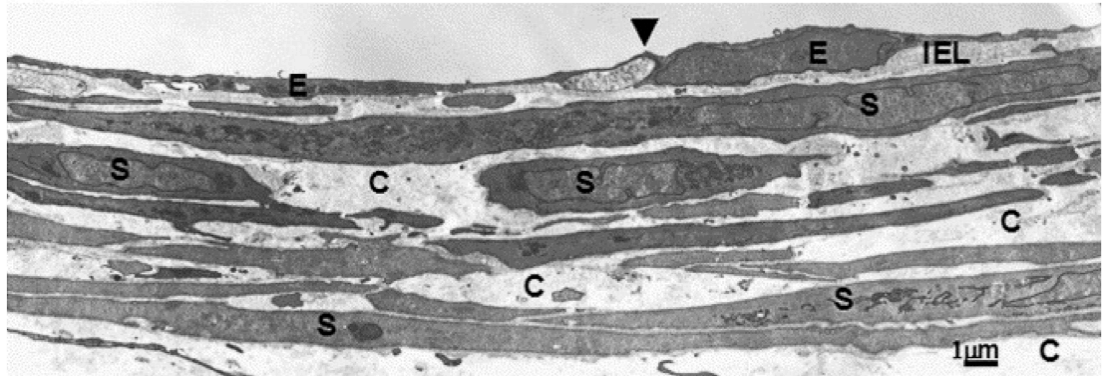
Ca²⁺-sensitisation and –desensitisation result from major physiological mechanisms regulating MCL₂₀ activity, i.e. phosphorylation and dephosphorylation (Gong et al., 1992a, Somlyo and Himpens, 1989, Tansey et al., 1994). However, the majority of the work on Ca²⁺-sensitisation and –desensitisation has been carried out on a variety of vascular and non-vascular tissues from animals. Our current knowledge of these signalling pathways in human SMC is limited, particularly in the reproductive vasculatures.

1.5.1. Structural properties of myometrial and placental arteries

Knowledge of the structural properties of human placental and uterine vascular SMC is limited. Studies have shown that placental arteries from the chorionic plate contain a thick medial layer with the SMC separated by an abundance of extracellular matrix (ECM), whilst (uterine) myometrial arteries displayed a more tightly packed SM layer with less ECM (Figure 1.9) (Sweeney et al., 2006a). A structure similar to chorionic plate placental arteries was also observed in placental arteries within the stem villi (Tanaka et al., 1999) and in human umbilical arteries at term gestation (Benirschke and Kaufmann, 2000). In addition, placental arteries, in contrast with myometrial arteries, lack a distinct IEL separating EC and SMC. As mentioned earlier, the placental vasculature offers little resistance to blood flow (Kleiner-Assaf et al., 1999), therefore placental blood vessels are likely exposed to lower pressures than myometrial blood vessels. It is possible that placental arteries evolved without an elastic component because of their exposure to low pressure/flow, in which case elasticity in these vessels may not have been an important requirement (Sweeney et al., 2006a). The placental

vasculature lacks innervation indicating that its regulation relies only upon paracrine, autocrine or mechanical stimuli (Fox and Khong, 1990).

A Myometrial



B Placental

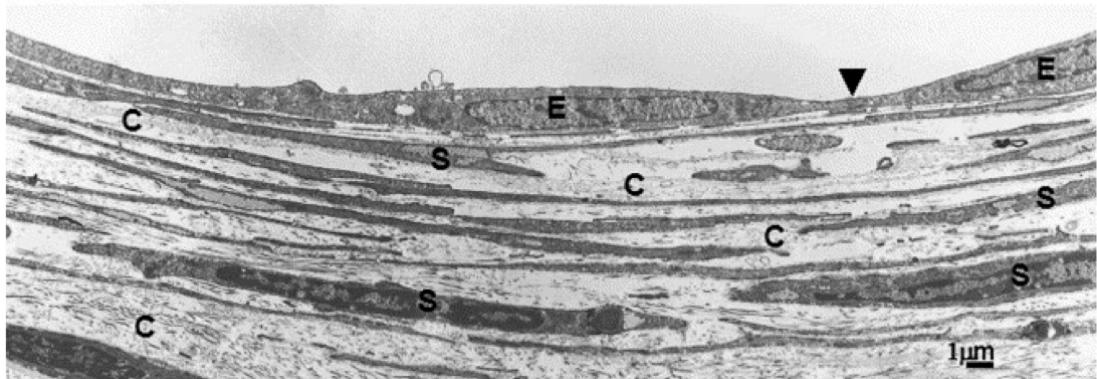


Figure 1.9: Electron micrographs of transverse sections of arterial walls from a myometrial (A) and placental artery (B). The myometrial artery consists of EC, an IEL and tightly packed SMC separated by little ECM compared to the placental artery, which does not display an IEL and whose SMC are interspersed with large amounts of ECM. The ECM is represented by collagen amounts. S: smooth muscle cell, E: endothelial cell, IEL: internal elastic lamina, C: collagen. Adapted from (Sweeney et al., 2006a).

1.5.2. Functional characteristics of myometrial and placental arteries

Electromechanical and pharmacomechanical stimuli are known to play a role in the regulation of vascular tone of the uterus and placenta. Studies have shown both human myometrial and placental arteries constrict to solution with high potassium (electromechanical) (Sweeney et al., 2008), and to a variety of contractile agents (pharmacomechanical) such as the eicosanoid, thromboxane A₂ (Sweeney et al., 2008, Wareing et al., 2006c), and the constrictive peptides ET-1 (Wareing et al., 2006c) and S1P (Hemmings et al., 2006, Hudson et al., 2007).

The importance of the endothelium-derived NO in the placental circulation was first shown in studies in the isolated perfused cotyledon, which reported that inhibition of NO production led to an increase in perfusion pressure (Myatt et al., 1991, Myatt et al., 1992). Tables 1.1 and 1.2 summarise our current knowledge of the effects of both endothelium-dependent and endothelium-independent vasodilators, respectively, on maternal and placental circulations. However, very few of these studies have compared effects between artery types, as a greater portion of studies seems to have been done on the placental vasculature and groups assessing one artery type rarely assessed the other. In a recent study, bradykinin-mediated endothelium-dependent relaxations induced minimal relaxations in placental arteries, in contrast to observations in myometrial arteries (Sweeney et al., 2008). It is unclear whether the difference in bradykinin response is the only dissimilarity within the NO/cGMP/PKG pathway between placental and myometrial arteries.

Table 1.1: Effect of receptor-coupled endothelium-dependent vasodilators on placental and maternal vasculatures.

Placental Vasculature			Myometrial Vasculature	
Vasodilators	Comments	References	Comments	References
Acetylcholine	No effect in perfused human placentas pre-constricted with U46619 or ET-1. No relaxation in small U46619-constricted human CPA.	(Myatt et al., 1992), (McCarthy et al., 1994), (Hull et al., 1994), (Amarnani et al., 1999).	Relaxation in U46619-constricted MA from pregnant sheep and pre- and post-menopausal UA constricted with 30 mM KPSS, MA from term pregnant women.	(McCarthy et al., 1993), (Kublickiene et al., 1997), (Anwar et al., 1999), (Kublickiene et al., 2000), (Spitaler et al., 2002).
Bradykinin	Relaxation in perfused human placental cotyledon; small/no relaxation in CPA constricted with high K ⁺ , U46619 or AVP. Increase in perfusion pressure in placentas.	(Myatt et al., 1992) (McCarthy et al., 1994), (Hull et al., 1994), (Amarnani et al., 1999), (Wareing, 2002), (Sweeney et al., 2008).	Relaxation in U46619-constricted MA from pregnant sheep; human MA from term pregnant women pre-constricted with AVP, NE, U46619, 60 mM KPSS.	(Anwar et al., 1999), (Sweeney et al., 2008), (Wareing et al., 2004).
Histamine	Relaxation in perfused human placentas and CPA constricted with sub-maximal concentrations of U46619, but not in maximally U46619- or KPSS-constricted CPA.	(Myatt et al., 1992), (McCarthy et al., 1994), (Hull et al., 1994), (Amarnani et al., 1999), (Mills et al., 2007b).	Relaxation in UA from non-pregnant post-menopausal women constricted with 30 mM KPSS.	(Spitaler et al., 2002)
Substance P	Minimal relaxation in human CPA.	(Hull et al., 1994)	Relaxation in PE-constricted MA from pre-eclamptic and term pregnant women.	(Wimalasundera et al., 2005)

UA: uterine arteries (animal), MA: myometrial arteries (human), CPA: chorionic plate placental arteries (human), U46619: thromboxane A₂ mimetic, 5-HT: serotonin, PGF₂: prostaglandin F₂, PE: phenylephrine, NE: norepinephrine, ET-1: endothelin-1, VP: vasopressin, NA: noradrenaline, AVP: arginine vasopressin.

Table 1.2: Effect of endothelium-independent vasodilators on placental and maternal vasculatures.

Placental Vasculature			Myometrial Vasculature	
Vasodilators	Comments	References	Comments	References
SNAP (NO donor)	Relaxation in U46619-constricted human CPA and perfused placentas constricted with PGF ₂ .	(Myatt et al., 1991), (Hull et al., 1994), (Zhang et al., 2001).	Dose-dependent relaxation in UA from pregnant rats pre-constricted with PE. Relaxation in MA from pregnant and non-pregnant women.	(Lu et al., 2008), (McCarthy et al., 1993), (McCarthy et al., 1994)
SNP (NO donor)	Concentration-dependent relaxation in sub-maximally U46619-constricted human CPA at low (7%) and high (20%) O ₂ . Relaxation in perfused human placentas constricted with PGF ₂ .	(Zhang et al., 2001), (Mills et al., 2007a), (McCarthy et al., 1994), (Mills et al., 2009), (Mills et al., 2005)		
SNG (NO donor)	Relaxation in (sub-) maximally U46619-constricted human CPA and in perfused human placentas constricted with PGF ₂ .	(Zhang et al., 2001)		
GTN (NO donor)	Relaxation in (sub-) maximally U46619-constricted human CPA and in perfused human placentas constricted with PGF ₂ , U46619 and ET-1.	(Myatt et al., 1991), (Myatt et al., 1992), (Zhang et al., 2001).		
YC-1 (sGC activator)	Increase in placental perfusion pressure.	(Bainbridge et al., 2002)		

SNAP: S-nitroso-N-acetyl-DL-penicillamine, SNP: sodium nitroprusside, SNG: S-nitroso-N-glutathione, GTN: glyceryl trinitrate.

Table 1.2 (continued): Effect of endothelium-independent vasodilators on placental and maternal vasculatures.

Placental Vasculature			Myometrial Vasculature	
Vasodilators	Comments	References	Comments	References
NaNO₂ (NO donor)	Relaxation in human U46619-constricted CPA. Relaxation in perfused human placentas constricted with PGF ₂ .	(Zhang et al., 2001)		
NIF (Ca ²⁺ channel blocker)	Concentration-dependent relaxation in human CPA constricted with 40 mM, 124mM KPSS or 5-HT. (Potency: NIF > VER).	(Lindow et al., 1988), (Reviriego and Marin, 1989) (Marin et al., 1990), (Blea et al., 1997), (Kook et al., 1996).	Small relaxation in 124 mM KPSS-constricted human non-pregnant MA, but not in VP- or NA-constricted MA.	(Maigaard et al., 1985)
VER (L-type Ca ²⁺ channel blocker)	Relaxation in human CPA (and umbilical) artery. (Potency: VER < NIF).	(Belfort et al., 1994), (Kook et al., 1996)	Relaxation in ovine UA. Inhibition of ANG II-induced prostacyclin increases in uterine arteries from pregnant ewes.	(Magness and Rosenfeld, 1993), (Belfort et al., 1994)
NIT (Ca ²⁺ channel blocker)	Almost full relaxation in 124 mM KPSS-constricted CPA from pregnant women.	(Maigaard et al., 1986)	Almost complete abolishment of 124 mM KPSS-constricted MA from pregnant women.	(Maigaard et al., 1986)
NKB	Decreased fetal-side arterial pressure in human perfused placenta pre-constricted with U46619.	(Brownbill et al., 2003)	No effect on BK-induced relaxations in AVP-constricted human MA.	(Wareing et al., 2003a)

NIF: Nifedipine, VER: Verapamil, NIT: nitrendipine, NKB: neurkinin B.

Whilst functional studies observing contractile and relaxatory responses of placental and myometrial SM have been carried out, studies pertaining to Ca^{2+} -sensitisation and –desensitisation in these arteries are very limited. Agonist-induced sensitisation of contractile filaments to calcium has been described in placental and myometrial SMC, albeit at only one concentration of sub-maximally, activating Ca^{2+} (Wareing et al., 2005b). Expression of $\text{ROK}\alpha$ has been reported in term human placental, myometrial and omental arteries and linked to thromboxane-induced Ca^{2+} -sensitisation (Wareing et al., 2005b). Similarly, it was shown that Ca^{2+} -sensitisation was effected at a single sub-maximal concentration of Ca^{2+} by another G protein-coupled agonist (S1P) and ROK involvement suggested (Hemmings et al., 2006). While Ca^{2+} -sensitisation has been demonstrated in myometrial and placental arteries, albeit at only one chosen level of sub-maximal activating Ca^{2+} , the phenomenon of Ca^{2+} -desensitisation has not yet been reported in these tissues. Several studies in a variety of animal SM tissues (vascular and non-vascular) have reported the phenomenon of Ca^{2+} -desensitisation, primarily via cyclic nucleotide (cAMP/cGMP) pathways. One may therefore speculate that desensitisation to activating Ca^{2+} may also occur in human myometrial and placental VSM.

Developing our understanding of these processes in healthy human vascular tissues and exploring whether the mediators involved are consistent with those reported in animal tissues will contribute significantly to our knowledge of the molecular mechanisms regulating arterial tone of myometrial and placental vessels during pregnancy. The findings may also have wider applications to human blood vessels in general.

1.6. Aims of the present study

To this end, this work sought to answer three biological queries:

- (i) whether myometrial and placental arteries develop Ca^{2+} -sensitisation over a wider range of concentrations,
- (ii) whether the phenomenon of Ca^{2+} -desensitisation occurs in these artery types and whether it may be mediated by cGMP-dependent pathways,
- (iii) whether myometrial and placental arteries display differing sensitivities in their contractile and/or relaxatory responses,

Chapter 2

Materials and Methods

2.1. Chemicals and Solutions

2.1.1. General chemicals

The following chemicals were obtained as powder, prepared as 10^{-2} M stock solutions in double-deionised water (ddH₂O) and stored at -20 °C in the freezer after their preparation, unless stated otherwise. They were used to assess contractile and relaxatory capacities of the human myometrial (MA) and placental (PA) arteries.

U46619 and YC-1 were purchased from Calbiochem. U46619 was made up by drying the ethanol (in which it was dissolved) by passing a flow of N₂ gas over the solution and then resuspending in a solution of 1:1.85 100 % ethanol: 1 mg/L Na₂CO₃ (Hemmings et al., 2006). YC-1 was prepared in Dimethyl Sulfoxide (DMSO).

8-bromo-cGMP was purchased from Biomol.

Spingosine-1-phosphate (S1P) was purchased from Enzo Life Sciences and made up as a 2.64×10^{-3} M stock by dissolving it in 1.5 mL of methanol at 80-100 °C for 45 minutes and aliquoted equally into glass vials. For each experiment, the methanol was dried off with N₂ gas and the S1P was re-suspended in the appropriate volume of 0.01 M NaOH (Hemmings et al., 2006).

Bradykinin (BK), histamine (His), sodium nitroprusside (SNP) and endothelin-1 (ET-1) were all purchased from Sigma-Aldrich. SNP was made up fresh for every experiment. ET-1 was prepared to a stock concentration of 10^{-4} M.

A23187 was purchased from EMD Biosciences.

2.1.2. General and controlled calcium (stock) solutions

2.1.2.1. Solution chemicals

The following chemicals were used to make up general solutions (Section 2.1.2.2) and controlled calcium stock solutions (Section 2.1.2.3).

Glucose, EDTA, EGTA and CaCl₂ were purchased from BDH Laboratories, NaCl, KCl, NaHCO₃ and KH₂PO₄ from Fisher Scientific and MgSO₄, MOPS, Magnesium Oxide (MgO), Methanesulphonic Acid (Ms), PIPES, Na₂CP, Na₂ATP and DMSO were purchased from Sigma-Aldrich.

2.1.2.2. General Solutions

Three solutions were used most regularly and prepared twice a week (Table 2.1). Tissue collection buffer (TCB) was used for the processing of human samples (see Section 2.1). Physiological salt solution (PSS) and high-potassium salt solution (60 mM KPSS) were used at the beginning of each experiment (see Section 2.4). All three solutions were prepared to a pH of 7.4 and CaCl_2 was added last in a physiological pH to avoid precipitation of Ca^{2+} . The pH of TCB was adjusted using 1 M KOH. PSS and 60 mM KPSS were prepared by gassing the solution with 5 % CO_2 in air to lower the pH to 7.4. Solutions were stored at 4 °C in the fridge. pH measurements were carried out using a pH electrode and pH meter.

Table 2.1: Composition of general solutions.

Chemicals	Tissue Collection Buffer (TCB)	Physiological Salt Solution (PSS)	High-potassium physiological salt solution (KPSS)
NaCl	154	119	63.7
KCl	5.4	4.7	60
MgSO ₄	1.2	2.4	2.4
MOPS	10	-	-
NaHCO ₃	-	25	25
KH ₂ PO ₄	-	1.17	1.17
Glucose	5.5	6.05	6.05
EDTA	-	0.0684	0.0684
CaCl ₂	1.6	1.6	1.6

The concentrations of chemicals are presented in mM.

2.1.2.3. Controlled calcium stock solutions

The following solutions were prepared as stock solutions for the controlled calcium solutions G₁, G₁₀ and CaG (Table 2.2), which were used in the permeabilisation experiments (Section 2.1).

0.1M K₂EGTA was made up as a 200 mL solution by using 7.60 g KOH and 2.26 g EGTA in ddH₂O, whilst heating at 50 - 100 °C.

0.1M CaEGTA was prepared as 100 mL solution using 3.80 g EGTA, 1.01 g CaCO₃ and 1.09 g KOH in ddH₂O.

0.1M Magnesium methanesulfonic acid (MgMS₂) was made up as a 200 mL solution using 0.80 g Magnesium oxide (MgO) and 2.60 mL Methanesulfonic acid (Ms) in ddH₂O.

Finally, 1M KMs was prepared using 11.22 g KOH and 12.98 mL Ms in ddH₂O and pH was adjusted to 7 using 1 M KOH.

Table 2.2: Compositions of the controlled calcium solutions G₁, G₁₀ and CaG.

Chemicals	Relaxing solution	Calcium-free	Calcium-activating
	G ₁	solution G ₁₀	solution CaG
PIPES	30	30	30
Na ₂ CP	10	10	10
Na ₂ ATP	5.16	5.16	5.16
MgMS ₂	7.31	7.92	7.25
KMs	43.1	46.6	47.1
K ₂ EGTA	1	10	-
CaEGTA	-	-	10

The concentrations of each chemical are given in mM.

G₁, G₁₀ and CaG were prepared in ddH₂O to a pH of 7.1 with 1M KOH. The three solutions were prepared once a week and their pH was checked before each experiment.

2.1.2.4. *Ca²⁺-containing solutions for experiments with α -toxin-permeabilised arteries*

Ca²⁺-containing or pCa solutions were prepared by adding accurate set volumes of G₁₀ and CaG, as indicated in the pCa table below (Table 2.3) (Horiuti, 1988).

Table 2.3: The G_{10} and CaG compositions of a range of pCa solutions.

pCa solutions	CaG	G_{10}
9	0.03607	9.96393
8	0.34935	9.65065
7.5	1.02715	8.97285
7	2.65792	7.34208
6.7	4.19403	5.80597
6.3	6.44778	3.55222
5.5	9.20459	0.79541
4.5	9.99378	0.00622

The volumes of CaG and G_{10} are in mL (Horiuti, 1988).

2.2. Human Tissue processing

2.2.1. Placental and myometrial biopsies

Placental and myometrial biopsies were obtained from healthy women with uncomplicated pregnancies either after vaginal delivery or following elective Caesarean section at 37-41 weeks' gestation. The study was approved by the Newcastle and North Tyneside 2 Research Ethics Committee (08/H0907/96 (myometrial biopsies, Appendix A, Section A.1) and 09/H0908/11 ((placental biopsies) Appendix A, Section A.2). All women were given an information sheet about the study (Appendix B, Sections B.1 (myometrial) and B.2 (placental)). Any questions about the study were answered by a research midwife. Those wishing to participate gave written informed consent in compliance with the Helsinki Declaration.

During this study, several problems were encountered with the supply of myometrial tissue from pregnant women. Figure 2.1 illustrates the number of consented samples compared to number collected. The discrepancy between the number of consenting women and the number of biopsies obtained, primarily related to the surgeon failing to take the biopsy. In some cases this was because of haemorrhage but in others no explanation was available. In addition, some samples were obtained from women delivered of a small-for-gestational age infant (birth weight for gestational age less than the 10th centile), which were not used for functional experimentation. Confirmation of FGR was determined by post-delivery calculation of the individualised birth ratio (IBR), which takes into account maternal factors including height, weight, parity and ethnicity (Wilcox et al., 1993). These represented another 4 % of all myometrial biopsies and 4 % of placental ones.

Myometrial Consents

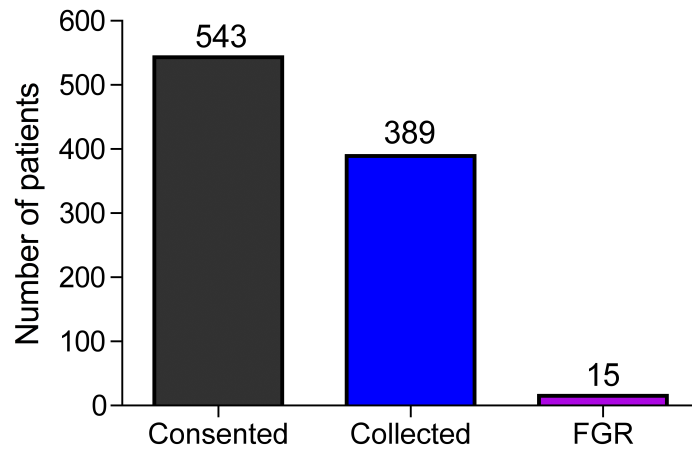


Figure 2.1: Histogram of human myometrial consents July 2009 – July 2011. Black: consented samples, Blue: collected biopsies, and Purple: biopsies from fetal growth restricted (FGR) pregnancies.

During the first six months of the project, several quality control measures were developed to ensure consistency in arterial profiles throughout the experiments. These measures were determined from personal experience as well as guidance from the literature. Section 2.4 gives a detailed overview of these. Figure 2.2 illustrates the number of collected samples compared to the number of samples used in the *in vitro* myography studies. The demographic data of the women who contributed samples to the myographic experiments are shown in Table 2.4.

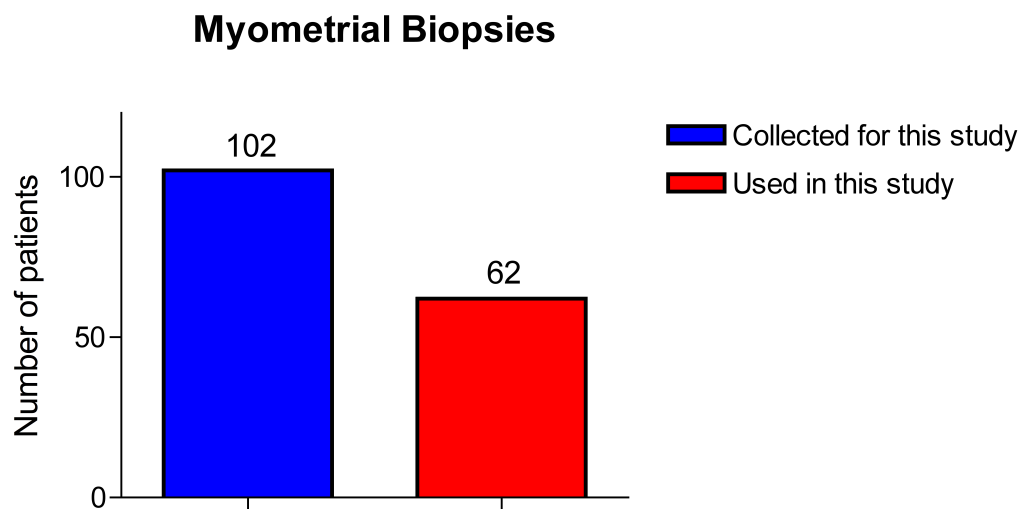


Figure 2.2: Summary of myometrial biopsies obtained and used for *in vitro* functional studies. Blue: Collected biopsies Red: Biopsies used in functional studies.

Table 2.4: Demographic details of the participants used in this study.

Characteristics	Myometrial Biopsies	Placental Biopsies
Number of patients	62	75
Age	31 ± 9.9	30 ± 4.4
Body Mass Index at booking	27 ± 3.7	27 ± 2.5
Smoker	12 %	10 %
Parity	1.2 ± 0.9	1.2 ± 1.1
Gravidity	2.6 ± 1.2	2.4 ± 1.1
Gestational age (weeks)	39 ± 0.8	39 ± 0.9
Birthweight (g)	3478 ± 23.6	3440 ± 21.7
Birthweight centile	62 ± 7.4	61 ± 6.2
Sex (%)	Female : 47 % Male : 53 %	Female : 41 % Male : 59 %

Figures are presented as mean ± SEM.

2.2.2. Tissue microdissections

Whole placentas were collected in cylindrical hospital buckets from rooms adjacent to the hospital theatres within minutes of vaginal delivery or completion of the Caesarean section. Placental arteries were dissected (as described below) within 30 - 60 minutes of delivery. This study used placental arteries dissected from eight placentas following vaginal delivery alongside placental arteries obtained from placentas following Caesarean sections, as a study by Mills *et al* (2007) reported that the mode of delivery (vaginal versus Caesarean section) did not alter arterial vascular contractility (Mills *et al.*, 2007a).

The chorionic plate arteries were identified on the surface of the whole placenta (Figure 2.3, left) by following the branches from the umbilical artery. Arterial branches, which are thicker-walled than veins and uppermost on the chorionic surface, were followed to the edge of the placenta. A biopsy of around 4 × 3 × 1 cm and containing small chorionic plate arteries was then cut from the whole placenta and placed in cold tissue collection buffer (TCB) in a dissecting dish containing a 2 cm thick layer of Sylgaard gel to hold fixing pins. Chorionic plate arteries (< 500 µm diameter) were carefully dissected free from surrounding tissue using 11 cm long Dumont number 5 stainless steel forceps and straight 10 cm Spring stainless steel dissecting scissors (both World Precision Instruments (WPI)) under a stereomicroscope (Leica, at 2 × magnification).

Dissected arteries were placed in a small petri glass dish filled with cold TCB, cleaned free of connective tissue using the same dissecting instruments and cut into 1-2 mm lengths for subsequent mounting onto the small-vessel wire myograph (see Section 2.3.1). Thereafter, arteries were kept on ice for immediate experimental use. When samples were obtained late in the afternoon, arteries were kept in cold TCB overnight for use in the morning, which did not alter vascular function. A bank of placental arteries was also created by freezing fresh cleaned arteries in liquid nitrogen and storing them at -80°C for later use in Western Blotting (see Chapter 4).

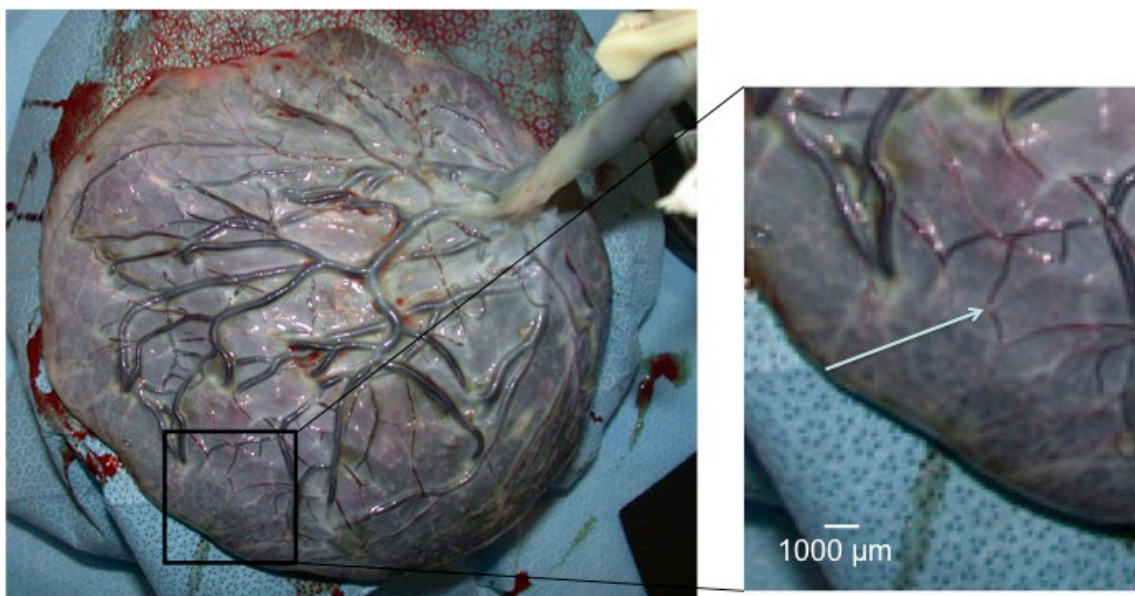


Figure 2.3: Photograph of a placenta following delivery by elective Caesarean section. Left: whole placenta. Right: magnified area of the edge of the placenta where a biopsy containing a third order placental artery branch (arrow) was taken.

Human myometrial biopsies were collected and transported to the laboratory similarly to whole placentas. Figure 2.4 illustrates a myometrial biopsy taken from the upper lip of the lower segment uterine incision at Caesarean section. The biopsy ($\sim 1.5 \times 1 \times 1$ cm) was pinned down in a dissecting dish containing Sylgaard gel in TCB. Myometrial arteries ($< 500\ \mu\text{m}$) were identified on the biopsy surface as white thick walled vessels. Arteries were distinguished from veins on the basis of their thicker walls and their failure to collapse when emptied of blood. They were isolated from the surrounding tissue using straight 8 cm long McPherson-Vannas stainless steel dissecting scissors and 11 cm long Dumont number 5 stainless steel forceps (both WPI). They were then placed in a petri glass dish with TCB and cleaned from surrounding myometrial and connective

tissue using the same instruments. Similarly to the placental arteries, the myometrial vessels were then cut into 1-2 mm lengths. When samples were obtained late in the afternoon, arteries were kept in cold TCB overnight for their use in the morning; otherwise they were used for an experiment immediately after cleaning. A bank of available myometrial arteries was also created by freezing arteries in liquid nitrogen and storing them at -80°C for later use for Western Blotting (see Chapter 4).

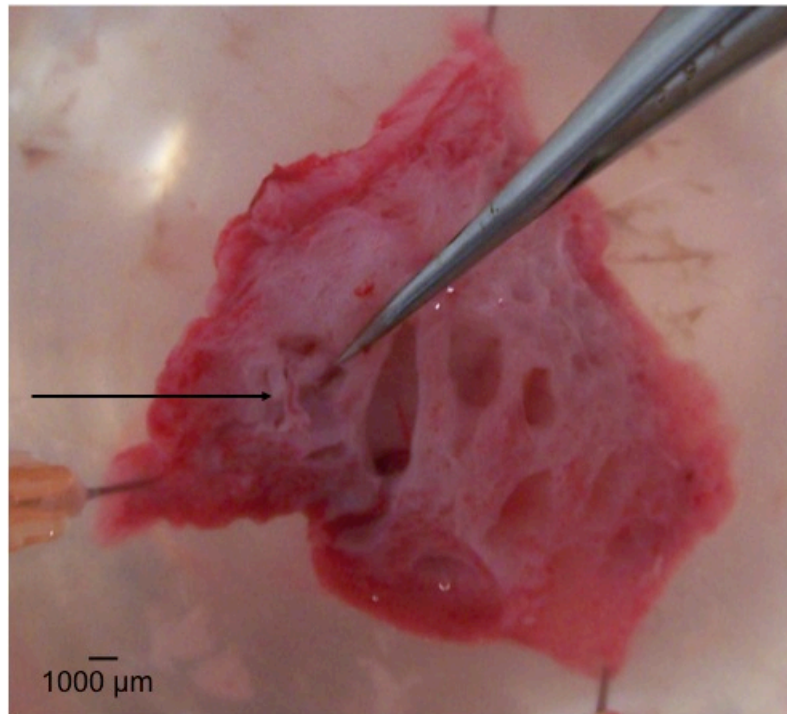


Figure 2.4: Photograph of a myometrial biopsy. The arrow indicates a myometrial artery prior to dissection from surrounding myometrial tissue.

2.3. The myograph system

2.3.1. The mounting procedure

Placental chorionic plate or myometrial arteries were mounted onto a Multi Wire Myograph System Model 610M manufactured by Danish Myo Technology in Aarhus N, Denmark. Each one of the four baths (Figure 2.5) composing the myograph system contains two jaws, one attached to a micrometer to allow stretching of the vessel, the other connected to a strain gauge for recording isometric tension development onto a computer using the MyoDaq software (version 2.2).

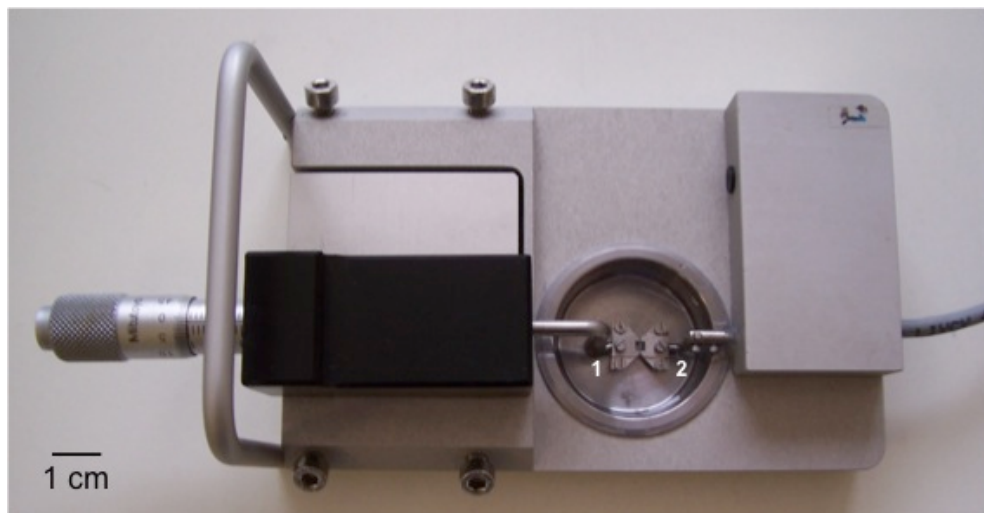


Figure 2.5: Photograph of a myograph bath. 1: Jaw connected to the micrometre. 2: Jaw connected to the tension transducer.

Figure 2.6 shows a zoomed-in photograph of the myograph bath and mounted vessel (Figure 2.6A) and a schematic drawing of a mounted vessel (Figure 2.6B). During the mounting procedure, the vessels were immersed in 6 mL PSS. To mount a vessel, two 40 μm wires were gently introduced along the lumen. The first wire was hooked onto the top left-side screw and stabilised between the two jaws pressed against each other. The vessel was then shimmied up the wire into the space between the jaws. The jaws were then moved apart slightly. The bottom end of the wire was then pulled tightly against the jaw and screwed onto the lower left-side screw and the top end was pulled equally tightly and screwed onto the upper left-side screw. A second wire was then introduced along the vessel lumen ensuring that the end of the wire did not traumatise

the vessel wall. The jaws were positioned back together and the bottom end of this wire was pulled tightly against the second jaw and screwed onto the top right-side screw. Finally, the top end was also pulled and screwed to the lower right-side screw. Both wires were then positioned side-by-side in a parallel manner. The exact length of the arteries was then measured under the microscope using the calibrated eyepiece graticule.

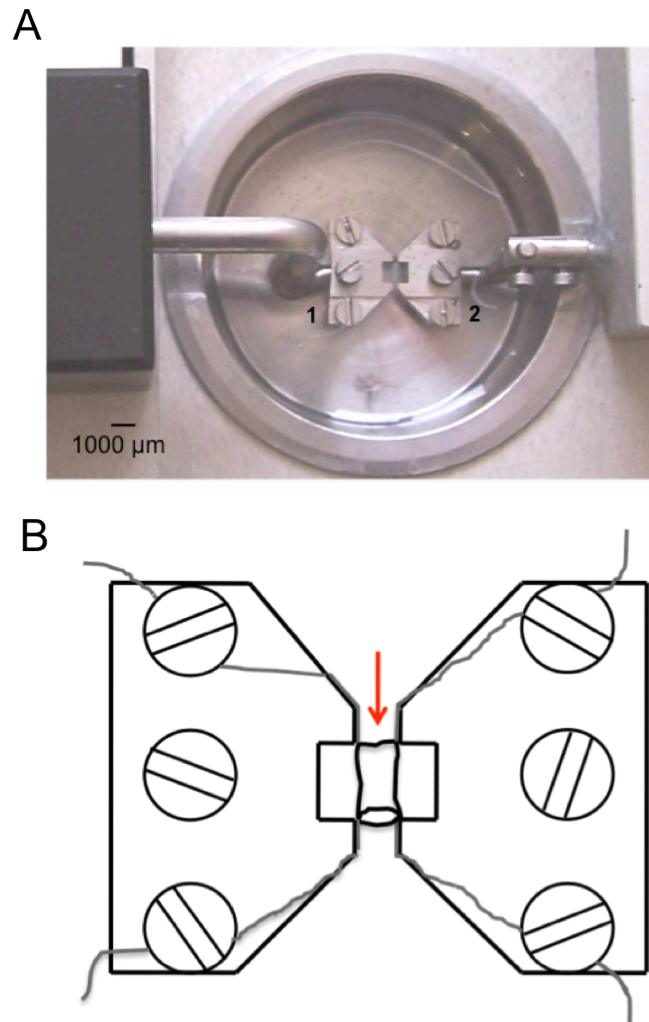


Figure 2.6: Representations of a mounted vessel onto myograph jaws. A: Photograph of the myograph bath with a mounted artery. B: Schematic drawing of a vessel mounted on the myograph jaws. The vessel, (red arrow) is positioned in the space between the jaws and the wires (grey), tightly secured on four screws, are parallel to each other.

2.3.2. The normalisation procedure

2.3.2.1. Theory

Normalisation is the procedure, carried out on each artery, to set it to a width intended to simulate its anticipated physiological intra-luminal pressure in vivo (Mulvany and Halpern, 1977). This procedure determined the internal circumference ($IC_{\text{set pressure}}$), which an artery would have had when relaxed. The starting width of each artery was noted and the vessel stretched in a step-wise manner (see Figure 2.7), the change in width and tension were continually monitored by the micrometer and strain gauge respectively, and the effective pressure (kPa) was calculated at each step:

$$\text{Effective pressure} = (\text{wall tension}_{(\text{mN/mm})} / (IC_{(\mu\text{m})} / 2\pi))$$

wall tension (mN) = tension_{plateau} – tension_{baseline} and IC = internal circumference of the artery in μm (= total stretch + diameters of the two wires).

An exponential curve was then fitted to the internal circumference versus effective pressure plot (Davis and Gore, 1989). Using the Laplace equation, the point on the exponential curve which corresponded to the set transmural pressure was determined and denoted $IC_{\text{set pressure}}$. The Laplace equation is derived from a formula developed independently by Thomas Young (Young, 1805) and Pierre-Simon Laplace (Laplace, 1806); it defines the relationship between pressure, tension and radius of a solid sphere. In this context it is assumed that an artery behaves as such,

$$P = (T \times K) / r$$

r = radius in meters, T = tension in Newton, K = a constant to be derived from the wall length and P = pressure in Pascals.

Finally, the internal circumference was set to 0.9 of $IC_{\text{set pressure}}$ (see Section 2.3.3), which has been shown to yield the maximal active wall tension in rat mesenteric arteries (Mulvany and Halpern, 1977, Mulvany and Nyborg, 1980, Mulvany and Warshaw, 1979, Davis and Gore, 1989).

The normalised lumen diameter was then calculated:

$$\text{Diameter} = (0.9 \text{ of } IC_{\text{set pressure}}) / \pi.$$

2.3.2.2. Practice

The MyoDaq software includes an algorithm that allows calculation of 0.9 of $IC_{\text{set pressure}}$. The vessel length was entered in the software program. Figure 2.7 shows a raw tracing of an artery undergoing the normalisation procedure. Initially, each artery was set to the ‘zero’ position. This was the position at which the artery had the smallest diameter, i.e. it had not yet developed any tension. This position was obtained by adjusting the jaws slowly until the wires touched without pushing against each other. The zero stretch and tension were entered into the software program. The artery was then stretched in a step-wise manner, leaving enough time after every stretch for the vessel to reach a steady-state tension, as illustrated in Figure 2.7 (1 to 6), with total stretch and tension entered at each step. The software program calculated the internal circumference at each step and stretching was stopped when the effective pressure exceeded the set pressure. The program then fitted the internal circumference versus effective pressure data to an exponential curve and used the Laplace relation to determine $IC_{\text{set pressure}}$ and calculate 0.9 of $IC_{\text{set pressure}}$ and the diameter of the vessel.

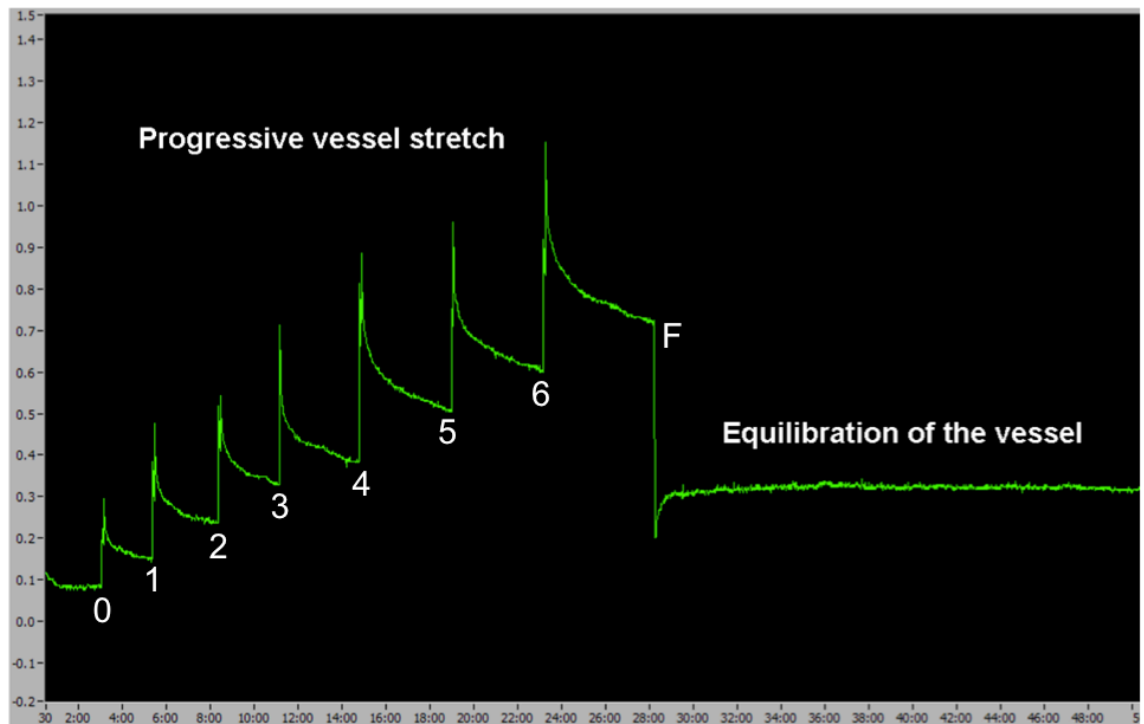


Figure 2.7: Schematic diagram of the normalisation procedure on a human myometrial artery. (0): starting point, ie. ‘zero’ tension. (1), (2), (3), (4), (5) and (6): positions at which the vessel was stretched progressively. (F): position at which, after having exceeded the desired ‘set pressure’ (see below), the stretch was adjusted (reduced) to 0.9 of the internal circumference anticipated at the desired simulated physiological ‘set pressure’. The vessel was then left to equilibrate. x axis: time in minutes. y axis: tension in mN/mm.

2.3.3. Normalisation of the myometrial and placental arteries

The myometrial and placental circulations are exposed to differing intraluminal blood pressures. The blood pressure in the myometrial vasculature is considered to be close to that in the systemic circulation, (80 - 100 mmHg or 13.3 kPa), whilst the placental vasculature is thought to be exposed to lower pressures (28 - 40 mmHg or 5.13 kPa) (Griffin et al., 1983, McCarthy et al., 1994, Kleiner-Assaf et al., 1999, Struijk et al., 2008). Pressures can be presented either in Pascals (1000 Pascals = 1 kPa) or mmHg. From a pressure in Pa, the conversion factor to mmHg is 0.0075 (Pellicer, 2000). Thus, throughout this study, MA were stretched in order to reach an internal circumference equivalent to 0.9 of IC_{13.3kPa} and PA were normalised to an internal circumference of 0.9 of IC_{5.13kPa} (Wareing et al., 2002, Hudson et al., 2007).

2.4. Quality assessment of human arteries

In this study, the mean \pm SEM diameter of MA was 314 ± 4.17 microns ($n = 62$), whilst that of PA was 297 ± 7.35 microns ($n = 75$). Normalisation and subsequent experimentations were carried out whilst gassing with 5 % CO₂ in air (oxygen content of 18 – 21 % - BOC Special Gases, British Oxygen Company, UK). Chapter 5 clarifies this choice of oxygenation for both MA and PA. Permeabilisation experiments (see Section 2.5) were carried out at 26 °C, whilst intact experiments were carried out in 37 °C.

All experiments were started as follows:

Following normalisation, human arteries (MA or PA) were left to equilibrate in PSS for 20 to 30 minutes. Addition of 60 mM of KPSS was intended to induce sustained constrictions in both artery types. High K⁺ depolarizes the vascular smooth muscle cell membrane and opens voltage-dependent Ca²⁺ channels, resulting in an influx of extracellular Ca²⁺ and an activation of contractile machinery (Somlyo and Somlyo, 2003). Figure 2.8 shows the extent of constriction induced by 60 mM KPSS in human MA and PA at 37 °C. PA constricted less than MA (MA: 8.2 ± 0.5 kPa, 54 arteries versus PA: 5.9 ± 0.2 kPa, 96 arteries, $P < 0.05$, unpaired *t-test*).

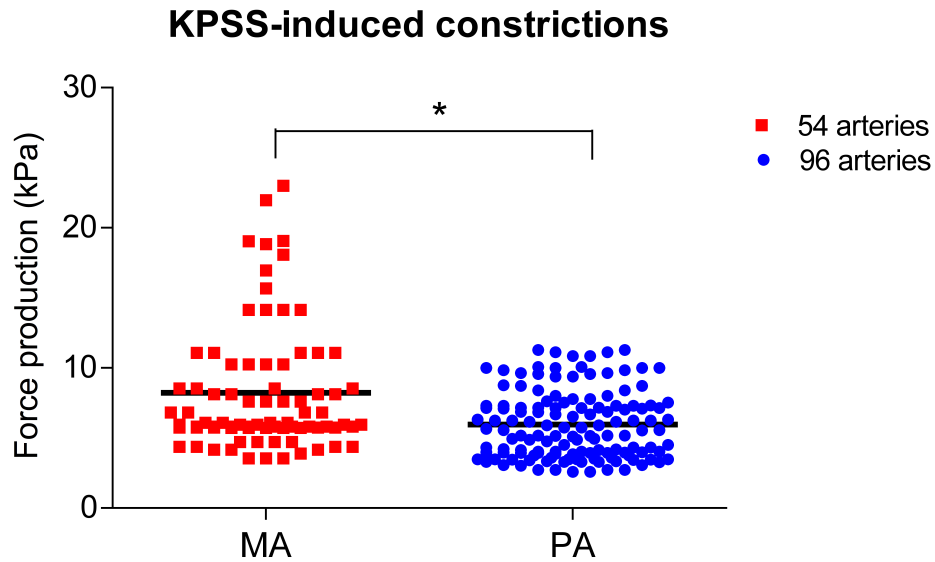


Figure 2.8: Constrictions to 60 mM KPSS in human myometrial (MA) and placental arteries (PA). y axis: Force production in kPa. * Statistical difference relative to PA ($P < 0.05$, unpaired *t-test*).

Arteries, which constricted with less than 3 kPa, were deemed of poor quality and were therefore discarded. They represented 5 % of MA and 6 % of PA of all experiments.

Once constriction to 60 mM KPSS had reached a plateau, arterial endothelial function was assessed with the addition of BK (1 μ M). MA relaxed to BK (by 36 ± 2.7 %, $n = 54$ at 37 °C). As MA are known to have a prominent agonist-mediated endothelial-dependent relaxatory capacity, any vessels, which relaxed less than 30 % to BK (1 μ M), were deemed of poor endothelial quality and discarded. These represented 6 % of all MA. The relaxations observed in this study were similar to those reported in the literature (Hudson et al., 2007, Sweeney et al., 2008). In contrast, pre-constricted PA did not relax substantially to this agonist (relaxation of 6.2 ± 1.1 %, $n = 92$ at 37 °C). Similar findings had previously been observed in PA pre-constricted to maximal concentrations of the thromboxane agonist U46619 (1 μ M) (Sweeney et al., 2008) and support the notion that PA are resistant to agonist-mediated endothelial-dependent relaxation.

Following exposure to BK, arteries were washed out with PSS and left to equilibrate for 10 minutes. Arteries were then either permeabilised (see Section 2.5) or left intact.

2.5. The permeabilisation procedure

The permeabilisation procedure was the method of choice to assess possible Ca^{2+} -sensitisation or –desensitisation phenomena in human arteries, as it enabled tight control of intracellular Ca^{2+} concentrations ($[\text{Ca}^{2+}]_i$). The procedure involved generation of small pores in the cell membrane using α -toxin, secreted naturally occurring toxin produced by the bacterium *Staphylococcus aureus*, and purchased under license from List Biological Laboratories (see Appendix D). α -toxin allowed only proteins and molecules of 1 - 4 kDa to escape from the cell (Fussle et al., 1981, Bhakdi et al., 1984, Lind et al., 1987). Thus, proteins essential to cellular contractile and relaxatory mechanisms were assumed to remain within the cell and functional. Membrane G protein-coupled receptors were also assumed to retain their function following permeabilisation (Bhakdi et al., 1984, Kitazawa et al., 1989).

2.5.1. Preparation of *Staphylococcus aureus* α -toxin stock aliquots

To permeabilise each artery, 300 units (U)/ml of α -toxin were used. Other groups had used 500 – 2000 U/ml (Hudson et al., 2007, Hemmings et al., 2006, Wareing et al., 2005b), but after running test experiments with 400 and 300 U/ml, I observed that 300 U/ml were enough to carry out successful permeabilisation.

Each stock vial of α -toxin came as 0.25 mg powder. Each vial had a specific activity in units per mg, which could change depending on the lot number. The procedure was as follows:

- 1) The number of active units present in the 0.25 mg vial was calculated.
- 2) Each α -toxin vial was then dissolved in 500 μl sterile double deionised water (ddH₂O)
- 3) The volume required to obtain 300 units of α -toxin in an aliquot was then calculated and aliquots of this volume were prepared.
- 4) The aliquots were stored at – 20 °C until use for experiments.

The α -toxin was prepared wearing a facemask and protective eyewear, in a fume hood. All the equipment used to prepare the aliquots, including pipettes and pipette tip boxes, were thoroughly cleaned in diluted bleach to remove all toxicity.

2.5.2. Preparation of the α -toxin permeabilisation cocktail

In each permeabilisation experiment, 25 μ l α -toxin permeabilisation cocktail was added directly onto each artery. For each experiment, four arteries were used, therefore 100 μ l α -toxin cocktail was needed. The cocktail contained 300 U/ml of α -toxin (in variable volumes according to the lot number), 10 μ M (1 μ l of stock) ionophore A23187, which rendered the intracellular stores permeable to Ca^{2+} , and variable volumes (μ l) of a pCa solution, to ensure the cocktail had a final pCa of 6.7. To determine the necessary pCa solution, the following steps were followed:

- 1) The volume of Ca^{2+} -activating solution, CaG, needed to make up pCa 6.7 was determined.
- 2) The dilution factor necessary to obtain a final pCa of 6.7 was determined.
- 3) The volume of CaG, which makes up pCa 6.7, was multiplied by the dilution factor. This provided the volume of CaG making up the unknown pCa solution.
- 4) The now known CaG volume was then searched in the pCa table (Table 2.3) and the corresponding pCa solution determined.
- 5) The pCa solution for the cocktail was prepared using G_{10} and CaG solutions in the compositions indicated in the pCa table.

2.5.3. The permeabilisation protocol

The raw tracing shown in Figure 2.9 illustrates the permeabilisation procedure. Following normalisation and assessment of contractile viability (Section 2.4), each intact artery was exposed to a mock intracellular relaxing solution (G_1 , Table 2.2). G_1 solution contains a high concentration of K^+ , which acts to open the membrane voltage-gated Ca^{2+} channels, allowing influx of Ca^{2+} and resulting in contraction of the artery. The chelator EGTA present in G_1 likely mops up any residual extracellular Ca^{2+} ions in the bath (from the previous PSS solution), resulting in arterial relaxation back to baseline. G_1 -induced constrictions were similar in MA and PA (MA: 5.6 ± 0.1 kPa, 151 arteries and PA: 4.7 ± 0.2 kPa, 189 arteries).

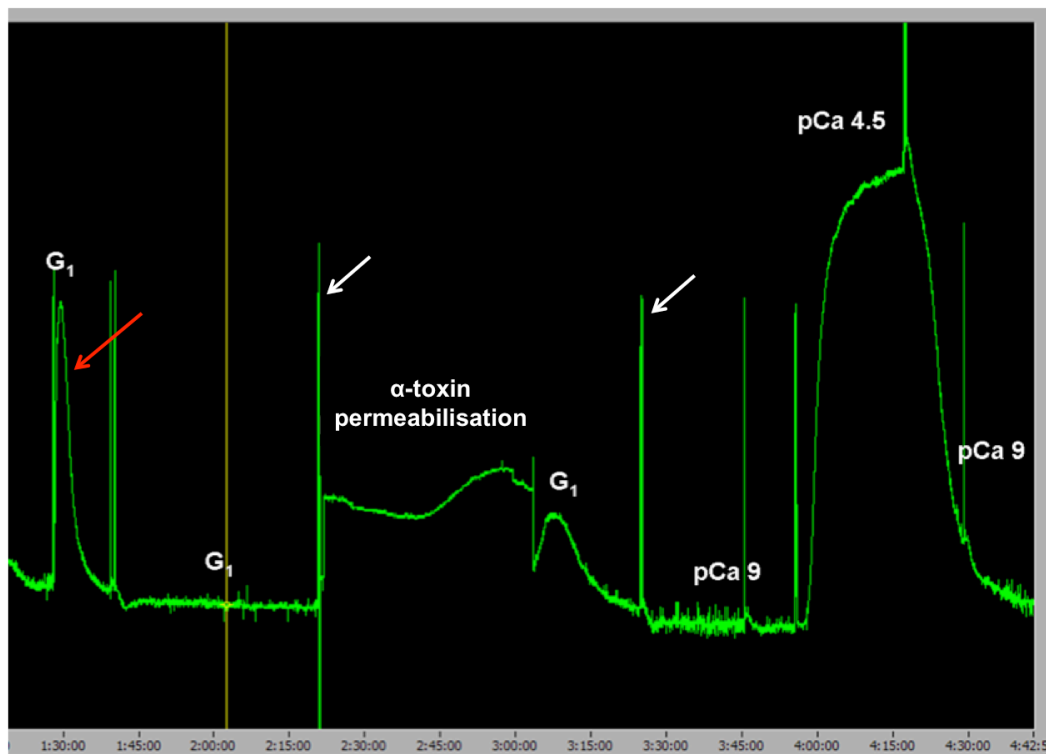


Figure 2.9: Raw tracing of the permeabilisation procedure in a human myometrial artery. The small increases, shown by the white arrows, represent changes in solutions and occur due to mechanical movements of the myograph transducer. Red arrow illustrates a relaxation resulting from EGTA mopping up Ca^{2+} ions. y axis: tension in mN/mm. x axis indicates time in hours:minutes:seconds.

Following removal of the relaxing solution from the bath, vessels devoid of all Ca^{2+} ions were ready for permeabilisation and each artery was incubated with a 25 μ l droplet of α -toxin cocktail. Incubation was carried out for 30 minutes or until the pCa 6.7-induced constriction had reached plateau.

Following permeabilisation, arteries were bathed in the relaxing solution G_1 , followed by exposure to a specified low-calcium solution (pCa 9, Table 2.3). Subsequent exposure to the activating solution pCa 4.5 (Table 2.3) was intended to induce substantial constriction of the artery, as this pCa solution contains maximal $[Ca^{2+}]$. To maximize chances of consistent results, arteries, which constricted to pCa 4.5 with less than 3 kPa, were deemed unsuitable for further experimentation and discarded (1 % placental arteries and 1 % myometrial arteries). Experimental experience indicated that arteries, which constricted with less than 3 kPa to pCa 4.5, became erratic. Raw tracings on the monitor were very noisy rather than smooth-lined, which would be representative of controlled tone of vessels. A further wash with pCa 9 relaxed the arteries back to baseline and experimental protocols were then started. Specific experimental protocols will be detailed in the materials and methods section of the relevant results chapter.

2.6. Immuno-blotting

The following experiments were kindly carried out in liaison with Julie Taggart. The final western blots presented in this thesis illustrating expression levels of proteins PKGI, telokin, MLCK, MYPT1 and CPI-17 were carried out by Julie Taggart. Homogenisations of frozen samples (myometrial and placental arteries, myometrial tissues, rat brain and rat aorta) used for the assessment of the protein expression were carried out in modified RIPA buffer (50 mM Tris HCl, 150 mM NaCl, 1% NP-40, 0.5% Na-deoxycholate, 1 mM EGTA pH 7.4) with 2 % (vol/vol) protease inhibitor and 0.5 % (vol/vol) phosphatase inhibitor (Sigma Chemicals, St. Louis, MO, USA) at 5 μ l buffer per mg of tissue. Homogenates were centrifuged at $10,000 \times g$ at 4 °C for 10 minutes and supernatants were collected. Protein concentrations were determined using Bio-Rad DC Protein Assay reagents (Bio-Rad Laboratories, Hercules, CA). Table 2.5 illustrates the conditions of immune-blots carried out for each protein. Human myometrial tissue from pregnant women was used as positive control for HSP20, MLCK, MYPT1 and CPI-17, whilst rat aorta and rat brain were the controls of choice for PKGI α and telokin, respectively. All protein samples were separated by SDS-PAGE at 80 mA for 90 minutes. Electro-blotting was carried out onto 0.2 μ M polyvinylidene difluoride (PVDF) membranes (Biorad Laboratories, Hercules, CA) with transfer voltage and time described in Table 2.5 for each protein. Membranes in preparation for immuno-blotting for PKGI α were blocked in 5 % Bovine Albumin Serum (BSA, Sigma-Aldrich)

overnight at 4 °C. All other membranes were blocked in 5 % milk in TBS-Tween (TBS-T: 100 mM Tris Base, 66 mM NaCl, 0.1 % Tween 20 (0.1 % w/v), pH 7.5) overnight at 4 °C. Following exposure to primary and secondary antibodies, membranes were washed 3 × 5 minutes in TBS-T. All secondary antibodies were conjugated with horseradish peroxidase. Membranes were stained with enhanced chemiluminescence (ECL) substrate (GE Healthcare, Buckinghamshire, UK) and visualised on photographic film (Thermo Scientific, IL, USA). Actin was used as a loading control by assessing membranes stained by incubating them with Ponceau Red (Sigma-Aldrich) for 30 mins at RT. Stained membranes and films were scanned using the UMAX Powerlook III Scanner and Softmax Pro Software.

Table 2.5: Summary of immuno-blotting conditions for PKGI α and PKG-interacting myofilament-associated proteins.

Antibody	Protein Concentration (μg)	PC	Percentage Acrylamide Gel	Electro-Blotting	Primary Antibody	Secondary Antibody
PKGIα	20	Rat Aorta	10 %	90 V for 90 mins	Goat IgG, 1:400 (sc-10335, Santa Cruz, CA), 5% BSA, o/n 4 °C	Rabbit anti-goat, 1:5,000 (Dako), 5% BSA, 1 hr RT
HSP20	5	Human Myometrium (pregnant)	15 %	100 V for 45 mins	Rabbit IgG, 1:7,500 (ab13491, Abcam), 1% milk, o/n 4 °C	Goat anti-rabbit, 1:5,000 (Dako), 1% milk, 1 hr RT
Telokin	10	Rat Brain	Pre-cast 4 – 15 %	100 V for 45 mins	Rabbit IgG, 1:2,000 (ab76092, Abcam), 1% milk, 1 hr RT	Goat anti-rabbit, 1:5,000 (Dako), 1% milk, 1 hr RT
MLCK	7.5	Human Myometrium (pregnant)	8 %	90 V for 110 mins	Rabbit IgG, 1:10,000 (ab76092, Abcam), 1% milk, 1 hr RT	Goat anti-rabbit, 1:5,000 (Dako), 1% milk, 1 hr RT
MYPT1	20	Human Myometrium (pregnant)	Pre-cast 4 – 15 %	90 V for 110 mins	Rabbit IgG, 1:200 (sc-25618, clone H-130, Santa Cruz, CA), 1% milk, o/n 4 °C	Goat anti-rabbit, 1:5,000 (Dako), 1% milk, 1 hr RT
CPI-17	10	Human Myometrium (pregnant)	12 %	100 V for 45 mins	Rabbit IgG, 1:500 (c-7905-50, US Biochemical), 1% milk, o/n 4 °C	Donkey anti-rabbit, 1:250 (ThermoScientific), 1% milk, 1 hr RT

Pre-cast gels were obtained from Bio-Rad Laboratories, Hercules, CA, BSA: Bovine Albumin Serum, mins: minutes, o/n: overnight, hr: hour, RT: room temperature, PC: positive control.

2.7. Analysis and Statistics

2.7.1. Analysis

2.7.1.1. Functional Studies

Vessel tone was measured in units of mN/mm, which were subsequently converted into active effective pressure (kPa) taking into account the diameter of the vessel.

$$\text{Active effective pressure} = (\text{wall tension}_{(\text{mN/mm})} / (\text{diameter}_{(\mu\text{m})} / 2000))$$

where wall tension = tension_{plateau} – tension_{baseline}

Raw tracings illustrating changes in tension are presented in kPa, except for Figures 2.7 and 2.9, which were presented in mN/mm in this Chapter.

Arterial relaxation to BK, His, SNP, YC-1 or 8-bromo-cGMP (8-br-cGMP) was measured as a percentage of constriction to 60 mM KPSS, contractile agonists or pCa solutions.

2.7.1.2. Immuno-blotting

Identification of the optical density of bands representing proteins in MA and PA allowed for quantification of protein expression. Optical densities from the western blot scans were determined using Intelligent Quantifier Software (BioImage Systems Inc.). Protein expression was quantified by normalising the optical density of each band in MA and PA to the optical density of the positive control following the subtraction of background. All resulting data sets were also normalised to the scans' background noise.

2.7.2. Statistics

n represents the number of patients. Throughout this study, statistical analyses were carried out using unpaired *t*-tests, one-way ANOVAs or two-way ANOVAs as appropriate. Values were quoted as mean ± standard error of the mean. Statistical analysis was carried out using the software GraphPad Prism, version 4.0. Statistical significance was taken at $P < 0.05$.

Chapter 3

Ca²⁺-sensitisation in human myometrial and placental arteries in the presence of G protein-coupled agonists

3.1. Introduction

Successful fetal growth and pregnancy outcome are dependent upon adequate blood flow in the uteroplacental circulations. In turn, this requires a balance of contractile and relaxatory factors within the maternal uterine and feto-placental circulations. Aberrant expression of several contractile agonists has been linked to pregnancy complications which display raised vascular resistance such as pre-eclampsia and hypertension in pregnancy (Wetzka et al., 1997, Faxen et al., 2000, Yamamoto et al., 2010). It is important, therefore, to develop our understanding of the regulation of blood vessel tone in placental and uterine circulations and to elucidate the mechanisms, which may regulate placental arteries (PA) differently from myometrial arteries (MA). As mentioned previously, it is reasonable to propose that maternal uterine and fetal placental vasculatures may experience different regulatory influences. Ca^{2+} activation of the contractile filaments of SM is the primary mechanism of contractile regulation in blood vessels. In addition, this pathway is often targeted by physiological agents effecting endothelial-dependent vasodilatory influences, which are known to differ between MA and PA (Chapter 5, Sweeney et al., 2008). Therefore, it is important to establish whether these arteries differ in their sensitivities to Ca^{2+} -dependent force production.

Studies have implicated the contractile agonist thromboxane, whose mimetic is U46619, in pregnancy complications. It has been shown that the ratio of prostacyclin:thromboxane production rate was decreased in the human placenta and placental bed from pre-eclamptic pregnancies compared to those from normal pregnancies, thus favouring the vasoconstrictive thromboxane (Wetzka et al., 1997) and, thereby, offering one mechanism for localised elevation in blood pressure associated with this condition. Similarly, S1P, a potent angiogenic factor, expressed in mammalian uteri and other tissues, has been shown to play an important role in the endometrial/placental angiogenesis during pregnancy in ewes (Dunlap et al., 2010, Hla, 2004, Mizugishi et al., 2007, Skaznik-Wikiel et al., 2006, Su et al., 2008). Insufficient endometrial/placental vascularisation can compromise pregnancy and lead to pathological conditions such as preeclampsia (Dunlap et al., 2010). These findings stress the importance of adequate control of S1P and thromboxane production/activity during pregnancy, highlighting the need to further understand their involvement in vascular tone regulation in arteries from the human placenta and myometrium. In

addition to these two agonists, a third vasoconstrictor, endothelin-1 (ET-1), has been associated with cardiovascular diseases and is considered to be one of the most potent naturally occurring peptidic agonists (Inoue et al., 1989). Overexpression of ET-1 has been reported in systemic hypertensive disorders and pregnancy related complications, such as preeclampsia (Tanfin et al., 2011, Agapitov and Haynes, 2002, Wang et al., 2008, Faxen et al., 2000). Additionally, ET-1 mRNA levels were found to be significantly higher in the placenta compared to myometrium from women with healthy pregnancies (Faxen et al., 2000). These findings highlight the importance of understanding the signalling mechanisms regulating vascular tone in these two human organs.

Previous studies have reported that both PA and MA constricted to sub-maximal concentrations of Ca^{2+} (pCa 6.7) when their membranes had been rendered permeable to small solutes by toxin permeabilisation. Such constrictions were further enhanced with the addition of the G protein-coupled agonists U46619 in both artery types and by S1P in chorionic plate PA (Wareing et al., 2005b, Hemmings et al., 2006). This indicated that enhancement of Ca^{2+} -dependent force production at one particular supra-basal and sub-maximal $[\text{Ca}^{2+}]_i$ occurred in both artery types. However, neither of these studies carried out rigorous comparisons of the Ca^{2+} -dependency of constriction, nor agonist-mediated Ca^{2+} -sensitisation of force, between PA and MA. There are currently no studies reporting Ca^{2+} -sensitisation induced by ET-1 in human arteries and knowledge on the contractile effects of this vasoconstrictor is also limited in arteries from the reproductive organs in humans (Cooper et al., 2005).

Consequently, in this study, I aimed to establish novel information regarding the role of these three physiologically important G protein-coupled agonists in regulating tone in human arteries from the placenta and myometrium. In particular, to assess (i) Ca^{2+} -dependent responses over a range of $[\text{Ca}^{2+}]_i$ (pCa 9 – 4.5), (ii) whether Ca^{2+} -sensitisations mediated by U46619, ET-1 and S1P occurred in PA and MA and (iii) whether responses differed between the two artery types. To do so, I utilised the experimental model of α -toxin permeabilisation, which allowed for tight experimental control of $[\text{Ca}^{2+}]_i$.

3.2. Materials and Methods

3.2.1. *Experimental protocol*

As described previously, permeabilisation experiments were carried out at 26 °C. Isolated human MA and PA, isometrically mounted on wire myographs, were constricted to 60 mM KPSS, permeabilised with α -toxin and constricted to pCa 4.5 (Section 2.5.3).

Contractile responses were then assessed to increasing Ca^{2+} concentrations (pCa 9, 8, 7.5, 7, 6.7, 6.3, 6, 5.5 and 4.5). Each individual artery was exposed to a pCa curve in one of the five following conditions:

1. pCa alone (Time Control or TC)
2. pCa + 10^{-6} M U46619
3. pCa + 10^{-8} M ET-1
4. pCa + 0.1 % BSA (TC + BSA)
5. pCa + 10^{-5} M SIP

For each tissue type (MA and PA), two experiments were run to accommodate the five experimental conditions. One myograph could only accommodate four vessels. Therefore, in one experiment, conditions 1, 2 and 3 were assessed and in a second experiment, conditions 4 and 5 were assessed from the same tissue.

These functional experiments lasted 9 -10 hours following normalisation of the vessels.

3.2.2. *Analysis and Statistics*

3.2.2.1. *Analysis*

Assessment of the constrictive responses of each artery type was carried out as an analysis of the change in tension (extrapolated as active effective pressure) of the TC compared to the contractile changes in the presence of the G protein-coupled agonist. Additionally, for each experimental condition, the level of tension production to every pCa (plus or minus agonist) was calculated as a percentage of the maximal tension development observed during that pCa dose-response protocol. This enabled a visual representation of possible changes in Ca^{2+} -sensitivity of contraction between conditions.

The log EC₅₀, which was the pCa value at which half (50%) of the maximal constriction was reached, was determined from the raw data obtained from each artery type exposed to every condition. Each raw data set was fitted onto a sigmoidal curve with nonlinear regression using the following equation

$$Y = \min + (\max - \min) / (1 + 10^{-(\text{Log EC}_{50} - X) * \text{Hill Slope}})$$

where min and max represent minimal and maximal raw values of tension development and Hill Slope represents the slope factor or steepness of the slope.

All the data sets presented in this chapter fitted onto sigmoidal curves with $r^2 > 0.90$. Log EC₅₀ values were compared between experimental conditions (in the presence or absence of G protein-coupled agonists) and between artery types.

3.2.2.2. *Statistics*

Contractile responses to 60 mM KPSS and pCa 4.5 were compared between MA and PA using unpaired *t-test*.

Tension development pCa curves were compared between experimental conditions for each artery type using two-way ANOVA, including a Bonferroni post-hoc test for detailed breakdown of the analysis. Paired comparisons between TC_{condition} and condition were made as follows:

- TC_{U46619} versus U46619
- TC_{ET-1} versus ET-1
- TC_{ALL} versus TC_{S1P} + BSA
- TC_{S1P} + BSA versus S1P

Tension development pCa curves were also compared between artery types for every experimental condition using two-way ANOVA, including a Bonferroni post-hoc test for detailed breakdown of the analysis. Comparisons were made as follows:

- With TC: PA versus MA
- With U46619: PA versus MA
- With ET-1: PA versus MA
- With S1P: PA versus MA

Log EC₅₀ values were compared between experimental conditions using paired Student's *t-test* as follows:

- EC₅₀ (TC) versus EC₅₀ (U46619)

- $EC_{50\text{ (TC)}}$ versus $EC_{50\text{ (ET-1)}}$
- $EC_{50\text{ (TC)}}$ versus $EC_{50\text{ (TC + BSA)}}$
- $EC_{50\text{ (TC)}}$ versus $EC_{50\text{ (S1P)}}$

Log EC_{50} values were also compared between artery types using unpaired Student's *t*-test as follows:

- With TC: $EC_{50\text{ (PA)}}$ versus $EC_{50\text{ (MA)}}$
- With U44619: $EC_{50\text{ (PA)}}$ versus $EC_{50\text{ (MA)}}$
- With ET-1: $EC_{50\text{ (PA)}}$ versus $EC_{50\text{ (MA)}}$
- With S1P: $EC_{50\text{ (PA)}}$ versus $EC_{50\text{ (MA)}}$

3.3. High K^+ - and Ca^{2+} -induced force production of human myometrial and placental arteries

Figure 3.1 shows the original tracings of an individual myometrial artery (A) and an individual placental artery (B) exposed to 60 mM KPSS pre-permeabilisation and pCa 4.5 post-permeabilisation. In this example, 60 mM KPSS and pCa 4.5 induced increases in tension both artery types. In MA, the KPSS-induced constriction was 8.2 kPa and similar to the pCa 4.5-induced constriction, which was 7.8 kPa. In PA, KPSS-induced constriction was 4.6 kPa, whilst that induced by pCa 4.5 was almost double the previous constriction, at 8.1 kPa.



Figure 3.1: Original raw tracings of responses in (A) a myometrial and (B) a placental artery to 60 mM KPSS pre-permeabilisation and to pCa 4.5 post-permeabilisation.

Figure 3.2 illustrates the contractile responses to high K^+ (60 mM KPSS) pre-permeabilisation and high Ca^{2+} (pCa 4.5) post-permeabilisation in human MA and PA. 60 mM KPSS-induced constrictions were greater in MA compared to PA (MA: 8.63 ± 0.31 kPa, $n = 49$ versus PA: 5.75 ± 0.14 kPa, $n = 51$). Constrictions to pCa 4.5 were similar to 60 mM KPSS-induced constrictions in MA, however in PA, they were 1.67 ± 0.06 -fold higher than those induced by KPSS. Consequently, mean constrictions to pCa 4.5 in PA exceeded those in MA (MA: 7.42 ± 0.22 kPa, $n = 49$ versus PA: 8.63 ± 0.24 kPa, $n = 51$).

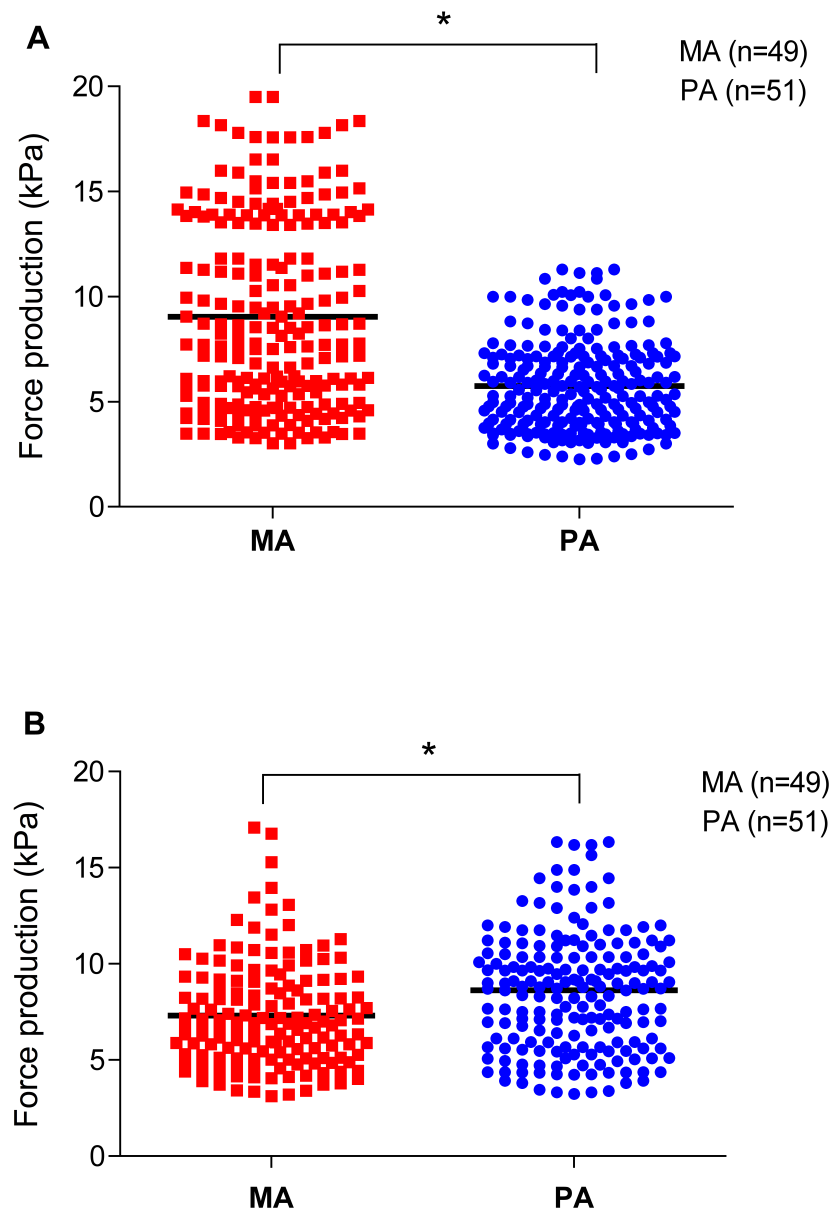


Figure 3.2: Summary data of contractile responses to 60 mM KPSS (A) and pCa 4.5 (B) in myometrial and placental arteries. Constrictions to 60 mM KPSS were assessed in *intact* arteries and constrictions to pCa 4.5 determined in *permeabilised* MA and PA. y axis: Force production in kPa. x axis: Red squares represent myometrial arteries (MA). Blue circles represent placental arteries (PA). * Statistical difference relative to PA.

3.4. Ca^{2+} -induced force production of human myometrial and placental arteries over increasing Ca^{2+} concentrations

Figure 3.3 shows an original tracing of the increasing force development in one individual permeabilised MA (Figure 3.3A) and one individual PA (Figure 3.3B) during assessment of responses to increasing Ca^{2+} concentrations or pCa (9 – 4.5). In these examples, tension development started at pCa 7 in MA, whilst in PA, the force production started at a lower pCa (pCa 6.7 i.e. at a higher $[\text{Ca}^{2+}]$). The magnitude of these constrictions appear similar over their respective ranges of $[\text{Ca}^{2+}]_i$ (i.e. pCa 7 to 4.5 in MA and pCa 6.7 to 4.5 in PA).

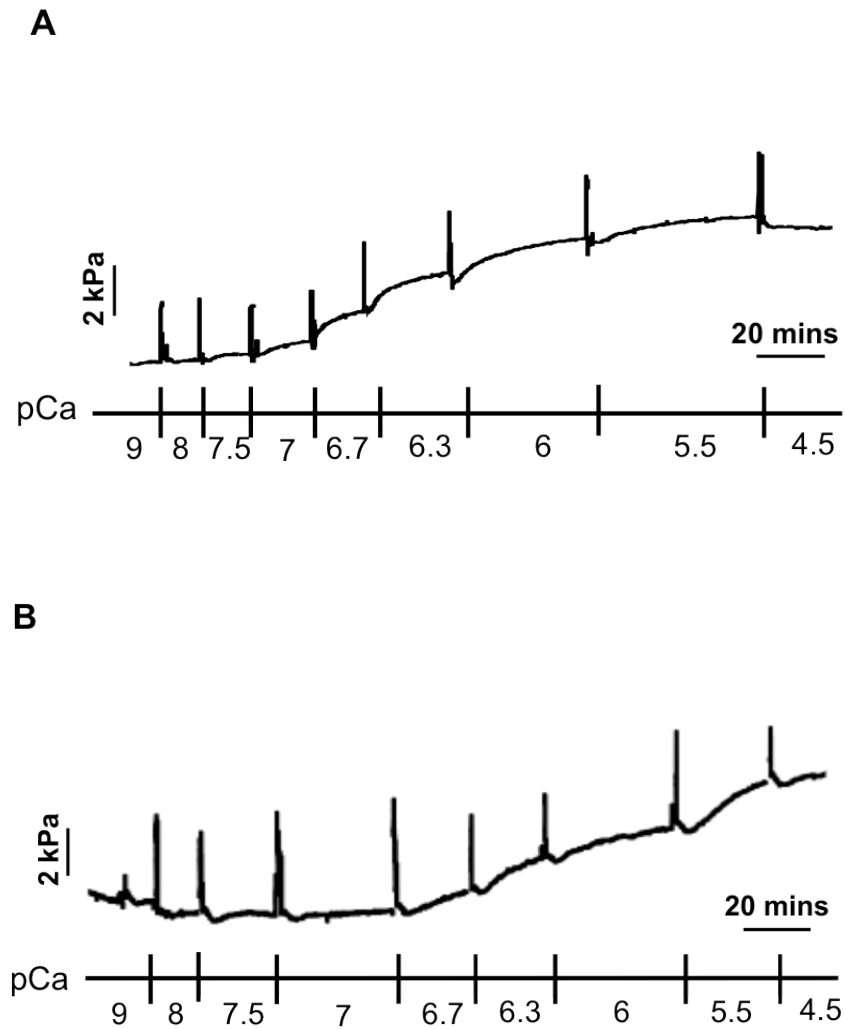


Figure 3.3: Original raw tracings of responses in (A) a myometrial and (B) a placental permeabilised artery to increasing Ca^{2+} concentrations.

Figure 3.4A illustrates the group mean \pm SEM comparisons of maximal constriction (kPa) pCa curves in MA versus PA. There was no difference in the maximal forces developed between these two artery types ($n = 8$). Figure 3.4B displays the comparison of the tension developed in MA or PA at each pCa when expressed as a percentage of the maximal force produced in each individual artery. The curve representing MA data sets is shifted to the left with a greater percentage constriction between pCa 7 and pCa 6 compared to PA. This indicates an increase in sensitivity to $[\text{Ca}^{2+}]_i$ in MA compared to PA; a suggestion which is supported by the lower EC_{50} compared to PA ($\log \text{EC}_{50 (\text{MA})} = -6.64 \pm 0.07$ and $\log \text{EC}_{50 (\text{PA})} = -6.26 \pm 0.05$). These results therefore illustrate that, whilst maximal constrictions were similar between MA and PA, the former artery type displayed a higher sensitivity to the same sub-maximal $[\text{Ca}^{2+}]_i$.

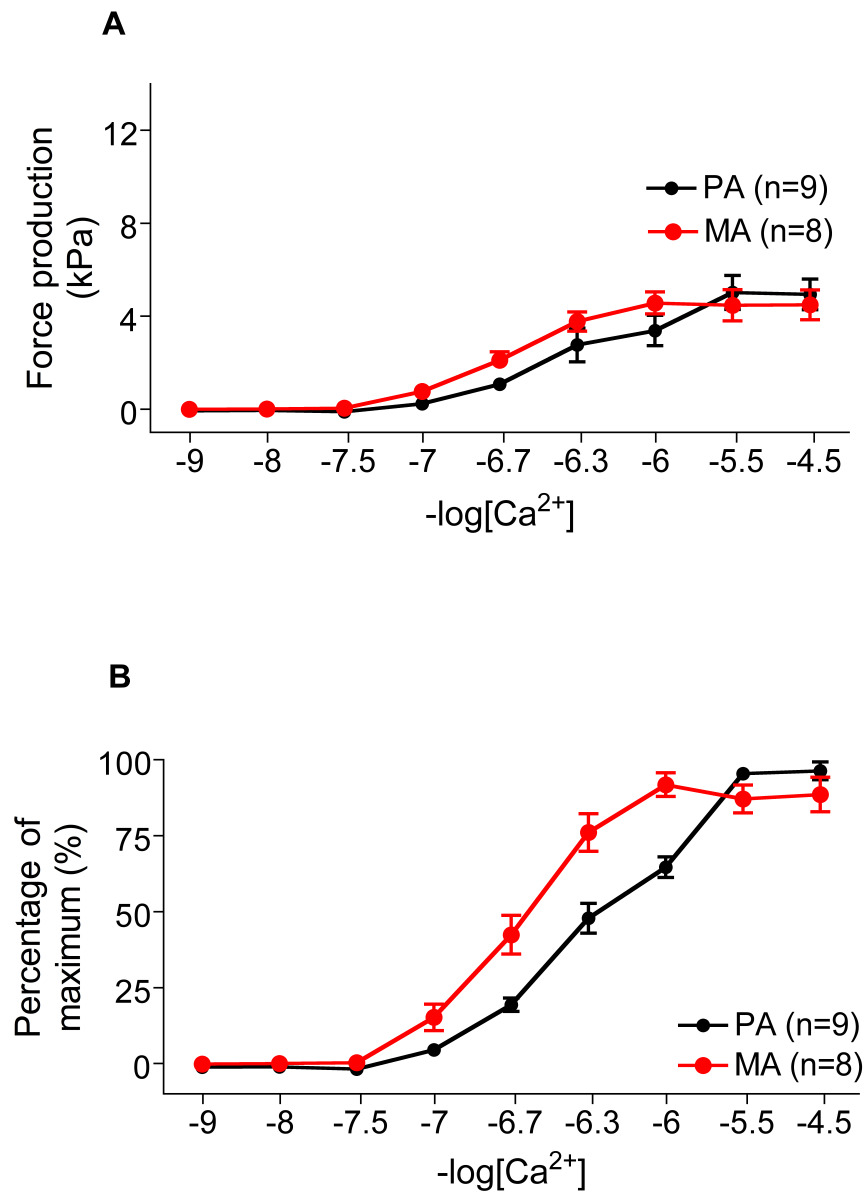


Figure 3.4: Summary data of contraction responses to increasing Ca²⁺ concentrations in myometrial (MA) and placental (PA) arteries. A: Mean maximal force productions (kPa) at each pCa (9 – 4.5) in MA and PA. B: The force developed at each pCa is expressed as a percentage of the maximal force developed in that individual artery type and the mean data shown for both MA and PA.

3.5. Agonist-induced enhancement of Ca^{2+} -dependent constriction in human myometrial and placental arteries

3.5.1. Assessment of agonist effects on Ca^{2+} -dependent constriction of human myometrial arteries

Figure 3.5 shows original tracings of the increasing force development in four individual permeabilised myometrial arteries during assessment of Ca^{2+} -sensitisation induced by three different G protein-coupled agonists. The first artery was exposed to pCa alone and small tension development started at pCa 7 (Figure 3.5A). The second artery was exposed to the same increasing pCa in the presence of 10^{-6} M U46619 (Figure 3.5B). Finally, the third and fourth arteries were exposed to the same increasing $[\text{Ca}^{2+}]_i$ in the presence of 10^{-8} M ET-1 and 10^{-5} M S1P (Figures 3.5C and 3.5D, respectively). Arteries exposed to any of the three agonists seem to develop greater tension over the same range of pCa, with a particular increase at pCa 7 (Figures 3.5A, 3.5B and 3.5C).

In MA, all TC data sets paired to U46619 were also paired to ET-1. However, it was important to confirm that there were no differences between the two TC data sets that were utilised (ie. TC for comparison to U46619 or ET-1 and TC + BSA for comparison to S1P as BSA was used as a carrier molecule for S1P). In the presence of BSA, the forces produced over the range of pCa were not different from those obtained in the presence of pCa alone (data not shown). In addition, their respective EC_{50} values were not different ($\log \text{EC}_{50 (\text{TC})} = -6.64 \pm 0.07$ vs. $\log \text{EC}_{50 (\text{TC}+\text{BSA})} = -6.62 \pm 0.06$). Thus, BSA had no constrictive nor Ca^{2+} -sensitising effect on MA. Consequently, only one original raw tracing representing TC was shown in Figure 3.5.

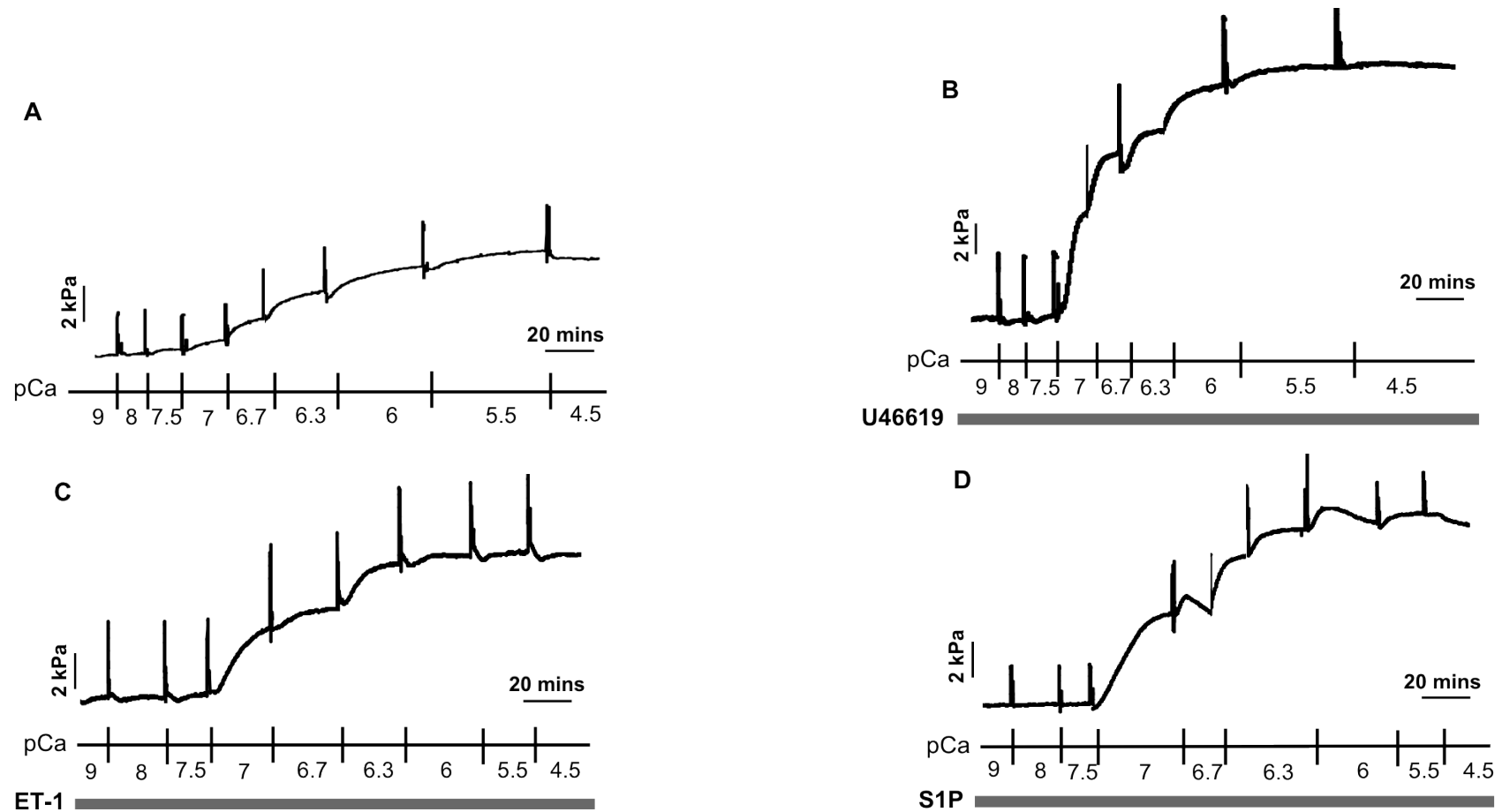


Figure 3.5: Original raw tracings of agonist effects on Ca^{2+} -dependent force of four individual permeabilised myometrial arteries. A: pCa curve showing arterial responses in a first artery to increasing $[\text{Ca}^{2+}]_i$ (pCa 9 - 4.5). B, C and D: pCa curves showing arterial responses to increasing $[\text{Ca}^{2+}]_i$ (pCa 9 - 4.5) in a second, third and fourth artery, in the presence of 10^{-6} M U46619, 10^{-8} M ET-1 or 10^{-5} M S1P, respectively.

Figure 3.6 shows the group comparisons of maximal constriction (kPa) of pCa curves in the three experimental conditions in human MA. In the presence of all three agonists, U46619, ET-1 and S1P, the forces produced over the range of pCa were greater than those observed in the TC (n = 8 Figure 3.6A, n = 5 Figure 3.6B and n = 4 Figure 3.6C, respectively). In arteries exposed to U46619 and ET-1, constrictions were greater than TC from pCa 7 onwards (pCa 7 – 4.5), whilst in the presence of S1P, significance was obtained particularly at pCa 6.3.

Figure 3.7 presents the mean forces developed at each pCa expressed as a percentage of the maximal force developed in each experimental condition. The curves representing U46619, ET-1 and S1P data sets are shifted to the left compared to the TC (Figures 3.7A, 3.7B and 3.7C, respectively), which indicates an increase in the sensitivity to Ca^{2+} in MA, induced by these agonists. This is supported by the lower EC_{50} values for the U46619 data sets ($\log \text{EC}_{50 (\text{TC})} = -6.64 \pm 0.07$ and $\log \text{EC}_{50 (\text{U46619})} = -7.05 \pm 0.05$), the ET-1 data sets ($\log \text{EC}_{50 (\text{TC})} = -6.64 \pm 0.07$ and $\log \text{EC}_{50 (\text{ET-1})} = -6.93 \pm 0.15$) and the S1P data sets ($\log \text{EC}_{50 (\text{TC})} = -6.64 \pm 0.07$ and $\log \text{EC}_{50 (\text{S1P})} = -6.78 \pm 0.05$).

Thus, taken together, these results indicate that agonists mediated the enhancement of Ca^{2+} -dependent force, and a sensitisation to the activating Ca^{2+} , in permeabilised human myometrial arteries.

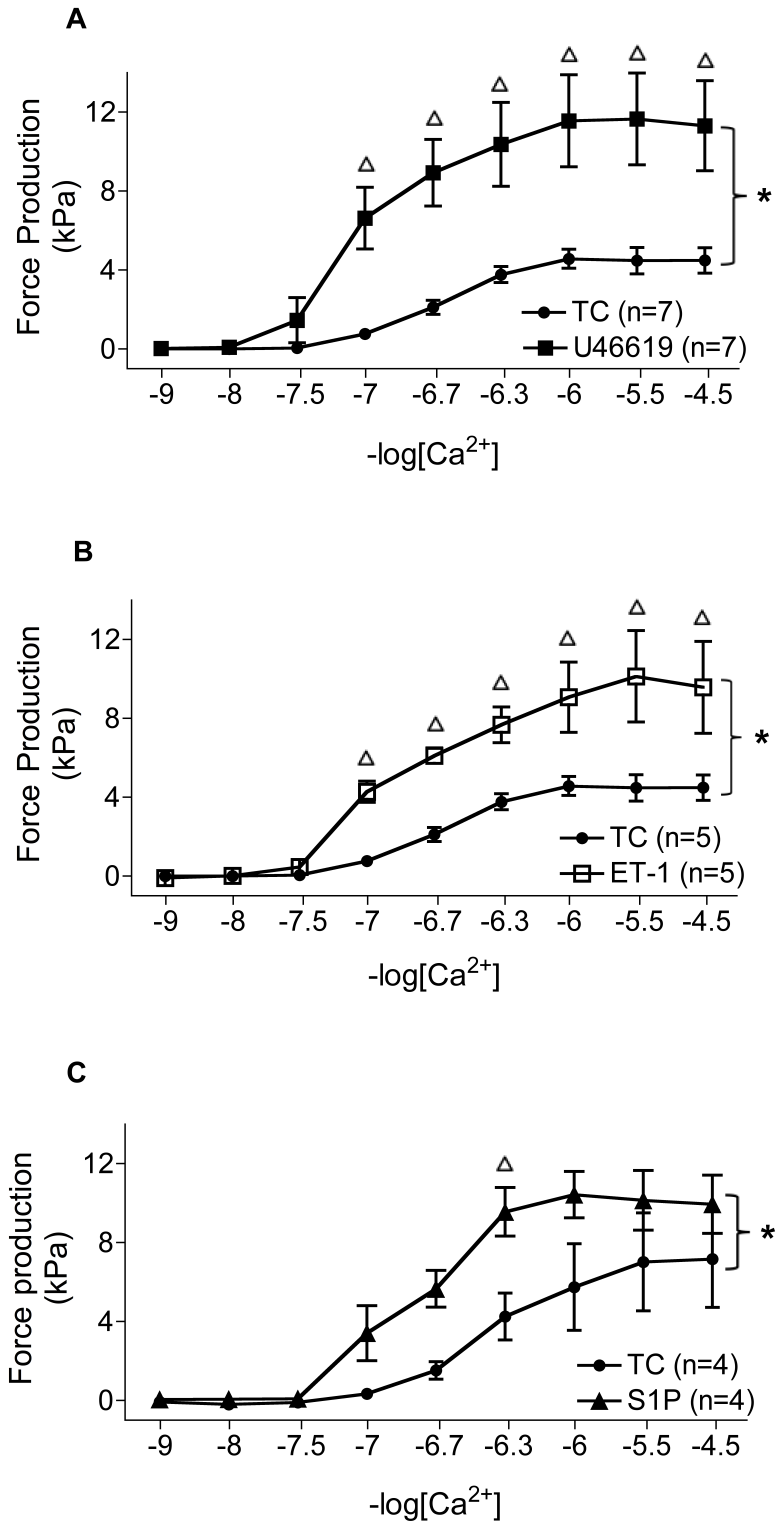


Figure 3.6: Summary force data in the presence of the G protein-coupled agonists, U46619, ET-1 and S1P, in permeabilised myometrial arteries. A, B and C: Mean (\pm SEM) maximal force productions (kPa) at each pCa in the presence of the G protein-coupled agonists U46619, endothelin-1 (ET-1) or sphingosine-1-phosphate (S1P), respectively. TC: time control, ie. increasing Ca^{2+} concentrations in the absence of a G protein-coupled agonist. * Statistical difference relative to TC. Δ Statistical difference relative to TC at the specific pCa.

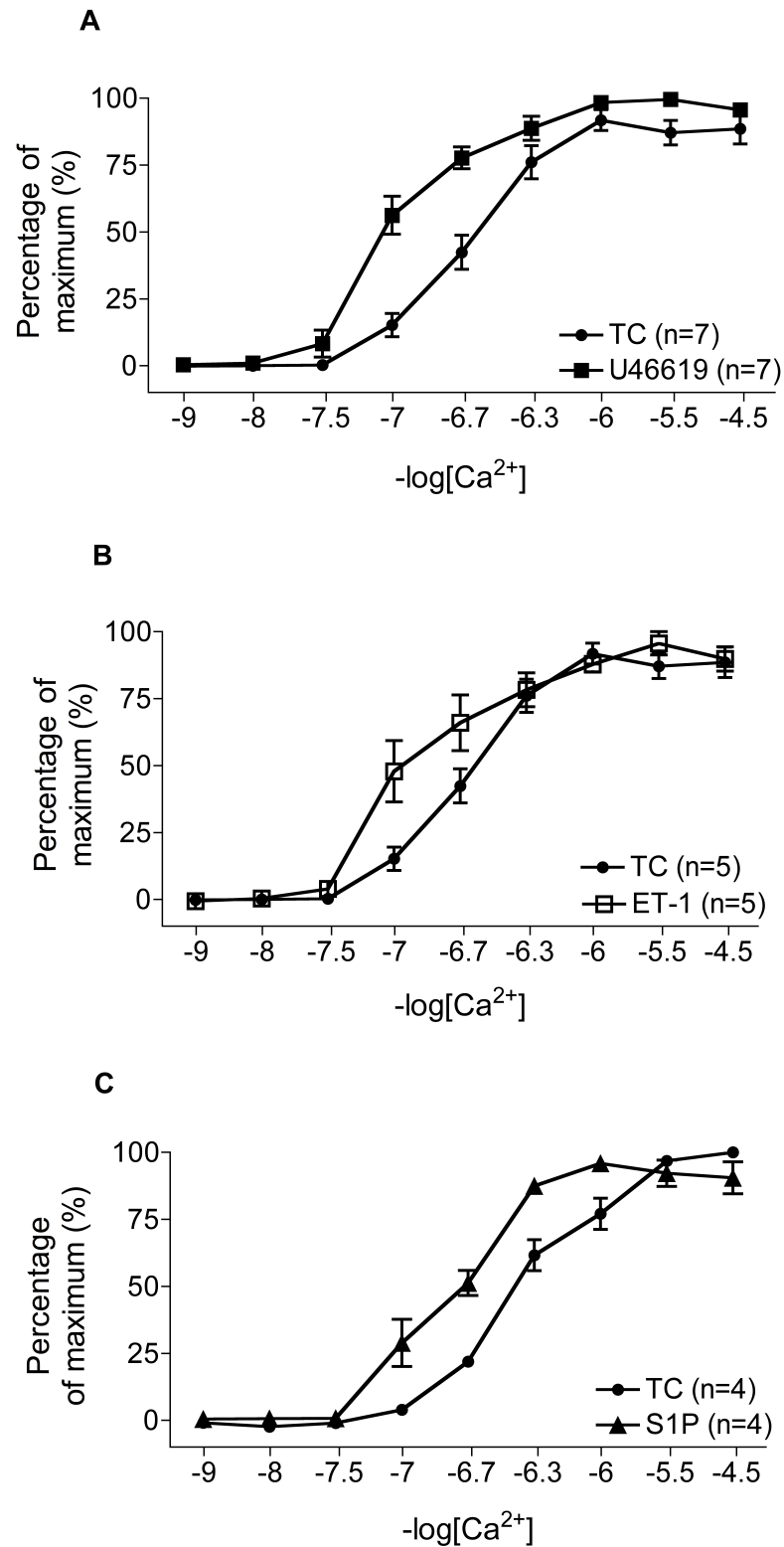


Figure 3.7: Normalised force data in the presence of the G protein-coupled agonists, U46619, ET-1 and S1P, in permeabilised myometrial arteries. A, B and C: Mean (\pm SEM) force developed at each pCa expressed as a percentage of the maximal force developed in each individual group over a range of nine pCa (9 – 4.5), in the presence of U46619, ET-1 or S1P, respectively.

3.5.2. Assessment of agonist effects on Ca^{2+} -dependent constriction of human placental arteries

Similarly to the experiments carried out in human MA, agonist-mediated Ca^{2+} -sensitisation was assessed in human PA in the same conditions. Figure 3.8 shows original tracings of the increasing force development in four individual permeabilised PA during the assessment of agonist effects on pCa-induced contractions. The first artery was exposed to increasing pCa amounts alone (time control, TC) and contraction started in pCa 6.7 (Figure 3.8A). The second artery was exposed to the same increasing pCa in the presence of 10^{-6} M U46619 (Figure 3.8B). Finally, the third and fourth arteries were exposed to the same increasing pCa with 10^{-8} M ET-1 or 10^{-5} M S1P (Figures 3.8C and 3.8D, respectively). In the presence of U46619, the force produced was greater over the same range of pCa (Figure 3.8B). ET-1 and S1P also seem to have induced greater tension development than pCa alone, although it appears, to a lesser extent than with U46616 (Figures 3.8C and 3.8D). In the presence of U46619, ET-1 and S1P, constrictions started at a lower $[\text{Ca}^{2+}]_i$ (pCa 7) compared to the TC.

In this set of results, the U46619 and ET-1 data sets were all paired to the TC data sets. However, I wished to verify that these TC (pCa alone) were not different from the TC + BSA data sets, which were paired to the pCa curves ran in the presence of S1P. No statistical comparison could be carried out between the two TC (TC and TC + BSA) due to the small n number for the TC + BSA data sets ($n = 2$). However, the mean EC_{50} values between these two conditions seemed similar ($\log \text{EC}_{50(\text{TC})} = -6.26$ vs. $\log \text{EC}_{50(\text{TC+BSA})} = -6.28$), indicating that BSA may not have affected the magnitude of constrictions nor sensitivities to Ca^{2+} in PA. As a result, only one original raw tracing representing the TC was shown in Figure 3.8.

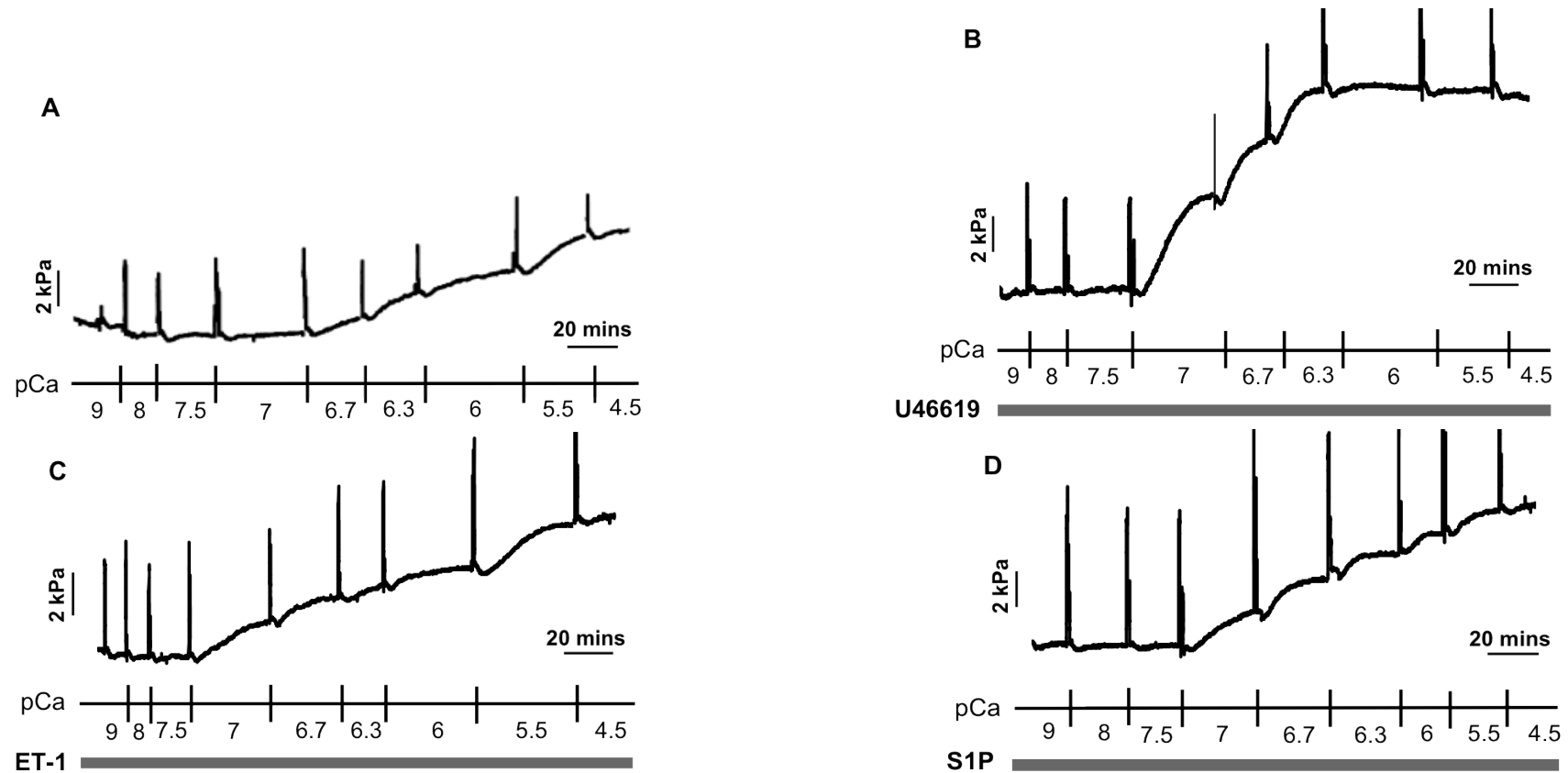


Figure 3.8: Original raw tracings of agonist effects on Ca^{2+} -dependent force of four individual permeabilised placental arteries. A: pCa curve showing arterial responses in a first artery to increasing $[\text{Ca}^{2+}]_i$ (pCa 9 - 4.5). B, C and D: pCa curves showing arterial responses to increasing $[\text{Ca}^{2+}]_i$ (pCa 9 - 4.5) in a second, third and fourth artery, in the presence of 10^{-6} M U46619, 10^{-8} M ET-1 or 10^{-5} M S1P, respectively.

Figure 3.9 shows the group comparisons of maximal constrictions (kPa) of pCa curves in the three experimental conditions in human PA. In the presence of U46619, the tension development was greater than that observed in TC (pCa alone) ($n = 8$, Figure 3.9A). Similarly, ET-1 induced greater constrictions compared to TC ($n = 9$, Figure 3.9B). Note that for the TC - S1P (Figure 3.9C), statistical comparison could not be carried out as there are only $n = 2$, however these preliminary data seem to indicate that S1P induces greater constriction over the range of pCa when compared to TC.

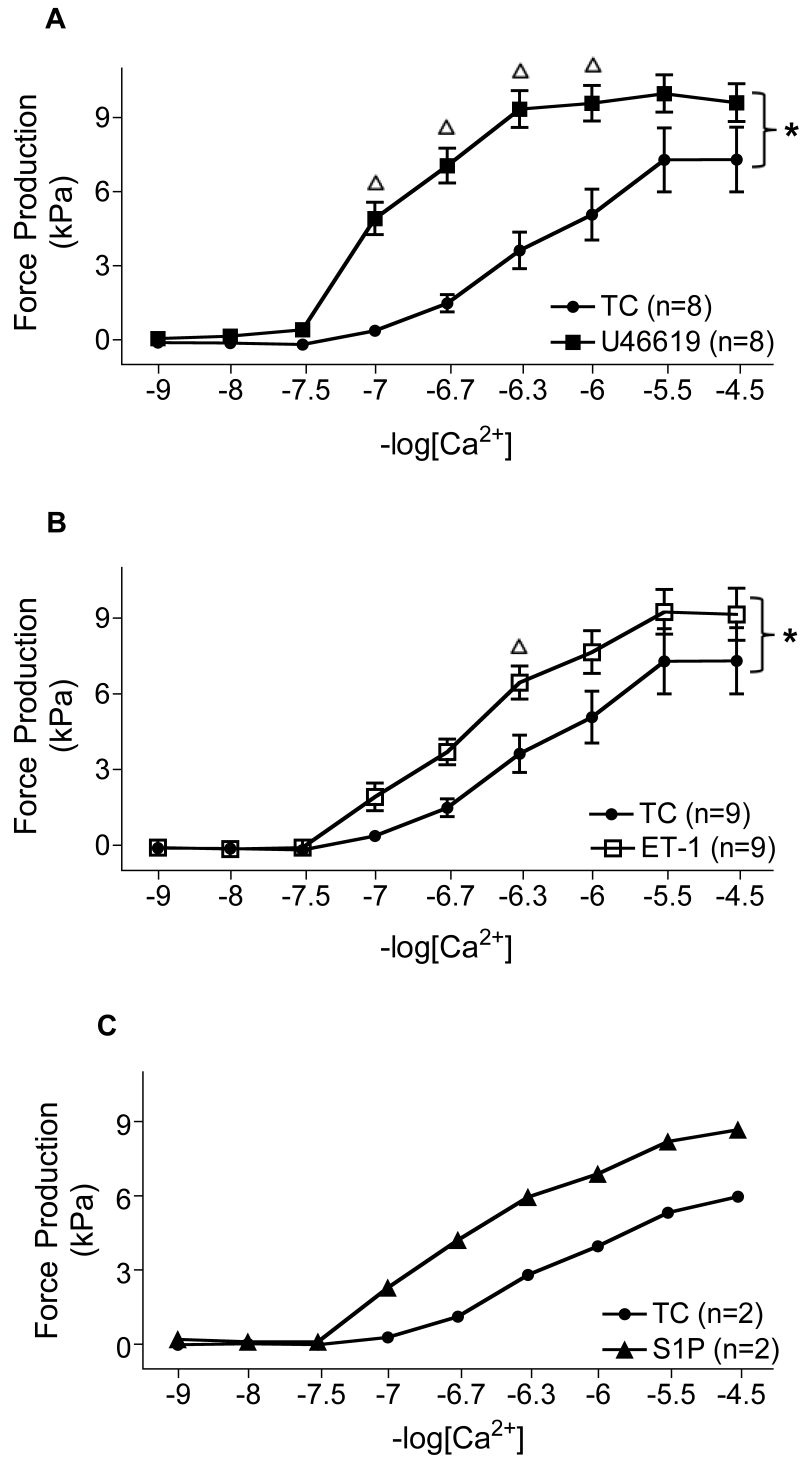


Figure 3.9: Summary of force production (kPa) in the presence of the G protein-coupled agonists, U46619, ET-1 and S1P, in permeabilised placental arteries. A, B and C: Mean (\pm SEM) maximal force productions (kPa) at each pCa in the presence of the G protein-coupled agonists U46619, endothelin-1 (ET-1) or sphingosine-1-phosphate (S1P), respectively. TC: time control, ie. increasing Ca²⁺ concentrations in the absence of a G protein-coupled agonist. * Statistical difference relative to TC. Δ Statistical difference relative to TC at the specific pCa.

Figure 3.10 displays the mean forces developed at each pCa expressed as a percentage of maximal force developed in each experimental condition. The curves representing U46619, ET-1 and S1P data sets are shifted to the left, which is indicative of an increase in sensitivity to Ca^{2+} induced by these agonists (Figures 3.10A, 3.10B and 3.10C, respectively). This notion is supported by lower EC_{50} values for the U46619 data ($\log \text{EC}_{50 (\text{TC})} = -6.26 \pm 0.05$ and $\log \text{EC}_{50 (\text{U46619})} = -6.97 \pm 0.06$) and the ET-1 data sets ($\log \text{EC}_{50 (\text{TC})} = -6.26 \pm 0.05$ and $\log \text{EC}_{50 (\text{ET-1})} = -6.63 \pm 0.1$). Statistical analysis was not carried out on the data sets for S1P, as the n number ($n = 2$) was too small. However, the average $\log \text{EC}_{50}$ is lower in the presence of S1P compared to the TC condition ($\log \text{EC}_{50 (\text{TC})} = -6.26$ and $\log \text{EC}_{50 (\text{S1P})} = -6.64$).

Consequently, these results illustrate that agonists mediated the enhancement of Ca^{2+} -dependent force, and a sensitisation to that activating Ca^{2+} , in permeabilised human placental arteries.

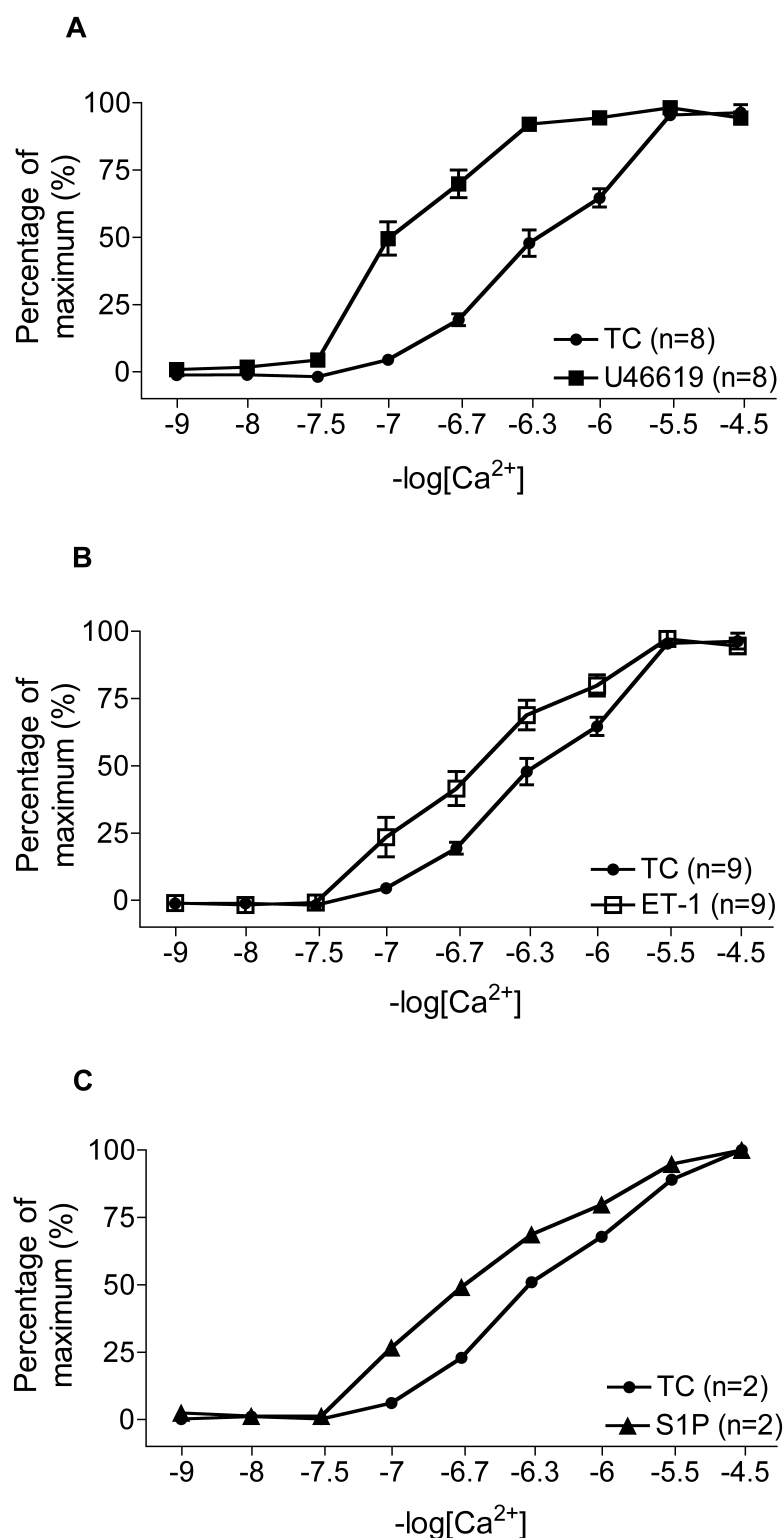


Figure 3.10: Normalised force data in the presence of the G protein-coupled agonists, U46619, ET-1 and S1P, in permeabilised placental arteries. A, B and C: Mean (\pm SEM) force developed at each pCa expressed as a percentage of the maximal force developed in each individual group over a range of pCa (9 – 4.5), in the presence of U46619, ET-1 or S1P, respectively.

3.6. Comparison of Ca^{2+} -dependent contractions between myometrial and placental arteries

Having established that the enhancement of Ca^{2+} -dependent force production, and Ca^{2+} -sensitisation, in both human MA and PA arteries are effected by a variety of G protein-coupled agonists, a comparison of the data between these artery types was subsequently investigated. As presented in Section 3.4, MA and PA constricted with a similar magnitude to a range of activating $[\text{Ca}^{2+}]_i$ (Figure 3.4A). However, MA displayed a greater sensitivity to the same $[\text{Ca}^{2+}]_i$ as compared to PA. This was illustrated by the shift to the left of the MA pCa-force curve relative to PA and by their different EC_{50} values (Figure 3.4B). It was of interest, therefore, to extend such assessment by comparing the responses to the same range of pCa in the presence of three G protein-coupled agonists, U46619, ET-1 and S1P, between these two artery types.

Figure 3.11 illustrates the comparisons of maximal constriction (kPa) of pCa curves in the four experimental conditions (TC, U46619, ET-1 and S1P) in human permeabilised MA and PA. The maximal force developed over the range of pCa alone (9 – 4.5) is similar in the two artery types (Figures 3.11A and 3.4A). Likewise, the forces produced with U46619 over the same range of pCa were not different between MA and PA (Figure 3.11B). However, as illustrated in Figure 3.11C, MA constricted more to the same range of pCa compared to PA in the presence of ET-1. Statistical analysis was not carried out to compare the contractile effect of S1P between these two arteries due to the small n number of S1P data sets in PA. Nonetheless it appears that MA constricted considerably more than PA, particularly over pCa 6.7 to 3.5 (Figure 3.11D).

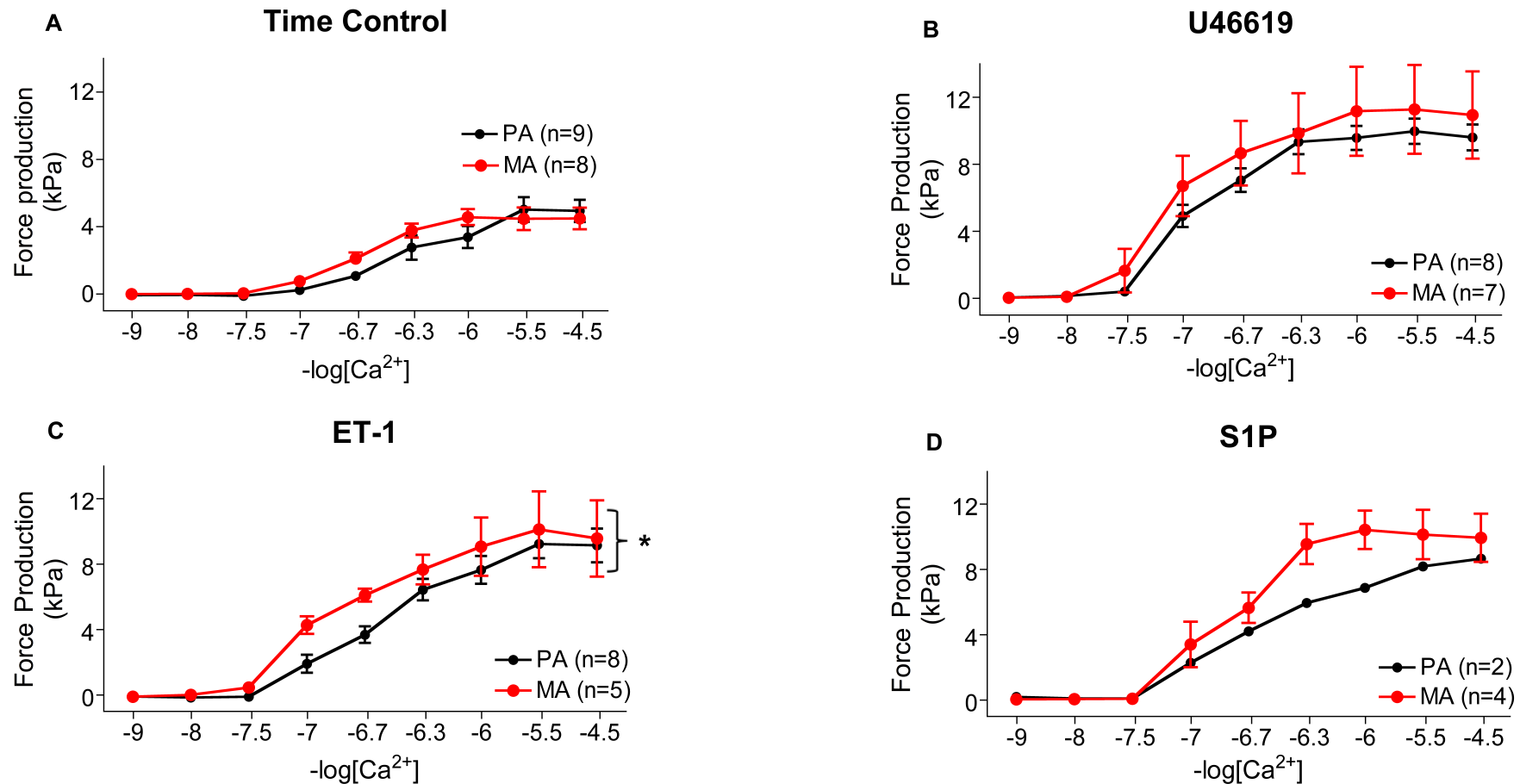


Figure 3.11: Comparison of force production in the presence and absence of the three G protein-coupled agonists in permeabilised myometrial (MA) and placental (PA) arteries. A: Mean (\pm SEM) maximal force productions (kPa) at each pCa in MA versus PA (Time Control). B, C and D: Mean maximal force productions (kPa) at each pCa between MA and PA in the presence of the G protein-coupled agonists U46619, endothelin-1 (ET-1) or sphingosine-1-phosphate (S1P), respectively. * Statistical difference relative to TC.

Figure 3.12 shows the mean tension developed at each pCa expressed as a percentage of the maximal force produced in each experimental condition in MA versus PA. As mentioned previously, the curve representing MA data is shifted to the left and force production started at a higher pCa (pCa 7) compared to PA data, indicating a greater sensitivity to Ca^{2+} in MA (Figures 3.12A and 3.4B). This was supported by the lower EC_{50} in MA compared to PA. Conversely, as illustrated in Figure 3.12B, there seem to be no differences between the curves representing MA and PA data sets in the presence of U46619 over the range of pCa, indicating that these two artery types display a similar sensitivity to Ca^{2+} in the presence of this agonist. This notion was maintained by the similar EC_{50} values in these two artery types ($\log \text{EC}_{50 (\text{PA})} = -6.97 \pm 0.06$ and $\log \text{EC}_{50 (\text{MA})} = -7.05 \pm 0.05$). In the presence of ET-1, the curve representing MA data is shifted to the left compared to that representing PA data, possibly illustrating a greater sensitivity to Ca^{2+} in MA compared to PA in the presence of this agonist (Figure 3.12C). Surprisingly, the EC_{50} values did not support this notion, as no difference was detected between EC_{50} values from these two artery types ($\log \text{EC}_{50 (\text{PA})} = -6.63 \pm 0.10$ and $\log \text{EC}_{50 (\text{MA})} = -6.93 \pm 0.15$). Finally, in the presence of S1P, the curves representing MA and PA data sets seem to differ, but only at pCa 6.3 and 6 (Figure 3.12D). This may be due to the small n number for PA.

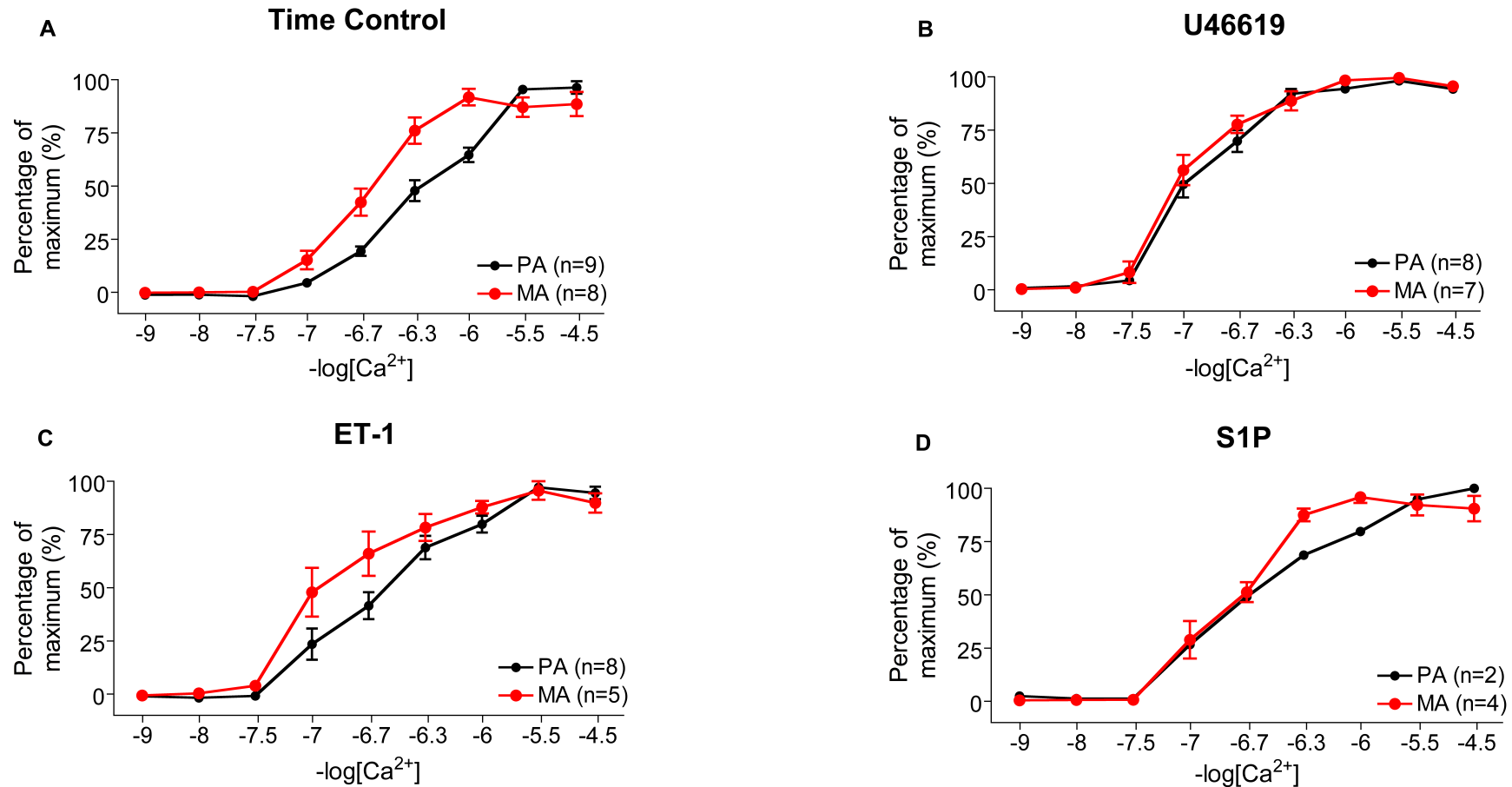


Figure 3.12: Comparison of normalised force data in the presence of three G protein-coupled agonists in permeabilised myometrial (MA) and placental (PA) arteries. A: Mean (\pm SEM) force developed at each pCa expressed as a percentage of the maximal force developed in PA versus MA. This data has been displayed before in Fig 3.2B. B, C and D: Mean force developed at each pCa expressed as a percentage of the maximal force developed between PA and MA arteries in the presence of U46619, ET-1 or S1P, respectively.

3.7. Discussion

The intention of this study was to establish whether agonist-mediated enhancement of Ca^{2+} -dependent constrictions occurred in human myometrial (MA) and placental (PA) arteries and whether there were any differences between the two artery types. Vessels were permeabilised with α -toxin, which facilitated discreet control of the activating Ca^{2+} concentrations acting on the myofilaments while retaining the G protein-coupled mechanisms. The key findings were that the sensitivity of MA and PA to activating Ca^{2+} differed, G protein-coupled agonists enhanced the Ca^{2+} -dependent force production in both MA and PA and that this was also associated in each case with increased Ca^{2+} -sensitisation of force.

To date, there are few reports of Ca^{2+} -dependent force production in α -toxin permeabilised human MA and PA (Wareing et al., 2005b, Hemmings et al., 2006). In both studies, sub-maximal constrictions produced by pCa 6.7 were further enhanced by exposure to either U46619 or S1P. However, there have been no reports of the development of force and sensitisation over incremental Ca^{2+} concentrations in these human arteries in the presence or absence of agonists.

Methods previously used to achieve selective permeabilisation (i.e. permeabilisation of the cell's plasma membrane only), have included the use of glycerol, which was the first detergent used for such purposes in skeletal (striated) and vascular (smooth) muscles (Filo et al., 1965), the application of high voltage discharges to bovine adrenal medullary chromaffin cells (Baker and Knight, 1981) and rat pancreatic islet cells (Stutchfield and Howell, 1984) and the use of non-ionic detergents such as digitonin, saponin or β -escin (a saponine derivative) on human cavernosa cells, guinea pig taenia cecae SM fibres or SM cells, respectively (Endo et al., 1982, Muraki et al., 1992, Krall et al., 1988). A permeabilising agent should create permanent 'leaks' but digitonin and saponin fail to achieve stable permeabilisation of erythrocytes with pores apparently resealing (Duncan and Schlegel, 1975). Additionally, permeabilisation using these detergents, although cheap and apparently technically simple, was unreliable due to the narrow range of concentrations, incubation time and temperature over which the desired selective effect could be obtained (Dunn and Holz, 1983, Baker et al., 1985). These different permeabilising agents also all induced leakage of intracellular key contractile proteins to the extracellular environment, which meant that, in (vascular) smooth

muscle preparations, the medium required supplementation with CaM to activate MLCK and to try and minimise the decrease in constrictions observed with successive contraction-relaxation cycles (Endo et al., 1982, Filo et al., 1965, Muraki et al., 1992). Moreover, with the exception of β -escin, permeabilisation with these agents did not retain the G protein-coupled receptor function, which for the purposes of this study was essential (Endo et al., 1982, Muraki et al., 1992).

The benefits of *Staphylococcal* α -toxin as a membrane permeabilising agent were initially established in 1985 (Ahnert-Hilger et al., 1985). *Staphylococcal* α -toxin pores are comprised of homogenous ring-structured hexamers forming pores of apparently uniform size with a functional diameter of around 1.5 nm regardless of the dose of toxin applied (Fussle et al., 1981, Bhakdi and Tranum-Jensen, 1991). It is therefore highly unlikely that the α -toxin molecules ($M_r = 34,000$) would permeate such pores and gain access to the cell interior with secondary effects on intracellular membranes or protein function (Bhakdi and Tranum-Jensen, 1991). The small size of the α -toxin pores also allows retention of intracellular molecules of ~ 4 kDa whilst maintaining G protein coupled receptor-mediated signalling integrity (Bhakdi et al., 1984, Bhakdi and Tranum-Jensen, 1984, Kitazawa et al., 1989). Kitazawa et al. (1989) showed that constrictions in α -toxin-permeabilised guinea pig SM strips were induced by activation of G protein-coupled α -adrenergic and muscarinic receptors by their respective agonists, phenylephrine and carbachol. Additionally, these constrictions were dependent on GTP, as addition of GDP β S inhibited them; this indicated that functionality of G protein-coupled receptors was retained following α -toxin permeabilisation (Kitazawa et al., 1989). Thus, this toxin was the permeabilising agent of choice for this study.

In the current study, addition of high K^+ (60 mM KPSS) induced greater constrictions in *intact* MA compared to PA. This difference was, however, not apparent in permeabilised arteries exposed to pCa 4.5. Thus, one possibility for the lower constrictions observed with KPSS in *intact* PA compared to MA may be differences in the sensitivity of myofilaments to the activating Ca^{2+} . It is commonly accepted that an increase in $[Ca^{2+}]_i$ induces constriction of VSMC via binding of Ca^{2+} to calmodulin, activation of MLCK and phosphorylation of the regulatory MLC_{20} (Somlyo, 1985, Somlyo and Himpens, 1989). Conversely, the activity of myosin light chain phosphatase (MLCP), and a decrease in $[Ca^{2+}]_i$ reducing MLCK activity, leads to MLC_{20} dephosphorylation and relaxation of VSMC (Hartshorne et al., 1998). Thus, the

ratio of kinase to phosphatase activities determines the contractile/relaxatory state of a VSMC. In this study, human MA and PA both displayed concentration-dependent increases in force production over a range of pCa and although, no differences in maximal force production were observed between MA and PA constricted with incremental $[Ca^{2+}]$ (pCa 9 - 4.5), MA contracted at lower $[Ca^{2+}]_i$ (pCa 7) compared to PA (pCa 6.7), suggesting a higher sensitivity of the regulatory contractile mechanism to Ca^{2+} in arteries from the myometrium compared to those from the placenta.

Work in different SM types offer possible explanations for this difference in sensitivities between PA and MA. It has been suggested, for example, that differences in Ca^{2+} sensitivity may occur between two SM 'types' (phasic versus tonic) and these may be due, at least in part, to differences in the MCLK/MLCP activity ratios between different SM types (Somlyo and Himpens, 1989). Thus, the observed differences in sensitivity between PA and MA may be due to differing MLCK/MLCP activity ratios within their respective VSMC. Studies have also shown that Ca^{2+} sensitivity of MLCK may be regulated by phosphorylation at its Ser-512 by protein kinase A (PKA), which leads to a reduction in the affinity of MLCK to Ca^{2+} /CaM by around 10 fold (Conti and Adelstein, 1981). Increased levels of PKA in PA would therefore induce a reduction in sensitivity to Ca^{2+} compared to MA, as was observed in this study. Levels of PKA have not yet been assessed in the two artery types. It has also been suggested that the inhibitory phosphorylation of MLCK is a result of an autoinhibitory mechanism mediated by Ca^{2+} -dependent phosphorylation of MLCK by the calmodulin kinase II (CaMKII) (Tansey et al., 1994, Miller et al., 1983). Higher levels of activated CaMKII in PA could thus result in MLCK inhibition and lowered sensitivity to Ca^{2+} . Finally, it is thought that SMC contain two isoforms of MLCK, long and small. The long MLCK has a higher binding affinity for actin filaments compared to the short MLCK, stimulating greater actinomyosin filaments interaction (Blue EK et al., 2002, Smith et al., 2002). Therefore, MA may have a different ratio of long MLCK/short MLCK than PA, explaining the greater Ca^{2+} -sensitivity in MA. Assessment of expression levels of short MLCK was carried out in MA and PA and no differences in expression were observed between the two artery types (see Chapter 4). Thus, further assessment of the long MLCK expression and post-translational modifications may be useful for future studies in order to elucidate if there was any role for MLCK in the difference of sensitisation to Ca^{2+} between the two artery types.

Only a handful of studies have assessed agonist-induced Ca^{2+} -sensitisation in human MA and PA and then at just one supra-basal $[\text{Ca}^{2+}]_i$ level (Hemmings et al., 2006, Hemmings, 2006, Wareing et al., 2005b). In the present study, human MA and PA developed a sensitisation to Ca^{2+} in the presence of three G protein-coupled agonists, U46619, ET-1 and S1P. It is commonly accepted that Ca^{2+} -sensitisation occurs via activation of heterotrimeric G proteins ($G_{\alpha q}$ or/and $G_{\alpha 12/13}$), stimulation of the small GTPase RhoA and subsequent activation of RhoA-associated kinase (ROK) (Gong et al., 1996, Sward et al., 2000). This sequence of events is entirely dependent upon presence of GTP, as activation of RhoA occurs by catalysis of the GDP–RhoA complex to GTP–RhoA and subsequent translocation of the complex to the G protein-coupled receptors on the plasma membrane (Fujihara et al., 1997, Gong et al., 1997). GTP was therefore added to each experiment with G protein-coupled agonists, as it is a small molecule, which may have escaped the cell during the permeabilisation procedure.

As discussed in the Introduction (Chapter 1, Section 1.4.2.2), the involvement of the RhoA/ROK pathway in Ca^{2+} -sensitisation has been reported previously. Wareing et al. (2005) have shown that inhibition of ROKI/II by Y27632 abolished Ca^{2+} -sensitisation in both permeabilised MA and PA. Similarly, S1P-induced Ca^{2+} -sensitisation in these two artery types was shown to be dependent upon activation of the RhoA/ROK pathway, as addition of Y27632 also inhibited the phenomenon (Hudson et al., 2007, Hemmings et al., 2006). This ROK-dependent mechanism was also reported in animal models showing that ROK stimulation, by RhoA, contributed to Ca^{2+} -sensitisation (Somlyo and Somlyo, 2000, Sward et al., 2000). In this study, the sensitisation to Ca^{2+} , observed in the presence of U46619 and S1P, was therefore likely mediated via stimulation of ROK following activation of RhoA. No prior studies have assessed the Ca^{2+} -sensitising effects of ET-1 in human arteries, however it is known that ET-1 induces vasoconstriction via activation of the G protein-coupled $\text{ET}_{A/B}$ receptors (Kublickiene et al., 2000). This could have therefore subsequently activated the RhoA/ROK pathway via $G_{\alpha q}$ and/or $G_{\alpha 12/13}$ and induce Ca^{2+} -sensitisation.

Inhibition of MLCP by thiophosphorylation of the targeting subunit, MYPT1, at Thr-696 by ROK has been shown in many SM preparations to induce sensitisation of the myofilaments to Ca^{2+} (Kitazawa et al., 1991a, Kitazawa et al., 1989, Sward et al., 2000, Ito et al., 2003, Kimura et al., 1996). Moreover, the small 17 kDa peptide, CPI-17, has also been shown to induce MLCP inhibition following its activation by phosphorylation

by both ROK and PKC (Koyama et al., 2000, Eto et al., 1995). Given the likely role of ROK in Ca^{2+} -sensitisation in this study's human arteries, this phenomenon may result at least in part from inhibition of MLCP.

The difference in sensitivity observed in the presence of Ca^{2+} alone between the two artery types did not persist in the presence of the G protein-coupled agonists U46619. There are a number of possible explanations for these findings. The structure of a vessel wall is an important factor in determining its mechanical performance. Studies have shown that in contrast to human MA, PA lack a distinct IEL, the barrier separating the vascular EC and SMC layers (Sweeney et al., 2006b). The physiological significance of this is not known. One may speculate, however, that the absence of the IEL may facilitate permeation of blood-borne circulating factors, such as contractile agonists, reaching the SMC quicker and affecting contractility of these arteries. This may have increased the ability of PA to sensitise to Ca^{2+} in the presence of U46619, allowing PA to 'catch up' with the sensitising abilities of MA. In this case, therefore, the sensitisation to Ca^{2+} was greater in PA than MA. However, it is unclear why similar observations were not made in the presence of ET-1. Conversely, compared to MA, PA have been shown to have a thicker medial layer with the SMC separated by considerable amounts of ECM (Sweeney et al., 2006b). The force development may therefore be reduced in PA compared to MA in the presence of ET-1. Finally, there is good evidence to suggest that the umbilical and placental vessels are not innervated, as immunohistological and neurohistochemical studies have shown the absence of adrenergic and cholinergic nerves. Contraction of these vessels can therefore not be elicited via neurotransmitters, such as noradrenaline and norepinephrine (Reilly and Russell, 1977, Fox and Khong, 1990). As a compensatory mechanism, PA may have evolved to give other circulating factors, such as U46619, and their signalling pathways a more prominent role. This may have explained the similar responses in MA and PA to U46619, but not the observed difference in contractile responses in the presence of ET-1.

Another explanation for these observations may be that the expression levels of key contractile proteins involved in Ca^{2+} -sensitisation, such as RhoA/ROK or CPI-17 differ between MA and PA. Upon addition of U46619, higher levels of (activated) RhoA/ROK may induce greater Ca^{2+} -sensitisation in PA compared to MA via inhibition of MLCP. Similarly, increased CPI-17 expression and phosphorylation thereof may induce greater phosphatase inhibition in PA compared to MA, thus allowing greater

sensitivity to Ca^{2+} in the former artery type. However, as will be described in the following chapter (Chapter 4), levels of CPI-17 did not differ between MA and PA. The differences in sensitisation capacity with U46619 may more likely be due to differences in activity of the signalling proteins involved. It is yet unclear, why ET-1 did not induce similar responses between MA and PA. This discrepancy in constriction and sensitisation to thromboxane A_2 and ET-1 illustrates a paucity in our knowledge of the pathways activated by these contractile factors in human arteries, highlighting a need for further investigation of the specific signalling mechanisms activated by these agonists.

This study has highlighted several novel findings in human myometrial and placental arteries. First, the pattern of Ca^{2+} -sensitivity of the myofilaments and agonist-dependent modulation of Ca^{2+} -sensitisation in both artery types. Second, that placental arteries display a lower sensitivity to Ca^{2+} alone as compared to myometrial arteries. Third, that this difference in Ca^{2+} -sensitivity does not persist in the presence of the thromboxane A_2 agonist. It was important to establish these phenomena as a prelude to subsequently investigating the actions of vasorelaxants on myofilament activation in each artery type.

Chapter 4

Ca²⁺-desensitisation in human myometrial and placental arteries

4.1. Introduction

Vascular smooth muscle (VSM) tone is primarily controlled by a balance between the levels of myosin light chain kinase (MLCK) and myosin light chain phosphatase (MLCP) activity and the ensuing phosphorylation state of the myosin light chains (MLC₂₀) (Somlyo and Somlyo, 1994). There are several signalling mechanisms modulating Ca²⁺ availability and Ca²⁺ sensitivity of the contractile apparatus, which also regulate the contractile and relaxatory responses of VSM to receptor agonists.

Studies in human placental and uterine vessels have shown that U46619-, ET-1- and S1P-induced contractile responses increased in the presence of nitric oxide synthase (NOS) inhibitors, such as L-NNA or L-NAME, highlighting these agonists' role in regulating vascular tone (Myatt et al., 1992, Fried and Liu, 1994, Hemmings et al., 2006, Hudson et al., 2007, Kublickiene et al., 2000). The importance of these G protein-coupled receptor proteins was further emphasised following reports of increased expression of these peptides in both placental and myometrial vasculatures in pathological pregnancies, which were characterised by raised vascular resistance (Wetzka et al., 1997, Faxen et al., 2000, Agapitov and Haynes, 2002, Hla, 2004, Wang et al., 2008, Dunlap et al., 2010). Concurrently, the development of endothelial dysfunction is thought to exacerbate the observed increase in resistance. Studies reported impaired endothelial-dependent relaxations in the vasculatures from women with pre-eclampsia, gestational diabetes, hypertension and fetal growth restriction, even though increased levels of the NO and/or aberrant (hyper-) activity of NOS were observed (McCarthy et al., 1993, Knock and Poston, 1996, Knock et al., 1997, VanWijk et al., 2000, Wareing et al., 2005a, Wareing et al., 2006d, Myers et al., 2006).

The potent vasodilator action of the cGMP/PKG pathway has been ascribed to a decrease in [Ca²⁺]_i through the activation of multiple Ca²⁺ lowering mechanisms (Lincoln and Cornwell, 1993) and/or to a decrease in Ca²⁺ sensitivity of myofilaments, referred to as Ca²⁺-desensitisation (Wu et al., 1996, Gong et al., 1996, Wooldridge et al., 2004, Lee et al., 1997).

This phenomenon has been fairly well established in animal tissues (vascular and non-vascular) and reported in human bronchial tissues (Yoshii et al., 1999). However, no studies have thus far presented this phenomenon in human arteries from the

myometrium and placenta. Nishimura and van Breemen (1989) first showed that desensitisation to Ca^{2+} could be mediated by cGMP. They studied rat mesenteric arteries, permeabilised with *Staphylococcal* α -toxin with $[\text{Ca}^{2+}]_i$ held constant by Ca^{2+} EGTA buffer (Nishimura and van Breemen, 1989). A similar role for cGMP was also reported in Triton X-100 skinned smooth muscle (SM) fibres from guinea-pig taenia coli and rat mesenteric arteries (Pfitzer et al., 1984, Pfitzer et al., 1986). Relaxations of the α -toxin-permeabilised rabbit ileum SM, which occurred at constant $[\text{Ca}^{2+}]_i$, were shown to result from activation of PKG isoform I (PKGI) by 8-br-cGMP. This also correlated with an increase in MLCP activity inducing increased MLC_{20} dephosphorylation (Wu et al., 1996). Further studies in intact swine carotid arteries and VSMC reported that stimulation of the cGMP/PKG axis induced an increase in MLCP activity, possibly via leucine-zipper interactions between PKGI and the targeting subunit of MLCP, MYPT1 (Surks et al., 1999, Etter et al., 2001, Bolz et al., 2003, Bonnevier et al., 2004, Khatri et al., 2001, Lu et al., 2008). These studies therefore inferred that Ca^{2+} -desensitisation occurred via activation of PKG and subsequent increase in MLCP activity to induce SM relaxation at constant $[\text{Ca}^{2+}]_i$. It is noteworthy, however, that the NO-cGMP/PKG axis has been suggested to induce relaxation via interaction with other proteins including HSP20 (Rembold et al., 2000), telokin (Wu et al., 1998) or CPI-17 (Bonnevier and Arner, 2004). There are no studies identifying expression of these proteins in arteries from the human placenta and/or uterus.

Thus far, assessment of the desensitisation mechanisms in permeabilised SM in the literature has been performed at individual concentrations of activating Ca^{2+} alone, such as pCa 6.0, 6.1, 6.2, 6.3, 6.5, 6.7 or pCa 4.5 in animal tissues (vascular and non-vascular) (Lee et al., 1997, Bonnevier and Arner, 2004, Choudhury et al., 2004, Wu et al., 1996, Wu et al., 1998, Shcherbakova et al., 2010), but not in tissues that were pre-sensitised to $[\text{Ca}^{2+}]$ using G protein-coupled receptor agonists.

Thus this body of work sought to determine:

- (i) whether the phenomenon of Ca^{2+} -desensitisation occurred in human myometrial and placental arteries constricted to $[\text{Ca}^{2+}]$ alone or to $[\text{Ca}^{2+}]$ in the presence of G-protein coupled receptor agonists U46619, ET-1 or S1P,
- (ii) if the extent of cGMP-induced relaxations differed between these two artery types,
- (iii) whether Ca^{2+} -desensitisation was mediated via the cGMP/PKG/MLCP axis,

- (iv) if PKGI α , HSP20, telokin, MYPT1 or CPI-17 are expressed in MA and PA and if expression levels of these proteins differed between the two artery types.

4.2. Materials and methods

4.2.1. *Experimental protocol*

4.2.1.1. *Functional Experiments*

Protocol 1: α -toxin-permeabilised human MA and PA were constricted with pCa 4.5 then exposed to pCa 9. Arteries were bathed in a sub-maximal Ca^{2+} solution (pCa 6.7 + 2 μM GTP) followed by addition of 1 μM U46619 to each artery. Finally, 8-br-cGMP was added to three individual arteries (10 μM , 1 μM or 0.1 μM) and the fourth artery was used as a time-matched control. The effect of 8-br-cGMP was monitored for 30 - 35 minutes until plateau.

Protocol 2: α -toxin-permeabilised human MA and PA were exposed to pCa 4.5, then pCa 9. Arteries were then bathed in pCa 6.7 + 2 μM GTP with the addition of either of two G protein-coupled agonists, 10^{-8} M ET-1 or 10^{-5} M S1P in two individual arteries. S1P was added with 0.1 % BSA. 10 μM 8-br-cGMP was subsequently added to one artery from each condition and the second artery was used as a time-matched control. The time control for S1P also contained 0.1 % BSA. The effect of 8-br-cGMP was monitored for 30 - 35 minutes until plateau.

Protocol 3: α -toxin-permeabilised MA and PA were exposed to the high-calcium solution (pCa 4.5) and left until plateau was reached at 15 minutes. 10 μM 8-bromo-cGMP (8-br-cGMP) was subsequently added and its effect was monitored until plateau at 30 - 35 minutes.

Protocol 4: α -toxin-permeabilised human MA and PA were incubated with a 30 μl droplet of either pCa 9 (lowest $[\text{Ca}^{2+}]$) or 1 μM calyculin A, a protein phosphatase PP1 and PP2A inhibitor. Incubations were carried out for 90 - 100 minutes (time to plateau). Next, arteries were exposed to pCa 4.5 until plateau. Finally, 10 μM 8-br-cGMP was added to the bath and the effect monitored for at 30 - 35 minutes.

These functional experiments lasted 5 - 6 hours following normalisation of the vessels.

4.2.1.2. *Immuno Blotting*

Expression levels of six proteins were assessed MA and PA: PKGI α , HSP20, telokin, MLCK, MYPT1, CPI-17. For detailed methodology, see Chapter 2, Section 2.6 and Table 2.5.

4.2.2. *Statistics*

The effect of 8-br-cGMP was compared between MA and PA for each separate experimental protocol using two-way ANOVA followed by Bonferroni post-hoc test.

Constrictions induced by pCa 6.7 were compared to total constrictions (pCa 6.7 + 2 μ M GTP + agonist) for each experimental condition (U46619, ET-1 and S1P), using paired Student *t-test*.

Unpaired *t-tests* were used to compare:

- Total constrictions between experimental conditions (U46619, ET-1 and S1P) for each artery type (MA and PA),
- Constrictions induced by pCa 6.7 and total constrictions between MA and PA for each experimental condition (U46619, ET-1 and S1P),
- $T_{1/2}$ (time to half maximal relaxation) between MA and PA for each protocol.

Protein expression levels of MA and PA were compared between the two artery types using unpaired *t-test*.

4.3. Ca^{2+} -desensitisation in arteries pre-sensitised with G-protein-coupled agonists

Initial assessment of Ca^{2+} -desensitisation was carried out using the non-hydrolysable cGMP mimetic, 8-br-cGMP, in arteries pre-sensitised with G-protein-coupled receptor agonist U46619.

4.3.1. Assessment of Ca^{2+} -desensitisation in U46619-induced Ca^{2+} -sensitised human myometrial and placental arteries

Figure 4.1 shows the response to 10 μM 8-br-cGMP of an individual permeabilised MA pre-sensitised with U46619. Figure 4.1A illustrates a first MA exposed to pCa 6.7, which induced a sub-maximal contraction to 36 % of the previous pCa 4.5 constriction. Subsequent addition of 1 μM U46619 led to a further pronounced tonic contraction at the same $[\text{Ca}^{2+}]$ to 61 % of the pCa 4.5 constriction. This indicated Ca^{2+} -sensitisation. Figure 4.1B illustrates a second MA constricted with pCa 6.7. The sub-maximal constriction elicited reached 22 % of the previous pCa 4.5 constriction. Subsequent sensitisation to Ca^{2+} was induced by 1 μM U46619 and the constriction elicited was 117 % of the pCa 4.5 constriction. Subsequent addition of 10 μM 8-br-cGMP induced a sustained relaxation of 69 % of total contraction. Figure 4.1A illustrates the time-matched MA, which showed no decrease.

Figure 4.2 shows the effect of 10 μM 8-br-cGMP on an individual permeabilised PA pre-sensitised with the thromboxane mimetic, U46619. Figure 4.2A illustrates a PA exposed to pCa 6.7, which induced a sub-maximal contraction to 31 % of the previous pCa 4.5 contraction. Subsequent addition of 1 μM U46619 led to further development of force at the same $[\text{Ca}^{2+}]$ to 55 % of the pCa 4.5 constriction. This indicated Ca^{2+} -sensitisation of force. Figure 4.2B illustrates a second PA constricted with pCa 6.7, which induced 23 % of the pCa 4.5 constriction. 1 μM U46619 sensitised the artery to Ca^{2+} , which reached 69 % of pCa 4.5. Subsequent addition of 10 μM 8-br-cGMP induced a relaxation of 37 % from total contraction. The time-matched PA, on the other hand, maintained the constriction throughout (Figure 4.2A).

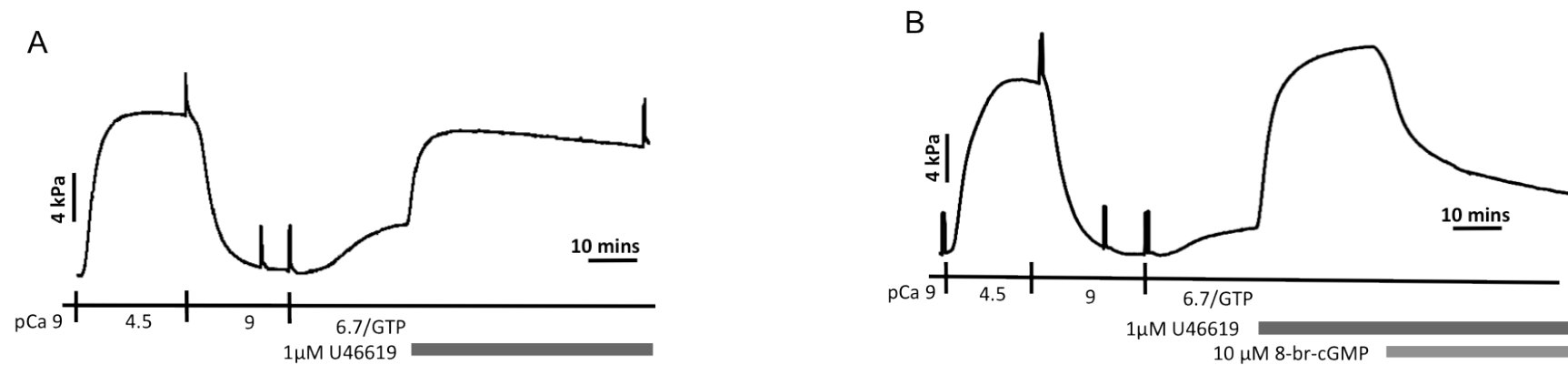


Figure 4.1: Effect of 10 μ M 8-bromo-cGMP in two individual permeabilised myometrial arteries pre-sensitised with U46619. A: First artery exposed to pCa 4.5, pCa 9, sub-maximal Ca^{2+} solution pCa 6.7 + 1 μ M U46619. B: Second artery exposed to pCa 4.5, pCa 9, sub-maximal Ca^{2+} solution pCa 6.7 + 1 μ M U46619 and 10 μ M 8-bromo-cGMP.

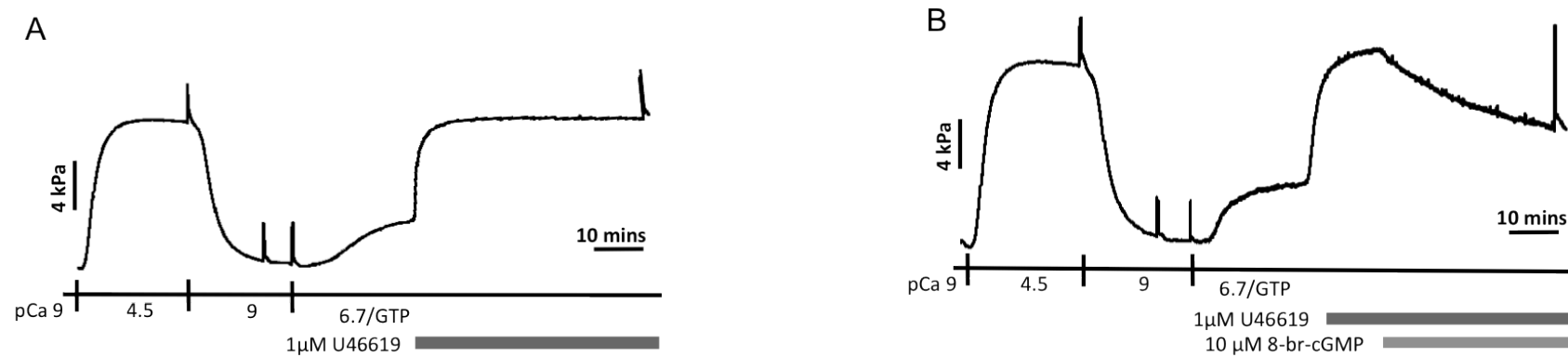


Figure 4.2: Effect of 10 μ M 8-bromo-cGMP in two individual permeabilised placental arteries pre-sensitised with U46619. A: First artery exposed to pCa 4.5, pCa 9, sub-maximal Ca^{2+} solution pCa 6.7 + 1 μ M U46619. B: Second artery exposed to pCa 4.5, pCa 9, sub-maximal Ca^{2+} solution pCa 6.7 + 1 μ M U46619 and 10 μ M 8-bromo-cGMP.

Figure 4.3 shows the group mean \pm SEM relaxation responses over 30 minutes to 10 μ M 8-br-cGMP in MA and PA. Total constrictions to pCa6.7/U46619 did not differ between the two artery types (MA: 7.52 ± 0.81 kPa, $n = 8$ versus PA: 7.45 ± 1.05 kPa, $n = 6$). Both artery types relaxed in the presence of the cGMP mimetic compared to their respective time controls (TC) (MA_{cGMP}: 69.5 ± 5.12 % versus MA_{TC}: 6.65 ± 1.71 %, $n = 8$ and PA_{cGMP}: 49.3 ± 6.04 % versus PA_{TC}: 8.95 ± 2.79 %, $n = 6$). The mean maximal relaxation to 10 μ M 8-br-cGMP in MA was greater than that in PA. Additionally, the rate of relaxation in MA was greater than that in PA, as highlighted by the time at which half the maximal relaxation ($t_{1/2}$) was reached. MA reached its $t_{1/2}$ at 4.67 ± 0.43 minutes, whilst PA reached it at 10.2 ± 1.02 minutes.

Thus, Ca^{2+} -desensitisation occurred in human MA and PA, which were constricted and sensitised to Ca^{2+} via activation of the G protein-coupled pathway by the thromboxane mimetic, U46619. In addition, MA displayed a greater relaxatory capacity in the presence of the cGMP mimetic compared to PA. The difference in their time(s) to maximal relaxation may highlight a difference in sensitivity to cGMP between these two artery types.

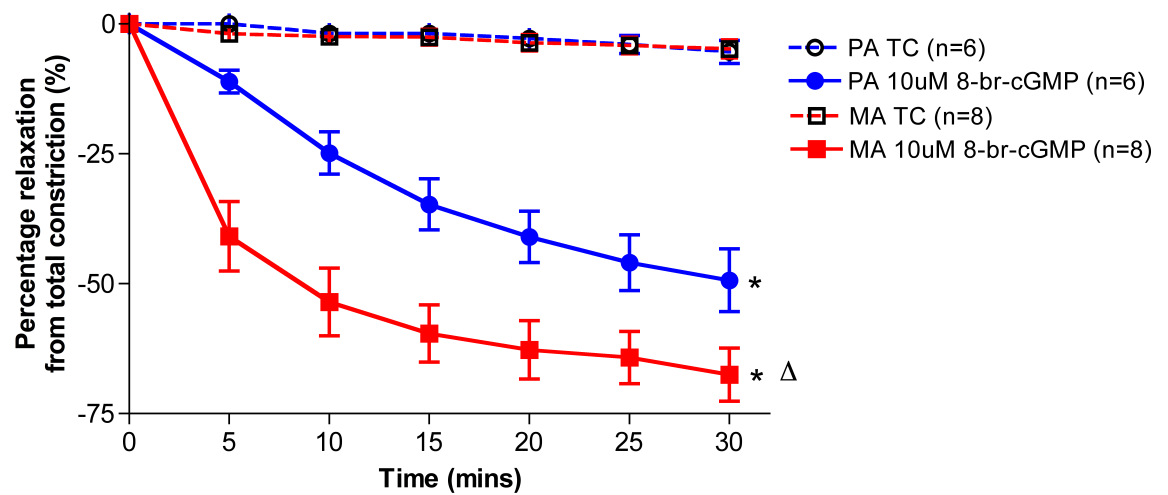


Figure 4.3: Summary data of responses induced by 10 μ M 8-bromo-cGMP in human myometrial and placental arteries pre-sensitised to the thromboxane mimetic, U46619. Responses to 10 μ M 8-br-cGMP are expressed as percentages of the total constriction obtained with pCa 6.7 + 1 μ M U46619 over a 30 minute time period. MA: Myometrial Arteries, PA: Placental Arteries, TC: Time Control. * Statistical difference relative to TC. Δ Statistical difference relative to PA.

Next, it was of interest to assess whether there was a concentration-dependency of this possible difference between MA and PA. Therefore, given the prominent action already witnessed at 10 μM , the influence of 8-br-cGMP at lower concentrations (1 μM and 0.1 μM) in arteries pre-sensitised to Ca^{2+} with U46619 was determined.

Figures 4.4A and 4.4B illustrate the mean \pm SEM responses to 1 μM and 0.1 μM 8-br-cGMP, respectively, in human permeabilised MA and PA pre-sensitised to Ca^{2+} with 1 μM U46619. Total constrictions (pCa 6.7 + 1 μM U46619) were similar in MA and PA (PA: 7.49 ± 1.55 kPa, $n = 6$ versus MA: 8.02 ± 1.01 kPa, $n = 7$). As illustrated in Figure 4.4A, both artery types relaxed to 1 μM 8-br-cGMP relative to their time controls (TC) (MA_{cGMP}: 62.6 ± 5.38 % versus MA_{TC}: 8.51 ± 2.25 %, $n = 7$ and PA_{cGMP}: 48.9 ± 3.63 % versus PA_{TC}: 6.58 ± 2.03 %, $n = 6$). Moreover, the mean maximal relaxation was greater in MA compared to PA, as was the rate of relaxation. $T_{1/2}$ in MA was 6.28 ± 0.95 minutes compared to 11.2 ± 0.55 minutes in PA.

Similarly, as illustrated in Figure 4.4B, 0.1 μM 8-br-cGMP relaxed both human MA and PA (MA_{cGMP}: 48.3 ± 6.02 %, $n = 7$ versus MA_{TC}: 8.51 ± 2.25 % and PA_{cGMP}: 33.1 ± 4.82 %, $n = 6$ versus PA_{TC}: 6.58 ± 2.03 %) and the mean maximal relaxation was greater in MA compared to PA. In addition, the rate of relaxation was also greater as MA reached its $t_{1/2}$ at 10.0 ± 1.21 minutes compared to 15.7 ± 0.44 minutes for PA.

Table 4.1 summarises the relaxatory responses induced by 8-br-cGMP in the human MA and PA. The differences in mean maximal relaxations and $t_{1/2}$ observed between MA and PA were consistent throughout the range of concentrations of 8-br-cGMP used. These results highlight that myofilament sensitivities to cGMP may be greater in human MA compared to PA.

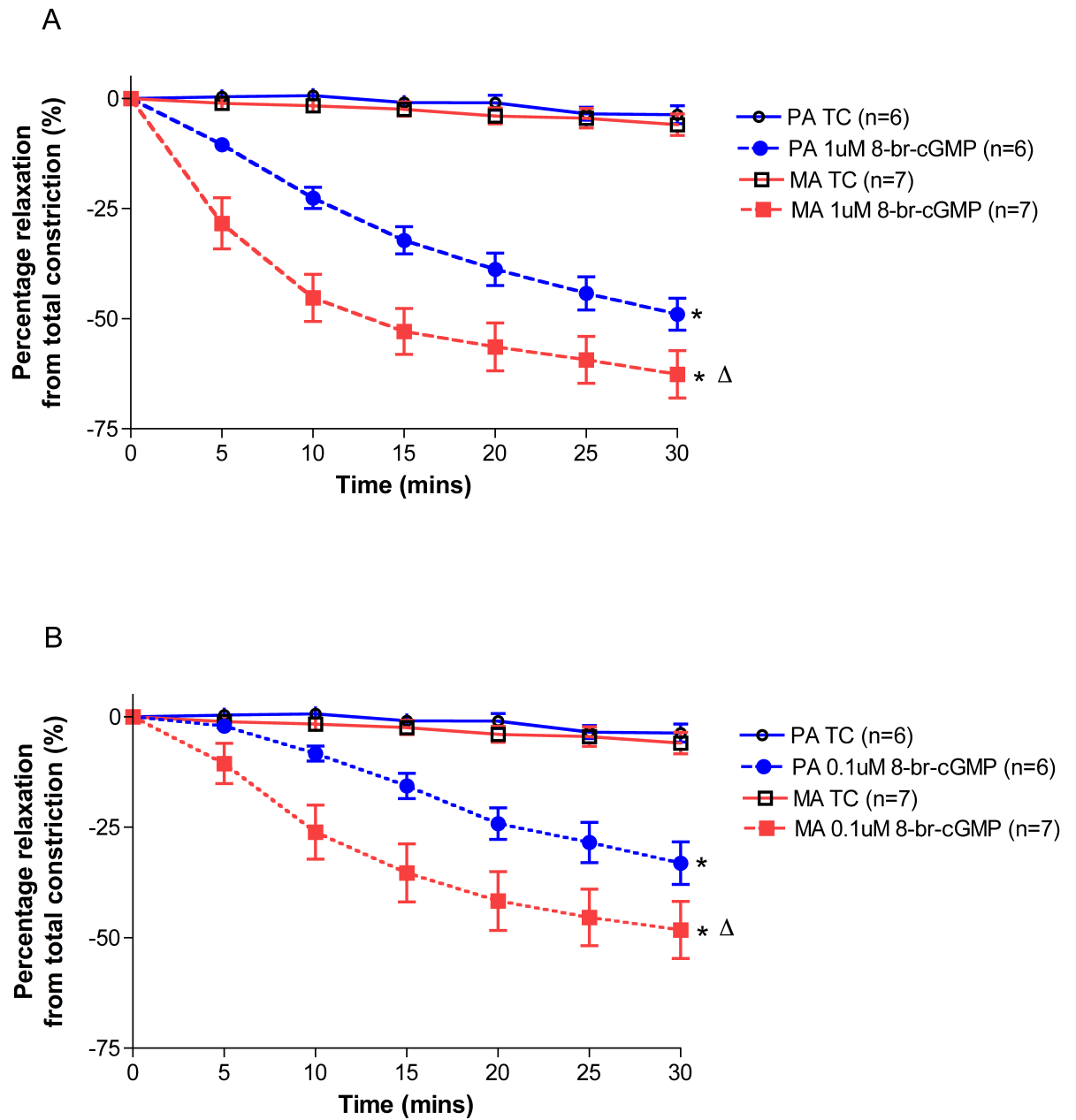


Figure 4.4: Summary data of responses induced by 1 μ M and 0.1 μ M 8-bromo-cGMP responses in human myometrial and placental arteries pre-sensitised to the thromboxane mimetic, U46619. Responses to 1 μ M 8-br-cGMP (A) and 0.1 μ M 8-br-cGMP (B) are expressed as percentages of the total constriction obtained with pCa 6.7 + 1 μ M U46619 over a 30 minute time period. MA: Myometrial Arteries, PA: Placental Arteries, TC: Time Control. * Statistical difference relative to TC. Δ Statistical difference relative to PA.

Table 4.1: Summary of maximal relaxations induced by 8-bromo-cGMP and time to reach half maximal relaxation in human permeabilised myometrial and placental arteries.

Myometrial Arteries			Placental Arteries	
Concentration of 8-br-cGMP (μM)	Maximal relaxation from constriction (%)	$T_{1/2}$ (minutes)	Maximal relaxation from constriction (%)	$T_{1/2}$ (minutes)
10	$69.5 \pm 5.12^*$	$4.67 \pm 0.43^{\blacksquare}$	49.3 ± 6.04	10.2 ± 1.02
1	$62.6 \pm 4.58^*$	$6.28 \pm 0.95^{\blacksquare\bullet}$	48.9 ± 3.63	11.2 ± 0.55
0.1	$48.3 \pm 6.02^{*\diamond}$	$10.0 \pm 1.21^{\blacksquare\diamond}$	$33.1 \pm 4.82^{\diamond}$	$15.7 \pm 0.44^{\diamond}$

* Statistical difference relative to the maximal relaxation in human placental arteries.

\blacksquare Statistical difference relative to the $t_{1/2}$ in human placental arteries. \diamond Statistical difference relative to 10 μM and 1 μM 8-br-cGMP. \bullet Statistical difference relative to 10 μM .

4.3.2. Ca^{2+} -desensitisation in human permeabilised myometrial and placental arteries pre-sensitised to Ca^{2+} with the G protein-coupled agonists, endothelin-1 or sphingosine-1-phosphate

Similarly to the assessment of Ca^{2+} -sensitisation using a variety of G protein-coupled agonists as described in Chapter 3, it was important to rigorously establish whether the phenomenon of Ca^{2+} -desensitisation in human permeabilised MA and PA also occurred when arteries were pre-sensitised with agonists other than U46619. To this effect, this set of experiments examined cGMP-induced Ca^{2+} -desensitisation in human arteries sensitised to Ca^{2+} by the G protein-coupled agonists, ET-1 or S1P.

Similarly to the previous experimental design using U46619 as the Ca^{2+} -sensitising agent, permeabilised MA and PA were constricted with submaximal $[\text{Ca}^{2+}]$ (pCa 6.7), after which addition of 10^{-8} M ET-1 or 10^{-5} M S1P induced further development of force, thus illustrating a sensitisation to the activating Ca^{2+} . Finally, addition of 10 μM 8-br-cGMP induced relaxations in both ET-1-induced- and S1P-induced pre-sensitised PA and MA. A time-matched artery for each condition was used as a control.

Figures 4.5 and 4.6 illustrate the mean \pm SEM responses to 10 μM 8-br-cGMP in human permeabilised MA and PA following pre-sensitisation to Ca^{2+} by 10^{-8} M ET-1 or 10^{-5} M S1P, respectively. The time controls (TC) used in experiments with S1P contained 0.1 % BSA (as described in Chapter 3). These were not different from the TC for ET-1-sensitised MA and PA.

As illustrated in Figure 4.5, MA and PA pre-sensitised with ET-1 relaxed to 8-br-cGMP compared to their TC (MA_{cGMP} : 84.5 ± 5.60 % versus MA_{TC} : 14.6 ± 3.59 %, $n = 7$ and PA_{cGMP} : 63.5 ± 6.89 % versus PA_{TC} : 7.19 ± 3.93 %, $n = 6$). Similarly, as demonstrated in Figure 4.6, the cGMP mimetic induced a relaxation in S1P-induced-sensitised MA and PA compared to their TC (MA_{cGMP} : 108.1 ± 7.18 %, versus MA_{TC} : 10.2 ± 9.23 %, $n = 4$ and PA_{cGMP} : 82.0 ± 1.70 % versus PA_{TC} : 9.69 ± 7.44 %, $n = 4$).

The mean maximal relaxations to 8-br-cGMP were greater in MA compared to PA following ET-1-induced Ca^{2+} -sensitisation. Importantly, the rate of relaxation was also greater in MA compared to PA. Indeed, $t_{1/2}$ in MA was reached at 6.04 ± 0.77 minutes compared to 11.8 ± 1.73 minutes in PA. In S1P-sensitised arteries, 8-br-cGMP induced

a greater relaxation in MA compared to PA and their respective rates of relaxation also differed. The $t_{1/2}$ in MA was reached at 3.57 ± 0.16 minutes, whilst that in PA was reached at 7.28 ± 0.87 minutes.

These results indicated therefore, that PKG-mediated Ca^{2+} -desensitisation occurs in human arteries when pre-sensitised to Ca^{2+} with a variety of agonists and that the desensitisation responses are greater in MA than PA.

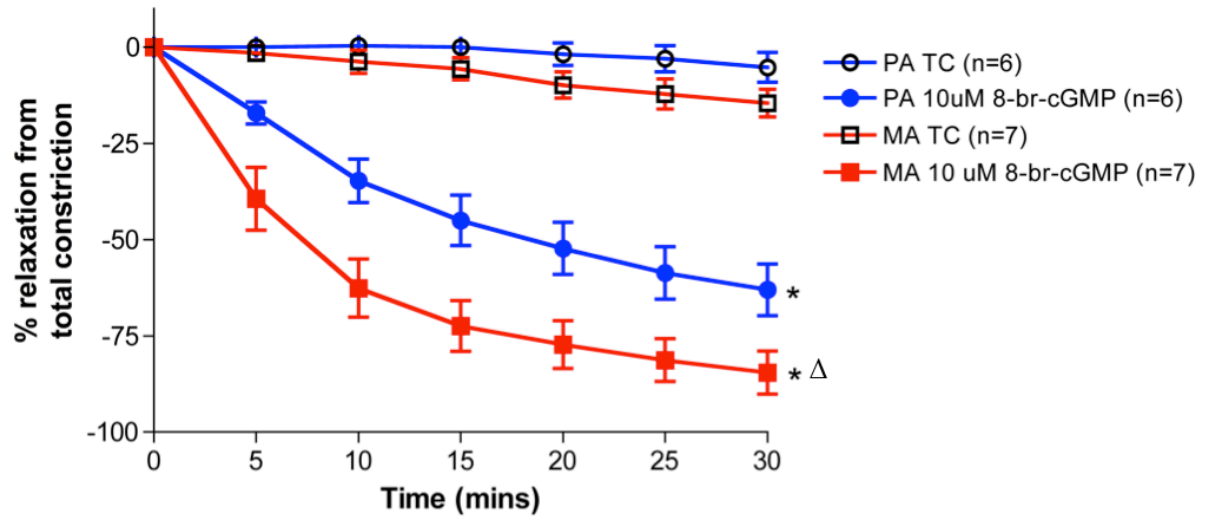


Figure 4.5: Summary data of 8-bromo-cGMP-induced responses in human myometrial and placental arteries pre-sensitised to the G protein-coupled agonist endothelin-1. Responses to 10 μ M 8-br-cGMP are expressed as percentages of the total constriction obtained with pCa 6.7 + 10^{-8} M ET-1 over a 30 minute time period. MA: Myometrial Arteries, PA: Placental Arteries, TC: Time Control. * Statistical difference relative to TC. Δ Statistical difference relative to PA.

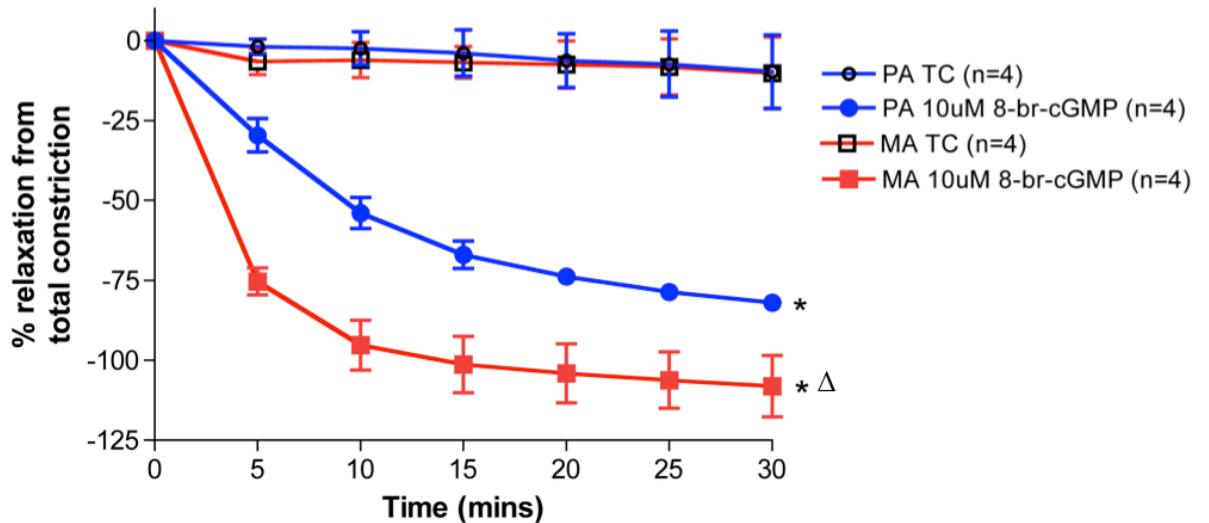


Figure 4.6: Summary data of 8-bromo-cGMP-induced responses in human myometrial and placental arteries pre-sensitized to the G protein-coupled agonist sphingosine-1-phosphate. Responses to 10 μ M 8-br-cGMP are expressed as percentages of the total constriction obtained with pCa 6.7 + 10^{-5} M S1P over a 30 minute time period. MA: Myometrial Arteries, PA: Placental Arteries, TC: Time Control. * Statistical difference relative to TC. Δ Statistical difference relative to PA.

Table 4.2 compares the constrictions induced by pCa 6.7 and the three G protein-coupled agonists, U46619, ET-1 and S1P in human permeabilised MA and PA. All three agonists induced sensitisation to Ca^{2+} , as evidenced by the increase in force production by U46619, ET-1 and S1P in both MA and PA.

Table 4.2: Constrictions induced by submaximal $[Ca^{2+}]$ and the G protein-coupled agonists, U46619, endothelin-1 and sphingosine-1-phosphate in human placental and myometrial arteries.

Myometrial Arteries					Placental Arteries			
Agonist	pCa 6.7-induced constriction (kPa)	Total Constriction (pCa 6.7 + agonist)	pCa 6.7-induced constriction relative to pCa 4.5 constriction (%)	Agonist-sensitised constriction relative to pCa 4.5 constriction (%)	pCa 6.7-induced constriction (kPa)	Total Constriction (kPa)	pCa 6.7-induced constriction relative to pCa 4.5 constriction (%)	Agonist-sensitised constriction relative to pCa 4.5 constriction (%)
U46619	1.81 ± 0.78	7.44 ± 1.05 ♦	35.3 ± 3.12	73.8 ± 1.12 Δ	2.51 ± 0.33	7.52 ± 0.81 ♦	32.3 ± 1.62	57.8 ± 2.42
ET-1	1.75 ± 0.49	5.06 ± 1.64 ♦	21.2 ± 3.67	53.3 ± 8.37	2.31 ± 0.43	6.08 ± 0.61 ♦	24.1 ± 2.96	56.4 ± 8.28
S1P	1.18 ± 0.22	2.31 ± 0.34 Δ *■	21.7 ± 2.51	24.1 ± 6.50 *■	1.65 ± 0.33	3.11 ± 0.58 Δ *■	24.3 ± 3.63	15.8 ± 4.73 *■

♦ Significant difference relative to the constriction induced by pCa 6.7 for each respective agonist and artery type. * Significant difference relative to U46619. ■ Significant difference relative to ET-1. Δ Significant difference relative to placental arteries.

4.4. Assessment of protein kinase G-mediated Ca^{2+} -desensitisation in human arteries pre-constricted with pCa 4.5

It was of interest to establish whether the phenomenon of cGMP-induced Ca^{2+} -desensitisation also occurred in human arteries constricted with activating Ca^{2+} in the absence of agonist stimulation. Ca^{2+} alone, or Ca^{2+} in the presence of constrictor agonists, activate, in part, alternative intracellular pathways acting on the myofilaments. This, in turn, may influence the ability of PKG to counteract the constrictions.

Figure 4.7 shows original tracings of two individual permeabilised human MA exposed to maximal $[\text{Ca}^{2+}]$ (pCa 4.5) alone (A) or to pCa 4.5 followed by 10 μM 8-br-cGMP (B). Figure 4.7A demonstrates that pCa 4.5 induced a sustained constriction over time. Figure 4.7B illustrates that 10 μM 8-br-cGMP induced a relaxatory response in the pre-constricted MA. The relaxation reached plateau after 20 minutes and represented, in this artery, 69 % of the previously induced constriction.

Figure 4.8 shows original raw tracings of two individual permeabilised human PA exposed to similar conditions. Figure 4.8A demonstrates that pCa 4.5 alone induced a sustained constriction over time. Figure 4.8B illustrates that addition of 8-br-cGMP induced a relaxation in the pCa 4.5 pre-constricted artery, which reached a plateau at 30 minutes. In this artery, the relaxation was 20 % of the pCa 4.5-induced constriction.

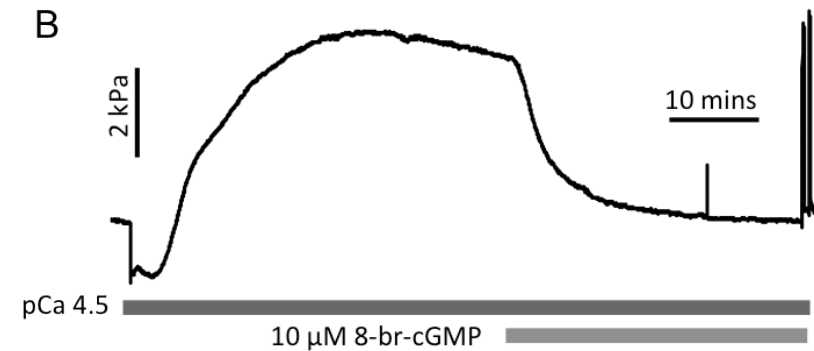
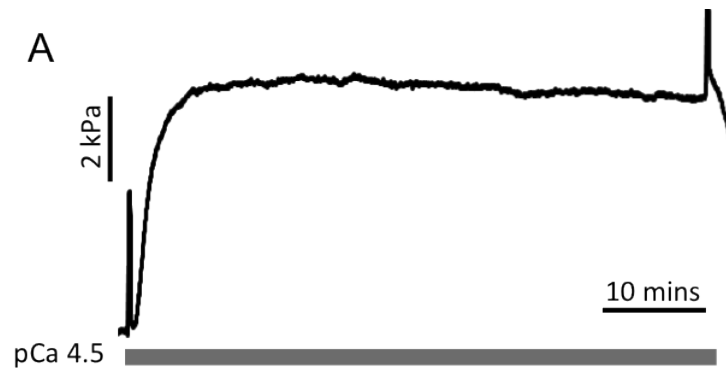


Figure 4.7: Original raw tracings of the relaxatory effects of 10 μ M 8-bromo-cGMP in two individual human myometrial arteries. A: Time-matched control exposed to pCa 4.5 shows a persistent contraction with only a slight drift downwards over time. B: A second artery, exposed to pCa 4.5, then to 10 μ M 8-bromo-cGMP, caused a large relaxation.

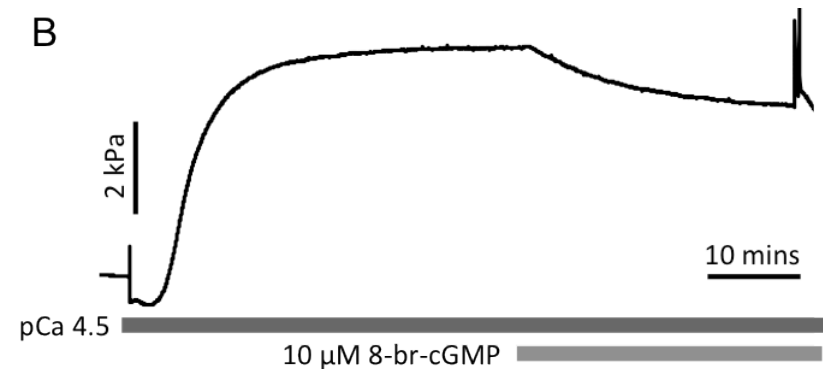
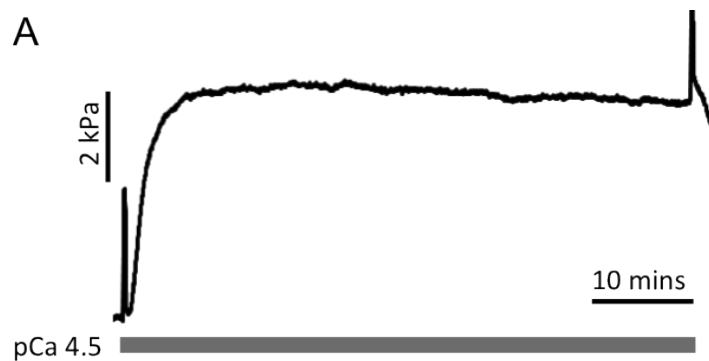


Figure 4.8: Original raw tracings of the relaxatory effect of 10 μ M 8-bromo-cGMP in two individual human placental arteries. A: Time-matched control exposed to pCa 4.5 shows a persistent contraction with only a slight drift downwards over time. B: Second artery, exposed to pCa 4.5, then to 10 μ M 8-bromo-cGMP, caused a small relaxation.

Figure 4.9 shows the group mean \pm SEM relaxation responses over 30 minutes to 10 μ M 8-br-cGMP in MA and PA, expressed as a percentage of their previous pCa 4.5 constrictions. Both MA and PA relaxed in the presence of the vasodilator compared to their respective time controls (TC) (MA_{cGMP}: 49.2 \pm 9.71 % versus MA_{TC}: 7.42 \pm 2.71 %, n = 7 and PA_{cGMP}: 22.8 \pm 6.6 % versus PA_{TC}: 4.81 \pm 2.11 %, n = 6). Time-matched responses in MA and PA were similar; therefore in the presented graph the data were pulled together in one time control data set. The mean maximal relaxation to 8-br-cGMP in MA was greater than that in PA. Additionally, the rate of relaxation was faster in MA compared to PA, which was highlighted by a shorter t_{1/2} in MA compared to PA (MA_{t(1/2)}: 3.66 \pm 0.19 minutes, n = 7 versus PA_{t(1/2)}: 8.75 \pm 0.33 minutes, n = 6).

As reported earlier, cGMP-induced mean maximal relaxations were greater in MA compared to PA, when arteries were pre-sensitised with the G protein-coupled agonists and when arteries were constricted to maximal [Ca²⁺]. Additionally, cGMP induced greater relaxations in MA sensitised with U46619 compared to arteries pre-constricted with pCa 4.5 (MA_{pCa 4.5}: 49.2 \pm 9.71 %, n = 7 versus MA_{U46619}: 67.5 \pm 5.12 %, n = 8), ET-1 (MA_{ET-1}: 84.5 \pm 5.60 %, n = 6) and with S1P (MA_{S1P}: 108.1 \pm 9.69 %, n = 4). Similarly, PA pre-constricted with pCa 4.5 relaxed less to 8-br-cGMP than arteries sensitised with U46619 (PA_{pCa 4.5}: 22.8 \pm 6.68 %, n = 6 versus PA_{U46619}: 49.3 \pm 6.04 %, n = 6), ET-1 (PA_{ET-1}: 63.5 \pm 6.89 %, n = 7) or with S1P (PA_{S1P}: 82.0 \pm 1.70 %, n = 4).

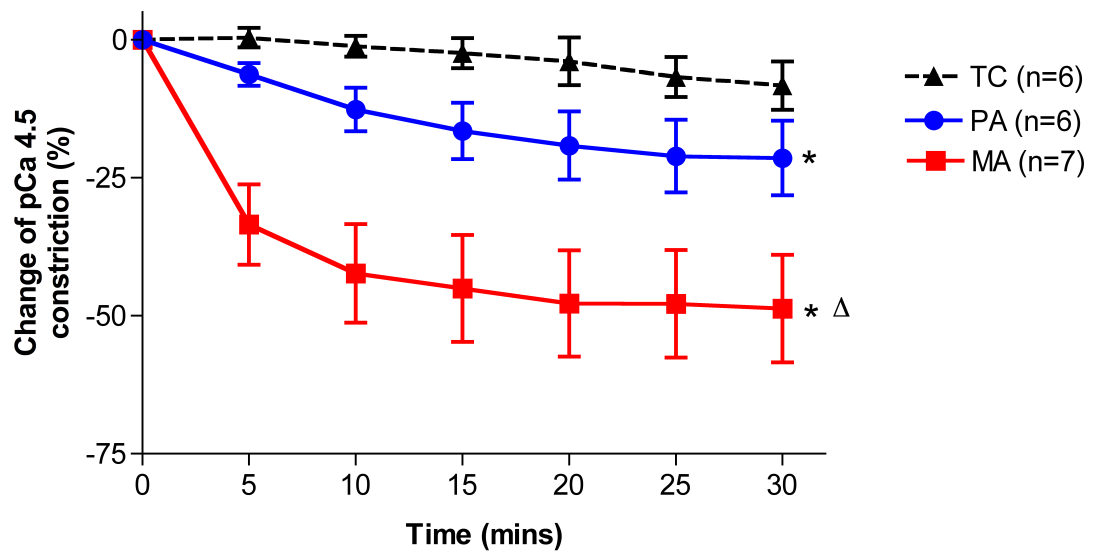


Figure 4.9: Summary data of 10 μ M 8-bromo-cGMP-induced responses in human myometrial and placental arteries. Responses to 8-br-cGMP are expressed as percentages of constrictions obtained with pCa 4.5 over 30 minutes. MA: Myometrial Arteries, PA: Placental Arteries, TC: Time Control. * Statistical difference relative to the time control (TC). Δ Statistical difference relative to PA.

4.5. Potential role of myosin light chain phosphatase (MLCP) in PKG-mediated relaxation of Ca^{2+} -constricted permeabilised arteries

Having observed cGMP-activated-PKG-mediated Ca^{2+} -desensitisation in human arteries from the myometrium and placenta, it was next of interest to establish whether this phenomenon was dependent upon an active MLCP by directly inhibiting the phosphatase using calyculin A (Suzuki and Itoh, 1993, Wareing et al., 2005b).

Figure 4.10 illustrates the effect of 1 μM calyculin A on a permeabilised human MA (A) and PA (B). Exposure to pCa 4.5 preceding addition of the MLCP inhibitor induced similar constrictions in both artery types. Following relaxation back to baseline, at resting $[\text{Ca}^{2+}]$ (pCa 9), calyculin A induced an increase in force production in MA and PA. Subsequent exposure to pCa 4.5 did not further constrict either artery. Finally, 10 μM 8-br-cGMP did not induce a relaxation in either artery type over 30 - 40 minutes.

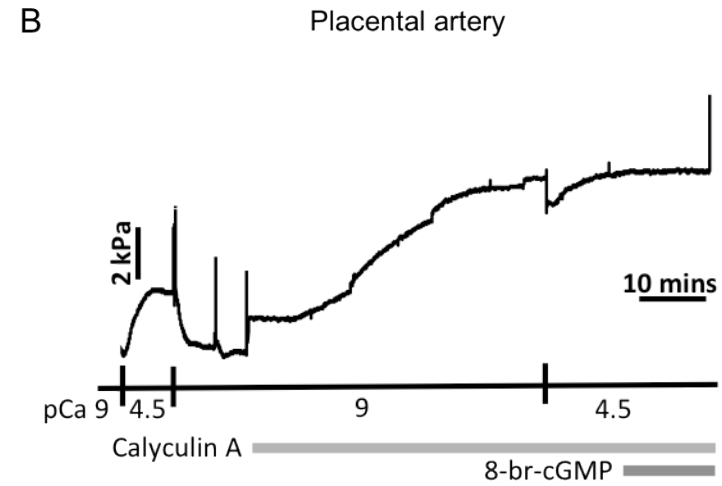
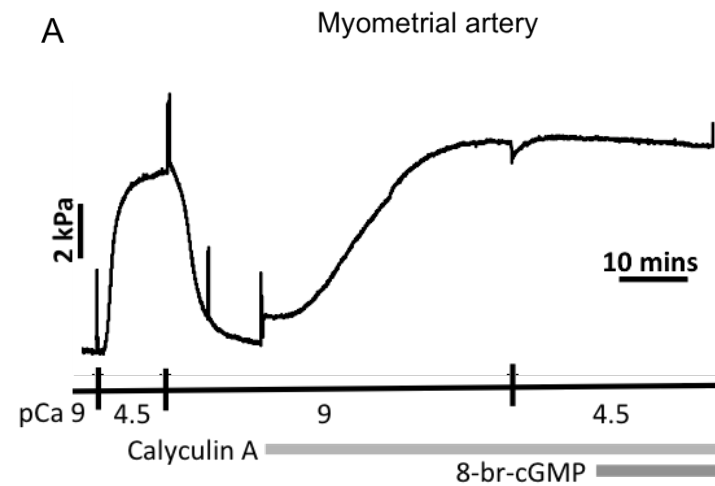


Figure 4.10: Effect of the phosphatase inhibitor, calyculin A (1 μM), on PKG-mediated relaxation of two human arteries at resting $[Ca^{2+}]$. Permeabilised MA (A) and PA (B) exposed to pCa 4.5, then pCa 9, followed by incubation with calyculin A (1 μM), a second exposure to pCa 4.5, and, finally, addition of 8-br-cGMP (10 μM).

Constrictions induced by pCa 4.5 were similar in MA and PA (MA: 7.83 ± 1.98 kPa, $n = 7$ versus PA: 8.78 ± 2.31 kPa, $n = 6$) as were those induced by calyculin A (MA: 8.63 ± 0.68 kPa, $n = 7$ versus PA: 10.6 ± 2.31 kPa, $n = 6$). Calyculin A-induced constrictions were also similar to previous pCa 4.5 constrictions in both MA and PA. Figure 4.11 shows the group mean \pm SEM relaxation responses to 10 μ M 8-br-cGMP in the presence of calyculin A in both MA and PA.

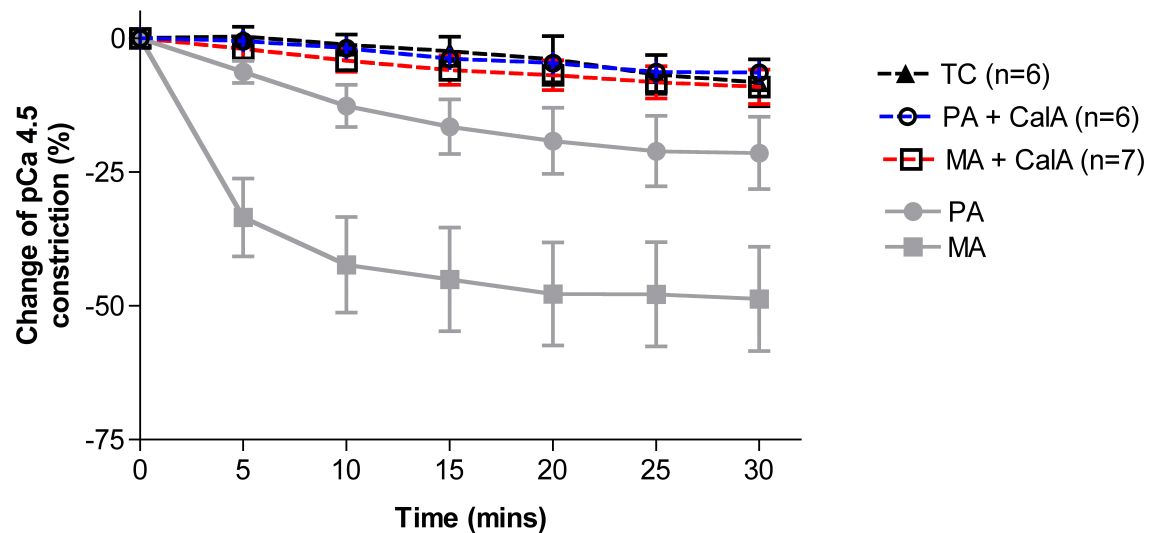


Figure 4.11: Summary data of 8-bromo-cGMP-induced responses in human myometrial and placental arteries in the presence of the phosphatase inhibitor, calyculin A. Responses to 8-br-cGMP are expressed as percentages of constrictions obtained with pCa 4.5 over a 30 minute time period. MA: Myometrial Arteries, PA: Placental Arteries, Caly A: calyculin A. The data displayed in grey in this figure was that illustrated previously in Figure 4.9.

4.6. Expression of PKG and putative PKG-interacting myofilament-associated proteins of human myometrial and placental arteries

PKG has been proposed to alter Ca^{2+} -sensitivity of contraction by interacting with one, or more, of a variety of myofilament-associated proteins. The differences in responsiveness to 8-br-cGMP reported herein between MA and PA may reflect tissue-specific expression profiles of such PKG effector proteins. Thus, it was of interest to explore this possibility by studying the expression of putative PKG-interacting proteins HSP20, telokin, MYPT1 and CPI-17, as well as PKGI α , the most abundant PKG isoform in SM (Francis et al., 2010).

4.6.1. PKGI α protein levels in myometrial and placental arteries

Figure 4.12 illustrates the expression patterns of PKGI α in six human MA and PA samples. Figure 4.12A shows that the expression of PKGI α was detected in human MA and PA and rat aorta (positive control, PC) at the expected molecular mass of around 75 kDa. There are higher levels of PKGI α in the rat aorta compared to the MA and PA samples. Figure 4.12B shows equal loading throughout the membrane from patient to patient samples as assessed by actin staining. There was no difference in the expression of PKGI α between MA and PA (MA: n = 11, PA: n = 12, Figure 4.13).

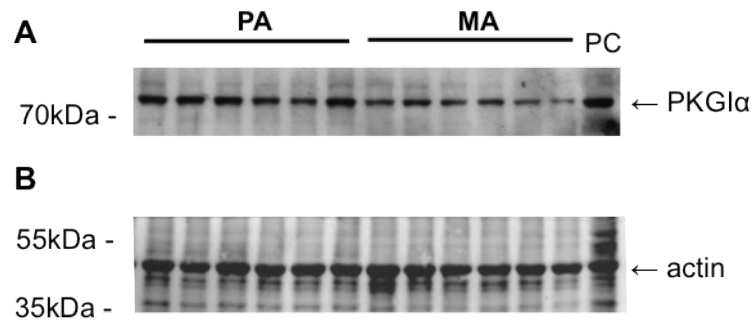


Figure 4.12: PKGIα protein expression in human myometrial and placental arteries. A: Representative immunoblot of total PKGIα abundance in human myometrial arteries (MA, 20 μg, n = 6) and placental arteries (PA, 20 μg, n = 6). PC: positive control, rat aorta, 20 μg. B: actin as a loading control.

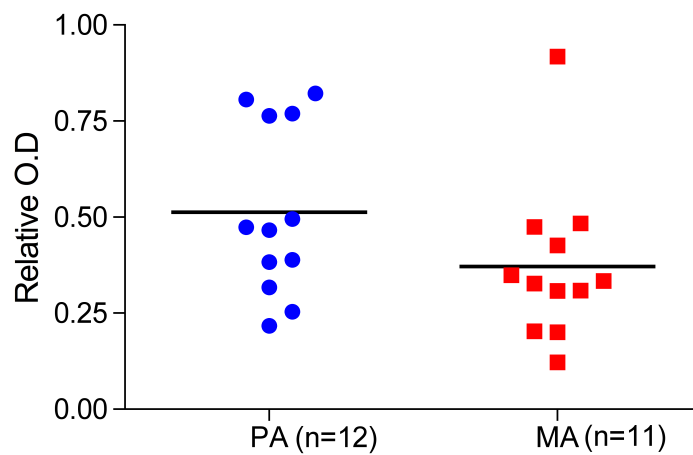


Figure 4.13: Quantified expression levels of PKGIα protein in human myometrial and placental arteries. Optical density of bands representing PKGIα in MA and PA was normalised to the optical density of PC. Relative O.D.: Relative Optical Density, MA: Myometrial Arteries, PA: Placental Arteries.

4.6.2. HSP20 protein levels in human myometrial and placental arteries

Figure 4.14 illustrates the expression patterns of HSP20 in six human MA and PA samples. Figure 4.14A shows that expression of HSP20 was detected in both artery types and in the myometrium from a pregnant woman (PC), at the expected molecular mass of 20 kDa. A second band was also observed around 17 kDa. Higher protein levels were detected in the myometrial tissue sample compared to the arteries. A degree of inter-patient variability can also be observed in both MA and PA. There was no difference in the expression of HSP20 between the two artery types (n = 12, Figure 4.15).

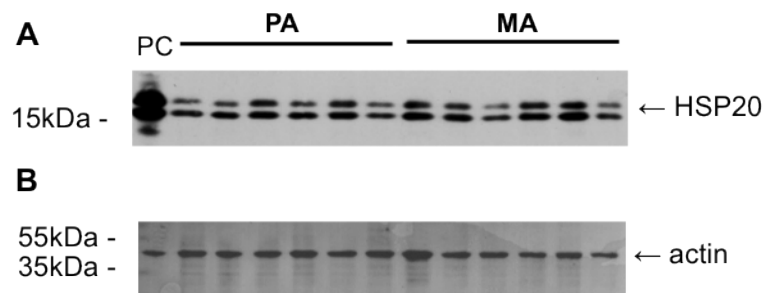


Figure 4.14: HSP20 protein expression in human myometrial and placental arteries. A: Representative immunoblot of total HSP20 abundance in human myometrial arteries (MA, 5 μ g, n = 6) and placental arteries (PA, 5 μ g, n = 6). PC: positive control, human myometrium (pregnant patient), 5 μ g. B: actin as a loading control.

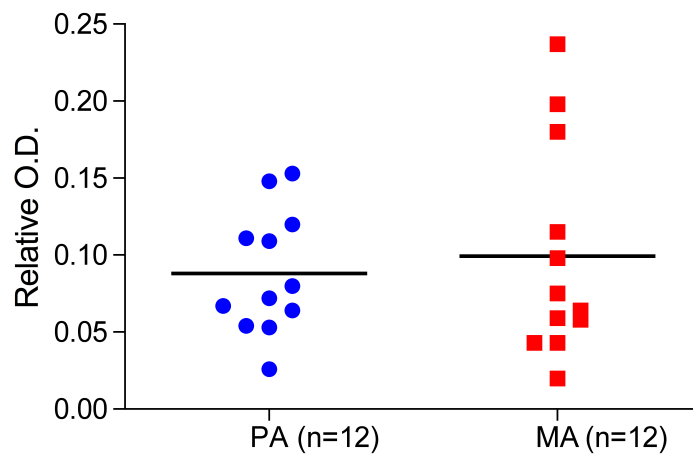


Figure 4.15: Quantified expression levels of HSP20 protein in human myometrial and placental arteries. Optical density of bands representing HSP20 in MA and PA was normalised to the optical density of PC. Relative O.D.: Relative Optical Density, MA: Myometrial Arteries, PA: Placental Arteries.

4.6.3. Telokin protein levels in human myometrial and placental arteries

Figure 4.16 illustrates the expression patterns of telokin in 4 - 6 human MA and PA samples. Figure 4.16A shows that expression of telokin was detected in both artery types and in rat brain (PC) at the expected molecular mass of around 17 kDa. A second band of lower intensity was also observed around 16 kDa. Considerable inter-patient variability in the expression of telokin was observed for both MA and PA. There was no difference in the expression of telokin between ten samples of MA and PA (Figure 4.17).

Telokin expression is under the control of an intronic promoter of the MLCK gene such that the amino acid composition of telokin is identical to a C-terminal portion of MLCK (Gallagher et al., 1991, Herring and Smith, 1996). Indeed, telokin expression was probed in these experiments by use of an anti-MLCK antibody whose epitope was shared with telokin. Thus, it was of curiosity to ascertain if MLCK expression probed by the same antibody displayed a similar patient-to-patient variability as telokin. Figure 4.18A shows the results of MLCK expression of six human MA and PA samples with a band at the anticipated molecular mass of approximately 130 kDa. There was less patient-to-patient variation in MLCK expression than telokin. No difference was observed for MLCK expression between twelve human MA and PA samples (Figure 4.19).

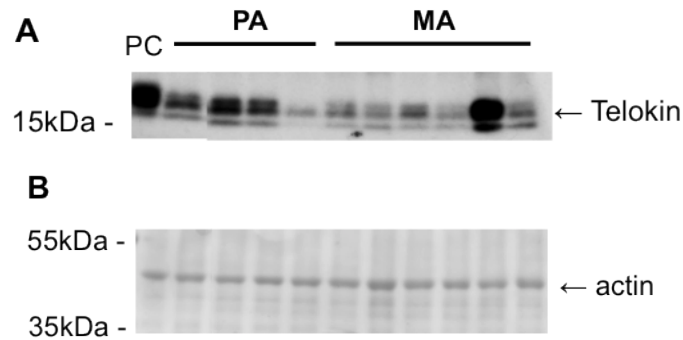


Figure 4.16: Telokin protein expression in human myometrial and placental arteries. A: Representative immunoblot of total telokin abundance in human myometrial arteries (MA, 10 μ g, n = 6) and placental arteries (PA, 10 μ g, n = 4). PC: positive control, rat brain, 10 μ g. B: actin as a loading control.

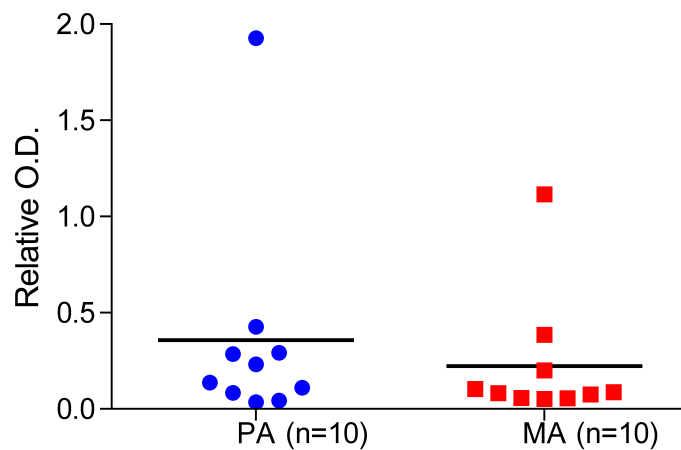


Figure 4.17: Quantified expression levels of telokin protein in human myometrial and placental arteries. Optical density of bands representing telokin in MA and PA was normalised to the optical density of PC. Relative O.D.: Relative Optical Density, MA: Myometrial Arteries, PA: Placental Arteries.

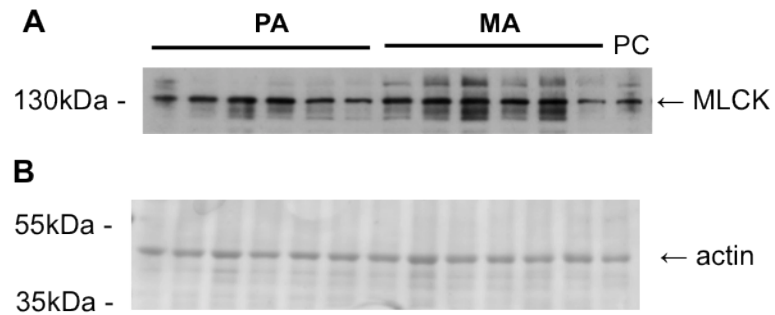


Figure 4.18: MLCK protein expression in human myometrial and placental arteries. A: Representative immunoblot of total MLCK abundance in human myometrial arteries (MA, 7.5 μ g, n = 6) and placental arteries (PA, 7.5 μ g, n = 6). PC: positive control, human myometrium (pregnant patient), 7.5 μ g. B: actin as a loading control.

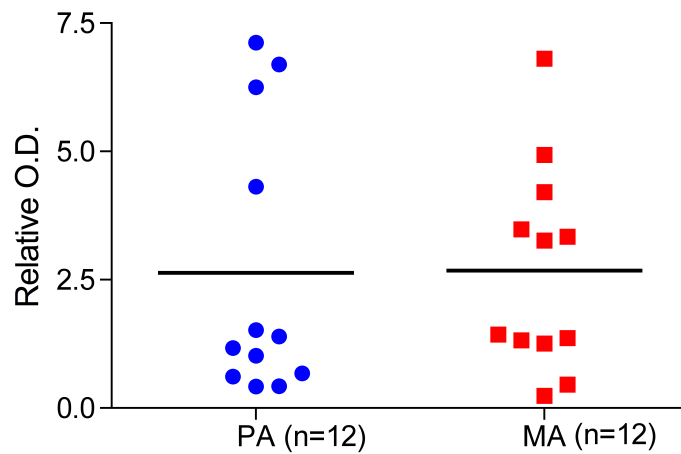


Figure 4.19: Quantified expression levels of MLCK protein human myometrial and placental arteries. Optical density of bands representing MLCK in MA and PA was normalised to the optical density of PC. Relative O.D.: Relative Optical Density, MA: Myometrial Arteries, PA: Placental Arteries.

4.6.4. MYPT1 protein levels in human myometrial and placental arteries

Figure 4.20 illustrates the expression patterns of the MLCP targeting subunit, MYPT1, in six human MA and PA samples. Figure 4.20A shows that expression of MYPT1 was detected in both artery types and in human myometrium (pregnant patient serving as the PC) at the expected molecular mass of around 115 kDa. There was no difference in the expression of this protein between MA and PA samples ($n = 12$, Figure 4.21).

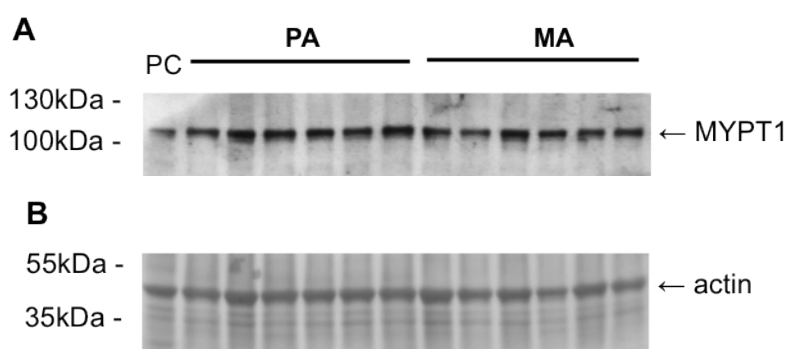


Figure 4.20: MYPT1 protein expression in human myometrial and placental arteries. A: Representative immunoblot of total MYPT1 abundance in human myometrial arteries (MA, 20 μ g, $n = 6$) and placental arteries (PA, 20 μ g, $n = 6$). PC: positive control, human myometrium (pregnant patient), 20 μ g. B: actin as a loading control.

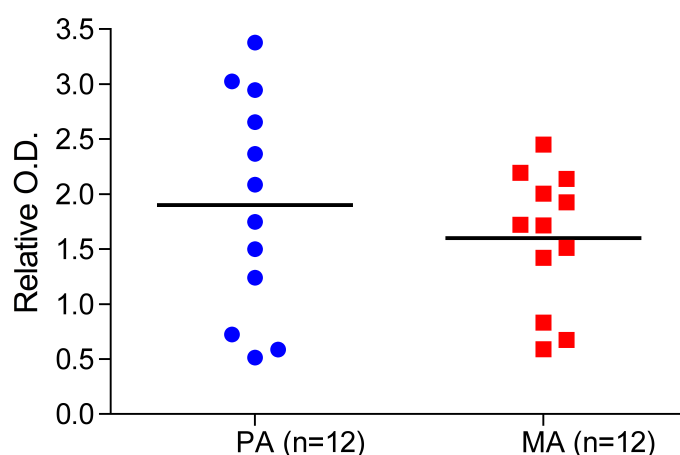


Figure 4.21: Quantified levels of MYPT1 protein in human myometrial and placental arteries. Optical density of bands representing MYPT1 in MA and PA was normalised to the optical density of PC. Relative O.D.: Relative Optical Density, MA: Myometrial Arteries, PA: Placental Arteries.

4.6.5. *CPI-17 protein levels in human myometrial and placental arteries*

Figure 4.22 illustrates the expression patterns of CPI-17 in six human MA and PA samples. Expression of CPI-17 was detected in both artery types and in rat brain (PC) was observed at the expected molecular mass of around 17 kDa. A second band of lower intensity was also observed around 16 kDa. Like for telokin, there is considerable patient-to-patient variation but, overall, there is no difference in the expression of this protein between MA and PA samples (n = 12, Figure 4.23).

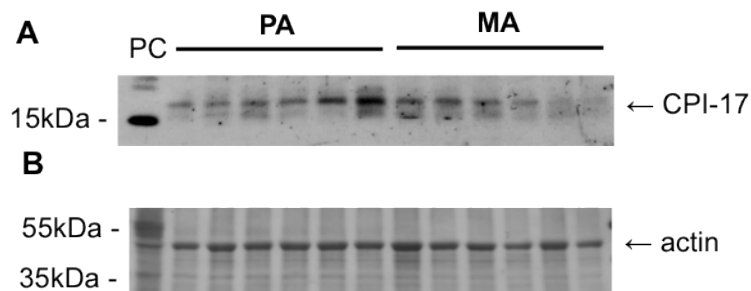


Figure 4.22: CPI-17 protein expression in human myometrial and placental arteries. A: Representative immunoblot of CPI-17 abundance in human myometrial arteries (MA, 10 μ g, n = 6) and placental arteries (PA, 10 μ g, n = 6). PC: positive control, rat brain, 20 μ g. B: actin as a loading control.

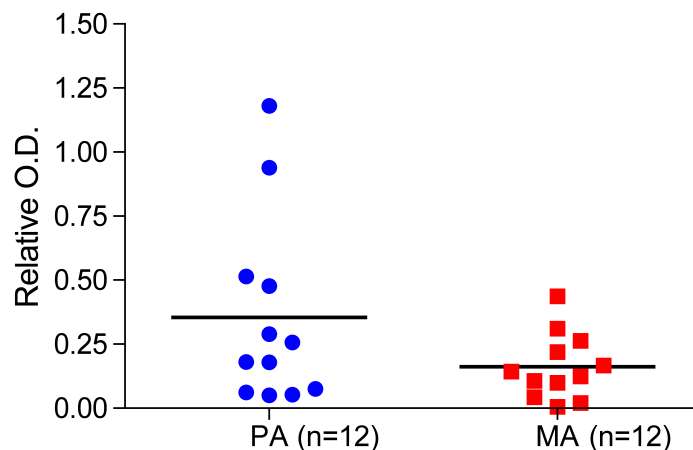


Figure 4.23: Quantified levels of CPI-17 protein in human myometrial and placental arteries. Optical density of bands representing CPI-17 in MA and PA was normalised to the optical density of PC. Relative O.D.: Relative Optical Density, MA: Myometrial Arteries, PA: Placental Arteries.

4.7. Discussion

This work sought to establish whether the phenomenon of cGMP-dependent Ca^{2+} -desensitisation occurred in human MA and PA. The main findings were: first, that both artery types exhibited decreases in Ca^{2+} -sensitivity in the presence of 8-br-cGMP in arteries constricted to either Ca^{2+} alone or sensitised to Ca^{2+} with a G protein-coupled receptor agonist. Second, that permeabilised MA displayed a greater relaxatory capacity to cGMP/PKG compared to PA. Third, that the mechanism of Ca^{2+} -desensitisation may be dependent upon an active MLCP. Fourth, that both MA and PA express myofilament-associated proteins thought to be involved in the cGMP/PKG relaxatory pathway and regulation of vascular tone but that no differences in expression levels for any of the proteins were demonstrated between the two artery types.

Both MA and PA sensitised to sub-maximal activating Ca^{2+} in the presence of the G protein-coupled agonists U46619, ET-1 and S1P. Constrictions induced by U46619 and ET-1 at pCa 6.7 in this set of experiments were similar to those observed at pCa 6.7 in arteries exposed to incremental $[\text{Ca}^{2+}]$ (Chapter 3) in both MA and PA. Both U46619 and ET-1 induced greater sensitisations than S1P in the two artery types. Additionally, the sensitisations induced by S1P were lower than those in arteries exposed to incremental $[\text{Ca}^{2+}]$. The sensitisation capacity of S1P has been documented in MA and PA and was reported as being rather variable, in that it did not occur to the same degree or in each experiment (Hemmings et al., 2006, Hudson et al., 2007). This may illustrate a degree of variability in vessel responses to this agonist. In addition, although the present study found a consistent U46619-induced Ca^{2+} -sensitisation in MA and PA, previous reports have shown greater sensitisations induced by this agonist in the two artery types. Wareing *et al.* (2005b) reports sensitisations of $131 \pm 19 \%$ and $54 \pm 15 \%$ of contraction to pCa 4.5 solution in α -toxin permeabilised from MA and PA from pregnant women, respectively (Wareing et al., 2005b). The present results were consistent with respect to PA ($57.8 \pm 2.42 \%$ from pCa 4.5 constriction). However, MA responded to a lesser extent compared to these reports ($73.8 \pm 1.12 \%$ from pCa 4.5 constriction), which may indicate a degree of variability in MA to U46619 also.

Agonist-mediated Ca^{2+} -sensitisation likely occurred, at least in part, from inhibition of MLCP. Several studies point to agonist-mediated Ca^{2+} -sensitisation involving ROK-induced phosphorylation of the MLCP targeting subunit MYPT1 at Thr-696 (Kitazawa

et al., 1991, Kitazawa et al., 1989, Sward et al., 2000, Ito et al., 2003, Kimura et al., 1996, Somlyo and Somlyo, 2000, Hudson et al., 2007, Hemmings et al., 2006, Wareing et al., 2005b). The likely involvement of this pathway in Ca^{2+} -sensitisation of MA or PA is supported by previous data showing that U46619- or S1P-induced Ca^{2+} -sensitisations were reduced upon addition of the ROK inhibitor, Y27632 (Hemmings et al., 2006, Hudson et al., 2007, Wareing et al., 2005b).

The present study is the first report of Ca^{2+} -desensitisation occurring in human arteries from the myometrium and placenta. Assessment of this phenomenon was carried out using the same permeabilisation technique as described and discussed in Chapter 3. Ca^{2+} -desensitisation occurred in a dose-responsive manner across a concentration range (0.1 - 10 μM) spanning estimates of physiological concentrations of cGMP (Francis et al., 2010). Basal concentrations of cGMP in VSMC are reported to be around 0.1 μM , with a 3 - 6 fold increase during active SM relaxation (Francis et al., 2010). The range of 8-br-cGMP concentrations used in this study were close to physiological and supra-physiological concentrations, assuming that all 8-br-GMP used was active and bearing in mind that the activity of 8-br-GMP may be slightly lower than native cGMP. The 10 μM used is actually one of the lower concentrations reported in the literature, where the range of concentrations more frequently used was 50 – 300 μM (Bonnevier and Arner, 2004, Khromov et al., 2006, Nakamura et al., 2007, Wu et al., 1996, Wu et al., 1998, Russo et al., 2008). A few animal studies have used lower concentrations between 0.5 – 10 μM 8-br-cGMP (Choudhury et al., 2004, Lee et al., 1997, Khatri et al., 2001, Pfitzer et al., 1986). In these studies, tissue-specific responses to 8-br-cGMP were also compared to assess possible differences in sensitivities between tissue types; Khatri *et al.* (2001) showed that 0.1 – 100 μM 8-br-GMP induced maximal (100 %) relaxation in permeabilised chicken aortic SM strips, but did not induce any responses in chicken gizzard SM. Choudhury *et al.* (2004) reported greater relaxations to 5 μM 8-br-cGMP in permeabilised rabbit tonic femoral arteries (30 %) compared to permeabilised phasic ileum SM (60 %) at pCa 6.3, highlighting a difference in sensitivities to the same concentrations of 8-br-cGMP between phasic and tonic SM. Differing levels of tonic versus phasic SM in MA and PA may also have influenced in the relaxatory capacities in the two artery types. In this study, MA and PA did not relax substantially more to 10 μM , compared to 1 μM 8-br-cGMP, but did relax faster. This may indicate a relaxatory threshold in these arteries, which might have developed to protect against acute changes within the fetal environment. In addition, this study found differences in mean maximal

relaxation to cGMP and in the times to half maximal relaxations over the three concentrations of 8-br-cGMP between the two artery types, suggesting different sensitivities to cGMP in MA compared to PA.

The decrease in Ca^{2+} sensitivity induced by 8-br-cGMP in both Ca^{2+} -constricted and Ca^{2+} -sensitised MA and PA likely occurred via activation of PKG. It is thought that relaxation in SMC may be induced via the NO-activated cGMP/PKG pathway (Waldman and Murad, 1987, Nishimura and van Breemen, 1989, Nakamura et al., 2007, Murad, 1994). Pfeifer *et al.* (1998) carried out an elegant study, which showed that intact aortic rings isolated from the PKGI-null mice had ablated 8-br-cGMP-induced relaxation compared to the PKGI control mice. Similarly, intact ileum strips from PKGI-deficient mice did not relax to 100 μM 8-br-cGMP, whilst those from WT mice did (Bonnevier et al., 2004).

PKGI has been proposed to potentially affect a variety of intracellular signalling proteins. Indeed, variations in the expression of several PKG-interacting proteins have been proposed to underlie SM tissue-specific sensitivities to NO/cGMP/PKG. These proteins include: (i) HSP20, whose phosphorylation state induced by both PKA and PKG on Ser-16 has been associated with active relaxation of permeabilised bovine carotid SM (Beall et al., 1997, Beall et al., 1999, Rembold et al., 2000); (ii) telokin, whose phosphorylation by PKG at Ser-13 has been shown to be increased by 8-br-cGMP and induce Ca^{2+} -desensitisation (Wu et al., 1998); (iii) MYPT1 LZ positive isoform of MLCP, which has been found to interact with the LZ domain of PKGI α (Surks et al., 1999, Khatri et al., 2001); (iv) CPI-17, whose increased dephosphorylation at residue Thr-38 following addition of 8-br-cGMP induced relaxation of mice femoral arteries and ileal SM (Bonnevier and Arner, 2004). Given the reported differences in response to 8-br-cGMP in permeabilised MA and PA it was possible that alterations in the expression of one or more of these proteins may be a contributory factor. However, levels of PKGI α , HSP20, telokin or CPI-17 protein were similar between MA and PA. There was considerable patient-to-patient variation between samples, particularly for telokin and CPI-17 expression. Levels of total MYPT1 protein were also similar for MA and PA. However, the antibody used to probe MYPT1 would not distinguish between LZ -positive and -negative isovariants of MYPT1. Thus, future experiments studying mRNA encoding each isovariant could be performed to ascertain if there is a variation in MYPT1 isoform ratio, rather than MYPT1 total protein, between MA and PA. It is

also possible that the activities of these proteins differ between the two artery types, rather than their expression levels, and future studies may assess this. Of note is the fact that protein expressions were assessed in full arterial samples, which included EC, IEL, SMC, ECM, rather than isolated SMC. Accurate quantification of the expression of PKGI and its putative interacting proteins was limited. Further studies may therefore use isolated SMC from fresh arterial samples for assessment of the aforementioned proteins.

MLCP is a known key regulator of vascular tone. The potential role of MLCP in Ca^{2+} -desensitisation was illustrated in this study with the broad class phosphatase inhibitor calyculin A, which prevented relaxant actions of 8-br-cGMP in both artery types. Calyculin A was first identified as a PP1 and PP2A inhibitor in SM fibers in 1989 (Ishihara et al., 1989) and shortly after was also found to induce contraction under Ca^{2+} -free conditions (Hartshorne et al., 1989). It exhibits a greater affinity for PP2A compared to PP1 similarly to the phosphatase inhibitor, MCLR (Takai et al., 1995). MCLR was reported to possess a higher affinity for PP2A and PP1 compared to calyculin A (Takai et al., 1995). Nonetheless, the efficiency of calyculin A in inhibiting MLCP has been shown in several studies, making it suitable for the present study. β -escin- and ionomycin-treated skinned SM strips of the rabbit mesenteric artery constricted with maximal amplitudes, similar to those evoked by $10\text{ }\mu\text{M}$ $[\text{Ca}^{2+}]$, in Ca^{2+} -free solutions (containing either 20 mM EGTA or 4 mM EGTA) and the threshold concentration of calyculin A required for the increase in tension or MLC-phosphorylation was $0.03\text{ }\mu\text{M}$, with maximum effects obtained at $3\text{ }\mu\text{M}$ (Suzuki and Itoh, 1993). In addition, $1\text{ }\mu\text{M}$ calyculin A was shown to inhibit MLCP in α -toxin-permeabilised rabbit trachea (Iizuka et al., 1999). Further, NO-induced Ca^{2+} -desensitisation was ablated in the presence of $0.12\text{ }\mu\text{M}$ calyculin A in rat aorta (Bolz et al., 2003) and in α -toxin-permeabilised human omental arteries from term pregnant women, $1\text{ }\mu\text{M}$ calyculin A induced substantial Ca^{2+} -sensitisations at sub-maximal $[\text{Ca}^{2+}]$ (pCa 6.7), which were of similar magnitude to those induced by the thromboxane mimetic U46619 (Wareing et al., 2005b). These studies, therefore, demonstrated that even at sub-maximal activating Ca^{2+} , calyculin A abolished MLCP activity.

Accordingly, the 8-br-cGMP-induced relaxations were inhibited following pre-incubation of MA and PA with calyculin A, inferring that MLCP was successfully inhibited. Measurements of MLC_{20} dephosphorylation would be valuable to support this

statement. Nevertheless, the present study indicated that Ca^{2+} -desensitisation was, at least in part, dependent upon an active MLCP. Lee *et al.* also showed that 10 μM 8-br-cGMP induced relaxations in sub-maximal activating Ca^{2+} solutions (pCa 6.7 or pCa 7), which were ablated following pre-incubations with either 10 μM MCLR or 1 μM calyculin A in both β -escin and α -toxin permeabilised rabbit femoral artery strips (Lee *et al.*, 1997). Additional studies in α -toxin permeabilised rabbit ileum SM constricted with pCa 6.2 showed that 100 μM 8-br-cGMP induced relaxation and also increased the rate of MLC_{20} dephosphorylation, whilst MLCK activity was blocked with ML-9 (50 μM) (Wu *et al.*, 1996). Following stimulation of PKG by 8-br-cGMP, the observed increase in MLC_{20} dephosphorylation likely occurred after the increase in MLCP activity and binding of the phosphatase to myosin filaments (Somlyo and Somlyo, 2003). Thus, Ca^{2+} -desensitisation was induced by activation of PKG and subsequent increase of MLCP activity.

Interestingly, this study showed that both MA and PA, which were pre-sensitised with U46619, ET-1 or S1P, relaxed to a greater extent than arteries pre-constricted with pCa 4.5. This suggests that arteries *sensitised* in sub-maximal $[\text{Ca}^{2+}]$ can evoke greater *desensitisation* compared to arteries constricted with Ca^{2+} alone. MLCP, and particularly MYPT1, may be a key checkpoint in the two processes. In this study, agonist-induced pre-sensitisation in MA and PA likely occurred via activation of the RhoA/ROK pathway and ROK-induced phosphorylation at Thr-853 of MYPT1 and subsequent inhibition of MLCP (Kitazawa *et al.*, 2009). Ca^{2+} -desensitisation may then have occurred partly via inhibition of the RhoA/ROK pathway and partly via increase of MLCP activity by PKGI activation. *In vitro* studies in rabbit femoral SM strips have shown that PKGI phosphorylated RhoA at Ser-188 (Sauzeau *et al.*, 2000a). This lifted phosphorylations at Thr-853 and at the predominantly endogenous Thr-696 of MYPT1, both of which are sites known to inhibit MLCP activity (Kitazawa *et al.*, 2009, Sauzeau *et al.*, 2000a, Gudi *et al.*, 2002). Studies in permeabilised ileum SM also showed that PKGI could directly phosphorylate MYPT1 at Ser-695 and that this phosphorylation blocked the adjacent endogenous Thr-696 inhibitory phosphorylation, which then increased MLCP activity (Kitazawa *et al.*, 2009, Wooldridge *et al.*, 2004). In MA and PA constricted with Ca^{2+} alone, Ca^{2+} -desensitisation likely occurred via PKGI-induced increase in MLCP activity. However, it is unlikely that inhibition of the RhoA/ROK pathway also played a role. RhoA is only active as a GTP/RhoA complex (Somlyo and Somlyo, 2003, Wang *et al.*, 2002) and it is likely that endogenous GTP escaped the cell

following permeabilisation. Therefore, in Ca^{2+} -constricted arteries, PKGI probably phosphorylated Ser-695, increasing MLCP activity and inducing Ca^{2+} -desensitisation. The reason for the difference in relaxations observed between pre-sensitised and pre-constricted arteries is still unclear; however, MYPT1 seems to place a key role in the regulation of PKGI-mediated Ca^{2+} -desensitisation.

This study also showed that constrictions were induced by calyculin A in human permeabilised MA and PA at sub-basal $[\text{Ca}^{2+}]$ (pCa 9), which were of similar magnitude to those induced by maximal activating Ca^{2+} (pCa 4.5, 31.6 μM). The pCa 4.5-induced constriction was likely elicited via the Ca^{2+} /calmodulin (CaM)-activated MLCK, which is known to phosphorylate MLC_{20} at Ser-19 and Thr-18 (Somlyo and Somlyo, 1994). It is unlikely that the subsequent constriction following addition of calyculin A was induced by MLCK, rather it may have been induced by a kinase with lower Ca^{2+} -sensitivity. Indeed, studies in rat caudal artery and chicken gizzard SM strips have shown that the activity of MLCK was dependent upon activating Ca^{2+} levels allowing formation of Ca^{2+} -CaM complex (Weber et al., 1999). Addition of the protein phosphatase 1 (PP1) inhibitor (predominantly), microcystin-LR (MCLR), to Triton X-100-skinned rat caudal arterial SM was found to elicit contractions at pCa 9 which correlated with the phosphorylation of MLC_{20} at Ser-19 and Thr-18 (Weber et al., 1999). This suggested that relatively Ca^{2+} -insensitive kinase(s) induced development of these constrictions. Using chicken gizzard SM, such a MLC_{20} kinase was isolated and identified as the integrin-linked kinase (IKL) (Deng et al., 2001). A second kinase, zipper-interacting protein kinase (ZIPK), was also found to induce SM constriction in a Ca^{2+} /CaM-independent manner. Both kinases were thought to induce constriction directly via both MLC_{20} and MYPT1 phosphorylations at Ser-19/Thr-18 and Thr-696, respectively (Murata-Hori et al., 1999, Niiro and Ikebe, 2001, Muranyi et al., 2002). In contrast, recent reports did not find a role for ZIPK in direct phosphorylation of MLC_{20} (Wilson et al., 2005b). No studies have yet determined if these relatively Ca^{2+} -insensitive kinases, ILK and ZIPK, are present human PA and MA, nor their functional significance.

In conclusion, the present report has shown for the first time that Ca^{2+} -desensitisation occurs in human MA and PA constricted to maximal $[\text{Ca}^{2+}]$ and is likely mediated via cGMP-activated PKG and active MLCP. MA displayed greater sensitivities to cGMP compared to PA; such differences were not obviously explicable by alterations in the expression levels of a number of myofilament-associated, and putatively PKG-

interacting, proteins. Differences in endothelial-dependent bradykinin-induced relaxations have also been shown in the two artery types (Sweeney et al., 2008). Thus, MA may possess a greater relaxatory capacity at both endothelial-dependent and – independent levels of the NO/cGMP/PKG pathway compared to PA. The next chapter set out to determine whether *intact* MA displayed greater relaxations than PA when exposed to agents that directly elevate NO, or activate sGC, independent of endothelial agonists.

Chapter 5

Effect of endothelium-dependent and -independent vasodilators on intact human myometrial and placental arteries

5.1. Introduction

There is strong evidence that, generally speaking, the NO/cGMP/PKG axis plays an important role in the relaxation of the vasculature (Francis et al., 2010). Notwithstanding this generalisation, there is also an appreciation that the influence of this signalling axis may vary across the vascular tree. Of particular interest to the studies highlighted in the previous chapter is the extent, and possible mechanisms therein, of such variations between the vasculatures of the human uterus and placenta.

The pO₂ in the myometrial vasculature is assumed to be close to that in the systemic circulation, namely around 100 mmHg, whilst that in the placental vasculature has been reported to range from 28 - 40 mmHg; these latter figures were determined by aspiration of intervillous blood through the chorionic plate at the time of cordocentesis (fetal blood sampling) (Soothill et al., 1986, Rodesch et al., 1992). A few studies have assessed the impact of O₂ concentrations on the dilation of human placental chorionic plate arteries when exposed to various relaxatory agonists. However, consensus has not been reached as to whether endothelium-dependent and/or –independent relaxations are impaired when placental arteries are exposed to superfusates of O₂ concentration assumed to be similar to that in the myometrial circulation *in vivo* (McCarthy et al., 1994, Poston, 1996, Poston et al., 1995, Mills et al., 2009, Wareing et al., 2006a). The most compelling work in this area has assessed *in vitro* placental artery function using superfusates bubbled with oxygen concentrations approaching those anticipated for pO₂ *in vivo* (Wareing et al., 2006a). However, in order to adequately assess any variations in endothelium-dependent and –independent responses between myometrial and placental arteries, it seemed necessary to determine whether varied oxygen levels would impact on the relaxation capacities of chorionic plate placental arteries.

Studies assessing the role of endothelial-dependent and –independent relaxation mechanisms in the *human* placental vasculature, as indicated in Chapter 1, Table 1.2, are conflicting. In some, the addition of the endothelium-independent nitrovasodilator sodium nitroprusside (SNP, 10⁻⁵ M) induced relaxation and the eNOS inhibitor L-NNA led to an increase in basal tone (Poston et al., 1995, McCarthy et al., 1994, Learmont and Poston, 1996). With these studies, an important role for NO in the regulation of vascular tone of the placenta was indicated. Further studies on small chorionic plate placental arteries (~ 300 µm diameter) also showed substantial vasodilation to

incremental concentrations of SNP ($10^{-9} - 10^{-4}$ M), where relaxations reached 70 % of pre-constrictions to U46619 (Mills et al., 2007a). SNP, along with other endothelium-independent vasodilators, such as SNAP or GTN, also induced relaxation in chorionic plate arterial segments of 1.5 – 2 mm diameter in a dose-dependent manner (1.3×10^{-8} M – 5.7×10^{-2} M) (Zhang et al., 2001). Yet, a variety of endothelial-dependent agents usually elicited only modest relaxatory responses from placental arteries (McCarthy et al., 1994, Sweeney et al., 2008).

The importance of NO in the *human* uterine vasculature has been shown in a variety of studies assessing vascular function in myometrial arteries from both healthy and/or pre-eclamptic pregnant women. Reductions in relaxations to bradykinin were reported following incubation with L-NAME (and a prostaglandin inhibitor, indomethacin) in myometrial arteries from healthy pregnant women mounted on a small-vessel wire myograph (Luksha et al., 2010). Endothelium-dependent relaxations, assessed by addition of acetylcholine or bradykinin, were impaired in myometrial arteries from preeclamptic women compared to those from healthy pregnancies (Kenny et al., 2002).

While the role of the NO-induced pathway has been assessed in both uterine and placental circulations, there are no studies comparing responses to a nitrovasodilator between myometrial and placental arteries under identical experimental conditions. In addition, studies in placental arteries which assessed responses induced by endothelium-independent vasodilators did so with pre-constrictions to G protein-coupled receptor agonists, such as the thromboxane A₂ mimetic (U46619) (McCarthy et al., 1994, Zhang et al., 2001, Mills et al., 2007a, Mills et al., 2007b, Mills et al., 2009), ET-1 (McCarthy et al., 1994), prostaglandins E₂ and F₂ (PGE₂ and PGF₂) (McCarthy et al., 1994), norepinephrine (NE) (McCarthy et al., 1993) or phenylephrine (PE) (Lu et al., 2008). Similarly, the effects of SNP concentrations were assessed in myometrial arteries pre-constricted to U46619 (McCarthy et al., 1993). None of these studies reported the effects of nitrovasodilators in arteries pre-constricted via an alternative pathway, such as via opening of Ca²⁺-channels by high K⁺ depolarisation.

There are currently no studies assessing the effects of a sGC activator in either human myometrial or placental arteries, although one study did report an increase in placental perfusion pressure, following carbon-monoxide exposure, by the sGC activator YC-1 (Bainbridge et al., 2002).

I, therefore, wished to

- (i) first, determine whether oxygen concentrations similar to those assumed in the uterine circulation affect endothelial-dependent and -independent responses in pre-constricted placental arteries,
- (ii) second, assess responses to endothelial-dependent and -independent vasodilators in both pre-constricted myometrial and placental arteries,
- (iii) and compare these responses between the two artery types.

5.2. Materials and Methods

5.2.1. Experimental Protocols

5.2.1.1. *Experimental design 1: assessing the effects of oxygen on the relaxation capacities on human placental arteries*

For each experiment, one set of four placental arteries (PA) was exposed to PSS bubbled with an $[O_2]$ similar to that assumed to be present in the myometrial circulation, ie. 100 mmHg. This was achieved by using a gas mixture with 20 % oxygen (5 % CO_2 in air - oxygen content of 18 - 21 % - BOC Special Gases, British Oxygen Company, UK). A second set of four PA from the same patient was exposed to PSS bubbled with an $[O_2]$ of ~38 mmHg, close to that assumed *in vivo* for the placental circulation, which was achieved using a gas mixture containing 7 % oxygen (5 % CO_2 /5 % O_2 in nitrogen (N_2) - oxygen content 6 - 8 % - BOC Special Gases, British Oxygen Company, UK).

Following normalisation, both sets of PA were exposed to 60 mM KPSS and left to plateau 10 – 15 minutes. They were then exposed to the endothelium-dependent vasodilator, bradykinin (BK, 10^{-6} M) for 15 minutes until plateau. After washout with PSS and a second KPSS exposure (left to plateau 10 – 15 minutes), the endothelium-dependent vasodilator histamine (His, 10^{-5} M) was added for 15 minutes until plateau and returned to PSS.

Arteries were then again constricted with KPSS and left to plateau 10 – 15 minutes. For each set of four arteries, two PA were exposed to one of two endothelium-independent vasodilators, the nitric oxide donor sodium nitroprusside (SNP, 10^{-5} μ M) or the soluble guanylate cyclase activator YC-1 (3×10^{-5} M) for 20 minutes or until plateau. YC-1 was used as it is a known potent sGC activator (Evgenov et al., 2006) and, as mentioned above, has been observed to exert vasoactive actions in perfused placental segments (Bainbridge et al., 2002). Therefore, it was the agent of choice in these studies. The other two PA were used as paired vehicle controls for each vasodilator (ddH₂O and DMSO, respectively).

Following normalisation, these functional experiments lasted 3 hours.

5.2.1.2. *Experimental design 2: assessing endothelium-dependent and – independent responses in human myometrial and placental arteries*

MA and PA were exposed to a first 60 mM KPSS addition, followed by 10^{-6} M BK and, following wash-out with PSS, they were exposed to a second 60 mM KPSS, followed by 10^{-5} M His. Subsequently, the following protocols were carried out:

Protocol 1: For both MA and PA, four arteries were constricted with 60 mM KPSS and left to plateau 10 – 15 minutes. Three arteries were exposed to one of nine concentrations of SNP (10^{-10} M, 10^{-9} M, 10^{-8} M, 3×10^{-8} M, 10^{-7} M, 10^{-6} M or 10^{-5} M), whilst the fourth was used as vehicle control (ddH₂O). Arteries exposed to SNP were left to plateau 15 – 20 minutes. This step was repeated three times, until all concentrations were assessed. Addition of a concentration of SNP was picked at random to add to each of three arteries and order of concentrations used was alternated for each experiment.

Protocol 2: For both MA and PA, four arteries were constricted to 60 mM KPSS and left to plateau 10 - 15 minutes. Three arteries were exposed to one of six concentrations of YC-1 (10^{-7} M, 3×10^{-7} M, 10^{-6} M, 3×10^{-6} M, 10^{-5} M or 3×10^{-5} M), whilst the fourth was used as vehicle control (DMSO). Arteries exposed to YC-1 were left to plateau 20 minutes. This was repeated twice, until all concentrations were assessed. Addition of a concentration of YC-1 was picked at random to add to one of three arteries and order of concentrations used was alternated for each experiment.

Following normalisation, these functional experiments lasted 5 hours.

5.2.2. *Statistics*

5.2.2.1. *Experimental design 1*

Responses to BK and His were expressed as percentages of the maximal constrictions to 60 mM KPSS. Comparisons between maximal responses to BK or His at 20 % versus 7 % O₂ were carried out using Kruskal-Wallis one-way ANOVA test.

The change in tension with the addition of SNP or YC-1 was calculated as a percentage of the change in tension to KPSS. Changes in tension were calculated at 5 minutes intervals. The responses to SNP or YC-1 were compared at 20 % versus 7 % O₂ using two-way ANOVA followed by Bonferroni post-hoc test.

5.2.2.2. *Experimental design 2*

Changes in tension to 60 mM KPSS were compared between MA and PA using unpaired *t-test*. Responses to BK and His were expressed as percentages of the maximal constrictions to 60 mM KPSS. The maximal effects of BK and His were compared between MA and PA using unpaired *t-test*.

Responses to SNP and YC-1 were expressed as percentages of the maximal constrictions to 60 mM KPSS. The effect of 3×10^{-8} M SNP was compared between MA and PA over 20 minutes using two-way ANOVA followed by Bonferroni post-hoc test. The effect of SNP was then compared between MA and PA over the range of concentrations used with two-way ANOVA followed by Bonferroni post-hoc test.

The effect of 3×10^{-6} M YC-1 was compared between MA and PA over 20 minutes using two-way ANOVA followed by Bonferroni post-hoc test.

Half times to maximal relaxations were compared between MA and PA using unpaired *t-test*.

5.3. Assessing the effects of percentage oxygen saturation on endothelium-dependent and –independent relaxations of placental arteries

5.3.1. *Endothelium-dependent relaxation in placental arteries exposed to 20 % and 7 % oxygen*

Maximal relaxations induced by the endothelium-dependent vasodilator, BK (10^{-6} M), were not significantly different at 20 % O₂ compared to 7 % (7.4 ± 1.8 % versus 8.3 ± 2.4 %, respectively, $n = 20$). Similarly, there was no significant difference in the His-induced maximal relaxations between 20 % and 7 % O₂ levels (6.2 ± 2.9 % versus 7.7 ± 1.4 %, respectively, $n = 20$).

5.3.2. *Endothelium-independent relaxations in placental arteries exposed to 20 % and 7 % oxygen*

Figure 5.1 illustrates the responses over time to 3×10^{-5} M YC-1 (A) and 10^{-5} M SNP (B) as percentages of constriction to KPSS in PA exposed to 20 % and 7 % O₂. Figure 5.1A shows YC-1 induced relaxations in KPSS pre-constricted PA at either 20 % and 7 % O₂ relative to their respective vehicle controls (VC) (YC-1_{20%}: 91 ± 3.3 % relaxation versus VC_{20%}: 2.7 ± 1.7 %, $n = 5$ and YC-1_{7%}: 86 ± 10 % relaxation versus VC_{7%}: 3.1 ± 1.3 %, $n = 5$). The relaxations induced by YC-1 were greater at 20 % oxygen than at 7 % O₂. Figure 5.1B shows that SNP-induced relaxations were invariant between 20 % and 7 % O₂ (SNP_{20%}: 65 ± 5.9 % versus VC_{20%}: 3.5 ± 1.3 %, $n = 5$ and SNP_{7%}: 65 ± 14 % versus VC_{7%}: 3.4 ± 1.7 %, $n = 5$).

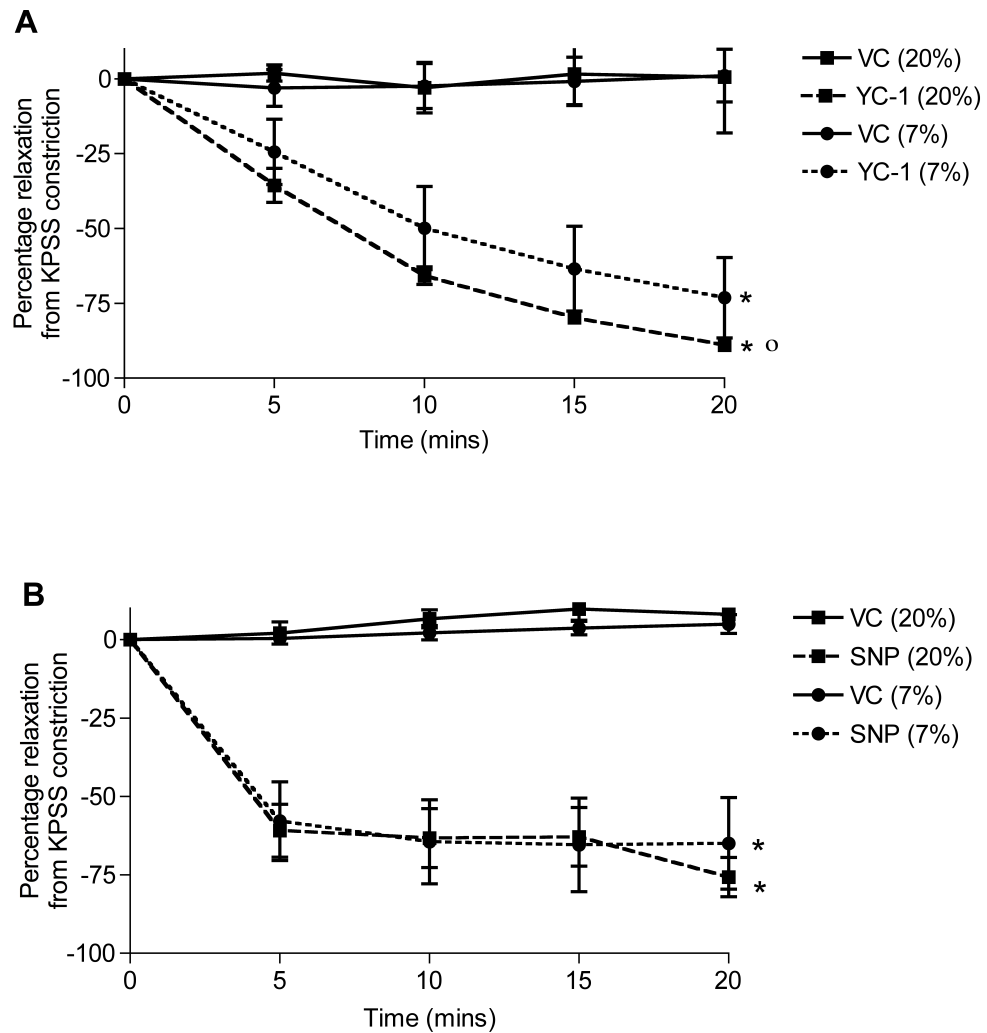


Figure 5.1: Responses to 3×10^{-5} M YC-1 (A) and 10^{-5} M SNP (B) in intact human placental arteries at 20 % and 7 % oxygen. A: Response to 3×10^{-5} M YC-1 in PA expressed as a percentage of 60 mM KPSS-induced constriction. B: Response to 10^{-5} M SNP in PA expressed as a percentage of 60 mM KPSS-induced constriction. VC: Vehicle Control, SNP: Sodium Nitroprusside. * Statistical difference relative to VC, ° Statistical difference relative to 7 % O₂.

Thus, these data indicate that oxygen levels similar to those present in the myometrial vasculature (around 20 %) do not impair the magnitude of endothelium-dependent or -independent relaxations in human PA. Therefore, in the subsequent experiments on *intact* arteries carried out throughout this study, the oxygen levels of PSS were kept at 20 % O₂ for both artery types.

5.4. Effects of endothelial-dependent agonists on pre-constricted human myometrial and placental arteries

Figure 5.2 shows original tracings of an intact human MA (A) and an intact human PA (B) exposed to 60mM KPSS followed by 10^{-6} M BK. Figure 5.2A demonstrates that 60 mM KPSS induced a sustained constriction and that 10^{-6} M BK induced a relaxatory response in the pre-constricted MA. The relaxation reached plateau after 5 minutes and, in this experiment, reflected a 34 % reduction of the KPSS pre-constriction. Figure 5.2B shows that 60 mM KPSS induced a sustained constriction and that 10^{-6} M BK induced a minimal response in the pre-constricted PA, which represented a 6 % reduction of the KPSS pre-constriction.

Figure 5.3 shows original tracings of an intact human MA (A) and an intact human PA (B) exposed to 60mM KPSS followed 10^{-5} M His. Figure 5.3A demonstrates that 60 mM KPSS induced a sustained constriction and that 10^{-5} M His induced a relaxatory response in the pre-constricted MA, which reached a plateau after 5 minutes. In this experiment, His induced a relaxation of 76 % of the KPSS pre-constriction. Figure 5.3B shows that 60 mM KPSS induced a sustained constriction and that 10^{-5} M His induced a small response in the pre-constricted PA, which represented a 7 % reduction of the KPSS constriction.

Overall constrictions induced by 60 mM KPSS were greater in MA compared to PA (MA: 12.7 ± 0.56 kPa, $n = 12$ versus PA: 6.15 ± 0.26 kPa, $n = 12$). Figure 5.4 illustrates the mean \pm SEM responses to BK (A) and His (B) in human MA and PA. Figure 5.4A shows that maximal relaxations induced by 10^{-6} M BK in 60 mM KPSS-constricted arteries were greater in MA compared to PA (MA: relaxation of 33.9 ± 1.91 %, $n = 12$ versus PA: relaxation of 6.91 ± 1.09 %, $n = 12$). Similarly, Figure 5.4B demonstrates that MA relaxed more to 10^{-5} M His compared to PA (MA: relaxation of 78.3 ± 1.90 %, $n = 12$ versus PA: relaxation of 8.30 ± 0.97 %, $n = 12$). His-induced relaxations were greater than those induced by BK.

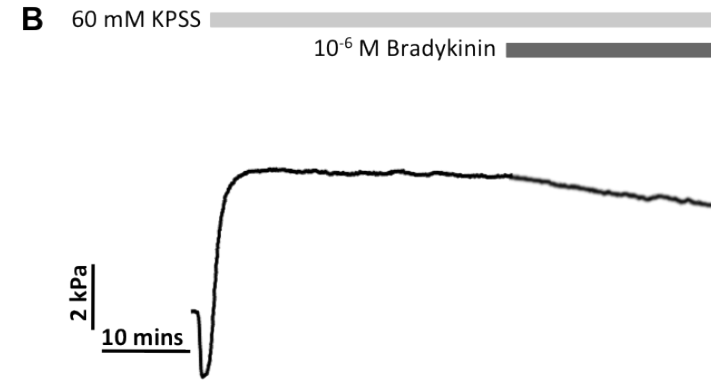
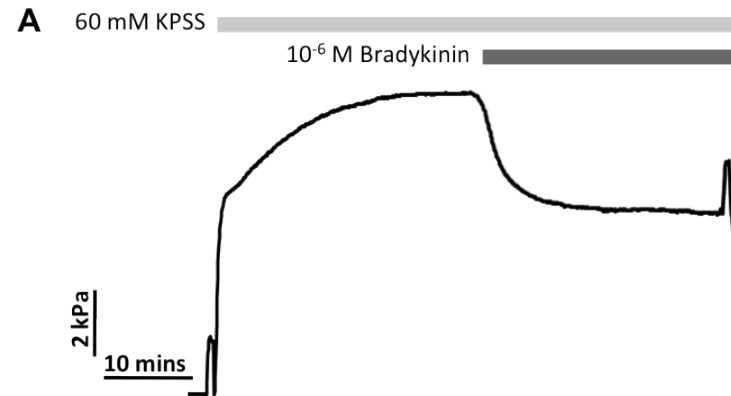


Figure 5.2: Effect of 10^{-6} M bradykinin in an intact myometrial artery (A) and an intact placental artery (B) pre-constricted with 60 mM KPSS. MA (A) and PA (B) exposed to 60 mM KPSS, followed 10^{-6} M bradykinin.

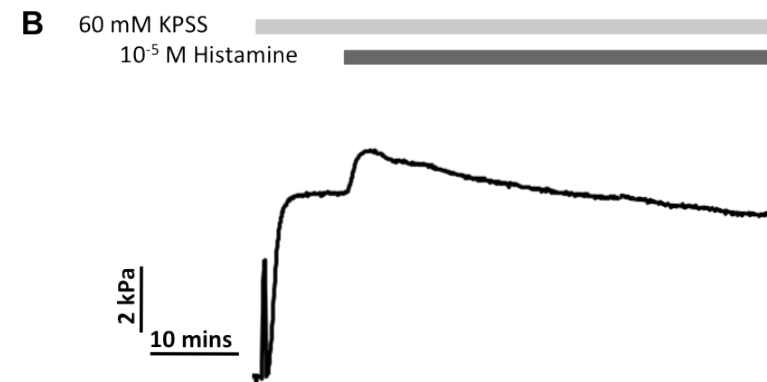
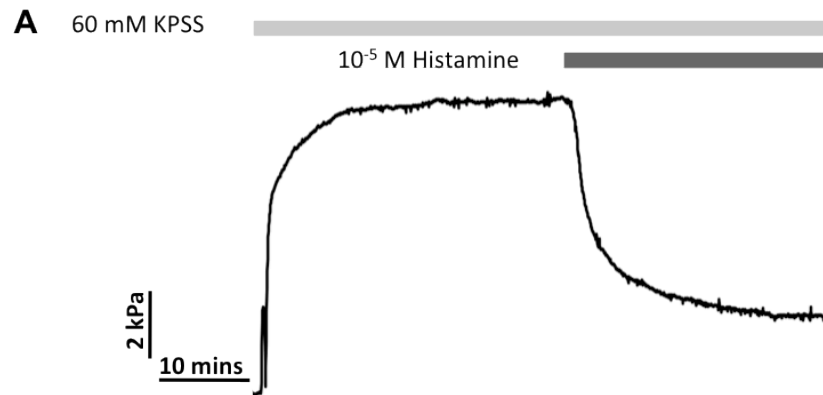


Figure 5.3: Effect of 10^{-5} M histamine in an intact myometrial artery (A) and an intact placental artery (B) pre-constricted with 60 mM KPSS. MA (A) and PA (B) exposed to 60 mM KPSS, followed 10^{-5} M histamine.

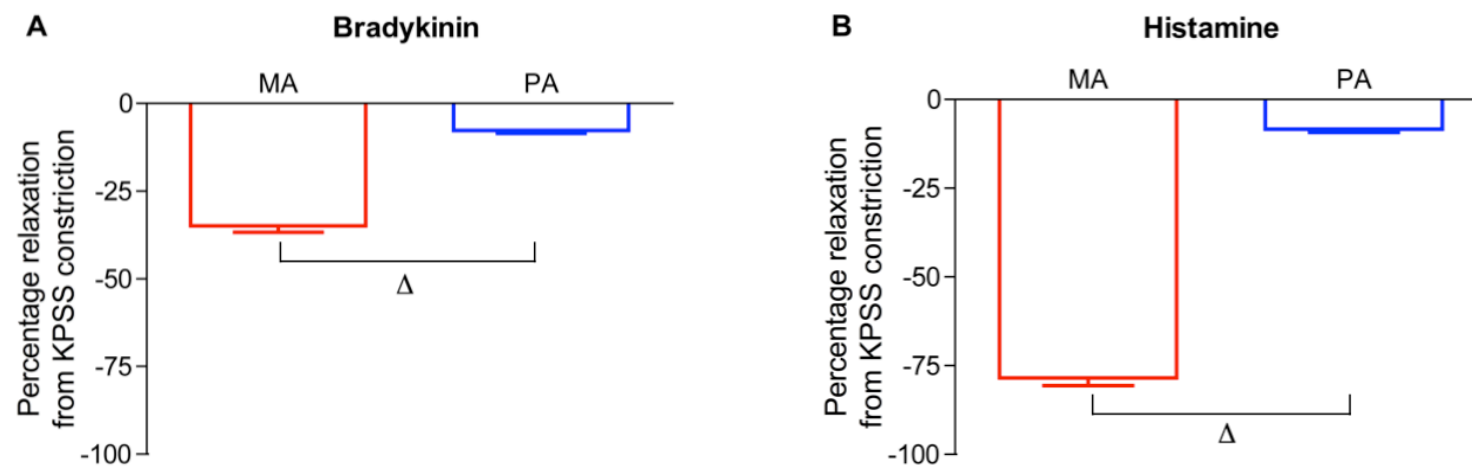


Figure 5.4: Summary data of maximal responses induced by bradykinin and histamine in human myometrial and placental arteries pre-constricted with 60 mM KPSS. Maximal responses to 10^{-6} M bradykinin (A) and to 10^{-5} M histamine (B) are expressed as percentages of the constriction obtained with 60 mM KPSS. MA: Myometrial Arteries, PA: Placental Arteries. Δ Statistical difference relative to MA.

5.5. Effects of YC-1 and SNP on pre-constricted human myometrial and placental arteries

5.5.1. Assessment of YC-1 induced responses in KPSS-constricted myometrial and placental arteries

Figure 5.5 shows original tracings of three individual intact human MA exposed to 60 mM KPSS followed by DMSO (A), 60 mM KPSS followed by 10^{-6} M YC-1 (B) or 60 mM KPSS followed by 3×10^{-5} M YC-1 (C). Figure 5.5A demonstrates that KPSS induced a sustained constriction. Figures 5.5B and 5.5C illustrate that 10^{-6} M and 3×10^{-5} M YC-1, respectively, induced relaxatory responses in the pre-constricted MA, which, in these experiments, reached 32 % and 99 % of the KPSS pre-constrictions, respectively. The relaxations reached plateau at 16 minutes and 7 minutes, respectively.

Figure 5.6 shows original tracings of three individual intact human PA exposed to similar conditions. Figure 5.6A demonstrates that 60 mM KPSS induced a constriction. Figures 5.6B and 5.6C illustrate that addition of both concentrations of YC-1 induced relaxations in the KPSS pre-constricted arteries. In this instance, 10^{-6} M YC-1 induced a relaxation of 9.5 % relative to the KPSS constriction, which reached plateau at 15 minutes, whilst 3×10^{-5} M YC-1 induced a relaxation of 97 %, which reached plateau at 12 minutes.

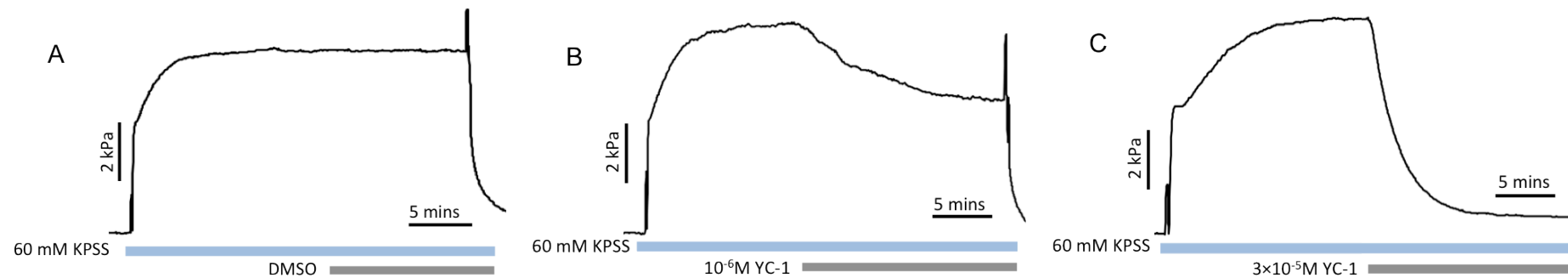


Figure 5.5: Effect of YC-1 in three individual intact myometrial arteries constricted with 60 mM KPSS. A: First artery exposed to 60 mM KPSS. B: Second artery exposed to 60 mM KPSS, followed by 10^{-6} M YC-1. C: Third artery exposed to 60mM KPSS, followed by 3×10^{-5} M YC-1.

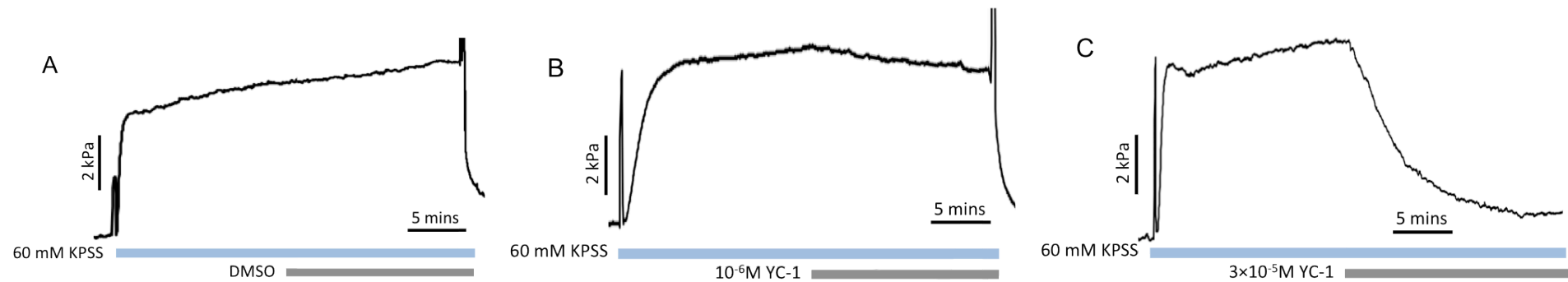


Figure 5.6: Effect of YC-1 in three individual intact placental arteries constricted with 60 mM KPSS. A: First artery exposed to 60 mM KPSS. B: Second artery exposed to 60 mM KPSS, followed by 10^{-6} M YC-1. C: Third artery exposed to 60mM KPSS, followed by 3×10^{-5} M YC-1.

Figure 5.7 shows the group mean \pm SEM responses to incrementing concentrations of YC-1 (10^{-7} M, 3×10^{-7} M, 10^{-6} M, 3×10^{-6} M, 10^{-5} M and 3×10^{-5} M) in MA and PA. YC-1 induced greater relaxations in MA compared to PA, particularly at the sub-maximal concentration 10^{-6} M (MA: relaxation of 32.7 ± 6.87 %, $n = 5$ versus PA: 6.41 ± 3.70 %, $n = 6$). Mean relaxations at maximal concentration of YC-1 (3×10^{-5} M) were not different between MA and PA (MA: relaxation of 94.6 ± 5.35 %, $n = 5$ versus 93.6 ± 2.72 %, $n = 6$), however the rate of relaxation in MA was greater than that in PA, as highlighted by the time at which half the maximal relaxation ($t_{1/2}$) was reached. MA reached its $t_{1/2}$ at 3.77 ± 1.35 minutes, whilst PA reached it at 6.36 ± 0.21 minutes.

Figure 5.8 shows the group mean \pm SEM responses over 20 minutes to 10^{-6} M YC-1 in MA and PA. The respective vehicle controls (VC) were different between MA and PA (MA_{VC}: increase of 1.71 ± 1.22 %, $n = 5$ versus PA_{VC}: increase of 10.3 ± 1.67 %, $n = 6$). Both artery types relaxed in the presence of the sGC activator compared to their respective vehicle controls (VC) (MA_{YC-1}: relaxation of 32.7 ± 6.87 %, $n = 5$ and PA_{YC-1}: relaxation of 6.41 ± 3.70 %, $n = 6$). Additionally, MA relaxed more to 10^{-6} M YC-1 than PA.

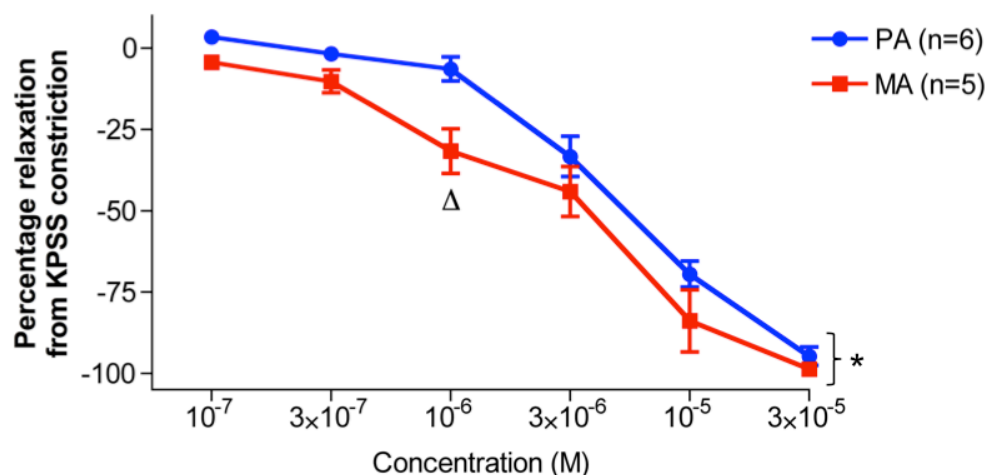


Figure 5.7: Summary data of maximal responses induced by YC-1 in human myometrial and placental arteries pre-constricted with 60 mM KPSS. Maximal responses to incrementing concentrations of YC-1 (10^{-7} M, 3×10^{-7} M, 10^{-6} M, 3×10^{-6} M, 10^{-5} M and 3×10^{-5} M) are expressed as percentages of the constriction obtained with 60 mM KPSS. MA: Myometrial Arteries, PA: Placental Arteries. * Statistical difference between MA and PA responses to YC-1. Δ Statistical difference relative to MA at the specified concentration.

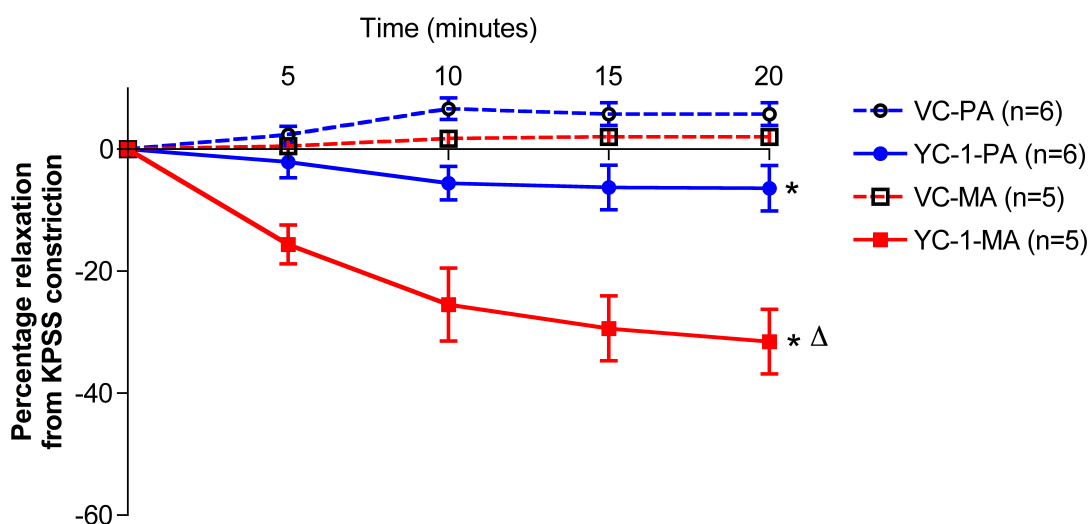


Figure 5.8: Summary data of responses induced by 10^{-6} M YC-1 in human myometrial and placental arteries pre-constricted with 60 mM KPSS. Responses to 10^{-6} M YC-1 are expressed as percentages of the constriction obtained with 60 mM KPSS over a 20-minute time period. MA: Myometrial Arteries, PA: Placental Arteries, VC-MA: Vehicle Control for MA, VC-PA: Vehicle Control for PA. * Statistical difference relative to the respective VC. Δ Statistical difference relative to MA.

5.5.2. Assessment of SNP-induced responses in KPSS-constricted myometrial and placental arteries

Figure 5.9 shows original tracings of three individual intact human MA exposed to 60 mM KPSS followed by ddH₂O (A), 60 mM KPSS followed by 3×10^{-8} M SNP (B) or 60 mM KPSS followed by 10^{-5} M SNP (C). Figure 5.9A demonstrates that KPSS induced a sustained constriction over time. Figures 5.9B and 5.9C illustrate that 3×10^{-8} M and 10^{-5} M SNP, respectively, induced relaxatory responses in the pre-constricted MA. In this experiment, the SNP-induced relaxations reached 14 % and 66 % of the KPSS constriction, which reached plateau at 9 minutes and 6 minutes, respectively.

Figure 5.10 shows original tracings of three individual intact human PA exposed to similar conditions. Figure 5.10A shows that 60 mM KPSS induced a constriction. Figures 5.10B and 5.10C demonstrate that both concentrations of SNP induced relaxations in the KPSS pre-constricted arteries. In this instance, 3×10^{-8} M SNP induced a relaxation of 52 % relative to the KPSS constriction, which reached plateau at 18 minutes and 10^{-5} M SNP induced a relaxation of 72 %, which reached plateau at 7 minutes.

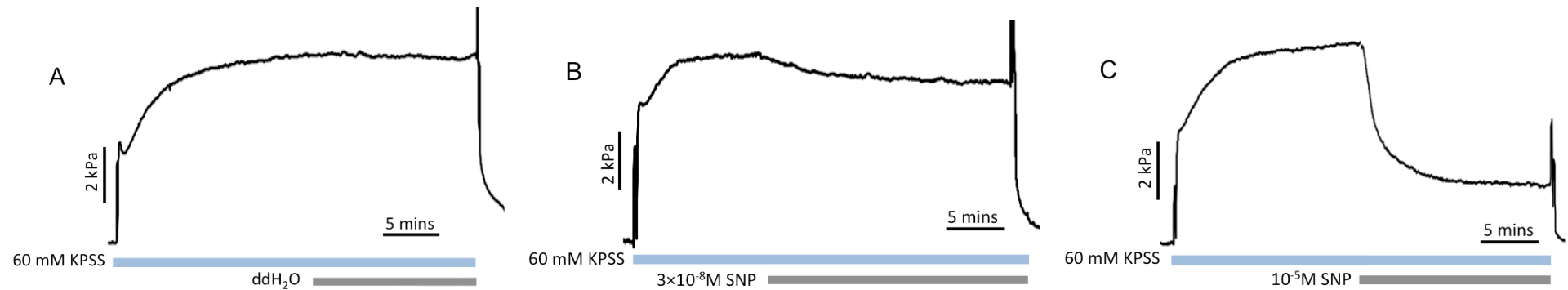


Figure 5.9: Effect of sodium nitroprusside in three individual intact myometrial arteries constricted with 60 mM KPSS. A: First artery exposed to 60 mM KPSS. B: Second artery exposed to 60 mM KPSS, followed by 3×10^{-8} M sodium nitroprusside (SNP). C: Third artery exposed to 60 mM KPSS, followed by 10^{-5} M SNP.

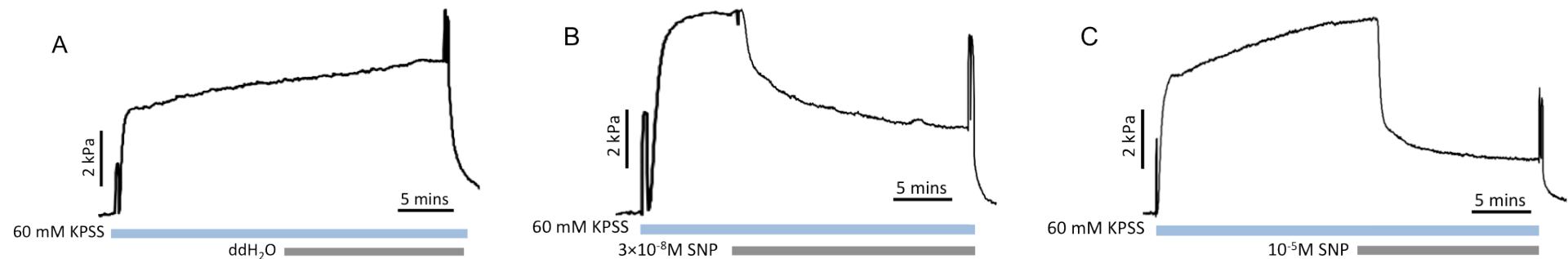


Figure 5.10: Effect of sodium nitroprusside in three individual intact placental arteries constricted with 60 mM KPSS. A: First artery exposed to 60 mM KPSS. B: Second artery exposed to 60 mM KPSS, followed by 3×10^{-8} M sodium nitroprusside (SNP). C: Third artery exposed to 60 mM KPSS, followed by 10^{-5} M SNP.

Figure 5.11 shows the group mean \pm SEM responses to incrementing concentrations of SNP (10^{-10} M, 10^{-9} M, 10^{-8} M, 3×10^{-8} M, 10^{-7} M, 10^{-6} M and 10^{-5} M) in MA and PA. There was no difference in the mean maximal relaxation at maximal concentration of SNP (10^{-5} M) between the artery types (MA: relaxation of 64.0 ± 4.46 %, $n = 7$ versus PA: relaxation of 73.6 ± 5.19 %, $n = 6$) and their rates of relaxation were similar, as highlighted by their $t_{1/2}$. MA reached its $t_{1/2}$ at 3.29 ± 1.25 minutes, whilst PA reached it at 3.52 ± 0.61 minutes. However, mean relaxations were greater in PA compared to MA at the following sub-maximal concentrations of SNP: 10^{-8} M (MA: relaxation of 3.99 ± 2.23 %, $n = 7$ versus PA: 43.6 ± 10.0 %, $n = 6$), 3×10^{-8} M (MA: relaxation of 14.5 ± 3.31 %, $n = 7$ versus PA: 55.1 ± 7.14 %, $n = 6$) and 10^{-7} M (MA: relaxation of 23.4 ± 5.25 %, $n = 7$ versus PA: 63.6 ± 2.84 %, $n = 6$).

Figure 5.12 shows the group mean \pm SEM responses over a time-course of 20 minutes to a sub-maximal dose of 3×10^{-8} M SNP in MA and PA. Constrictions to KPSS differed between MA and PA (MA: 10.7 ± 0.60 kPa, $n = 7$ versus PA: 6.35 ± 0.38 kPa, $n = 6$). Both artery types relaxed in the presence of the NO donor compared to their respective VC (MA_{SNP}: relaxation of 14.5 ± 3.31 % versus MA_{VC}: no change at 0.01 ± 0.22 %, $n = 7$ and PA_{SNP}: relaxation of 55.1 ± 7.14 % versus PA_{VC}: increase of 15.1 ± 6.06 %, $n = 6$). The mean maximal relaxation to 3×10^{-8} M SNP in MA was lower than that in PA.

These results may highlight a greater sensitivity to SNP in placental compared to myometrial arteries pre-constricted with high K^+ .

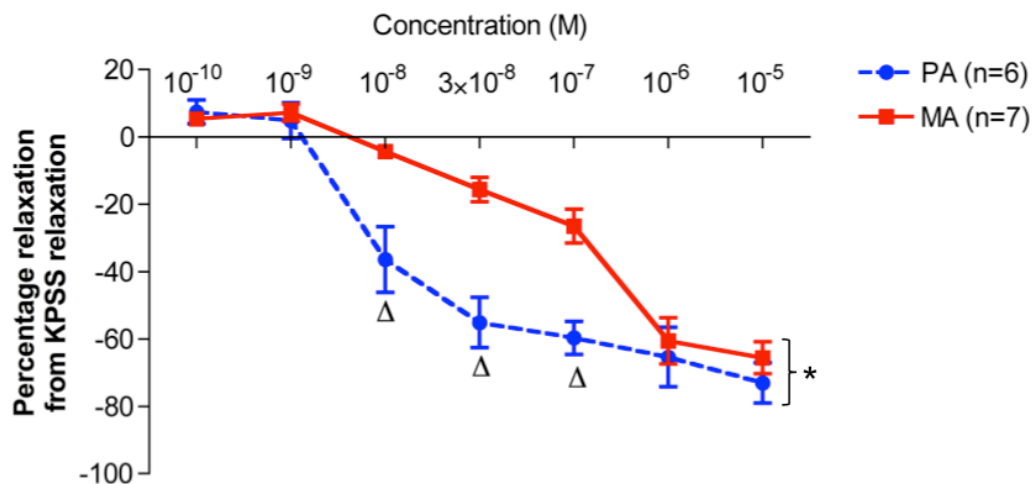


Figure 5.11: Summary data of responses induced by sodium nitroprusside in human myometrial and placental arteries pre-constricted with 60 mM KPSS. Responses to incrementing concentrations of SNP (10^{-10} M, 10^{-9} M, 10^{-8} M, 3×10^{-8} M, 10^{-7} M, 10^{-6} M and 10^{-5} M) are expressed as percentages of the constriction obtained with 60 mM KPSS. MA: Myometrial Arteries, PA: Placental Arteries. * Statistical difference between MA and PA responses to SNP. Δ Statistical difference relative to MA at the specified concentrations.

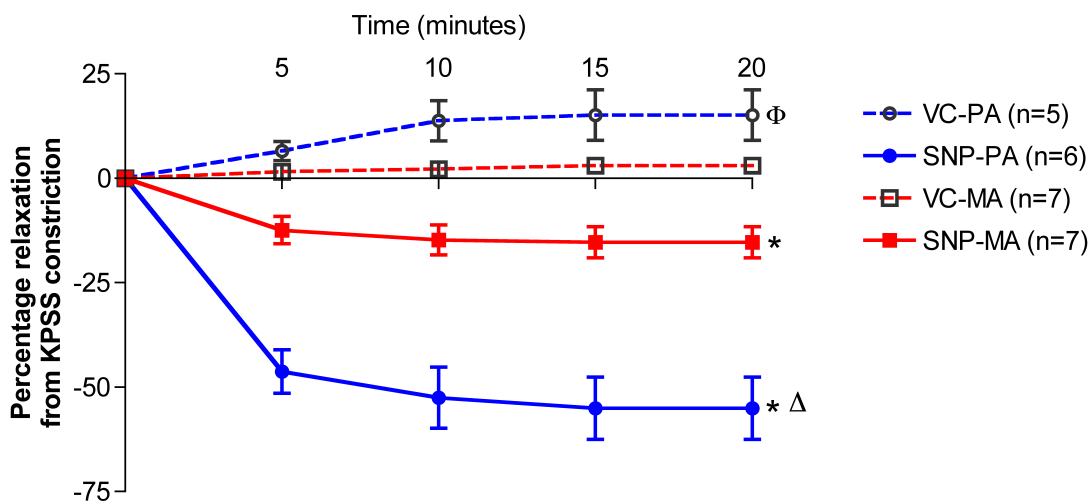


Figure 5.12: Summary data of responses induced by 3×10^{-8} M sodium nitroprusside in human myometrial and placental arteries pre-constricted with 60 mM KPSS. Responses to 3×10^{-8} M SNP are expressed as percentages of the constriction obtained with 60 mM KPSS over a 20 minute time period. MA: Myometrial Arteries, PA: Placental Arteries, VC-MA: Vehicle Control for MA, VC-PA: Vehicle Control for PA. SNP: sodium nitroprusside. * Statistical difference relative to the respective VC. Δ Statistical difference relative to SNP-MA. Φ Statistical difference relative to VC-MA.

5.6. Discussion

This study sought to assess the effects of endothelial-dependent and –independent relaxatory agents on pre-constricted human MA and PA. Bradykinin, or histamine, had considerable relaxatory influences on MA but limited effect on PA. The sGC activator, YC-1, and the NO donor SNP, induced significant relaxations in pre-constricted human MA and PA. YC-1 induced greater effects in MA than PA. These results again pointed to the possibility of greater relaxatory sensitivities over the sGC/PKG axis in MA compared to PA. A surprising finding was that PA displayed greater relaxations at sub-maximal concentrations of SNP compared to MA. This may indicate higher sensitivities to the NO donor in arteries from the placenta compared to those from the myometrium.

Prior to the assessments of SNP- and YC-1-induced relaxations in human MA and PA, an initial evaluation of the effects of O₂ was carried out in PA to determine whether similar O₂ levels as those observed in the myometrial circulation (20 %) (Rodesch et al., 1992) would alter vascular relaxation capacity of PA. This study showed that endothelium-dependent relaxations, as assessed by BK and His, were similar (and small) at 20 % and 7 % O₂, as were endothelium-independent relaxations induced by the NO donor, SNP. YC-1-induced relaxations were, however, greater at higher (20 %) than lower (7 %) O₂ levels. Smaller relaxations in PA at low versus high O₂ may have falsely highlighted differences in relaxations between MA and PA. Previous studies had not reached a consensus as to the effects of O₂ on PA vascular reactivity and were carried primarily in U46619-pre-constricted arteries. McCarthy *et al* (1994) reported that the sensitivity to SNP was reduced at high O₂ (20 %) (McCarthy et al., 1994), whilst Wareing *et al* showed that responses to SNP were similar at higher (20 %) and lower (7 %) O₂ levels and only altered relaxation capacity in hypoxic conditions (2 % O₂) (Wareing et al., 2003b, Wareing et al., 2006b). Thus, the present results and prior studies supported the use of similar O₂ levels in both PA and MA in the assessment of SNP- and YC-1-induced effects on the two artery types, as it would not likely highlight any differences, which may not have physiological relevance.

In this study, the assessment of YC-1 and SNP-induced responses in arteries pre-constricted via activation of Ca²⁺ channels, following addition of 60 mM K⁺, was a novel experimental design in human arteries. Most studies have carried out endothelial-independent relaxatory studies on arteries pre-constricted via activation of G protein-

coupled receptors with agonists such as U46619 (McCarthy et al., 1994, Mills et al., 2007a), ET-1 (McCarthy et al., 1994), NE (McCarthy et al., 1993) or PE (Lu et al., 2008). In this study, 60 mM K^+ induced substantial constrictions in both MA and PA and these constrictions were greater in MA than PA. High K^+ depolarises the VSMC membrane, activating voltage-gated Ca^{2+} -channels, which allow an influx of Ca^{2+} in the cell (Himpens and Somlyo, 1988). Constriction of VSMC is then initiated via formation of the Ca^{2+} -CaM complex, activation of MLCK and subsequent phosphorylation of MLC₂₀ (Himpens and Somlyo, 1988, Somlyo and Himpens, 1989). Several explanations may account for the difference in contractile capacities observed between MA and PA. First, it has been suggested that SMC contain two isoforms of MLCK, long and small. The long MLCK is thought to display a higher binding affinity for actin filaments compared to the short MLCK (Blue EK et al., 2002, Smith et al., 2002). A higher level of long MLCK in MA may induce greater contractile capacities to high K^+ in MA compared to PA. However, telokin and short (130 kDa) MLCK expression levels were found to be similar between MA and PA (Chapter 4), therefore long MLCK levels may also be similar between the two artery types. A second explanation may lie in the vessel structure of MA and PA. It has been shown that PA contain a thicker medial layer with the SMC separated by considerably more amounts of ECM than MA (Sweeney et al., 2006b). The development of force in PA may therefore be greatly reduced due to a lower number of SMC per selected area and thus less communication between SMC to propagate the contraction. Finally, differing expression levels of the voltage-gated Ca^{2+} -channels may also lead to differing contractile capabilities between the two artery types, although, to date, there are no reports comparing the expression levels of these channels between MA and PA. In addition to the lower K^+ -induced contractile capacity of PA versus MA, PA also presented a steady increase to high K^+ over time and, contrary to MA, did not plateau. The reason for this response is yet to be determined. Such observations were not reported in the literature, however similar slow steady increases were shown in U46619-constricted PA (Mills et al., 2007b), which may reflect a more tonic SM phenotype of PA compared to MA (Sweeney et al., 2008).

This study also extended previous suggestions that relaxatory capacities to endothelial-dependent vasodilators differed between MA and PA, by comparing for the first time in the same controlled experimental circumstances, the effects of two different agents across each artery type. As detailed in Chapter 2, Section 2.4, endothelial function of arteries was routinely tested by the actions of BK on KPSS pre-constricted arteries. The

relaxations of arteries to BK reported in the experimental sub-series of this chapter were similar to the responses observed overall in MA and PA presented in Chapter 2. MA displayed greater relaxations to both BK and His compared to PA, also consistent with former reports. Sweeney *et al* (2008) showed that BK induced relaxations up to 94 % in U46619-constricted (10^{-6} M) MA, whilst relaxations in PA were small (10 %) (Sweeney et al., 2008). Additionally, Wareing *et al* (2004) reported BK-induced (10^{-10} – 10^{-6} M) relaxations of up to 78 % and 69 % from arginine vasopressin (AVP)- and U46619-constricted MA, respectively (Wareing et al., 2004). The same group also highlighted the lack of significant responses to BK (10^{-10} – 10^{-6} M) of term PA pre-constricted with either AVP (10^{-8} M), U46619 (10^{-6} M) or high K^{+} (Wareing, 2002). Moreover, incremental doses of His (10^{-8} - 10^{-6} M) induced small relaxations (up to 17 %) in PA pre-constricted to sub-maximal, but not maximal, concentrations of U46619 (10^{-7} M) (Mills et al., 2007b). The same vasodilator also induced concentration-dependent relaxations (10^{-10} – 10^{-5} M), which reached 70 %, in intact isolated small uterine arteries pre-constricted with 30 mM KCl (Spitaler et al., 2002). Thus, relaxations to BK and His observed in this study in MA and PA confirmed the difference in endothelial-dependent responses between the myometrial and placental circulations.

The study also reported greater relaxations in MA compared to PA at the sGC/PKG level as shown with the addition of the sGC activator, YC-1, at sub-maximal concentrations (10^{-7} M, 3×10^{-7} M, 10^{-6} M). This difference was not observed over the higher concentrations of YC-1 (3×10^{-6} M, 10^{-5} M, 3×10^{-5} M), although relaxations at maximal concentrations of YC-1 were faster in MA than PA. These results may highlight a greater sensitivity at the sGC level in MA compared to PA. The concentrations of YC-1 using in this study were similar or higher to those reported. Bainbridge *et al* (2002) used 10^{-4} M to show an increase in perfusion pressure in a placental cotyledon, whilst Seitz *et al* (1999) reported relaxations induced by 3×10^{-5} M YC-1, albeit in KPSS-constricted rat aorta (Seitz et al., 1999).

YC-1, a benzyl indazole cell-permeable derivative (Tulis et al., 2000) is known to activate sGC, increasing its activity by around 10 fold, independently of NO (Mulsch et al., 1997). The activating effects of YC-1 were thought to be highly dependent upon the presence of the reduced Fe^{2+} prosthetic heme moiety of sGC. Its removal was thought to abolish any NO- or heme-dependent activator-induced enzyme activation (Ignarro et al., 1986, Foerster et al., 1996). However, YC-1 has also been suggested to activate sGC

independently of the heme moiety, with greater activation potential in the presence of the heme nonetheless (Martin, 2001). YC-1 may have induced relaxations in MA and PA via: (i) PKG activation and modification of myofilament-associated events (cf. Chapter 1, Figure 1.8) and/or (ii) PKG-induced activation of large-conductance Ca^{2+} -activated K^{+} -channels (BK_{Ca}) (cf. Chapter 1, Figure 1.7). Following activation of sGC by YC-1, production of cGMP and activation of PKG likely induced vasodilation in MA and PA (Waldman and Murad, 1987, Friebe and Koesling, 2003). The effect of YC-1 on PKG (and sGC) was shown in studies on human alveolar basal epithelial cells, which reported that addition of a PKG inhibitor, KT5823, and a sGC inhibitor, ODQ, reversed the stimulatory effect of YC-1 on the expression of the cyclooxygenase enzyme 2 (Chang et al., 2002). PA (300 – 700 μm) are known to express BK_{Ca} in both EC and VSMC (Sand et al., 2006). A role for PKG in the activation of BK_{Ca} channels was shown in studies in human coronary arterioles, which reported that inhibition of PKG (by Rp-8-Br-PET-cGMP), but not sGC (by ODQ), mimicked the inhibition of flow and H_2O_2 -induced dilation observed following BK_{Ca} inhibition by iberiotoxin (Zhang et al., 2012). Meanwhile, a direct effect of YC-1 was shown on another K^{+} channel, namely the voltage-dependent K^{+} channel. A recent study in rabbit coronary SMC showed a YC-1-induced inhibition of these channels, which was not observed following pre-treatment with another sGC activator (Bay 41-2272), a sGC inhibitor (ODQ) or a PKG inhibitor (Rp-8-Br-PET-cGMP) (Park et al., 2010). Thus, the putative actions of YC-1 on the contractile filaments and/or BK_{Ca} channels are likely via direct activation of PKG. Measurements of PKG activation and/or cGMP elevation would be necessary to confirm these results.

This study also assessed the role of NO in human MA and PA, using SNP. This was the nitrovasodilator of choice, as Zhang *et al* (2001) had shown that, in PA, SNP and GTN were equipotent and represented the two nitrovasodilators with the highest potency, compared to other vasodilators, such as SNAP, SNG or NaNO_2 (Zhang, 2001). SNP is a “spontaneous” NO donor, which releases NO rapidly upon distribution in aqueous solvents and does not require enzymatic reduction or hydrolysis for this process (Verner, 1974). Degradation of SNP also generates two other biologically active products besides NO, notably cyanide and free iron (Verner, 1974, Schroeder, 2006). The free cyanide radicals, which are released following reaction of the iron atom from the nitroprusside radical with free sulphydryl groups, are thought to then be linked to sulphydryl groups and form thiocyanate, which is less toxic (Verner, 1974). Rapid

actions of SNP were observed in this study as relaxations reached a plateau within 5 – 10 minutes in both MA and PA. This study has shown that SNP induced relaxations in human MA and PA over a range of concentrations ($3 \times 10^{-8} - 10^{-5}$ M). Relaxations observed in pre-constricted MA and PA were similar to those reported in previous studies, in which the main contractile agent was U46619. McCarthy *et al* (1994) reported concentration-dependent relaxations to SNP ($10^{-9} - 10^{-5}$ M), with maximal relaxations of 65 % in U46619-constricted arteries (McCarthy *et al.*, 1994), while Zhang *et al* (2001) showed that PA, pre-constricted with submaximal concentrations of U46619 ($3 \times 10^{-9} - 10^{-7}$ M), also displayed concentration-dependent relaxations ($1.3 \times 10^{-8} - 5.7 \times 10^{-5}$), which reached a maximum of 98 % (Zhang *et al.*, 2001). Wareing *et al* (2006) further confirmed these findings when U46619-constricted PA were shown to relax up to 90 % to a range of SNP ($10^{-10} - 10^{-4}$ M) (Wareing *et al.*, 2006b). Finally, SNP-induced relaxations of U46619-constricted term MA were shown to reach 65 – 70 % to a similar range of SNP as used in this study ($10^{-10} - 10^{-5}$ M) (Andersen *et al.*, 2011).

In this study, SNP-induced vasodilation likely occurred via two pathways working in synergy. The first involved activation of the NO/cGMP/PKG pathway. The release of NO is known to activate sGC (Friebe and Koesling, 2003) leading to the production of cGMP (Waldman and Murad, 1987), activation of PKG and VSMC relaxation (Warner *et al.*, 1994). The second may involve direct activation of BK_{Ca} by NO and, as highlighted above, the downstream-activated PKG. The direct effect of NO on BK_{Ca} was shown following addition of a BK_{Ca} inhibitor, charybdotoxin, which partly inhibited SNAP-induced relaxations and which were further inhibited following addition of ODQ (sGC inhibitor) (Sand *et al.*, 2006). The exact mechanisms by which NO may directly activate BK_{Ca} are still unknown. Studies in human skin fibroblasts highlighted the stimulatory effect of PKG on BK_{Ca} via SNP following inhibition of these channels with the addition of a sGC inhibitor (ODQ) and PKG inhibitor (KT5823) (Lim *et al.*, 2005). Voltage-dependent K⁺ channels may also play a role in hyperpolarising the membrane, as studies in rat mesenteric arteries have suggested that NO activates both sGC and voltage-dependent K⁺ channels (Irvine *et al.*, 2003). Thus, SNP seems to influence both the SMC membrane potential, with its direct effect on K⁺ channels, and myofilaments with its stimulus on the sGC/PKG axis.

A surprising finding in this study was the observation that sub-maximal concentrations of SNP (10^{-8} M, 3×10^{-8} M and 10^{-7} M) induced greater relaxations in PA compared to MA. Mean maximal relaxations at higher concentrations of SNP (10^{-6} M and 10^{-5} M) were not different between the two artery types. This may highlight a difference in sensitivity to SNP, rather than a difference in relaxatory capacity between MA and PA. The increased oxidative effect elicited by SNP may, at least partly, explain this observation. Onset of circulation during fetoplacental development is associated with an increase in oxygen concentration (Jauniaux et al., 2000) and in rates of ROS generation (Wisdom et al., 1991). A study on intact PA reported greater relaxations to SNP in the presence of ROS generating agonists (xanthine and xanthine oxidase) compared to controls (Mills, 2009), highlighting a sensitivity of PA to ROS. This sensitivity may not be present in MA, eliciting the observed difference in relaxations at sub-maximal concentrations of SNP. A second explanation for the differences in responses to SNP and YC-1 between the two artery types considers the lower constrictions to high K^+ in PA compared to MA. Membrane voltage change resulting from depolarisation to high K^+ may be lower in PA than MA, resulting in less Ca^{2+} influx into the cell acting on the myofilaments in PA. The direct actions of SNP on K^+ channels may therefore be effected on a less depolarised membrane, making it more susceptible to inhibition of these channels, thereby generating greater relaxations of PA compared to MA. Meanwhile, the main effects of YC-1 may be via PKG activation and its actions on myofilaments, resulting in greater relaxations in MA compared to PA. A third explanation may reside in differing expression levels and/or activities of K^+ channels between MA and PA.

In summary, this study has reported a surprising finding in the potential difference in sensitivity to the NO donor between MA and PA. However, upon activation of sGC with YC-1, MA displayed greater sensitivities than PA, in accordance with previous observations at the PKG level (Chapter 4). It is unclear, why PA exhibited low endothelial-dependent relaxations and lower endothelial-independent sensitivities at the sGC and PKG levels compared to MA, yet presented enhanced sensitivities at the NO level. However, they may likely result from differing interactions between the actin-myosin filaments and membrane channel stimulations, rather than differing expressions of proteins involved in the relaxatory pathway, since assessment of some of these proteins revealed no difference in expression between the two artery types (Chapter 4).

Chapter 6

General Discussion

This study set out to answer three principal physiological queries:

- (i) Do human MA and PA display agonist-mediated Ca^{2+} -sensitising responses over a range of $[\text{Ca}^{2+}]$?
- (ii) Does the phenomenon of Ca^{2+} -desensitisation occur in MA and PA and is it mediated via the cGMP/PKG pathway?
- (iii) Are there any differences in the contractile and/or relaxatory responses between the two artery types?

A first contribution of this study reported that the phenomenon of Ca^{2+} -sensitisation occurs over a range of $[\text{Ca}^{2+}]$ in human permeabilised arteries from the myometrium and placenta. Whilst constrictions to Ca^{2+} alone were shown to be similar between the two artery types, PA displayed lower sensitivities to Ca^{2+} than MA. SM force is predominantly determined by a balance between activities of MLCK and MLCP, with Ca^{2+} directly increasing the activity of MLCK (Fisher, 2010). The observed difference between MA and PA may originate from an innate difference in sensitivities to Ca^{2+} of the myofilaments. Table 6.1 illustrates differences in concentrations of solutes, vasoconstrictors and vasodilators present in the fetal (placental) and maternal circulations and thought to participate in regulating their tone. Of note is the fact that concentrations of several tone regulatory contractile and relaxatory agents have not been recorded in fetal circulations. This highlights a lack of knowledge of the building blocks involved in regulating vascular tone of the fetoplacental circulation. Concentrations of the physiologically important potassium, sodium, calcium and chloride have all been reported higher in the fetal compared to maternal vasculature (Delivoria-Papadopoulos et al., 1967, Faber and Thornburg, 1981, Mohammed et al., 1992, Bissonnette et al., 1994), which may explain the observed differences in their contractile and/or relaxatory responses. Indeed, this difference in concentrations of Ca^{2+} may have rendered the maternal circulation more sensitive to lower $[\text{Ca}^{2+}]$ than the placental vasculature, leading to the greater contractile responses at sub-maximal Ca^{2+} observed in MA compared to PA. Similarly, greater $[\text{K}^+]$ and $[\text{Na}^+]$ in the fetal versus maternal circulation may also have impacted on the amplitude of high K^+ -induced constrictions in intact MA and PA. Opening of voltage-gated Ca^{2+} channels is the result of a change in membrane potential towards more positive values (depolarisation). Greater initial K^+ levels in PA may regulate the membrane potential at rest to be more positive. Addition of high K^+ may therefore result in less membrane voltage changes or depolarisation and less Ca^{2+} entering the cell to induce SMC constriction, which may explain the observed

lower high K^+ -induced constrictions in PA compared to MA. Indeed, constrictions induced by high Ca^{2+} (pCa4.5) reached similar magnitudes in both artery types; the differences between MA and PA may therefore reside at the membrane potential, rather than general contractile capacities.

Table 6.1: Concentrations of ions, vasodilators and vasoconstrictors in human maternal and fetal circulations.

Solute	Mean maternal concentration (\pm SEM)	Mean fetal concentration (\pm SEM)	References
Calcium	2.1 \pm 0.1 mmol/L water	2.6 \pm 0.1 mmol/L water	(Faber and Thornburg, 1981), (Delivoria-Papadopoulos et al., 1967), (Abramovich et al., 1987)
Sodium	135.4 \pm 2.4 mmol/L water	137.0 \pm 2.8 mmol/L water	(Faber and Thornburg, 1981), (Flexner et al., 1948)
Potassium	4.3 \pm 0.1 mmol/L water	4.8 \pm 0.2 mmol/L water	(Mohammed et al., 1992), (Canning and Boyd, 1984)
Chloride	107 \pm 2.0 mmol/L water	109 \pm 2.3 mmol/L water	(Faber and Thornburg, 1981), (Bissonnette et al., 1994)
Thromboxane A₂	0.76 nmol/L	0.510 nmol/L (term gestation) 0.286 nmol/L (peripheral plasma)	(Mitchell and Robinson, 1978), (Sellers et al., 1981)
Bradykinin	10 nmol/L		(Melmon et al., 1968)
Prostaglandin F_{2α}	19 nmol/L		(Craft et al., 1973)
Prostaglandin E₂	0.36 nmol/L		(MacKenzie et al., 1980)
Endothelin-1	1.08 pmol/L	0.361 pmol/L	(Bracero et al., 1995)
Histamine		470.9 \pm 109.8 nmol/L	(Lorenz et al., 1972), (Kimera, 1999)
Angiotensin II	0.49 nmol/L		(Broughton Pipkin and Smales, 1975)

Conversely to major ion concentrations, other central vasoactive agents were reported much lower in the fetal compared to the maternal circulation (Table 6.1), such as thromboxane A₂ (TXA₂) or ET-1, which may explain the results obtained in agonist-mediated Ca²⁺-sensitisation. Following addition of the potent TXA₂ mimetic, U46619, the sensitisation capacities in PA were raised, resulting in constrictions in this artery type to reach those in MA. The lower agonist levels in fetoplacental blood vessels may have led to an increase in sensitivity of this vasculature to contractile factors. The assessment of responses to vasoconstrictive agonists in controlled Ca²⁺ conditions attempted to elucidate differences in sensitivities to both solute Ca²⁺ and agonist (TXA₂, ET-1, SIP) in MA and PA. During pregnancy complications, such as preeclampsia and gestational hypertension, levels of the vasoconstrictors TXA₂, ET-1 and angiotensin II have been shown to greatly increase (VanWijk et al., 2000, George and Granger, 2011). These are, in part, responsible for the increased peripheral vascular resistance and vasoconstriction observed in these disorders (Visser and Wallenburg, 1991). The increased sensitivity of PA myofilaments to Ca²⁺ in the presence of TXA₂, as observed in the present study, may be exacerbated in the fetoplacental circulations of women with preeclampsia, intensifying existing differences between maternal and placental vasculature.

The central contribution of this study underlined differences in the relaxatory patterns of MA and PA, which may highlight differing sensitivities to vasodilators involved in the regulation of myometrial and placental circulations.

The first assessment highlighted the phenomenon of Ca²⁺-desensitisation. The vasodilator mimetic 8-br-cGMP induced relaxations in MA and PA via activation of PKG and desensitisation of the myofilaments to constant [Ca²⁺]. PKG induced greater relaxations in both constricted and sensitised MA compared to PA, however the difference in sensitivity between the two artery types was not due to differing levels of PKG, as expression of this protein was similar in MA and PA. It may be due to a redistribution of actin-interacting proteins in MA to enhance dissociation of actin filaments with myosin filaments and induce greater and faster relaxation. MA develop phasic-like responses, in that frequent oscillations rising in amplitude develop upon constriction with TXA₂, whilst PA develop steady constrictions at the same agonist concentration (Sweeney et al., 2008), conferring PA a more slow tonic phenotype.

Surprisingly, pregnant (phasic) myometrial SM strips failed to relax upon addition of 8-br-cGMP and PKG levels decreased throughout pregnancy, inferring that the pregnant human myometrium may be insensitive to cGMP/PKG (Cornwell et al., 2001). However, expression levels of two actin filament-associated proteins, caldesmon and calponin, were found to increase during pregnancy and increase cross-bridge dissociation of actin and myosin filaments to induce relaxation (Cornwell et al., 2001). Thus, should MA be predominantly phasic, the difference in responsiveness to cGMP between the myometrial and placental vasculature may result from a decrease in the accessibility of actin to myosin following redistribution of actin-interacting proteins.

PKG is thought to interact with a variety of proteins, which have also been shown to interact with actin or myosin filaments in their phosphorylated state to induce relaxation. Ca^{2+} -desensitisation may have been induced via the direct effects of PKG-interacting proteins on the myofilaments and via the increase in MLCP activity by PKG. Figure 6.1 illustrates the possible signalling mechanisms involved in PKG-mediated desensitisation to Ca^{2+} .

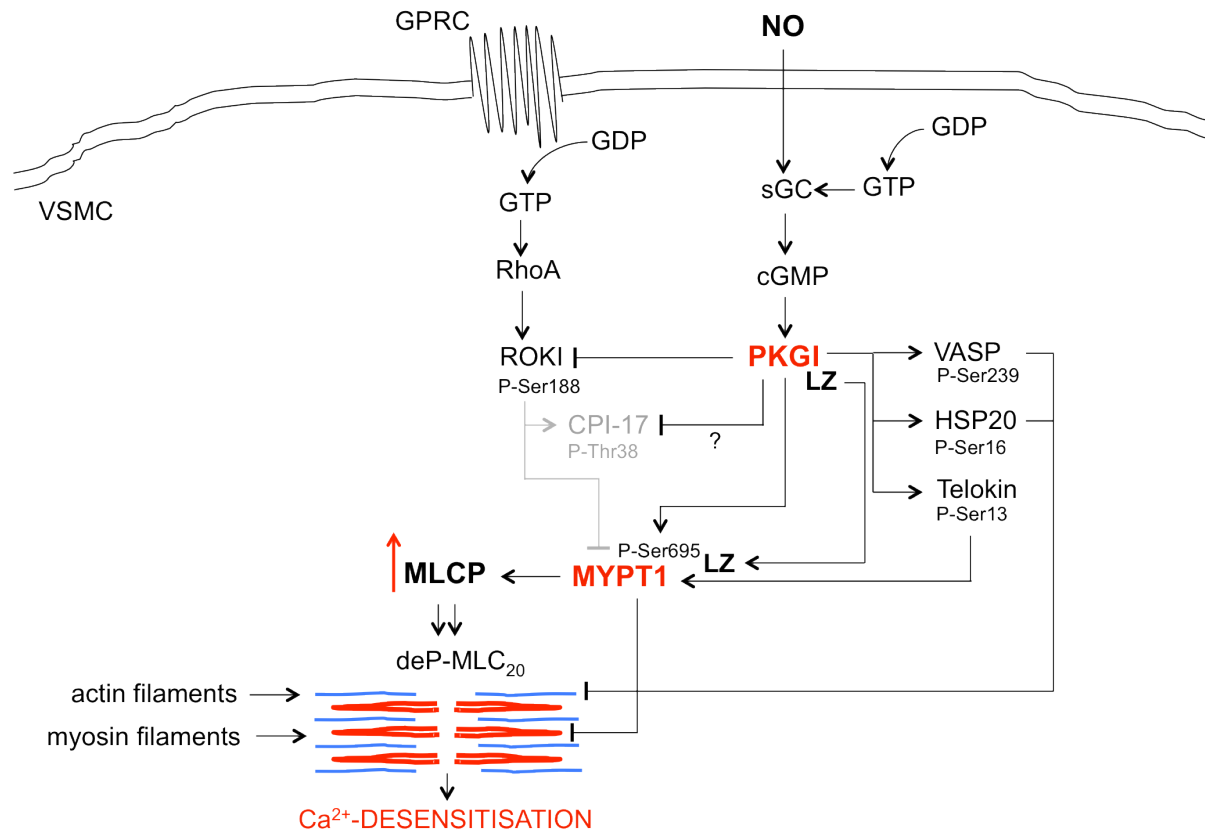


Figure 6.1: Potential mechanisms inducing PKG-mediated Ca^{2+} -desensitisation in human myometrial and placental arteries. VSMC: vascular smooth muscle cell, GPCR: G-protein-coupled receptor, NO: nitric oxide, sGC: soluble guanylate cyclase, GTP: guanosine-5'-triphosphate, GDP: guanosine diphosphate, PKGI: protein kinase G isoform I, LZ: leucine zipper, HSP20: heat shock protein 20, VASP: vasodilator-stimulated phosphoprotein, MLCP: myosin light chain phosphatase, MLC₂₀: myosin light chain 20. P-: phosphorylation site, deP-: dephosphorylation, Ca^{2+} : calcium ion. Red arrow represents an increase in activity. Black arrows: stimulation. Black stop: inhibition. ?: uncertain mechanism. Grey lines: inhibited signalling.

The small heat shock protein 20 (HSP20) likely induced PKG-mediated Ca^{2+} -desensitisation in MA and PA via its interaction with actin filaments following its phosphorylation at Ser-16 by PKG. Phospho-HSP20 was associated with active relaxation of permeabilised bovine carotid SM, but not with MLC_{20} dephosphorylation (Beall et al., 1997, Beall et al., 1999, Rembold et al., 2000). Thus its effects were unlikely mediated via MLCP-induced actions on myosin filaments, rather by its direct association with actin filaments and a second heat shock protein, HSP27 (Tyson et al., 2008a). Both HSP20 and HSP27 were found to co-localise with α -smooth muscle actin in the cytoplasm in human myometrium, although to differing degrees (MacIntyre et al., 2008, Tyson et al., 2008a). HSP27 has also been shown to relocate from the cytoplasm of nonlabouring myometria to the actin cytoskeleton in labouring myometria (MacIntyre et al., 2008). While phospho-HSP27 would stabilise actin filaments for VSMC constriction, phospho-HSP20 may therefore induce relaxation through breaking the actin-myosin cross-bridge following alteration of the actin filaments via its association with HSP27 (and/or other proteins). Thus, Ca^{2+} -desensitisation in MA and PA may have occurred both via phospho-HSP20 interaction with actin filaments inducing their dissociation from myosin filaments and via sequestration of HSP27 to the cytoplasm. This study has found that expression levels of HSP20 were similar in MA and PA. The difference in relaxation observed between MA and PA may therefore result from differences in the phosphorylated states of HSP20 affecting actino-myosin filament interactions.

A second actin-binding protein, known as the small vasodilator-stimulated phosphoprotein (VASP), may also have been involved in inducing Ca^{2+} -desensitisation in MA and PA, by inhibiting actin polymerisation (Reinhard et al., 2001, Kim et al., 2010) and thus actin-myosin interactions following its activation and phosphorylation at Ser-239 by PKG (Smolenski et al., 1998, Schulz et al., 2002, Schafer et al., 2003). There are currently no studies reporting on levels of VASP or phospho-VASP in human MA and/or PA. The differences in relaxations between the two artery types may be due either to differing levels of VASP or, more likely, to greater levels of the phosphoprotein in MA compared to PA, which may result in greater actinomyosin filament dissociations in SMC from the myometrial versus placental circulation.

PKG may also have desensitised the myofilaments of MA and PA to Ca^{2+} via inhibition of the RhoA/ROK pathway by PKGI-induced phosphorylation of ROK at Ser-188

(Sauzeau et al., 2000b, Gudi et al., 2002), which prevented inhibition of MLCP (Dong et al., 1998, Sward et al., 2003, Wang et al., 2002). Similarly, inhibition of the PKC- and ROK-activated CPI-17 by PKGI may also have induced Ca^{2+} -desensitisation by accelerating dephosphorylation of CPI-17 at residue Thr-38 and releasing MLCP inhibition (Bonnevier and Arner, 2004). In addition, greater 8-br-cGMP-induced relaxations were reported in SM sensitised with GTP γ S, ROK and PKC compared to unsensitised (sub-maximally Ca^{2+} -constricted) SM (Bonnevier and Arner, 2004). Similar findings were also observed in the present study and may have resulted from higher levels of dephosphorylated CPI-17 in Ca^{2+} -sensitised compared to Ca^{2+} -constricted arteries. The phosphorylated state of CPI-17 relies upon G protein-coupled-receptor-dependent activation of PKC and ROK, which occurs in pre-sensitised arteries, but unlikely does so in unsensitised arteries. Greater dephosphorylated levels of CPI-17, releasing MLCP inhibition, may have stimulated increases in MLCP activity in Ca^{2+} -sensitised arteries to levels exceeding those observed in Ca^{2+} -constricted vessels, where a balance between MLCK and MLCP activities may have still existed; thus inducing greater relaxations in sensitised arteries compared to Ca^{2+} -constricted ones. MLCP-induced increases in dephosphorylated MLC₂₀ may highlight variations in the accessibility of actin to myosin in SMC from myometrial and placental circulations. CPI-17 protein levels have been reported to be lower in phasic (non-vascular) SM, which incidentally often presented lower sensitivities to NO and/or PKG, than those in arterial, more tonic SM (Woodsome et al., 2001, Fisher, 2010). One may have expected greater levels of CPI-17 in MA compared to PA to explain the increased relaxatory abilities of the former artery type, however, CPI-17 expression levels were found to be similar between MA and PA; the differences may therefore reside in the phosphorylated/dephosphorylated ratios of this protein.

Another suggested mediator of cGMP-mediated Ca^{2+} -desensitisation is telokin, whose phosphorylation at Ser-13 by PKG has been shown to induce relaxations in permeabilised rabbit ileal SM (Wu et al., 1998, Walker et al., 2001) and to enhance MYPT1/MLCP activity (Khromov et al., 2006); however only in conditions, in which the phosphatase was already inhibited (by phosphorylations at Ser-696/853, numbering of human isoform) (Khromov et al., 2012). Relaxations were greater and faster in MA than in PA and studies showed that predominantly fast phasic SM displayed higher telokin levels and greater relaxations compared to slow tonic SM (Choudhury et al., 2004). However, the differences in relaxation between the two artery types, in this

instance, were not explained by differing expressions of telokin, as these were found to be similar in MA and PA. This, once more, underlines the subtle differences between the two circulations, which may not only be explained by differing protein levels. Assessment of phosphorylated telokin at Ser-13 may reveal greater levels in MA compared to PA, which would enhance MLCP affinity for myosin filaments in MA and displace their interaction with actin filaments via dephosphorylation of MLC₂₀ (Khromov et al., 2012).

These protein expression studies highlighted that differences between the two circulations likely occur at the level of their SMC actin and myosin filament interactions.

PKGI may also affect MLCP activity directly, partly via phosphorylating MYPT1 at Ser-695 (human isoform) (Nakamura et al., 1999, Wooldridge et al., 2004) and partly by interacting with its leucine-zipper (LZ) region at its C-terminus (Surks et al., 1999). Phosphorylation of Ser-695 by 8-br-cGMP was shown to prevent phosphorylation of the MLCP-inactivating Thr-696, which is immediately adjacent to Ser-695; thus preventing inhibition of MLCP (Wooldridge et al., 2004). However, phosphorylation at Thr-696 was also shown to decrease by only 50 % with 8-br-cGMP stimulation, whilst the tension of phenylephrine-pre-contracted rabbit femoral arteries and the MLC₂₀ phosphorylation fell to baseline (Nakamura et al., 2007), which indicated that Ser-695 phosphorylation was not solely responsible for PKG-mediated Ca²⁺-desensitisation. The aforementioned PKG-interacting putative proteins and their effects on myofilaments and/or MLCP activity may have induced the remaining fall in tension observed. Such mechanisms may also have been in play in human MA and PA.

Additional regulation of MLCP activity via LZ-LZ interaction with PKGI may also have played a role. Chicken gizzard and aorta SM expression of LZ-negative isoforms were shown to develop a resistance to cGMP as relaxation in response to 8-br-cGMP after Ca²⁺ activation of the myofilaments was abolished as was MLC₂₀ dephosphorylation (Khatri et al., 2001). Additionally, the LZ-negative isoform has been shown to predominate in fast-phasic VSM phenotypes (Huang et al., 2004, Payne, 2004). Consistent with this consensus, small rat mesenteric arteries were found to express predominantly the LZ-negative isoform and to be less responsive to NO/cGMP signalling compared to large conductance vessels signalling (Feletou et al., 1989, Nagao et al., 1992, Sauzeau et al., 2000a). It was proposed that MYPT1 isoforms may be

expressed in a tissue-specific manner throughout the vasculature (Payne, 2004) and that even in mature vasculatures, SMC retain their plasticity, such that they can undergo relatively rapid and reversible phenotypic changes in response to accommodate demands of the local environmental signals (Owens, 1995, Payne, 2004), such as those leading to remodelling and vasodilatory adaptations during pregnancy. Should MA contain mostly phasic SM, this artery type may have been expected to express predominantly LZ positive isoforms. However, the differences between two resistance artery types, such as MA and PA, may be more delicate than those observed between small (phasic) resistance arteries and large (tonic) conductance arteries. Assessing LZ-positive and -negative MYPT1 isoforms may elucidate small differences between the two artery types, as assessment of MYPT1 expression levels, undifferentiating between LZ isoforms, were found to be similar in MA and PA.

These subtle variations in LZ-positive isoform expression between MA and PA may result from differing O₂ levels present in myometrial and placental circulations and may impact on MYPT1/PKG LZ-LZ interactions. Physiologically, it is thought that the placental circulation is exposed to lower O₂ levels compared to the myometrial vasculature (Soothill et al., 1986, Rodesch et al., 1992) and recent studies reported that hypoxia reduced expression of LZ-positive MYPT1 in ovine fetal pulmonary arterial SMC and that interactions between LZ-positive MYPT1 and PKG were decreased, whilst those between LZ-positive MYPT1 and RhoA/ROKI were increased, resulting in increased phosphorylated MLC₂₀ and contraction (Singh et al., 2011). In normoxic conditions, an increase in LZ-positive MYPT1 and PKG expressions was observed (Singh et al., 2011). The placental circulation may therefore display lower LZ-positive MYPT1 levels and, importantly, fewer LZ-positive MYPT1/PKGI interactions, resulting in smaller cGMP-induced Ca²⁺-dependent relaxations than in the myometrial circulation. Although O₂ levels were kept similar for both artery types in the permeabilisation experiments, the disparity in MYPT1/PKG interactions between MA and PA may still have been highlighted, but may be even wider under physiological conditions.

The second assessment highlighted that the greater relaxations observed in *permeabilised* MA compared to PA persisted over the sGC/PKG axis, in *intact* arteries; but, surprisingly, they were reversed at the NO level.

The sGC activator YC-1 likely acted via PKG, inducing subsequent increase in MLCP activity and stimulation of the BK_{Ca} for efflux of K⁺, hyperpolarisation and relaxation (Chang et al., 2002, Zhang et al., 2012). Following activation of PKG, the aforementioned PKG-interacting proteins likely intervened to induce relaxation in MA and PA, pre-constricted with high K⁺. HSP20 phosphorylation may have sequestered HSP27 and destabilised actin-myosin interactions (Tyson et al., 2008a, MacIntyre et al., 2008). Similarly, phosphorylation of VASP likely induced relaxation as studies in rat platelets reported increases in Ser-239 phosphorylated VASP (and cGMP levels) upon addition of YC-1 *in vitro* (Becker et al., 2000). Phospho-telokin also participated in relaxing high K⁺-constricted MA and PA by directly enhancing MLCP affinity for myosin filaments (Khromov et al., 2012). Finally, PKG acted upon MYPT1 activity via their LZ-LZ interactions and resulting increase in MLCP activity (Surks and Mendelsohn, 2003, Nakamura et al., 2007).

Similarly, SNP induced relaxations via activation of PKG and its putative signalling pathways, as HSP20 phosphorylations at Ser-16 were found to increase in PKG-expressing SMC upon treatment with SNP (Brophy et al., 2002) and increases in VASP Ser-239 phosphorylation following addition of SNP were shown to induce concentration-dependent relaxation of phenylephrine-constricted rat aorta (Schafer et al., 2003). Phosphorylated telokin and LZ-LZ interactions of SNP-activated PKG and MYPT1 may have also contributed to induce MLCP-mediated vasodilation. Surprisingly, in these conditions, SNP-mediated relaxations were greater in PA compared to MA. A likely explanation for this observation may lie in the actions of SNP on the K⁺ channels and the sensitivity of PA to oxidative conditions, which may result from the lower O₂ levels in the placental versus myometrial circulation (Rodesch et al., 1992). SNP-induced relaxations were greater in PA exposed to ROS generating agonists compared to controls (Mills et al., 2009). In addition, a recent study on rat retinal vessels inferred that ATP-sensitive K⁺ (K_{ATP}) channels were activated during exposure to ROS (Fukumoto et al., 2012). With PA presenting a particular sensitivity to ROS compared to MA, K_{ATP} channels along with other K⁺ channels (BK_{Ca} and voltage-dependent) may also respond with greater sensitivity to oxidative stress in PA compared to MA, resulting in increased hyperpolarisation and greater relaxations in arteries from the placenta. These K⁺ channel sensitivities were also reduced in complicated pregnancy, such as fetal growth restriction, in which overall peripheral vascular resistance is also increased (Corcoran et al., 2008). SNP actions may have therefore

primarily affected membrane potentials, whilst YC-1 may have directed its effects towards the SMC's actin-myosin filaments. Thus, regulation of myometrial vascular tone may result primarily from a sensitivity of the SM contractile apparatus to vasoactive and -dilatory agents, while regulation of the placental circulation may depend more on the membrane potential and channel activity states.

The relaxatory patterns in MA and PA reported in the present study were assessed principally by functional experimentation and further evaluated by protein expression analyses. Additional studies to determine levels of the phospho-proteins directly involved in regulating the activity of MLCP and actin-myosin filament interactions may serve to further elucidate the tight balance required in the regulation of vascular tone in myometrial and placental circulations. However, it is noteworthy to mention that such studies would be carried out with great difficulty due to the very small amount of protein to be yielded from such small arteries, particularly when dealing with MA. For each functional experiment, four small 200 – 400 μm arteries of 1 – 2 mm length were mounted onto four myography baths. On average, a minimum of eight arterial lengths such as those was necessary to provide enough protein (5 μg) to load onto *one* lane of a western blot. From one myometrial biopsy and thus one patient, one could dissect enough arterial material to yield around 60 - 80 μg of protein. Antibody and protein concentration optimisations thus required the use of several myometrial samples. In addition, phospho-antibodies are notoriously unspecific and obtaining a reliable one recognising human sequences was proving rather difficult.


This study may also have used a larger variety of compounds to confirm signalling pathways involved in the observed relaxations. Indeed, 8-br-cGMP is one cGMP mimetic and PKG activator that may be used; 8-pCPT-cGMP is another activator, which may have been used to assess Ca^{2+} -desensitisation in the human arteries (El-Awady et al., 2008). As the role of MLCP was established with the use of the phosphatase inhibitor calyculin A; a PKG inhibitor, such as KT5823 or Rp-8-Br-PET-cGMP, may also have been used to confirm its role in the desensitisation phenomenon (Kang et al., 2012, Zhang et al., 2012). Similarly, the role of RhoA/ROK in Ca^{2+} -sensitisation may also have been directly confirmed using specific ROK inhibitors, such as fasudil or Y-27632 (Masumoto et al., 2001, Wareing et al., 2005b), although previous studies in human term MA and PA had already reported inhibition of TXA_2 -

induced Ca^{2+} -sensitisation following addition of Y-27632 (Wareing et al., 2005b). Thus, the involvement of the RhoA/ROK pathway was readily assumed in this study.

Nonetheless, this study has highlighted novel scientific contributions in the differences in both constrictions and relaxations in isolated *human* arteries from the myometrium and the placental at term of healthy pregnancies. Whilst, putative signalling mechanisms may be similar in these two artery types, their sensitivities within these pathways showed great dissimilarities. Most importantly, it seems that the myometrial vasculature displays greater sensitivities across the sGC/PKG axis, which may result from differences in levels of MYPT1 isoforms and phosphorylated states of PKG-interacting proteins; thus directly affecting the activity of the central MLCP and actin-myosin filament interactions. The complex network of pathways involved may offer a plethora of possible leads for novel drug targets and further studies may highlight tissue-specific differences in the regulation of vascular tone of myometrial and placental circulations. This may not only allow development of more tissue-specific, and hopefully effective, therapeutics against pathophysiologies encountered during pregnancy, but may also extend for the treatment of other vascular disorders, such as asthma, functional bowel disease or cardiovascular disease.

Appendix A: Ethical approval forms

A.1 Myometrial ethical approval forms



National Research Ethics Service
Newcastle & North Tyneside 2 Research Ethics Committee
Room G14
Dental School
Framlington Place
Newcastle upon Tyne
NE2 4BW

Telephone: 0191 222 3581
Facsimile: 0191 222 3582
Email: gillian.mayer@ncl.ac.uk

23 September 2008

Professor Stephen C Robson
Professor of Fetal Medicine
Institute of Cellular Medicine
Newcastle University
3rd Floor William Leech Building
Framlington Place
Newcastle upon Tyne
NE2 4HH

Dear Professor Robson

Full title of study: **Novel regulation of human myometrial contractility by histone deacetylase 8 (HDAC8): the use of specific inhibitors as tocolytics**

REC reference number: **08/H0907/96**

Thank you for your letter of 17 September 2008, responding to the Committee's request for further information on the above research and submitting revised documentation.

The further information has been considered on behalf of the Committee by the Chair.

Confirmation of ethical opinion

On behalf of the Committee, I am pleased to confirm a favourable ethical opinion for the above research on the basis described in the application form, protocol and supporting documentation as revised, subject to the conditions specified below.

Ethical review of research sites

The Committee has designated this study as exempt from site-specific assessment (SSA). The favourable opinion for the study applies to all sites involved in the research. There is no requirement for other Research Ethics Committees to be informed or SSA to be carried out at each site.

Conditions of the favourable opinion

The favourable opinion is subject to the following conditions being met prior to the start of the study.

Management permission or approval must be obtained from each host organisation prior to the start of the study at the site concerned.

Management permission at NHS sites ("R&D approval") should be obtained from the relevant care organisation(s) in accordance with NHS research governance arrangements.

This Research Ethics Committee is an advisory committee to North East Strategic Health Authority
The National Research Ethics Service (NRES) represents the NRES Directorate within
the National Patient Safety Agency and Research Ethics Committees in England

Guidance on applying for NHS permission is available in the Integrated Research Application System or at <http://www.rdforum.nhs.uk>.

Approved documents

The final list of documents reviewed and approved by the Committee is as follows:

<i>Document</i>	<i>Version</i>	<i>Date</i>
Application	(5.6) AB/136009/1	06 June 2008
Investigator CV		
Protocol	v 1	17 May 2008
Peer Review		15 May 2008
Response to Request for Further Information	v 2	17 September 2008
Participant Information Sheet: Non-Pregnant	v 3	17 September 2008
Participant Information Sheet: Pregnant	v 3	17 September 2008
Participant Consent Form	v 3	17 September 2008
Research Leaflet	v 2	05 September 2008
Letter re funding from MRC		09 July 2008

Statement of compliance

The Committee is constituted in accordance with the Governance Arrangements for Research Ethics Committees (July 2001) and complies fully with the Standard Operating Procedures for Research Ethics Committees in the UK.

After ethical review

Now that you have completed the application process please visit the National Research Ethics Website > After Review

You are invited to give your view of the service that you have received from the National Research Ethics Service and the application procedure. If you wish to make your views known please use the feedback form available on the website.

The attached document "After ethical review – guidance for researchers" gives detailed guidance on reporting requirements for studies with a favourable opinion, including:

- Notifying substantial amendments
- Progress and safety reports
- Notifying the end of the study

The NRES website also provides guidance on these topics, which is updated in the light of changes in reporting requirements or procedures.

We would also like to inform you that we consult regularly with stakeholders to improve our service. If you would like to join our Reference Group please email referencegroup@nres.npsa.nhs.uk.

08/H0907/96

Please quote this number on all correspondence

This Research Ethics Committee is an advisory committee to North East Strategic Health Authority
*The National Research Ethics Service (NRES) represents the NRES Directorate within
the National Patient Safety Agency and Research Ethics Committees in England*

With the Committee's best wishes for the success of this project

Yours sincerely

Handwritten signature of Dr Philip Preshaw, consisting of the initials 'PP' followed by a stylized 'G. Mayer'.

Dr Philip Preshaw
Chair

Enclosures: 'After ethical review – guidance for researcher'

Copy to: *Joint Research Office – Royal Victoria Infirmary, Newcastle upon Tyne Hospitals NHS Foundation Trust*

A.2 Placental ethical approval forms



National Research Ethics Service

County Durham & Tees Valley Research Ethics Committee

Room 002
TEDCO Business Centre
Viking Industrial Park
Rolling Mill Road
Jarrow
Tyne & Wear
NE32 3DT

Tel: 0191 428 3566
Fax: 0191 428 3432

28 May 2010

Professor Stephen C Robson
Professor of Fetal Medicine
Newcastle University
Institute of Cellular Medicine
3rd Floor Leech building
NE2 4HH

Dear Professor Robson

Study title: Ca²⁺-signalling mechanisms controlling uteroplacental function in pregnancy
REC reference: 09/H0908/11
Protocol number: 1
Amendment number: 1
Amendment date: 17 May 2010
Reason for amendment: Notification of temporary halt of research now lifted
Amendment of information sheet and consent form for full term group to reflect timing of withdrawal from study

The above amendment was reviewed by the Sub-Committee in correspondence.

Ethical opinion

Favourable Opinion

The members of the Committee taking part in the review gave a favourable ethical opinion of the amendment on the basis described in the notice of amendment form and supporting documentation.

Approved documents

The documents reviewed and approved at the meeting were:

Document	Version	Date
Letter from R&D confirming study has now received full research governance approval	1	23 April 2010
Participant Consent Form: Full term Group	3	17 May 2010
Participant Information Sheet: Full Term Group	3	17 May 2010
Notice of Substantial Amendment (non-CTIMPs)	1	17 May 2010

This Research Ethics Committee is an advisory committee to the North East Strategic Health Authority
The National Research Ethics Service (NRES) represents the NRES Directorate within
the National Patient Safety Agency and Research Ethics Committees in England

Covering Letter	1	17 May 2010
-----------------	---	-------------

Membership of the Committee

The members of the Committee who took part in the review are listed on the attached sheet.

R&D approval

All investigators and research collaborators in the NHS should notify the R&D office for the relevant NHS care organisation of this amendment and check whether it affects R&D approval of the research.

Statement of compliance

The Committee is constituted in accordance with the Governance Arrangements for Research Ethics Committees (July 2001) and complies fully with the Standard Operating Procedures for Research Ethics Committees in the UK.

09/H0908/11:	Please quote this number on all correspondence
--------------	--

Yours sincerely

Leigh Pollard

Leigh Pollard
Committee Co-ordinator

E-mail: leigh.pollard@nhs.net

Enclosures: List of names and professions of members who took part in the review

Copy to: Research & Development, 4th Floor, Leazes Wing, Royal Victoria Infirmary, Queen Victoria Road, Newcastle upon Tyne, NE1 4LP

Appendix B: Consent forms

B.1 Myometrial consent forms

The Newcastle upon Tyne Hospitals 
NHS Foundation Trust



CONSENT FORM

Title of project: **Novel regulation of human myometrial contractility by HDAC8**

Name of researchers: Professor S. Robson, Dr N. Europe-Finner

initial box

Please

1. I confirm that I have read the information sheet dated 17th September 2008 for the above study and have had the opportunity to ask questions.
2. I understand that my participation is voluntary and that I am free to withdraw, without giving any reason, without my medical care or legal rights being affected.
3. I understand that relevant sections of my medical notes and data collected during the study, may be looked at by individuals from regulatory authorities or from the NHS Trust, where it is relevant to my taking part in this research. I give permission to these individuals to have access to my records.
4. I agree to take part in the above study.

☐☐☐☐

Name of patient

Date

Signature

*Name of person taking consent
(if different from researcher)*

Date

Signature

Researcher

Date

Signature

1 for patient; 1 to be kept with medical notes

Novel regulation of human myometrial contractility by HDAC8

Professor S. Robson, Dr N. Europe-Finner

1. Introduction

You are being invited to take part in a research study. It is important for you to understand why the research is being done and what it will involve before you decide whether to take part. Please take time to read the following information carefully and discuss it with others if you wish. Ask us if there is anything that is not clear or if you would like more information.

2. What is the purpose of the study?

During pregnancy, the upper part of the womb (uterus) is relaxed while the lower part (cervix) is closed. In labour the upper part contracts and the lower part relaxes, allowing the baby to be born. If this occurs early, preterm birth results with major consequences for the baby. The drugs we use to treat premature labour are not very effective. In order to develop better drugs we need to understand how the womb contracts and relaxes. This study is investigating the effect of HDAC8 (an enzyme present in the womb).

3. Why have I been chosen and do I have to take part?

You have been chosen to take part because you are having a caesarean section. It is up to you to decide whether or not to take part. If you do decide to take part you will be asked to sign a consent form; a copy of your consent and this information sheet will be given to you to keep. If you decide to take part you are still free to withdraw at any time and without giving a reason. A decision to withdraw, or a decision not to take part, will not affect the standard of the care you receive.

4. What will happen to me if I take part?

In order to undertake this study we need small samples of myometrium (the muscle layer of the womb). After the baby and placenta have been delivered a small piece of muscle (about the size of a pea) will be taken from the lower part of the womb (from the site where the womb was opened to deliver the baby). Collecting the muscle sample adds less than a minute to the operation and will not affect your recovery in any way.

5. What are the risks and benefits of taking part?

Extensive experience of taking these samples suggests the procedure is not associated with any risk. You will not directly benefit from taking part in the study. We will be

using the sample to study how the muscle contracts. This should help us understand why some women labour early and may allow us to develop better drugs to prevent premature birth.

6. Will my taking part in this study be kept confidential?

Participation in the study will be recorded in your hospital notes but no personal information will be kept by the research team.

7. What will happen to the results of the research study?

The study will take just over 3 years to complete. We anticipate the results will be published in a medical journal. You will not be identified in any report or publication.

8. What will happen if I don't want to carry on with the study?

If you withdraw from the study, we will destroy all your identifiable samples, but we will need to use the data collected up to your withdrawal.

9. What if there is a problem?

In the event that something does go wrong and you are harmed during the research and this is due to someone's negligence then you may have grounds for legal action for compensation against the Newcastle upon Tyne NHS Foundation Trust but you may have to pay your legal costs. If you have a concern about any aspect of this study, you should ask to speak to the researchers who will do their best to answer your questions. If you remain unhappy and wish to complain formally, you can do this through the NHS Complaints Procedure (or Private Institution). Details can be obtained from the hospital.

10. Who is organising and funding the research and who has reviewed the study?


The study is funded by the Medical Research Council. The study has been approved by the Newcastle & North Tyneside Research Ethics Committee. It is being carried out by a team of researchers at Newcastle University.

11. Contact for further information

If you have any questions about the study please contact: Professor S. Robson (Tel: 2824132)

Thank you for reading this information sheet.

B.2 Placental consent forms

The Newcastle upon Tyne Hospitals 
NHS Foundation Trust



Consent Form

Title of project: **Calcium signalling mechanisms in the human placenta**

Name of researchers: **Professor M. Taggart, Professor S. Robson**
Institute of Cellular Medicine, Newcastle University

Please initial box

1. I confirm I have read the information sheet for the above study (dated 3rd April 2009) and have had the opportunity to ask questions.
2. I understand that my participation is voluntary and that I can withdraw from the study (by informing the nursing or medical staff), without giving a reason, up to the time I leave hospital. I understand that withdrawal from the study will not affect my medical care.
3. I agree to the retention of any placental tissue that remains unused after the completion of the study and the use of this tissue for future research studies.
4. I agree to take part in the above study.

☐☐☐☐

Name of patient

Date

Signature

*Name of person taking consent
(if different from researcher)*

Date

Signature

Name of researcher

Date

Signature

1 for patient; 1 to be kept in medical notes

PIS (P) v2
Date: 3.4.2009

Calcium signalling mechanisms in the human placenta

Professor M. Taggart, Professor S. Robson

You are being invited to take part in a research study. Before you decide it is important for you to understand why the research is being done and what it will involve. Please take time to read the following information carefully.

What is the purpose of the study?

During pregnancy the placenta (afterbirth) transfers nutrients to the growing baby. These nutrients reach the baby through the blood vessels of the placenta. If these blood vessels don't work normally then this can affect the growth and health of the baby. The aim of this study is to find out how these blood vessels work and specifically the role of calcium.

What will happen to me if I take part?

In order to undertake this research we need to study what makes the blood vessels in the placenta contract and relax using a range of drugs. These blood vessels can be collected from the placenta after delivery. After collection the samples of the placenta are stored in a tissue bank in Newcastle University.

Do I have to take part?

It is up to you to decide whether or not to take part. If you decide to take part you will be given this information sheet and be asked to sign a consent form. If you decide to take part you are free to withdraw up to the time you leave the delivery suite (as, once in the tissue bank, there is no way of identifying who the samples came from). A decision not to take part will not affect the care you receive.

What are the possible disadvantages and risks of taking part?

As you have already delivered the placenta there are no risks to you.

Will my taking part in the study be kept confidential?

Participation in the study will be recorded in your hospital notes but no personal information will be kept by the research team.

What will happen to the results of the research study?

When the study is finished findings will be published in medical journals.

Who has reviewed the study? Who is funding the study?

The study has been approved by the County Durham & Tees Valley Research Ethics Committee and funded by Newcastle University.

Contact for further information.

If you have any questions or concerns about the study you should contact Professor S. Robson (Tel. 2824132). If you remain unhappy and wish to complain formally you should contact Dr A. Tortice in the NHS Research Office (Tel. 2825959).

Thank you for reading this information sheet

PIS (P) v2
Date: 3.4.2009

Appendix C: Patient Information Form

				Biobank #	
<u>Uterine Cell Signalling Group Tissue Collection</u>					
Date of sample collection.....		Hospital Number.....			
Gestation (wk + day).....		Age.....			
Gravidity	Parity.....	Height	Weight	BMI	
Ethnicity		Term BMI.....			
Birthweight M / F		Smoker: True <input type="checkbox"/> False <input type="checkbox"/>			
Birth Centile					
<u>Consented:</u>			<u>Samples Collected</u>		
Placenta	<input type="checkbox"/>	Placenta	<input type="checkbox"/>	(PTO for other outcomes)	
Amnion/chorion	<input type="checkbox"/>	Amnion/chorion	<input type="checkbox"/>		
Placental bed	<input type="checkbox"/>	Placental bed	<input type="checkbox"/>		
Myometrium	Upper <input type="checkbox"/> Lower <input type="checkbox"/>	Myometrium	Upper <input type="checkbox"/> Lower <input type="checkbox"/>		
Cervix	<input type="checkbox"/>	Cervix	<input type="checkbox"/>		
<u>Delivery:</u>					
Vaginal delivery	<input type="checkbox"/>	Elective CS	<input type="checkbox"/>	Indication.....	
Emergency CS	<input type="checkbox"/>	Dilatation.....cm)		Indication.....	
Hysterectomy	<input type="checkbox"/>	LMP		Indication.....	
TOP	<input type="checkbox"/>				
ERPC	<input type="checkbox"/>				
<u>Drugs:</u>					
This patient does not take any prescribed medications <input type="checkbox"/>					
Prostaglandin	True <input type="checkbox"/>	False <input type="checkbox"/>	Other medications:		
Oxytocin	True <input type="checkbox"/>	False <input type="checkbox"/>			
Steroids (within 48h)	True <input type="checkbox"/>	False <input type="checkbox"/>			
Tocolytic (within 48h)	True <input type="checkbox"/>	False <input type="checkbox"/>			
Progesterone (inc Mirena)	True <input type="checkbox"/>	False <input type="checkbox"/>			
GnRH analogue	True <input type="checkbox"/>	False <input type="checkbox"/>			
<u>Other medical conditions:</u>					
Preclampsia	<input type="checkbox"/>	Diabetes	<input type="checkbox"/>	Prolonged ROM	<input type="checkbox"/>
Infection	<input type="checkbox"/>				
<u>Consent:</u>					
I confirm that this patient has given informed written consent for this sample					
True <input type="checkbox"/>		False <input type="checkbox"/>			
Signed.....		Print name.....			
Thank you for filling in this form. Please ring RVI Ext 24132 for sample collection					
Page 1 of 2		JO Jan 2012 v3.2			

For theatre staff to complete:

Operating surgeon:

Date of surgery:

For scientist to complete:

If samples were consented but not collected why?

Was sample useful? Yes ☐

No ☐

If not, why?

If non-pregnant was endometrial sample obtained? Yes ☐

No ☐

N.b Above to be completed in addition to 'Samples collected' overleaf.

Appendix D: α -Toxin Export Licence



540 DIVISION STREET • CAMPBELL • CALIFORNIA 95008-6906 • USA
408-866-6363 • 800-726-3213 • FAX 408-866-6364 • EMAIL info@listlabs.com
WEBSITE www.listlabs.com

June 14, 2011

Michael Taggart, Ph.D., Michele Sweeney, Ph.D.
Newcastle University
Institute of Cellular Medicine
3rd Floor, Leech Bldg.
Framlington Place
Newcastle upon Tyne, UK NE2 4HH

Dear Researcher:

This is to inform you that your export license to order through Quadrtech Diagnostics Limited from the U.S. Department of Commerce has been approved and is valid through June 30, 2013. Your license has some specific conditions that we would like to make you aware of:

1. End use is limited to the end use as stated on the license application.
2. No resale, transfer, or re-export of the items listed on the license is authorized without prior authorization by the U.S. Government.
3. No use in chemical or biological weapons manufacture or applications.
4. The license is issued based on the dollar amount of the product, not the quantity ordered. The value listed on the license cannot be exceeded.
5. These products are for research purposes only, not for human use.

The license has been approved for 20 vials of product #120, Alpha toxin from *staphylococcus aureus*. We will be able to ship this product to you when we have received an official purchase order through Quadrtech. Thank you for your interest in our products.

Sincerely,

Nancey Ferguson
Administration, Export Licensing

cc: T. Turner, G. Jones, Quadrtech



UNITED STATES DEPARTMENT OF COMMERCE
BUREAU OF INDUSTRY AND SECURITY
WASHINGTON, D.C. 20230

EXPORT LICENSE U.S. DEPARTMENT OF COMMERCE
INDUSTRY AND SECURITY

D463791

VALIDATED: JUN 14 2011

EXPIRES: JUN 30 2013

THIS LICENSE AUTHORIZES THE LICENSEE TO CARRY OUT THE EXPORT TRANSACTION DESCRIBED ON THE LICENSE (INCLUDING ALL ATTACHMENTS). IT MAY NOT BE TRANSFERRED WITHOUT PRIOR WRITTEN APPROVAL OF THE OFFICE OF EXPORT LICENSING. THIS LICENSE HAS BEEN GRANTED IN RELIANCE ON REPRESENTATIONS MADE BY THE LICENSEE AND OTHERS IN CONNECTION WITH THE APPLICATION FOR EXPORT AND IS EXPRESSLY SUBJECT TO ANY CONDITIONS STATED ON THE LICENSE, AS WELL AS ALL APPLICABLE EXPORT CONTROL LAWS, REGULATIONS, RULES, AND ORDERS. THIS LICENSE IS SUBJECT TO REVISION, SUSPENSION, OR REVOCATION WITHOUT PRIOR NOTICE.

APPLICANT REFERENCE NUMBER: LIS1002

LIST BIOLOGICAL LABORATORIES, INC.
540 DIVISION ST
CAMPBELL, CA 95008

PURCHASER:
QUADRATECH DIAGNOSTICS LIMITED
64 SOUTH STREET
EPSOM SURREY, UNITED KINGDOM

ULTIMATE CONSIGNEE:
NEWCASTLE UNIVERSITY
INST. OF CELLULAR MEDICINE
3RD FL. LEECH BLDG, FRAMLINGTON PLA
NEWCASTLE UPON TYNE, UNITED KINGDOM

INTERMEDIATE CONSIGNEE:

COMMODITIES:		TOTAL
QTY	DESCRIPTION	PRICE
20	MODEL: 120, ALPHA TOXIN FROM STAPHYLOCOCCUS AUREUS 20 X 0.25 VIALS. THIS PRODUCT IS NOT A LABELED CONJUGATE AND IS NOT EXEMPT UNDER EAR99. FOR RESEARCH PURPOSES ONLY, NOT FOR HUMAN USE	\$5,400
TOTAL:		\$5,400

THE EXPORT ADMINISTRATION REGULATIONS REQUIRE YOU TO TAKE THE FOLLOWING ACTIONS WHEN EXPORTING UNDER THE AUTHORITY OF THIS LICENSE.

GENERATED BY SNAP-R



UNITED STATES DEPARTMENT OF COMMERCE
BUREAU OF INDUSTRY AND SECURITY
WASHINGTON, D.C. 20230

- A. RECORD THE EXPORT COMMODITY CONTROL NUMBER IN THE BLOCK
PROVIDED ON EACH SHIPPER'S EXPORT DECLARATION (SED).
- B. RECORD YOUR VALIDATED LICENSE NUMBER IN THE BLOCK
PROVIDED ON EACH SED.
- C. PLACE A DESTINATION CONTROL STATEMENT ON ALL BILLS OF LADING,
AIRWAY BILLS, AND COMMERCIAL INVOICES.

RIDERS AND CONDITIONS:

D463791

VALIDATED: JUN 14 2011

EXPIRES: JUN 30 2013

-
1. FOR STATED END USE ONLY.
 2. APPLICANT MUST INFORM CONSIGNEE OF ALL LICENSE CONDITIONS.
 3. NO RESALE, TRANSFER, OR REEXPORT OF THE ITEMS LISTED ON THIS LICENSE
IS AUTHORIZED WITHOUT PRIOR AUTHORIZATION BY THE U.S. GOVERNMENT.
 4. NO USE IN CHEMICAL OR BIOLOGICAL WEAPONS MANUFACTURE OR APPLICATIONS.

GENERATED BY SNAP-R

Appendix E: Presentations and Publications

E.1 Presentations and Awards

June 2009:	Oral Presentation (40 minutes). Institute of Cellular Medicine Science Forum, Newcastle University.
June 2009:	Oral Presentation (10 minutes). Alternative Muscle Conference, University of Manchester. Conference organised by PhD students for fellow PhD students and young PostDocs.
November 2009:	First Prize (£300) , Oral Presentation (10 minutes). North-East Postgraduate Conference, Newcastle University.
June 2010:	Oral Presentation (10 minutes). Annual Physiological Society Meeting, University of Manchester. <i>Travel Grant obtained from the Physiological Society.</i>
June 2010:	First Prize (£100) , Poster Presentation. Annual Institute of Cellular Medicine Research Day, Newcastle University.
July 2010:	Poster Presentation. Vascular Biology Summer School, Bristol University.
November 2010:	Poster Presentation. Royal College of Obstetricians and Gynaecologists (RCOG) Annual Academic Meeting, RCOG, London.
March 2011:	Oral Presentation (25 minutes). Institute of Cellular Medicine Research Seminar, Newcastle University.
April 2011:	Oral Presentation (10 minutes). Northern Cardiac Research Group (NCRG) Meeting, Hull University.
March 2012:	Poster Presentation. 59 th Annual Meeting for the Society for Gynecological Investigation, San Diego, CA, USA. <i>Travel Grants obtained from the Physiological Society and Newcastle University.</i>

E.2 Publications (scientific and non-scientific)

A. C. Dordea, M. Sweeney, S. C. Robson, M. J. Taggart (2010), 8-br-cGMP-induced Ca²⁺-desensitisation mechanisms in human blood vessels – evidence of tissue specificity, Proc. Physiol Soc, 19, C136. Abstract.

A. C. Dordea, M. Sweeney, S.C. Robson, M.J. Taggart (2012), **Human placental and myometrial arteries differ in their Ca^{2+} -sensitivities of force production**, Official J Soc Gynecol Invest, Suppl. Reprod Sciences, 19, T210. *Abstract*.

A.C. Dordea (2012), Travel Grant Connections, *Physiology News*, Issue 87, Summer 2012. Contribution about an International Meeting attended in San Diego, CA, March 2012.

A.C. Dordea (2012), Lab Profile: The Reproductive and Vascular Biology Group, Newcastle University, *Physiology News*, Issue 87, Summer 2012. Contribution about the research carried out in our laboratory.

E.3 Society Affiliations

2009 – Present: Affiliate member of the Physiological Society

References

- ABRAMOVICH, D. R., DACKE, C. G., ELCOCK, C. & PAGE, K. R. 1987. Calcium transport across the isolated dually perfused human placental lobule. *J Physiol*, 382, 397-410.
- AGAPITOV, A. V. & HAYNES, W. G. 2002. Role of endothelin in cardiovascular disease. *J Renin Angiotensin Aldosterone Syst*, 3, 1-15.
- AHNERT-HILGER, G., BHAKDI, S. & GRATZL, M. 1985. Alpha-toxin permeabilized rat pheochromocytoma cells: a new approach to investigate stimulus-secretion coupling. *Neurosci Lett*, 58, 107-10.
- AMARNANI, S., SANGRAT, B. & CHAUDHURI, G. 1999. Effects of selected endothelium-dependent vasodilators on fetoplacental vasculature: physiological implications. *Am J Physiol*, 277, H842-7.
- ANDERSEN, M. R., ULDBJERG, N., STENDER, S., SANDAGER, P. & AALKJAER, C. 2011. Maternal smoking and impaired endothelium-dependent nitric oxide-mediated relaxation of uterine small arteries in vitro. *Am J Obstet Gynecol*, 204, 177 e1-7.
- ANWAR, M. A., DOCHERTY, C., POSTON, L. & NATHANIELSZ, P. W. 1999. A comparative study of vascular responsiveness of myometrial and omental small resistance arteries in late-gestation sheep. *Am J Obstet Gynecol*, 181, 663-8.
- ASHWORTH, J. R., WARREN, A. Y., BAKER, P. N. & JOHNSON, I. R. 1997. Loss of endothelium-dependent relaxation in myometrial resistance arteries in pre-eclampsia. *Br J Obstet Gynaecol*, 104, 1152-8.
- BAINBRIDGE, S. A., FARLEY, A. E., MCLAUGHLIN, B. E., GRAHAM, C. H., MARKS, G. S., NAKATSU, K., BRIEN, J. F. & SMITH, G. N. 2002. Carbon monoxide decreases perfusion pressure in isolated human placenta. *Placenta*, 23, 563-9.
- BAKER, P. F. & KNIGHT, D. E. 1981. Calcium control of exocytosis and endocytosis in bovine adrenal medullary cells. *Philos Trans R Soc Lond B Biol Sci*, 296, 83-103.
- BAKER, P. F., KNIGHT, D. E. & UMBACH, J. A. 1985. Calcium clamp of the intracellular environment. *Cell Calcium*, 6, 5-14.
- BEALL, A., BAGWELL, D., WOODRUM, D., STOMING, T. A., KATO, K., SUZUKI, A., RASMUSSEN, H. & BROPHY, C. M. 1999. The small heat shock-related protein, HSP20, is phosphorylated on serine 16 during cyclic nucleotide-dependent relaxation. *J Biol Chem*, 274, 11344-51.
- BEALL, A. C., KATO, K., GOLDENRING, J. R., RASMUSSEN, H. & BROPHY, C. M. 1997. Cyclic nucleotide-dependent vasorelaxation is associated with the phosphorylation of a small heat shock-related protein. *J Biol Chem*, 272, 11283-7.
- BECKER, E. M., SCHMIDT, P., SCHRAMM, M., SCHRODER, H., WALTER, U., HOENICKA, M., GERZER, R. & STASCH, J. P. 2000. The vasodilator-stimulated phosphoprotein (VASP): target of YC-1 and nitric oxide effects in human and rat platelets. *J Cardiovasc Pharmacol*, 35, 390-7.
- BELFORT, M., AKOVIC, K., ANTHONY, J., SAADE, G., KIRSHON, B. & MOISE, K., JR. 1994. The effect of acute volume expansion and vasodilatation with verapamil on uterine and umbilical artery Doppler indices in severe preeclampsia. *J Clin Ultrasound*, 22, 317-25.
- BENIRSCHKE, K. & KAUFMANN, P. 1991. *Early development of the human placenta*, New York, Springer-Verlag.
- BENIRSCHKE, K. & KAUFMANN, P. 2000. *Architecture of normal villous tree*, New York, Springer-Verlag.

- BERGH, C. M., BROPHY, C. M., DRANSFIELD, D. T., LINCOLN, T., GOLDENRING, J. R. & RASMUSSEN, H. 1995. Impaired cyclic nucleotide-dependent vasorelaxation in human umbilical artery smooth muscle. *Am J Physiol*, 268, H202-12.
- BHAKDI, S., SUTTORP, N., SEEGER, W., FUSSLE, R. & TRANUM-JENSEN, J. 1984. [Molecular basis for the pathogenicity of *S. aureus* alpha-toxins]. *Immun Infekt*, 12, 279-85.
- BHAKDI, S. & TRANUM-JENSEN, J. 1984. Mechanism of complement cytolysis and the concept of channel-forming proteins. *Philos Trans R Soc Lond B Biol Sci*, 306, 311-24.
- BHAKDI, S. & TRANUM-JENSEN, J. 1991. Alpha-toxin of *Staphylococcus aureus*. *Microbiol Rev*, 55, 733-51.
- BISSONNETTE, J. M., WEINER, C. P. & POWER, G. G., JR. 1994. Amino acid uptake and chloride conductances in human placenta. *Placenta*, 15, 445-6.
- BLEA, C. W., BARNARD, J. M., MAGNESS, R. R., PHERNETTON, T. M. & HENDRICKS, S. K. 1997. Effect of nifedipine on fetal and maternal hemodynamics and blood gases in the pregnant ewe. *Am J Obstet Gynecol*, 176, 922-30.
- BLUE EK, GOECKELER ZM, JIN Y, HOU L, DIXON SA, HERRING BP, WYSOLMERSKI RB & PJ., A. G. 2002. 220- and 130-kDa MLCKs have distinct tissue distributions and intracellular localization patterns. *Am J Physiol Cell Physiol*, 282, C451-C460.
- BOLZ, S. S., VOGEL, L., SOLLINGER, D., DERWAND, R., DE WIT, C., LOIRAND, G. & POHL, U. 2003. Nitric oxide-induced decrease in calcium sensitivity of resistance arteries is attributable to activation of the myosin light chain phosphatase and antagonized by the RhoA/Rho kinase pathway. *Circulation*, 107, 3081-7.
- BOND, M., KITAZAWA, T., SOMLYO, A. P. & SOMLYO, A. V. 1984. Release and recycling of calcium by the sarcoplasmic reticulum in guinea-pig portal vein smooth muscle. *J Physiol*, 355, 677-95.
- BONNEVIER, J. & ARNER, A. 2004. Actions downstream of cyclic GMP/protein kinase G can reverse protein kinase C-mediated phosphorylation of CPI-17 and Ca(2+) sensitization in smooth muscle. *J Biol Chem*, 279, 28998-9003.
- BONNEVIER, J., FASSLER, R., SOMLYO, A. P., SOMLYO, A. V. & ARNER, A. 2004. Modulation of Ca²⁺ sensitivity by cyclic nucleotides in smooth muscle from protein kinase G-deficient mice. *J Biol Chem*, 279, 5146-51.
- BOSIO, P. M., MCKENNA, P. J., CONROY, R. & O'HERLIHY, C. 1999. Maternal central hemodynamics in hypertensive disorders of pregnancy. *Obstet Gynecol*, 94, 978-84.
- BOURA, A. L., LEITCH I.M., READ M.A. AND WALTERS A.W. 1998. The control of fetal vascular resistance in the human placenta. *Trophoblast Res.*, 11, 299-313.
- BOVING, B. G. 1959a. The biology of trophoblast. *Ann N Y Acad Sci*, 80, 21-43.
- BOVING, B. G. 1959b. Implantation. *Ann N Y Acad Sci*, 75, 700-25.
- BOYD, J. D. & HAMILTON, W. J. 1966. Electron microscopic observations on the cytotrophoblast contribution to the syncytium in the human placenta. *J Anat*, 100, 535-48.
- BRACERO, L. A., REALE, M. R., TE, M. N., ZEBALLOS, G. A. & DWECK, H. S. 1995. Endothelin-1 levels in the maternal-fetal dyad. *Gynecol Obstet Invest*, 39, 221-5.
- BRADLEY, A. B. & MORGAN, K. G. 1987. Alterations in cytoplasmic calcium sensitivity during porcine coronary artery contractions as detected by aequorin. *J Physiol*, 385, 437-48.

- BROPHY, C. M., WOODRUM, D. A., POLLOCK, J., DICKINSON, M., KOMALAVILAS, P., CORNWELL, T. L. & LINCOLN, T. M. 2002. cGMP-dependent protein kinase expression restores contractile function in cultured vascular smooth muscle cells. *J Vasc Res*, 39, 95-103.
- BROSENS, I., ROBERTSON, W. B. & DIXON, H. G. 1967. The physiological response of the vessels of the placental bed to normal pregnancy. *J Pathol Bacteriol*, 93, 569-79.
- BROUGHTON PIPKIN, F. & SMALES, O. R. 1975. Proceedings: Blood pressure and angiotensin II in the newborn. *Arch Dis Child*, 50, 330.
- BROWNBILL, P., BELL, N. J., WOODS, R. J., LOWRY, P. J., PAGE, N. M. & SIBLEY, C. P. 2003. Neurokinin B is a paracrine vasodilator in the human fetal placental circulation. *J Clin Endocrinol Metab*, 88, 2164-70.
- BURNETT, A. L. 1995. Role of nitric oxide in the physiology of erection. *Biol Reprod*, 52, 485-9.
- BURNETT, A. L. 2006. The role of nitric oxide in erectile dysfunction: implications for medical therapy. *J Clin Hypertens (Greenwich)*, 8, 53-62.
- BURTON, G. J., HEMPSTOCK, J. & JAUNIAUX, E. 2003. Oxygen, early embryonic metabolism and free radical-mediated embryopathies. *Reprod Biomed Online*, 6, 84-96.
- BURTON, G. J., JAUNIAUX, E. & WATSON, A. L. 1999. Maternal arterial connections to the placental intervillous space during the first trimester of human pregnancy: the Boyd collection revisited. *Am J Obstet Gynecol*, 181, 718-24.
- BURTON, G. J., WOODS, A. W., JAUNIAUX, E. & KINGDOM, J. C. 2009. Rheological and physiological consequences of conversion of the maternal spiral arteries for uteroplacental blood flow during human pregnancy. *Placenta*, 30, 473-82.
- CANNING, J. F. & BOYD, R. D. H. 1984. In *Fetal Physiology and Medicine. The Basis of Perinatology*, New York, Dekker, New York.
- CASTELLUCCI, M., KOSANKE, G., VERDENELLI, F., HUPPERTZ, B. & KAUFMANN, P. 2000. Villous sprouting: fundamental mechanisms of human placental development. *Hum Reprod Update*, 6, 485-94.
- CASTELLUCCI, M., SCHEPER, M., SCHEFFEN, I., CELONA, A. & KAUFMANN, P. 1990. The development of the human placental villous tree. *Anat Embryol (Berl)*, 181, 117-28.
- CELERMAJER, D. S., CULLEN, S. & DEANFIELD, J. E. 1993. Impairment of endothelium-dependent pulmonary artery relaxation in children with congenital heart disease and abnormal pulmonary hemodynamics. *Circulation*, 87, 440-6.
- CHANG, M. S., LEE, W. S., TENG, C. M., LEE, H. M., SHEU, J. R., HSIAO, G. & LIN, C. H. 2002. YC-1 increases cyclo-oxygenase-2 expression through protein kinase G- and p44/42 mitogen-activated protein kinase-dependent pathways in A549 cells. *Br J Pharmacol*, 136, 558-67.
- CHOUDHURY, N., KHROMOV, A. S., SOMLYO, A. P. & SOMLYO, A. V. 2004. Telokin mediates Ca²⁺-desensitization through activation of myosin phosphatase in phasic and tonic smooth muscle. *J Muscle Res Cell Motil*, 25, 657-65.
- CHRISTENSEN, E. N. & MENDELSON, M. E. 2006. Cyclic GMP-dependent protein kinase I α inhibits thrombin receptor-mediated calcium mobilization in vascular smooth muscle cells. *J Biol Chem*, 281, 8409-16.
- CLAPP, J. F., 3RD & CAPELESS, E. 1997. Cardiovascular function before, during, and after the first and subsequent pregnancies. *Am J Cardiol*, 80, 1469-73.

- CLAPP, J. F., 3RD, SEAWARD, B. L., SLEAMAKER, R. H. & HISER, J. 1988. Maternal physiologic adaptations to early human pregnancy. *Am J Obstet Gynecol*, 159, 1456-60.
- CLARK, S. L., COTTON, D. B., LEE, W., BISHOP, C., HILL, T., SOUTHWICK, J., PIVARNIK, J., SPILLMAN, T., DEVORE, G. R., PHELAN, J. & ET AL. 1989. Central hemodynamic assessment of normal term pregnancy. *Am J Obstet Gynecol*, 161, 1439-42.
- CONTI, M. A. & ADELSTEIN, R. S. 1981. The relationship between calmodulin binding and phosphorylation of smooth muscle myosin kinase by the catalytic subunit of 3':5' cAMP-dependent protein kinase. *J Biol Chem*, 256, 3178-81.
- COOPER, E. J., WAREING, M., GREENWOOD, S. L. & BAKER, P. N. 2005. Effects of oxygen tension and normalization pressure on endothelin-induced constriction of human placental chorionic plate arteries. *J Soc Gynecol Investig*, 12, 488-94.
- CORCORAN, J., LACEY, H., BAKER, P. N. & WAREING, M. 2008. Altered potassium channel expression in the human placental vasculature of pregnancies complicated by fetal growth restriction. *Hypertens Pregnancy*, 27, 75-86.
- CORNWELL, T. L., LI, J., SELLAK, H., MILLER, R. T. & WORD, R. A. 2001. Reorganization of myofilament proteins and decreased cGMP-dependent protein kinase in the human uterus during pregnancy. *J Clin Endocrinol Metab*, 86, 3981-8.
- CRAFT, I. L., FERGUSSON, I. L., SMITH, B. & YOUSSEFNEJADIAN, E. 1973. Sex steroid hormone levels in plasma following intra-amniotic injection of urea and prostaglandin E2. *J Obstet Gynaecol Br Commonw*, 80, 1095-9.
- CROSS, B. E., O'DEA, H. M. & MACPHEE, D. J. 2007. Expression of small heat shock-related protein 20 (HSP20) in rat myometrium is markedly decreased during late pregnancy and labour. *Reproduction*, 133, 807-17.
- CROSS, J. C., WERB, Z. & FISHER, S. J. 1994. Implantation and the placenta: key pieces of the development puzzle. *Science*, 266, 1508-18.
- DAVIS, M. J. & GORE, R. W. 1989. Length-tension relationship of vascular smooth muscle in single arterioles. *Am J Physiol*, 256, H630-40.
- DAVISON, J. M. & HYTTEN, F. E. 1975. The effect of pregnancy on the renal handling of glucose. *Br J Obstet Gynaecol*, 82, 374-81.
- DAVISON, J. M., VALLOTTON, M. B. & LINDHEIMER, M. D. 1981. Plasma osmolality and urinary concentration and dilution during and after pregnancy: evidence that lateral recumbency inhibits maximal urinary concentrating ability. *Br J Obstet Gynaecol*, 88, 472-9.
- DELIVORIA-PAPADOPOULOS, M., BATTAGLIA, F. C., BRUNS, P. D. & MESCHIA, G. 1967. Total, protein-bound, and ultrafilterable calcium in maternal and fetal plasmas. *Am J Physiol*, 213, 363-6.
- DEMIR, R., KAUFMANN, P., CASTELLUCCI, M., ERBENGI, T. & KOTOWSKI, A. 1989. Fetal vasculogenesis and angiogenesis in human placental villi. *Acta Anat (Basel)*, 136, 190-203.
- DEMIR, R., KAYISLI, U. A., CAYLI, S. & HUPPERTZ, B. 2006. Sequential steps during vasculogenesis and angiogenesis in the very early human placenta. *Placenta*, 27, 535-9.
- DEMIR, R., YABA, A. & HUPPERTZ, B. 2010. Vasculogenesis and angiogenesis in the endometrium during menstrual cycle and implantation. *Acta Histochem*, 112, 203-14.
- DEMPSEY, E. W. 1972. The development of capillaries in the villi of early human placentas. *Am J Anat*, 134, 221-37.

- DENG, J. T., VAN LIEROP, J. E., SUTHERLAND, C. & WALSH, M. P. 2001. Ca^{2+} -independent smooth muscle contraction. a novel function for integrin-linked kinase. *J Biol Chem*, 276, 16365-73.
- DONG, J. M., LEUNG, T., MANSER, E. & LIM, L. 1998. cAMP-induced morphological changes are counteracted by the activated RhoA small GTPase and the Rho kinase ROKalpha. *J Biol Chem*, 273, 22554-62.
- DUNCAN, J. L. & SCHLEGEL, R. 1975. Effect of streptolysin O on erythrocyte membranes, liposomes, and lipid dispersions. A protein-cholesterol interaction. *J Cell Biol*, 67, 160-74.
- DUNLAP, K. A., KWAK, H. I., BURGHARDT, R. C., BAZER, F. W., MAGNESS, R. R., JOHNSON, G. A. & BAYLESS, K. J. 2010. The sphingosine 1-phosphate (S1P) signaling pathway is regulated during pregnancy in sheep. *Biol Reprod*, 82, 876-87.
- DUNN, L. A. & HOLZ, R. W. 1983. Catecholamine secretion from digitonin-treated adrenal medullary chromaffin cells. *J Biol Chem*, 258, 4989-93.
- EASTERLING, T. R., WATTS, D. H., SCHMUCKER, B. C. & BENEDETTI, T. J. 1987. Measurement of cardiac output during pregnancy: validation of Doppler technique and clinical observations in preeclampsia. *Obstet Gynecol*, 69, 845-50.
- EDELMAN, A. M., LIN, W. H., OSTERHOUT, D. J., BENNETT, M. K., KENNEDY, M. B. & KREBS, E. G. 1990. Phosphorylation of smooth muscle myosin by type II Ca^{2+} /calmodulin-dependent protein kinase. *Mol Cell Biochem*, 97, 87-98.
- EDWARDS, G., DORA, K. A., GARDENER, M. J., GARLAND, C. J. & WESTON, A. H. 1998. K^{+} is an endothelium-derived hyperpolarizing factor in rat arteries. *Nature*, 396, 269-72.
- EDWARDS, G., FÉLÉTOU, M. & WESTON, A. H. 2010. Endothelium-derived hyperpolarising factors and associated pathways: a synopsis. *Pflügers Archiv - European Journal of Physiology*, 459, 863-879.
- EDWARDS, G. & WESTON, A. H. 1998. Endothelium-derived hyperpolarizing factor-a critical appraisal. *Prog Drug Res*, 50, 107-33.
- EL-AWADY, M. S., SMIRNOV, S. V. & WATSON, M. L. 2008. Desensitization of the soluble guanylyl cyclase/cGMP pathway by lipopolysaccharide in rat isolated pulmonary artery but not aorta. *Br J Pharmacol*, 155, 1164-73.
- ELDER, M. G. 2002. *Early Development*, Imperial College Press.
- ENDO, M., YAGI, S. & IINO, M. 1982. Tension-pCa relation and sarcoplasmic reticulum responses in chemically skinned smooth muscle fibers. *Fed Proc*, 41, 2245-50.
- ETO, M., OHMORI, T., SUZUKI, M., FURUYA, K. & MORITA, F. 1995. A novel protein phosphatase-1 inhibitory protein potentiated by protein kinase C. Isolation from porcine aorta media and characterization. *J Biochem*, 118, 1104-7.
- ETTER, E. F., ETO, M., WARDLE, R. L., BRAUTIGAN, D. L. & MURPHY, R. A. 2001. Activation of myosin light chain phosphatase in intact arterial smooth muscle during nitric oxide-induced relaxation. *J Biol Chem*, 276, 34681-5.
- EVGENOV, O. V., PACHER, P., SCHMIDT, P. M., HASKO, G., SCHMIDT, H. H. & STASCH, J. P. 2006. NO-independent stimulators and activators of soluble guanylate cyclase: discovery and therapeutic potential. *Nat Rev Drug Discov*, 5, 755-68.
- FABER, J. J. & THORNBURG, K. L. 1981. *Placental Transfer: Methods and Interpretations*, London, WB Saunders, London.
- FAXEN, M., NISELL, H. & KUBICKIENE, K. R. 2000. Altered gene expression of endothelin-A and endothelin-B receptors, but not endothelin-1, in myometrium and placenta from pregnancies complicated by preeclampsia. *Arch Gynecol Obstet*, 264, 143-9.

- FEIL, R., GAPPA, N., RUTZ, M., SCHLOSSMANN, J., ROSE, C. R., KONNERTH, A., BRUMMER, S., KUHNBANDNER, S. & HOFMANN, F. 2002. Functional reconstitution of vascular smooth muscle cells with cGMP-dependent protein kinase I isoforms. *Circ Res*, 90, 1080-6.
- FELETOU, M., HOEFFNER, U. & VANHOUTTE, P. M. 1989. Endothelium-dependent relaxing factors do not affect the smooth muscle of portal-mesenteric veins. *Blood Vessels*, 26, 21-32.
- FENELEY, M. R. & BURTON, G. J. 1991. Villous composition and membrane thickness in the human placenta at term: a stereological study using unbiased estimators and optimal fixation techniques. *Placenta*, 12, 131-42.
- FERRE, F. 2001. [Regulation of fetal placental circulation]. *Gynecol Obstet Fertil*, 29, 512-7.
- FILO, R. S., BOHR, D. F. & RUEGG, J. C. 1965. Glycerinated Skeletal and Smooth Muscle: Calcium and Magnesium Dependence. *Science*, 147, 1581-3.
- FISHER, S. A. 2010. Vascular smooth muscle phenotypic diversity and function. *Physiol Genomics*, 42A, 169-87.
- FLEXNER, L. B., COWIE, D. B. & ET AL. 1948. The permeability of the human placenta to sodium in normal and abnormal pregnancies and the supply of sodium to the human fetus as determined with radioactive sodium. *Am J Obstet Gynecol*, 55, 469-80.
- FOERSTER, J., HARTENECK, C., MALKEWITZ, J., SCHULTZ, G. & KOESLING, D. 1996. A functional heme-binding site of soluble guanylyl cyclase requires intact N-termini of alpha 1 and beta 1 subunits. *Eur J Biochem*, 240, 380-6.
- FOIDART, J. M., HUSTIN, J., DUBOIS, M. & SCHAAPS, J. P. 1992. The human placenta becomes haemochorial at the 13th week of pregnancy. *Int J Dev Biol*, 36, 451-3.
- FOX, S. B. & KHONG, T. Y. 1990. Lack of innervation of human umbilical cord. An immunohistological and histochemical study. *Placenta*, 11, 59-62.
- FRANCIS, S. H., BUSCH, J. L. & CORBIN, J. D. 2010. cGMP-Dependent Protein Kinases and cGMP Phosphodiesterases in Nitric Oxide and cGMP Action. *Pharmacological Reviews*, 62, 525-563.
- FRANCIS, S. H. & CORBIN, J. D. 1994. Structure and function of cyclic nucleotide-dependent protein kinases. *Annu Rev Physiol*, 56, 237-72.
- FRANCIS, S. H., NOBLETT, B. D., TODD, B. W., WELLS, J. N. & CORBIN, J. D. 1988. Relaxation of vascular and tracheal smooth muscle by cyclic nucleotide analogs that preferentially activate purified cGMP-dependent protein kinase. *Mol Pharmacol*, 34, 506-17.
- FRIEBE, A. & KOESLING, D. 2003. Regulation of nitric oxide-sensitive guanylyl cyclase. *Circ Res*, 93, 96-105.
- FRIED, G. & LIU, Y. A. 1994. Effects of endothelin, calcium channel blockade and EDRF inhibition on the contractility of human uteroplacental arteries. *Acta Physiol Scand*, 151, 477-84.
- FUJIHARA, H., WALKER, L. A., GONG, M. C., LEMICHEZ, E., BOQUET, P., SOMLYO, A. V. & SOMLYO, A. P. 1997. Inhibition of RhoA translocation and calcium sensitization by in vivo ADP-ribosylation with the chimeric toxin DC3B. *Mol Biol Cell*, 8, 2437-47.
- FUKUMOTO, M., NAKAIZUMI, A., ZHANG, T., LENTZ, S. I., SHIBATA, M. & PURO, D. G. 2012. Vulnerability of the retinal microvasculature to oxidative stress: ion channel-dependent mechanisms. *Am J Physiol Cell Physiol*, 302, C1413-20.

- FURCHGOTT, R. F. & ZAWADZKI, J. V. 1980. The obligatory role of endothelial cells in the relaxation of arterial smooth muscle by acetylcholine. *Nature*, 288, 373-6.
- FUSSLE, R., BHAKDI, S., SZIEGOLEIT, A., TRANUM-JENSEN, J., KRANZ, T. & WELLENSIEK, H. J. 1981. On the mechanism of membrane damage by *Staphylococcus aureus* alpha-toxin. *J Cell Biol*, 91, 83-94.
- GALLAGHER, P. J., HERRING, B. P., GRIFFIN, S. A. & STULL, J. T. 1991. Molecular characterization of a mammalian smooth muscle myosin light chain kinase. *J Biol Chem*, 266, 23936-44.
- GANITKEVICH, V. Y. & ISENBERG, G. 1992. Contribution of Ca^{2+} -induced Ca^{2+} release to the $[\text{Ca}^{2+}]_i$ transients in myocytes from guinea-pig urinary bladder. *J Physiol*, 458, 119-37.
- GEORGE, E. M. & GRANGER, J. P. 2011. Endothelin: key mediator of hypertension in preeclampsia. *Am J Hypertens*, 24, 964-9.
- GOKINA, N. I., MANDALÀ, M. & OSOL, G. 2003. Induction of localized differences in rat uterine radial artery behavior and structure during gestation. *American Journal of Obstetrics and Gynecology*, 189, 1489-1493.
- GOLDENBERG, R. L., CULHANE, J. F., IAMS, J. D. & ROMERO, R. 2008. Epidemiology and causes of preterm birth. *Lancet*, 371, 75-84.
- GONG, M. C., COHEN, P., KITAZAWA, T., IKEBE, M., MASUO, M., SOMLYO, A. P. & SOMLYO, A. V. 1992a. Myosin light chain phosphatase activities and the effects of phosphatase inhibitors in tonic and phasic smooth muscle. *J Biol Chem*, 267, 14662-8.
- GONG, M. C., FUGLSANG, A., ALESSI, D., KOBAYASHI, S., COHEN, P., SOMLYO, A. V. & SOMLYO, A. P. 1992b. Arachidonic acid inhibits myosin light chain phosphatase and sensitizes smooth muscle to calcium. *J Biol Chem*, 267, 21492-8.
- GONG, M. C., FUJIHARA, H., SOMLYO, A. V. & SOMLYO, A. P. 1997. Translocation of rhoA associated with Ca^{2+} sensitization of smooth muscle. *J Biol Chem*, 272, 10704-9.
- GONG, M. C., IIZUKA, K., NIXON, G., BROWNE, J. P., HALL, A., ECCLESTON, J. F., SUGAI, M., KOBAYASHI, S., SOMLYO, A. V. & SOMLYO, A. P. 1996. Role of guanine nucleotide-binding proteins--ras-family or trimeric proteins or both--in Ca^{2+} sensitization of smooth muscle. *Proc Natl Acad Sci U S A*, 93, 1340-5.
- GONG, M. C., KINTER, M. T., SOMLYO, A. V. & SOMLYO, A. P. 1995. Arachidonic acid and diacylglycerol release associated with inhibition of myosin light chain dephosphorylation in rabbit smooth muscle. *J Physiol*, 486 (Pt 1), 113-22.
- GRAY, H. 1975. *Early Development of the Human Embryo*, Longman.
- GRIFFIN, D., COHEN-OVERBEEK, T. & CAMPBELL, S. 1983. Fetal and utero-placental blood flow. *Clin Obstet Gynaecol*, 10, 565-602.
- GUDI, T., CHEN, J. C., CASTEEL, D. E., SEASHOLTZ, T. M., BOSS, G. R. & PILZ, R. B. 2002. cGMP-dependent protein kinase inhibits serum-response element-dependent transcription by inhibiting rho activation and functions. *J Biol Chem*, 277, 37382-93.
- HANAHAN, D. 1997. Signaling vascular morphogenesis and maintenance. *Science*, 277, 48-50.
- HARTSHORNE, D. J., ITO, M. & ERDODI, F. 1998. Myosin light chain phosphatase: subunit composition, interactions and regulation. *J Muscle Res Cell Motil*, 19, 325-41.

- HARTSHORNE, D. J., ITO, M. & IKEBE, M. 1989. Myosin and contractile activity in smooth muscle. *Adv Exp Med Biol*, 255, 269-77.
- HASHIMOTO, R., YUMOTO, M., WATANABE, M., KONISHI, M., HARAOKA, J. & MIKI, T. 2009. Differential effects of an expected actin-tropomyosin binding region of heat shock protein 20 on the relaxation in skinned carotid artery and taenia cecum from guinea pig. *J Smooth Muscle Res*, 45, 63-74.
- HEMMINGS, D. G. 2006. Signal transduction underlying the vascular effects of sphingosine 1-phosphate and sphingosylphosphorylcholine. *Naunyn Schmiedebergs Arch Pharmacol*, 373, 18-29.
- HEMMINGS, D. G., HUDSON, N. K., HALLIDAY, D., O'HARA, M., BAKER, P. N., DAVIDGE, S. T. & TAGGART, M. J. 2006. Sphingosine-1-phosphate acts via rho-associated kinase and nitric oxide to regulate human placental vascular tone. *Biol Reprod*, 74, 88-94.
- HERRING, B. P. & SMITH, A. F. 1996. Telokin expression is mediated by a smooth muscle cell-specific promoter. *Am J Physiol*, 270, C1656-65.
- HIGBY, K., SUITER, C. R., PHELPS, J. Y., SILER-KHODR, T. & LANGER, O. 1994. Normal values of urinary albumin and total protein excretion during pregnancy. *Am J Obstet Gynecol*, 171, 984-9.
- HIMPENS, B., KITAZAWA, T. & SOMLYO, A. P. 1990. Agonist-dependent modulation of Ca²⁺ sensitivity in rabbit pulmonary artery smooth muscle. *Pflugers Arch*, 417, 21-8.
- HIMPENS, B. & SOMLYO, A. P. 1988. Free-calcium and force transients during depolarization and pharmacomechanical coupling in guinea-pig smooth muscle. *J Physiol*, 395, 507-30.
- HLA, T. 2004. Physiological and pathological actions of sphingosine 1-phosphate. *Semin Cell Dev Biol*, 15, 513-20.
- HOLLIER, L. M. 2005. Preventing preterm birth: what works, what doesn't. *Obstet Gynecol Surv*, 60, 124-31.
- HORIUTI, K. 1988. Mechanism of contracture on cooling of caffeine-treated frog skeletal muscle fibres. *J Physiol*, 398, 131-48.
- HUANG, J., ZHOU, H., MAHAVADI, S., SRIWAI, W. & MURTHY, K. S. 2007. Inhibition of Gα_q-dependent PLC-β1 activity by PKG and PKA is mediated by phosphorylation of RGS4 and GRK2. *Am J Physiol Cell Physiol*, 292, C200-8.
- HUANG, Q. Q., FISHER, S. A. & BROZOVICH, F. V. 2004. Unzipping the role of myosin light chain phosphatase in smooth muscle cell relaxation. *J Biol Chem*, 279, 597-603.
- HUDSON, N. K., O'HARA, M., LACEY, H. A., CORCORAN, J., HEMMINGS, D. G., WAREING, M., BAKER, P. & TAGGART, M. J. 2007. Modulation of human arterial tone during pregnancy: the effect of the bioactive metabolite sphingosine-1-phosphate. *Biol Reprod*, 77, 45-52.
- HULL, A. D., WHITE, C. R. & PEARCE, W. J. 1994. Endothelium-derived relaxing factor and cyclic GMP-dependent vasorelaxation in human chorionic plate arteries. *Placenta*, 15, 365-75.
- HUPPERTZ, B. & PEETERS, L. L. 2005. Vascular biology in implantation and placentation. *Angiogenesis*, 8, 157-67.
- HYTTEN, F. 1985. Blood volume changes in normal pregnancy. *Clin Haematol*, 14, 601-12.
- IGNARRO, L. J. 1999. Nitric oxide: a unique endogenous signaling molecule in vascular biology. *Biosci Rep*, 19, 51-71.
- IGNARRO, L. J. 2005. Nitric oxide. *Curr Top Med Chem*, 5, 595.

- IGNARRO, L. J., BYRNS, R. E., BUGA, G. M. & WOOD, K. S. 1987. Mechanisms of endothelium-dependent vascular smooth muscle relaxation elicited by bradykinin and VIP. *Am J Physiol*, 253, H1074-82.
- IGNARRO, L. J., HARBISON, R. G., WOOD, K. S. & KADOWITZ, P. J. 1986. Activation of purified soluble guanylate cyclase by endothelium-derived relaxing factor from intrapulmonary artery and vein: stimulation by acetylcholine, bradykinin and arachidonic acid. *J Pharmacol Exp Ther*, 237, 893-900.
- IINO, M. 1990. Biphasic Ca^{2+} dependence of inositol 1,4,5-trisphosphate-induced Ca^{2+} release in smooth muscle cells of the guinea pig taenia caeci. *J Gen Physiol*, 95, 1103-22.
- IINO, M. & ENDO, M. 1992. Calcium-dependent immediate feedback control of inositol 1,4,5-trisphosphate-induced Ca^{2+} release. *Nature*, 360, 76-8.
- IIZUKA, K., YOSHII, A., SAMIZO, K., TSUKAGOSHI, H., ISHIZUKA, T., DOBASHI, K., NAKAZAWA, T. & MORI, M. 1999. A major role for the rho-associated coiled coil forming protein kinase in G-protein-mediated Ca^{2+} sensitization through inhibition of myosin phosphatase in rabbit trachea. *Br J Pharmacol*, 128, 925-33.
- INOUE, A., YANAGISAWA, M., KIMURA, S., KASUYA, Y., MIYAUCHI, T., GOTO, K. & MASAKI, T. 1989. The human endothelin family: three structurally and pharmacologically distinct isopeptides predicted by three separate genes. *Proc Natl Acad Sci U S A*, 86, 2863-7.
- IRVINE, J. C., FAVALORO, J. L. & KEMP-HARPER, B. K. 2003. NO- activates soluble guanylate cyclase and Kv channels to vasodilate resistance arteries. *Hypertension*, 41, 1301-7.
- ISHIHARA, H., MARTIN, B. L., BRAUTIGAN, D. L., KARAKI, H., OZAKI, H., KATO, Y., FUSEYANI, N., WATABE, S., HASHIMOTO, K., UEMURA, D. & ET AL. 1989. Calyculin A and okadaic acid: inhibitors of protein phosphatase activity. *Biochem Biophys Res Commun*, 159, 871-7.
- ITO, K., IKEMOTO, T. & TAKAKURA, S. 1991. Involvement of Ca^{2+} influx-induced Ca^{2+} release in contractions of intact vascular smooth muscles. *Am J Physiol*, 261, H1464-70.
- ITO, K., SHIMOMURA, E., IWANAGA, T., SHIRAISHI, M., SHINDO, K., NAKAMURA, J., NAGUMO, H., SETO, M., SASAKI, Y. & TAKUWA, Y. 2003. Essential role of rho kinase in the Ca^{2+} sensitization of prostaglandin F(2 α)-induced contraction of rabbit aortae. *J Physiol*, 546, 823-36.
- ITO, M., DABROWSKA, R., GUERRIERO, V., JR. & HARTSHORNE, D. J. 1989. Identification in turkey gizzard of an acidic protein related to the C-terminal portion of smooth muscle myosin light chain kinase. *J Biol Chem*, 264, 13971-4.
- JAUNIAUX, E., WATSON, A. L., HEMPSTOCK, J., BAO, Y. P., SKEPPER, J. N. & BURTON, G. J. 2000. Onset of maternal arterial blood flow and placental oxidative stress. A possible factor in human early pregnancy failure. *Am J Pathol*, 157, 2111-22.
- JENSEN, P. E., GONG, M. C., SOMLYO, A. V. & SOMLYO, A. P. 1996. Separate upstream and convergent downstream pathways of G-protein- and phorbol ester-mediated Ca^{2+} sensitization of myosin light chain phosphorylation in smooth muscle. *Biochem J*, 318 (Pt 2), 469-75.
- KANG, Y. H., KANG, J. S. & SHIN, H. M. 2012. Vasodilatory Effects of Cinnamic Acid via the Nitric Oxide-cGMP-PKG Pathway in Rat Thoracic Aorta. *Phytother Res*.
- KARAKI, H., OZAKI, H., HORI, M., MITSUI-SAITO, M., AMANO, K., HARADA, K., MIYAMOTO, S., NAKAZAWA, H., WON, K. J. & SATO, K. 1997.

- Calcium movements, distribution, and functions in smooth muscle. *Pharmacol Rev*, 49, 157-230.
- KATO, K., GOTO, S., INAGUMA, Y., HASEGAWA, K., MORISHITA, R. & ASANO, T. 1994. Purification and characterization of a 20-kDa protein that is highly homologous to alpha B crystallin. *J Biol Chem*, 269, 15302-9.
- KAUFMANN, P., BLACK, S. & HUPPERTZ, B. 2003. Endovascular trophoblast invasion: implications for the pathogenesis of intrauterine growth retardation and preeclampsia. *Biol Reprod*, 69, 1-7.
- KAUFMANN, P., MAYHEW, T. M. & CHARNOCK-JONES, D. S. 2004. Aspects of human fetoplacental vasculogenesis and angiogenesis. II. Changes during normal pregnancy. *Placenta*, 25, 114-26.
- KAUFMANN, P. A. S., I. 1998. *Placental development*, Philadelphia, W.B. Saunders.
- KENNY, L. C., BAKER, P. N., KENDALL, D. A., RANDALL, M. D. & DUNN, W. R. 2002. Differential mechanisms of endothelium-dependent vasodilator responses in human myometrial small arteries in normal pregnancy and pre-eclampsia. *Clin Sci (Lond)*, 103, 67-73.
- KHATRI, J. J., JOYCE, K. M., BROZOVICH, F. V. & FISHER, S. A. 2001. Role of myosin phosphatase isoforms in cGMP-mediated smooth muscle relaxation. *J Biol Chem*, 276, 37250-7.
- KHONG, T. Y., DE WOLF, F., ROBERTSON, W. B. & BROSENS, I. 1986. Inadequate maternal vascular response to placentation in pregnancies complicated by pre-eclampsia and by small-for-gestational age infants. *Br J Obstet Gynaecol*, 93, 1049-59.
- KHROMOV, A. S., MOMOTANI, K., JIN, L., ARTAMONOV, M. V., SHANNON, J., ETO, M. & SOMLYO, A. V. 2012. Molecular Mechanism of Telokin-mediated Disinhibition of Myosin Light Chain Phosphatase and cAMP/cGMP-induced Relaxation of Gastrointestinal Smooth Muscle. *J Biol Chem*, 287, 20975-85.
- KHROMOV, A. S., WANG, H., CHOUDHURY, N., MCDUFFIE, M., HERRING, B. P., NAKAMOTO, R., OWENS, G. K., SOMLYO, A. P. & SOMLYO, A. V. 2006. Smooth muscle of telokin-deficient mice exhibits increased sensitivity to Ca²⁺ and decreased cGMP-induced relaxation. *Proc Natl Acad Sci U S A*, 103, 2440-5.
- KILMAN, H. J. 1993. The placenta revealed. *Am J Pathol*, 143, 332-36.
- KILMAN, H. J. 2000. The story of decidualization, menstruation, and trophoblast invasion. *Am J Pathol*, 157, 1759-68.
- KIM, H. R., GRACEFFA, P., FERRON, F., GALLANT, C., BOCZKOWSKA, M., DOMINGUEZ, R. & MORGAN, K. G. 2010. Actin polymerization in differentiated vascular smooth muscle cells requires vasodilator-stimulated phosphoprotein. *Am J Physiol Cell Physiol*, 298, C559-71.
- KIM, K. H., MORIARTY, K. & BENDER, J. R. 2008. Vascular cell signaling by membrane estrogen receptors. *Steroids*, 73, 864-9.
- KIMERA, K. 1999. *Fukuoka Igaku Zasshi*, 90, 457-463.
- KIMURA, K., ITO, M., AMANO, M., CHIHARA, K., FUKATA, Y., NAKAFUKU, M., YAMAMORI, B., FENG, J., NAKANO, T., OKAWA, K., IWAMATSU, A. & KAIBUCHI, K. 1996. Regulation of myosin phosphatase by Rho and Rho-associated kinase (Rho-kinase). *Science*, 273, 245-8.
- KITAZAWA, T., ETO, M., WOODSOME, T. P. & BRAUTIGAN, D. L. 2000. Agonists trigger G protein-mediated activation of the CPI-17 inhibitor phosphoprotein of myosin light chain phosphatase to enhance vascular smooth muscle contractility. *J Biol Chem*, 275, 9897-900.

- KITAZAWA, T., GAYLINN, B. D., DENNEY, G. H. & SOMLYO, A. P. 1991a. G-protein-mediated Ca^{2+} sensitization of smooth muscle contraction through myosin light chain phosphorylation. *J Biol Chem*, 266, 1708-15.
- KITAZAWA, T., KOBAYASHI, S., HORIUTI, K., SOMLYO, A. V. & SOMLYO, A. P. 1989. Receptor-coupled, permeabilized smooth muscle. Role of the phosphatidylinositol cascade, G-proteins, and modulation of the contractile response to Ca^{2+} . *J Biol Chem*, 264, 5339-42.
- KITAZAWA, T., MASUO, M. & SOMLYO, A. P. 1991b. G protein-mediated inhibition of myosin light-chain phosphatase in vascular smooth muscle. *Proc Natl Acad Sci U S A*, 88, 9307-10.
- KITAZAWA, T., SEMBA, S., HUH, Y. H., KITAZAWA, K. & ETO, M. 2009. Nitric oxide-induced biphasic mechanism of vascular relaxation via dephosphorylation of CPI-17 and MYPT1. *J Physiol*, 587, 3587-603.
- KITAZAWA, T. & SOMLYO, A. P. 1990. Desensitization and muscarinic re-sensitization of force and myosin light chain phosphorylation to cytoplasmic Ca^{2+} in smooth muscle. *Biochem Biophys Res Commun*, 172, 1291-7.
- KLEINER-ASSAF, A., JAFFA, A. J. & ELAD, D. 1999. Hemodynamic model for analysis of Doppler ultrasound indexes of umbilical blood flow. *Am J Physiol*, 276, H2204-14.
- KNOCK, G. A., MCCARTHY, A. L., LOWY, C. & POSTON, L. 1997. Association of gestational diabetes with abnormal maternal vascular endothelial function. *Br J Obstet Gynaecol*, 104, 229-34.
- KNOCK, G. A. & POSTON, L. 1996. Bradykinin-mediated relaxation of isolated maternal resistance arteries in normal pregnancy and preeclampsia. *Am J Obstet Gynecol*, 175, 1668-74.
- KOOK, H., YOON, Y. D. & BAIK, Y. H. 1996. Effects of calcium antagonists on contractions of chorionic arteries in normal and preeclampsia placenta. *J Korean Med Sci*, 11, 250-7.
- KOYAMA, M., ITO, M., FENG, J., SEKO, T., SHIRAKI, K., TAKASE, K., HARTSHORNE, D. J. & NAKANO, T. 2000. Phosphorylation of CPI-17, an inhibitory phosphoprotein of smooth muscle myosin phosphatase, by Rho-kinase. *FEBS Lett*, 475, 197-200.
- KRALL, J. F., FITTINGOFF, M. & RAJFER, J. 1988. Characterization of cyclic nucleotide and inositol 1,4,5-trisphosphate-sensitive calcium-exchange activity of smooth muscle cells cultured from the human corpora cavernosa. *Biol Reprod*, 39, 913-22.
- KUBLICKIENE, K. R., COCKELL, A. P., NISELL, H. & POSTON, L. 1997. Role of nitric oxide in the regulation of vascular tone in pressurized and perfused resistance myometrial arteries from term pregnant women. *Am J Obstet Gynecol*, 177, 1263-9.
- KUBLICKIENE, K. R., NISELL, H., POSTON, L., KRUGER, K. & LINDBLOM, B. 2000. Modulation of vascular tone by nitric oxide and endothelin 1 in myometrial resistance arteries from pregnant women at term. *Am J Obstet Gynecol*, 182, 87-93.
- KUBOTA, Y., NOMURA, M., KAMM, K. E. & STULL, J. T. 1992. Mechanism of GTP gamma S-dependent regulation of smooth muscle contraction. *Jpn J Pharmacol*, 58 Suppl 2, 421P.
- LAPLACE, P.-S. 1806. L'equation de Young-Laplace. *Mecanique celeste*, Supplement to the tenth edition.
- LEARMONT, J. G. & POSTON, L. 1996. Nitric oxide is involved in flow-induced dilation of isolated human small fetoplacental arteries. *Am J Obstet Gynecol*, 174, 583-8.

- LEE, E., HAYES, D. B., LANGSETMO, K., SUNDBERG, E. J. & TAO, T. C. 2007. Interactions between the leucine-zipper motif of cGMP-dependent protein kinase and the C-terminal region of the targeting subunit of myosin light chain phosphatase. *J Mol Biol*, 373, 1198-212.
- LEE, M. R., LI, L. & KITAZAWA, T. 1997. Cyclic GMP causes Ca²⁺ desensitization in vascular smooth muscle by activating the myosin light chain phosphatase. *J Biol Chem*, 272, 5063-8.
- LEIBERMAN, J. R., WIZNITZER, A., GLEZERMAN, M., FELDMAN, B., LEVY, J. & SHARONI, Y. 1993. Estrogen and progesterone receptors in the uterine artery of rats during and after pregnancy. *Eur J Obstet Gynecol Reprod Biol*, 51, 35-40.
- LIM, I., YUN, J., KIM, S., LEE, C., SEO, S., KIM, T. & BANG, H. 2005. Nitric oxide stimulates a large-conductance Ca-activated K⁺ channel in human skin fibroblasts through protein kinase G pathway. *Skin Pharmacol Physiol*, 18, 279-87.
- LINCOLN, T. M. & CORNWELL, T. L. 1993. Intracellular cyclic GMP receptor proteins. *FASEB J*, 7, 328-38.
- LINCOLN, T. M., DILLS, W. L., JR. & CORBIN, J. D. 1977. Purification and subunit composition of guanosine 3':5'-monophosphate-dependent protein kinase from bovine lung. *J Biol Chem*, 252, 4269-75.
- LINCOLN, T. M., FLOCKHART, D. A. & CORBIN, J. D. 1978. Studies on the structure and mechanism of activation of the guanosine 3':5'-monophosphate-dependent protein kinase. *J Biol Chem*, 253, 6002-9.
- LIND, I., AHNERT-HILGER, G., FUCHS, G. & GRATZL, M. 1987. Purification of alpha-toxin from *Staphylococcus aureus* and application to cell permeabilization. *Anal Biochem*, 164, 84-9.
- LINDHEIMER, M. & BARRON, W. M. 1998. *Renal Function and volume homeostasis*, Stanford.
- LINDOW, S. W., DAVIES, N., DAVEY, D. A. & SMITH, J. A. 1988. The effect of sublingual nifedipine on uteroplacental blood flow in hypertensive pregnancy. *Br J Obstet Gynaecol*, 95, 1276-81.
- LORENZ, W., DOENICKE, A., MEYER, R., REIMANN, H. J., KUSCHE, J., BARTH, H., GEESING, H., HUTZEL, M. & WEISSENBACHER, B. 1972. An improved method for the determination of histamine release in man: its application in studies with propanidid and thiopentone. *Eur J Pharmacol*, 19, 180-90.
- LU, Y., ZHANG, H., GOKINA, N., MANDALA, M., SATO, O., IKEBE, M., OSOL, G. & FISHER, S. A. 2008. Uterine artery myosin phosphatase isoform switching and increased sensitivity to SNP in a rat L-NAME model of hypertension of pregnancy. *Am J Physiol Cell Physiol*, 294, C564-71.
- LUKSHA, L., LUKSHA, N., KUBLICKAS, M., NISELL, H. & KUBLICKIENE, K. 2010. Diverse mechanisms of endothelium-derived hyperpolarizing factor-mediated dilatation in small myometrial arteries in normal human pregnancy and preeclampsia. *Biol Reprod*, 83, 728-35.
- LYNDRUP, J. & LAMONT, R. F. 2007. The choice of a tocolytic for the treatment of preterm labor: a critical evaluation of nifedipine versus atosiban. *Expert Opin Investig Drugs*, 16, 843-53.
- MACDONALD, J. A., ETO, M., BORMAN, M. A., BRAUTIGAN, D. L. & HAYSTEAD, T. A. 2001. Dual Ser and Thr phosphorylation of CPI-17, an inhibitor of myosin phosphatase, by MYPT-associated kinase. *FEBS Lett*, 493, 91-4.
- MACINTYRE, D. A., TYSON, E. K., READ, M., SMITH, R., YEO, G., KWEK, K. & CHAN, E. C. 2008. Contraction in human myometrium is associated with changes in small heat shock proteins. *Endocrinology*, 149, 245-52.

- MACKENZIE, I. Z., MACLEAN, D. A. & MITCHELL, M. D. 1980. Prostaglandins in the human fetal circulation in mid-trimester and term pregnancy. *Prostaglandins*, 20, 649-54.
- MACLEAN, M. R., TEMPLETON, A. G. & MCGRATH, J. C. 1992. The influence of endothelin-1 on human foeto-placental blood vessels: a comparison with 5-hydroxytryptamine. *Br J Pharmacol*, 106, 937-41.
- MAGNESS, R. R. & ROSENFELD, C. R. 1993. Calcium modulation of endothelium-derived prostacyclin production in ovine pregnancy. *Endocrinology*, 132, 2445-52.
- MAIGAARD, S., FORMAN, A. & ANDERSSON, K. E. 1985. Differences in contractile activation between human myometrium and intramyometrial arteries. *Acta Physiol Scand*, 124, 371-9.
- MAIGAARD, S., FORMAN, A., BROGAARD-HANSEN, K. P. & ANDERSSON, K. E. 1986. Inhibitory effects of nitrendipine on myometrial and vascular smooth muscle in human pregnant uterus and placenta. *Acta Pharmacol Toxicol (Copenh)*, 59, 1-10.
- MANDALA, M. & OSOL, G. 2012. Physiological remodelling of the maternal uterine circulation during pregnancy. *Basic Clin Pharmacol Toxicol*, 110, 12-8.
- MARIN, J., REVIRIEGO, J., FERNANDEZ-ALFONSO, M. S. & GUERRA, P. 1990. Effect of nifedipine in arterial vasculature of human placenta. *Gen Pharmacol*, 21, 629-33.
- MARTIN, E., LEE, Y-C., MURAD, F. 2001. YC-1 activation of human soluble guanylyl cyclase has both heme-dependent and heme-independent components. *Proc Natl Acad Sci U S A*, 98, 12938-12942.
- MASUMOTO, A., HIROOKA, Y., SHIMOKAWA, H., HIRONAGA, K., SETOGUCHI, S. & TAKESHITA, A. 2001. Possible involvement of Rho-kinase in the pathogenesis of hypertension in humans. *Hypertension*, 38, 1307-10.
- MATCHKOV, V. V. 2004. A Cyclic GMP-dependent Calcium-activated Chloride Current in Smooth-muscle Cells from Rat Mesenteric Resistance Arteries. *The Journal of General Physiology*, 123, 121-134.
- MCCARTHY, A. L., WOOLFSON, R. G., EVANS, B. J., DAVIES, D. R., RAJU, S. K. & POSTON, L. 1994. Functional characteristics of small placental arteries. *Am J Obstet Gynecol*, 170, 945-51.
- MCCARTHY, A. L., WOOLFSON, R. G., RAJU, S. K. & POSTON, L. 1993. Abnormal endothelial cell function of resistance arteries from women with preeclampsia. *Am J Obstet Gynecol*, 168, 1323-30.
- MELMON, K. L., CLINE, M. J., HUGHES, T. & NIES, A. S. 1968. Kinins: possible mediators of neonatal circulatory changes in man. *J Clin Invest*, 47, 1295-302.
- MILLER, J. R., SILVER, P. J. & STULL, J. T. 1983. The role of myosin light chain kinase phosphorylation in beta-adrenergic relaxation of tracheal smooth muscle. *Mol Pharmacol*, 24, 235-42.
- MILLS, T. A., WAREING, M., BUGG, G. J., GREENWOOD, S. L. & BAKER, P. N. 2005. Chorionic plate artery function and Doppler indices in normal pregnancy and intrauterine growth restriction. *Eur J Clin Invest*, 35, 758-64.
- MILLS, T. A., BAKER, P. N. & WAREING, M. 2007a. The effect of mode of delivery on placental chorionic plate vascular reactivity. *Hypertens Pregnancy*, 26, 201-10.
- MILLS, T. A., TAGGART, M. J., GREENWOOD, S. L., BAKER, P. N. & WAREING, M. 2007b. Histamine-induced contraction and relaxation of placental chorionic plate arteries. *Placenta*, 28, 1158-64.

- MILLS, T. 2009. Acute and chronic modulation of placental chorionic plate artery reactivity by reactive oxygen species. *Free Radical Biology and Medicine*, 47, 159-166.
- MILLS, T. A., WAREING, M., SHENNAN, A. H., POSTON, L., BAKER, P. N. & GREENWOOD, S. L. 2009. Acute and chronic modulation of placental chorionic plate artery reactivity by reactive oxygen species. *Free Radic Biol Med*, 47, 159-66.
- MITCHELL, M. D. & ROBINSON, J. S. 1978. Concentrations of 6-oxo-prostaglandin F1 alpha and thromboxane B2 in the tracheal fluid of foetal sheep. *J Endocrinol*, 79, 403-4.
- MIZUGISHI, K., LI, C., OLIVERA, A., BIELAWSKI, J., BIELAWSKA, A., DENG, C. X. & PROIA, R. L. 2007. Maternal disturbance in activated sphingolipid metabolism causes pregnancy loss in mice. *J Clin Invest*, 117, 2993-3006.
- MOHAMMED, T., STULC, J., SIBLEY, C. P. & BOYD, R. D. 1992. Effect of maternal hypokalaemia on unidirectional maternofetal and net potassium fluxes across the placenta of the anaesthetized rat. *Placenta*, 13, 231-40.
- MULSCH, A., BAUERSACHS, J., SCHAFER, A., STASCH, J. P., KAST, R. & BUSSE, R. 1997. Effect of YC-1, an NO-independent, superoxide-sensitive stimulator of soluble guanylyl cyclase, on smooth muscle responsiveness to nitrovasodilators. *Br J Pharmacol*, 120, 681-9.
- MULSCH, A., OELZE, M., KLOSS, S., MOLLNAU, H., TOPFER, A., SMOLENSKI, A., WALTER, U., STASCH, J. P., WARNHOLTZ, A., HINK, U., MEINERTZ, T. & MUNZEL, T. 2001. Effects of in vivo nitroglycerin treatment on activity and expression of the guanylyl cyclase and cGMP-dependent protein kinase and their downstream target vasodilator-stimulated phosphoprotein in aorta. *Circulation*, 103, 2188-94.
- MULVANY, M. J. 1987. Relations between vascular structure and blood pressure. *J Clin Hypertens*, 3, 313-6.
- MULVANY, M. J. & AALKJAER, C. 1990. Structure and function of small arteries. *Physiol Rev*, 70, 921-61.
- MULVANY, M. J. & HALPERN, W. 1977. Contractile properties of small arterial resistance vessels in spontaneously hypertensive and normotensive rats. *Circ Res*, 41, 19-26.
- MULVANY, M. J. & KORSGAARD, N. 1983. Correlations and otherwise between blood pressure, cardiac mass and resistance vessel characteristics in hypertensive, normotensive and hypertensive/normotensive hybrid rats. *J Hypertens*, 1, 235-44.
- MULVANY, M. J. & NYBORG, N. 1980. An increased calcium sensitivity of mesenteric resistance vessels in young and adult spontaneously hypertensive rats. *Br J Pharmacol*, 71, 585-96.
- MULVANY, M. J. & WARSHAW, D. M. 1979. The active tension-length curve of vascular smooth muscle related to its cellular components. *J Gen Physiol*, 74, 85-104.
- MURAD, F. 1994. Regulation of cytosolic guanylyl cyclase by nitric oxide: the NO-cyclic GMP signal transduction system. *Adv Pharmacol*, 26, 19-33.
- MURAKI, K., IMAIZUMI, Y. & WATANABE, M. 1992. Ca-dependent K channels in smooth muscle cells permeabilized by beta-escin recorded using the cell-attached patch-clamp technique. *Pflugers Arch*, 420, 461-9.
- MURANYI, A., MACDONALD, J. A., DENG, J. T., WILSON, D. P., HAYSTEAD, T. A., WALSH, M. P., ERDODI, F., KISS, E., WU, Y. & HARTSHORNE, D. J. 2002. Phosphorylation of the myosin phosphatase target subunit by integrin-linked kinase. *Biochem J*, 366, 211-6.

- MURATA-HORI, M., SUIZU, F., IWASAKI, T., KIKUCHI, A. & HOSOYA, H. 1999. ZIP kinase identified as a novel myosin regulatory light chain kinase in HeLa cells. *FEBS Lett*, 451, 81-4.
- MYATT, L., BREWER, A. & BROCKMAN, D. E. 1991. The action of nitric oxide in the perfused human fetal-placental circulation. *Am J Obstet Gynecol*, 164, 687-92.
- MYATT, L., BREWER, A. S., LANGDON, G. & BROCKMAN, D. E. 1992. Attenuation of the vasoconstrictor effects of thromboxane and endothelin by nitric oxide in the human fetal-placental circulation. *Am J Obstet Gynecol*, 166, 224-30.
- MYERS, J., HALL, C., WAREING, M., GILLHAM, J. & BAKER, P. 2006. The effect of maternal characteristics on endothelial-dependent relaxation of myometrial arteries. *Eur J Obstet Gynecol Reprod Biol*, 124, 158-63.
- NAGAO, T., ILLIANO, S. & VANHOUTTE, P. M. 1992. Heterogeneous distribution of endothelium-dependent relaxations resistant to NG-nitro-L-arginine in rats. *Am J Physiol*, 263, H1090-4.
- NAKAMURA, K., KOGA, Y., SAKAI, H., HOMMA, K. & IKEBE, M. 2007. cGMP-dependent relaxation of smooth muscle is coupled with the change in the phosphorylation of myosin phosphatase. *Circ Res*, 101, 712-22.
- NAKAMURA, M., ICHIKAWA, K., ITO, M., YAMAMORI, B., OKINAKA, T., ISAKA, N., YOSHIDA, Y., FUJITA, S. & NAKANO, T. 1999. Effects of the phosphorylation of myosin phosphatase by cyclic GMP-dependent protein kinase. *Cell Signal*, 11, 671-6.
- NIIRO, N. & IKEBE, M. 2001. Zipper-interacting protein kinase induces Ca(2+)-free smooth muscle contraction via myosin light chain phosphorylation. *J Biol Chem*, 276, 29567-74.
- NISHIMURA, J., KHALIL, R. A., DRENTH, J. P. & VAN BREEMEN, C. 1990. Evidence for increased myofilament Ca²⁺ sensitivity in norepinephrine-activated vascular smooth muscle. *Am J Physiol*, 259, H2-8.
- NISHIMURA, J. & VAN BREEMEN, C. 1989. Direct regulation of smooth muscle contractile elements by second messengers. *Biochem Biophys Res Commun*, 163, 929-35.
- NORWITZ, E. R., SCHUST, D. J. & FISHER, S. J. 2001. Implantation and the survival of early pregnancy. *N Engl J Med*, 345, 1400-8.
- OELZE, M., MOLLNAU, H., HOFFMANN, N., WARNHOLTZ, A., BODENSCHATZ, M., SMOLENSKI, A., WALTER, U., SKATCHKOV, M., MEINERTZ, T. & MUNZEL, T. 2000. Vasodilator-stimulated phosphoprotein serine 239 phosphorylation as a sensitive monitor of defective nitric oxide/cGMP signaling and endothelial dysfunction. *Circ Res*, 87, 999-1005.
- OGAWA, Y. 1994. Role of ryanodine receptors. *Crit Rev Biochem Mol Biol*, 29, 229-74.
- OSOL, G., BARRON, C., GOKINA, N. & MANDALA, M. 2009. Inhibition of Nitric Oxide Synthases Abrogates Pregnancy-Induced Uterine Vascular Expansive Remodeling. *J Vasc Res*, 46, 478-486.
- OSOL, G. & MANDALA, M. 2009. Maternal uterine vascular remodeling during pregnancy. *Physiology (Bethesda)*, 24, 58-71.
- OWENS, G. K. 1995. Regulation of differentiation of vascular smooth muscle cells. *Physiol Rev*, 75, 487-517.
- OWENS, G. K., KUMAR, M. S. & WAMHOFF, B. R. 2004. Molecular regulation of vascular smooth muscle cell differentiation in development and disease. *Physiol Rev*, 84, 767-801.

- PARK, W. S., KO, J.-H., KO, E. A., SON, Y. K., HONG, D. H., JUNG, I. D., PARK, Y.-M., CHOI, T.-H., KIM, N. & HAN, J. 2010. The Guanylyl Cyclase Activator YC-1 Directly Inhibits the Voltage-Dependent K⁺ Channels in Rabbit Coronary Arterial Smooth Muscle Cells. *Journal of Pharmacological Sciences*, 112, 64-72.
- PAYNE, M., ZHANG, H., PROSDOCIMO, T., JOYCE, K., KOGA, Y., IKEBE, M. & FISHER, S. 2006. Myosin phosphatase isoform switching in vascular smooth muscle development. *Journal of Molecular and Cellular Cardiology*, 40, 274-282.
- PAYNE, M. C. 2004. Dynamic changes in expression of myosin phosphatase in a model of portal hypertension. *AJP: Heart and Circulatory Physiology*, 286, H1801-H1810.
- PELLICER 2000. On the demonstration of the Young-Laplace equation in introductory physics courses. *Phys Educ*, 35, 126-29.
- PETROU, S., EDDAMA, O. & MANGHAM, L. 2011. A structured review of the recent literature on the economic consequences of preterm birth. *Arch Dis Child Fetal Neonatal Ed*, 96, F225-32.
- PFITZER, G., HOFMANN, F., DISALVO, J. & RUEGG, J. C. 1984. cGMP and cAMP inhibit tension development in skinned coronary arteries. *Pflugers Arch*, 401, 277-80.
- PFITZER, G., MERKEL, L., RUEGG, J. C. & HOFMANN, F. 1986. Cyclic GMP-dependent protein kinase relaxes skinned fibers from guinea pig taenia coli but not from chicken gizzard. *Pflugers Arch*, 407, 87-91.
- PHIPPARD, A. F., HORVATH, J. S., GLYNN, E. M., GARNER, M. G., FLETCHER, P. J., DUGGIN, G. G. & TILLER, D. J. 1986. Circulatory adaptation to pregnancy--serial studies of haemodynamics, blood volume, renin and aldosterone in the baboon (*Papio hamadryas*). *J Hypertens*, 4, 773-9.
- PIJNENBORG, R. 1990. Trophoblast invasion and placentation in the human: morphological aspects. *Trophoblast Res.*, 4, 33-47.
- PIJNENBORG, R., DIXON, G., ROBERTSON, W. B. & BROSENS, I. 1980. Trophoblastic invasion of human decidua from 8 to 18 weeks of pregnancy. *Placenta*, 1, 3-19.
- PIJNENBORG, R., VERCRUYSSSE, L. & HANSSSENS, M. 2006. The uterine spiral arteries in human pregnancy: facts and controversies. *Placenta*, 27, 939-58.
- POPPE, H., RYBALKIN, S. D., REHMANN, H., HINDS, T. R., TANG, X. B., CHRISTENSEN, A. E., SCHWEDE, F., GENIESER, H. G., BOS, J. L., DOSKELAND, S. O., BEAVO, J. A. & BUTT, E. 2008. Cyclic nucleotide analogs as probes of signaling pathways. *Nat Methods*, 5, 277-8.
- POSTON, L. 1996. Maternal vascular function in pregnancy. *J Hum Hypertens*, 10, 391-4.
- POSTON, L., MCCARTHY, A. L. & RITTER, J. M. 1995. Control of vascular resistance in the maternal and feto-placental arterial beds. *Pharmacol Ther*, 65, 215-39.
- RAMSEY, E. M. 1981. The story of the spiral arteries. *J Reprod Med*, 26, 393-9.
- REED, R. B., SANDBERG, M., JAHNSEN, T., LOHMANN, S. M., FRANCIS, S. H. & CORBIN, J. D. 1997. Structural order of the slow and fast intrasubunit cGMP-binding sites of type I alpha cGMP-dependent protein kinase. *Adv Second Messenger Phosphoprotein Res*, 31, 205-17.
- REILLY, R. D. & RUSSELL, P. T. 1977. Neurohistochemical evidence supporting an absence of adrenergic and cholinergic innervation in the human placenta and umbilical cord. *Anat Rec*, 188, 277-86.
- REINHARD, M., JARCHAU, T. & WALTER, U. 2001. Actin-based motility: stop and go with Ena/VASP proteins. *Trends Biochem Sci*, 26, 243-9.

- REMBOLD, C. M., FOSTER, D. B., STRAUSS, J. D., WINGARD, C. J. & EYK, J. E. 2000. cGMP-mediated phosphorylation of heat shock protein 20 may cause smooth muscle relaxation without myosin light chain dephosphorylation in swine carotid artery. *J Physiol*, 524 Pt 3, 865-78.
- REVIRIEGO, J. & MARIN, J. 1989. Effects of 5-hydroxytryptamine on human isolated placental chorionic arteries and veins. *Br J Pharmacol*, 96, 961-9.
- RIBATTI, D., VACCA, A., NICO, B., RIA, R. & DAMMACCO, F. 2002. Cross-talk between hematopoiesis and angiogenesis signaling pathways. *Curr Mol Med*, 2, 537-43.
- RICHIE-JANNETTA, R., FRANCIS, S. H. & CORBIN, J. D. 2003. Dimerization of cGMP-dependent protein kinase I β is mediated by an extensive amino-terminal leucine zipper motif, and dimerization modulates enzyme function. *J Biol Chem*, 278, 50070-9.
- ROBSON, S. C., HUNTER, S., BOYS, R. J. & DUNLOP, W. 1989. Serial study of factors influencing changes in cardiac output during human pregnancy. *Am J Physiol*, 256, H1060-5.
- RODESCH, F., SIMON, P., DONNER, C. & JAUNIAUX, E. 1992. Oxygen measurements in endometrial and trophoblastic tissues during early pregnancy. *Obstet Gynecol*, 80, 283-5.
- ROSENBERG, E. I. 1998. *Regulation of the placental circulation*, Philadelphia, W.B. Saunders.
- RUSSO, I., DEL MESE, P., DORONZO, G., MATTIELLO, L., VIRETTO, M., BOSIA, A., ANFOSSI, G. & TROVATI, M. 2008. Resistance to the Nitric Oxide/Cyclic Guanosine 5'-Monophosphate/Protein Kinase G Pathway in Vascular Smooth Muscle Cells from the Obese Zucker Rat, a Classical Animal Model of Insulin Resistance: Role of Oxidative Stress. *Endocrinology*, 149, 1480-1489.
- RUTH, P., PFEIFER, A., KAMM, S., KLATT, P., DOSTMANN, W. R. & HOFMANN, F. 1997. Identification of the amino acid sequences responsible for high affinity activation of cGMP kinase I α . *J Biol Chem*, 272, 10522-8.
- SAND, A., ANDERSSON, E. & FRIED, G. 2006. Nitric Oxide Donors Mediate Vasodilation in Human Placental Arteries Partly Through a Direct Effect on Potassium Channels. *Placenta*, 27, 181-190.
- SAUZEAU, V., LE JEUNE, H., CARIO-TOUMANIANTZ, C., SMOLENSKI, A., LOHMANN, S. M., BERTOGLIO, J., CHARDIN, P., PACAUD, P. & LOIRAND, G. 2000a. Cyclic GMP-dependent protein kinase signaling pathway inhibits RhoA-induced Ca²⁺ sensitization of contraction in vascular smooth muscle. *J Biol Chem*, 275, 21722-9.
- SAUZEAU, V., LE JEUNE, H., CARIO-TOUMANIANTZ, C., VAILLANT, N., GADEAU, A. P., DESGRANGES, C., SCALBERT, E., CHARDIN, P., PACAUD, P. & LOIRAND, G. 2000b. P2Y(1), P2Y(2), P2Y(4), and P2Y(6) receptors are coupled to Rho and Rho kinase activation in vascular myocytes. *Am J Physiol Heart Circ Physiol*, 278, H1751-61.
- SCHAFER, A., BURKHARDT, M., VOLLKOMMER, T., BAUERSACHS, J., MUNZEL, T., WALTER, U. & SMOLENSKI, A. 2003. Endothelium-dependent and -independent relaxation and VASP serines 157/239 phosphorylation by cyclic nucleotide-elevating vasodilators in rat aorta. *Biochem Pharmacol*, 65, 397-405.
- SCHLOSSMANN, J., AMMENDOLA, A., ASHMAN, K., ZONG, X., HUBER, A., NEUBAUER, G., WANG, G. X., ALLESCHER, H. D., KORTH, M., WILM, M., HOFMANN, F. & RUTH, P. 2000. Regulation of intracellular calcium by a signalling complex of IRAG, IP3 receptor and cGMP kinase I β . *Nature*, 404, 197-201.

- SCHROEDER, H. 2006. No Nitric Oxide for HO-1 from Sodium Nitroprusside. *Mol Pharmacol*, 69, 1507-1509.
- SCHULZ, E., TSILIMINGAS, N., RINZE, R., REITER, B., WENDT, M., OELZE, M., WOELKEN-WECKMULLER, S., WALTER, U., REICHENSPURNER, H., MEINERTZ, T. & MUNZEL, T. 2002. Functional and biochemical analysis of endothelial (dys)function and NO/cGMP signaling in human blood vessels with and without nitroglycerin pretreatment. *Circulation*, 105, 1170-5.
- SEITZ, S., WEGENER, J. W., RUPP, J., WATANABE, M., JOST, A., GERHARD, R., SHAINBERG, A., OCHI, R. & NAWRATH, H. 1999. Involvement of K(+) channels in the relaxant effects of YC-1 in vascular smooth muscle. *Eur J Pharmacol*, 382, 11-8.
- SELLERS, S. M., MITCHELL, M. D., BIBBY, J. G., ANDERSON, A. B. & TURNBULL, A. C. 1981. A comparison of plasma prostaglandin levels in term and preterm labour. *Br J Obstet Gynaecol*, 88, 362-6.
- SHARMA, A. K., ZHOU, G. P., KUPFERMAN, J., SURKS, H. K., CHRISTENSEN, E. N., CHOU, J. J., MENDELSON, M. E. & RIGBY, A. C. 2008. Probing the interaction between the coiled coil leucine zipper of cGMP-dependent protein kinase I α and the C terminus of the myosin binding subunit of the myosin light chain phosphatase. *J Biol Chem*, 283, 32860-9.
- SHCHERBAKOVA, O. V., SEREBRYANAYA, D. V., POSTNIKOV, A. B., SCHROETER, M. M., ZITTRICH, S., NOEGEL, A. A., SHIRINSKY, V. P., VOROTNIKOV, A. V. & PFITZER, G. 2010. Kinase-related protein/telokin inhibits Ca²⁺-independent contraction in Triton-skinned guinea pig taenia coli. *Biochem J*, 429, 291-302.
- SINGH, D. K., SARKAR, J., RAGHAVAN, A., REDDY, S. P. & RAJ, J. U. 2011. Hypoxia modulates the expression of leucine zipper-positive MYPT1 and its interaction with protein kinase G and Rho kinases in pulmonary arterial smooth muscle cells. *Pulm Circ*, 1, 487-98.
- SKAZNIK-WIKIEL, M. E., KANEKO-TARUI, T., KASHIWAGI, A. & PRU, J. K. 2006. Sphingosine-1-phosphate receptor expression and signaling correlate with uterine prostaglandin-endoperoxide synthase 2 expression and angiogenesis during early pregnancy. *Biol Reprod*, 74, 569-76.
- SLADEK, S. M., MAGNESS, R. R. & CONRAD, K. P. 1997. Nitric oxide and pregnancy. *Am J Physiol*, 272, R441-63.
- SMITH, L., PARIZI-ROBINSON, M., ZHU, M. S., ZHI, G., FUKUI, R., KAMM, K. E. & STULL, J. T. 2002. Properties of long myosin light chain kinase binding to F-actin in vitro and in vivo. *J Biol Chem*, 277, 35597-604.
- SMOLENSKI, A., BACHMANN, C., REINHARD, K., HONIG-LIEDL, P., JARCHAU, T., HOSCHUETZKY, H. & WALTER, U. 1998. Analysis and regulation of vasodilator-stimulated phosphoprotein serine 239 phosphorylation in vitro and in intact cells using a phosphospecific monoclonal antibody. *J Biol Chem*, 273, 20029-35.
- SOMLYO, A. P. 1985. Excitation-contraction coupling and the ultrastructure of smooth muscle. *Circ Res*, 57, 497-507.
- SOMLYO, A. P. & HIMPENS, B. 1989. Cell calcium and its regulation in smooth muscle. *FASEB J*, 3, 2266-76.
- SOMLYO, A. P. & SOMLYO, A. V. 1990. Flash photolysis studies of excitation-contraction coupling, regulation, and contraction in smooth muscle. *Annu Rev Physiol*, 52, 857-74.
- SOMLYO, A. P. & SOMLYO, A. V. 1992. Pharmacomechanical coupling: the role of G-proteins in Ca(2+)-release and modulation of Ca(2+)-sensitivity. *Jpn J Pharmacol*, 58 Suppl 2, 54P-59P.

- SOMLYO, A. P. & SOMLYO, A. V. 1994. Signal transduction and regulation in smooth muscle. *Nature*, 372, 231-6.
- SOMLYO, A. P. & SOMLYO, A. V. 2000. Signal transduction by G-proteins, rho-kinase and protein phosphatase to smooth muscle and non-muscle myosin II. *J Physiol*, 522 Pt 2, 177-85.
- SOMLYO, A. P. & SOMLYO, A. V. 2003. Ca²⁺ sensitivity of smooth muscle and nonmuscle myosin II: modulated by G proteins, kinases, and myosin phosphatase. *Physiol Rev*, 83, 1325-58.
- SOMLYO, A. P., WALKER, J. W., GOLDMAN, Y. E., TRENTHAM, D. R., KOBAYASHI, S., KITAZAWA, T. & SOMLYO, A. V. 1988. Inositol trisphosphate, calcium and muscle contraction. *Philos Trans R Soc Lond B Biol Sci*, 320, 399-414.
- SOMLYO, A. V. & SOMLYO, A. P. 1968. Electromechanical and pharmacomechanical coupling in vascular smooth muscle. *J Pharmacol Exp Ther*, 159, 129-45.
- SOOTHILL, P. W., NICOLAIDES, K. H., RODECK, C. H. & CAMPBELL, S. 1986. Effect of gestational age on fetal and intervillous blood gas and acid-base values in human pregnancy. *Fetal Ther*, 1, 168-75.
- SPITALER, M. M., HAMMER, A., MALLI, R. & GRAIER, W. F. 2002. Functional analysis of histamine receptor subtypes involved in endothelium-mediated relaxation of the human uterine artery. *Clin Exp Pharmacol Physiol*, 29, 711-6.
- ST-LOUIS, J., SICOTTE, B., BEAUSEJOUR, A. & BROCHU, M. 2006. Remodeling and angiotensin II responses of the uterine arcuate arteries of pregnant rats are altered by low- and high-sodium intake. *Reproduction*, 131, 331-9.
- STRUIJK, P. C., MATHEWS, V. J., LOUPAS, T., STEWART, P. A., CLARK, E. B., STEEGERS, E. A. & WLADIMIROFF, J. W. 2008. Blood pressure estimation in the human fetal descending aorta. *Ultrasound Obstet Gynecol*, 32, 673-81.
- STULC, J., STULCOVA, B., SMID, M. & SACH, I. 1994. Parallel mechanisms of Ca⁺⁺ transfer across the perfused human placental cotyledon. *Am J Obstet Gynecol*, 170, 162-7.
- STULL, J. T., HSU, L. C., TANSEY, M. G. & KAMM, K. E. 1990. Myosin light chain kinase phosphorylation in tracheal smooth muscle. *J Biol Chem*, 265, 16683-90.
- STUTCHFIELD, J. & HOWELL, S. L. 1984. The effect of phalloidin on insulin secretion from islets of Langerhans isolated from rat pancreas. *FEBS Lett*, 175, 393-6.
- SU, S. C., MENDOZA, E. A., KWAK, H. I. & BAYLESS, K. J. 2008. Molecular profile of endothelial invasion of three-dimensional collagen matrices: insights into angiogenic sprout induction in wound healing. *Am J Physiol Cell Physiol*, 295, C1215-29.
- SURKS, H. K. & MENDELSON, M. E. 2003. Dimerization of cGMP-dependent protein kinase 1 α and the myosin-binding subunit of myosin phosphatase: role of leucine zipper domains. *Cell Signal*, 15, 937-44.
- SURKS, H. K., MOCHIZUKI, N., KASAI, Y., GEORGESCU, S. P., TANG, K. M., ITO, M., LINCOLN, T. M. & MENDELSON, M. E. 1999. Regulation of myosin phosphatase by a specific interaction with cGMP- dependent protein kinase 1 α . *Science*, 286, 1583-7.
- SUZUKI, A. & ITOH, T. 1993. Effects of calyculin A on tension and myosin phosphorylation in skinned smooth muscle of the rabbit mesenteric artery. *Br J Pharmacol*, 109, 703-12.
- SWARD, K., DREJA, K., SUSNJAR, M., HELLSTRAND, P., HARTSHORNE, D. J. & WALSH, M. P. 2000. Inhibition of Rho-associated kinase blocks agonist-

- induced Ca^{2+} sensitization of myosin phosphorylation and force in guinea-pig ileum. *J Physiol*, 522 Pt 1, 33-49.
- SWARD, K., MITA, M., WILSON, D. P., DENG, J. T., SUSNJAR, M. & WALSH, M. P. 2003. The role of RhoA and Rho-associated kinase in vascular smooth muscle contraction. *Curr Hypertens Rep*, 5, 66-72.
- SWEENEY, M., JONES, C. J., GREENWOOD, S. L., BAKER, P. N. & TAGGART, M. J. 2006a. Ultrastructural features of smooth muscle and endothelial cells of isolated isobaric human placental and maternal arteries. *Placenta*, 27, 635-47.
- SWEENEY, M., JONES, C. J. P., GREENWOOD, S. L., BAKER, P. N. & TAGGART, M. J. 2006b. Ultrastructural Features of Smooth Muscle and Endothelial Cells of Isolated Isobaric Human Placental and Maternal Arteries. *Placenta*, 27, 635-647.
- SWEENEY, M., WAREING, M., MILLS, T. A., BAKER, P. N. & TAGGART, M. J. 2008. Characterisation of tone oscillations in placental and myometrial arteries from normal pregnancies and those complicated by pre-eclampsia and growth restriction. *Placenta*, 29, 356-65.
- TAGGART, M. J. & MORGAN, K. G. 2007. Regulation of the uterine contractile apparatus and cytoskeleton. *Semin Cell Dev Biol*, 18, 296-304.
- TAKAI, A., SASAKI, K., NAGAI, H., MIESKES, G., ISOBE, M., ISONO, K. & YASUMOTO, T. 1995. Inhibition of specific binding of okadaic acid to protein phosphatase 2A by microcystin-LR, calyculin-A and tautomycin: method of analysis of interactions of tight-binding ligands with target protein. *Biochem J*, 306 (Pt 3), 657-65.
- TANAKA, C., KUWABARA, Y. & SAKAI, T. 1999. Structural identification and characterization of arteries and veins in the placental stem villi. *Anat Embryol (Berl)*, 199, 407-18.
- TANFIN, Z., LEIBER, D., ROBIN, P., OYENIRAN, C. & BREUILLER-FOUCHE, M. 2011. Endothelin-1: physiological and pathological roles in myometrium. *Int J Biochem Cell Biol*, 43, 299-302.
- TANG, D. C., STULL, J. T., KUBOTA, Y. & KAMM, K. E. 1992. Regulation of the Ca^{2+} dependence of smooth muscle contraction. *J Biol Chem*, 267, 11839-45.
- TANSEY, M. G., LUBY-PHELPS, K., KAMM, K. E. & STULL, J. T. 1994. Ca^{2+} -dependent phosphorylation of myosin light chain kinase decreases the Ca^{2+} sensitivity of light chain phosphorylation within smooth muscle cells. *J Biol Chem*, 269, 9912-20.
- TAYLOR, S. G. & WESTON, A. H. 1988. Endothelium-derived hyperpolarizing factor: a new endogenous inhibitor from the vascular endothelium. *Trends Pharmacol Sci*, 9, 272-4.
- TULIS, D. A., DURANTE, W., PEYTON, K. J., CHAPMAN, G. B., EVANS, A. J. & SCHAFER, A. I. 2000. YC-1, a benzyl indazole derivative, stimulates vascular cGMP and inhibits neointima formation. *Biochem Biophys Res Commun*, 279, 646-52.
- TURNBULL, A. 2001. *Turnbull's Obstetrics*, London, Churchill Livingstone.
- TYSON, E. K., MACINTYRE, D. A., SMITH, R., CHAN, E. C. & READ, M. 2008a. Evidence that a protein kinase A substrate, small heat-shock protein 20, modulates myometrial relaxation in human pregnancy. *Endocrinology*, 149, 6157-65.
- TYSON, E. K., MACINTYRE, D. A., SMITH, R., CHAN, E. C. & READ, M. 2008b. Evidence that a Protein Kinase A Substrate, Small Heat-Shock Protein 20, Modulates Myometrial Relaxation in Human Pregnancy. *Endocrinology*, 149, 6157-6165.
- VAN DER HEIJDEN, O. W., ESSERS, Y. P., FAZZI, G., PEETERS, L. L., DE MEY, J. G. & VAN EYS, G. J. 2005. Uterine artery remodeling and reproductive

- performance are impaired in endothelial nitric oxide synthase-deficient mice. *Biol Reprod*, 72, 1161-8.
- VAN RIPER, D. A., WEAVER, B. A., STULL, J. T. & REMBOLD, C. M. 1995. Myosin light chain kinase phosphorylation in swine carotid artery contraction and relaxation. *Am J Physiol*, 268, H2466-75.
- VANWIJK, M. J., KUBLICKIENE, K., BOER, K. & VANBAVEL, E. 2000. Vascular function in preeclampsia. *Cardiovasc Res*, 47, 38-48.
- VERNER, I. R. 1974. Sodium nitroprusside: theory and practice. *Postgrad Med J*, 50, 576-81.
- VISSER, W. & WALLENBURG, H. C. 1991. Central hemodynamic observations in untreated preeclamptic patients. *Hypertension*, 17, 1072-7.
- WALDMAN, S. A. & MURAD, F. 1987. Cyclic GMP synthesis and function. *Pharmacol Rev*, 39, 163-96.
- WALKER, L. A., MACDONALD, J. A., LIU, X., NAKAMOTO, R. K., HAYSTEAD, T. A., SOMLYO, A. V. & SOMLYO, A. P. 2001. Site-specific phosphorylation and point mutations of telokin modulate its Ca^{2+} -desensitizing effect in smooth muscle. *J Biol Chem*, 276, 24519-24.
- WALLIS, A. B., SAFTLAS, A. F., HSIA, J. & ATRASH, H. K. 2008. Secular trends in the rates of preeclampsia, eclampsia, and gestational hypertension, United States, 1987-2004. *Am J Hypertens*, 21, 521-6.
- WANG, H., ETO, M., STEERS, W. D., SOMLYO, A. P. & SOMLYO, A. V. 2002. RhoA-mediated Ca^{2+} sensitization in erectile function. *J Biol Chem*, 277, 30614-21.
- WANG, W., YEN, H., CHEN, C. H., SONI, R., JASANI, N., SYLVESTRE, G. & REZNIK, S. E. 2008. The endothelin-converting enzyme-1/endothelin-1 pathway plays a critical role in inflammation-associated premature delivery in a mouse model. *Am J Pathol*, 173, 1077-84.
- WAREING, M. 2002. Characterization of Small Arteries Isolated From the Human Placental Chorionic Plate. *Placenta*, 23, 400-409.
- WAREING, M. & BAKER, P. N. 2004. Vasoconstriction of small arteries isolated from the human placental chorionic plate in normal and compromised pregnancy. *Hypertens Pregnancy*, 23, 237-46.
- WAREING, M., BHATTI, H., O'HARA, M., KENNY, L., WARREN, A. Y., TAGGART, M. J. & BAKER, P. N. 2003a. Vasoactive effects of neurokinin B on human blood vessels. *Am J Obstet Gynecol*, 188, 196-202.
- WAREING, M., CROCKER, I. P., WARREN, A. Y., TAGGART, M. J. & BAKER, P. N. 2002. Characterization of small arteries isolated from the human placental chorionic plate. *Placenta*, 23, 400-9.
- WAREING, M., GREENWOOD, S. & BAKER, P. 2006a. Reactivity of human placental chorionic plate vessels is modified by level of oxygenation: Differences between arteries and veins. *Placenta*, 27, 42-48.
- WAREING, M., GREENWOOD, S. L. & BAKER, P. N. 2006b. Reactivity of human placental chorionic plate vessels is modified by level of oxygenation: differences between arteries and veins. *Placenta*, 27, 42-8.
- WAREING, M., GREENWOOD, S. L., FYFE, G. K., BAKER, P. N. & TAGGART, M. J. 2006c. Glibenclamide inhibits agonist-induced vasoconstriction of placental chorionic plate arteries. *Placenta*, 27, 660-8.
- WAREING, M., GREENWOOD, S. L., TAGGART, M. J. & BAKER, P. N. 2003b. Vasoactive responses of veins isolated from the human placental chorionic plate. *Placenta*, 24, 790-6.

- WAREING, M., MYERS, J. E., O'HARA, M. & BAKER, P. N. 2005a. Sildenafil citrate (Viagra) enhances vasodilatation in fetal growth restriction. *J Clin Endocrinol Metab*, 90, 2550-5.
- WAREING, M., MYERS, J. E., O'HARA, M., KENNY, L. C., TAGGART, M. J., SKILLERN, L., MACHIN, I. & BAKER, P. N. 2006d. Phosphodiesterase-5 inhibitors and omental and placental small artery function in normal pregnancy and pre-eclampsia. *Eur J Obstet Gynecol Reprod Biol*, 127, 41-9.
- WAREING, M., MYERS, J. E., O'HARA, M., KENNY, L. C., WARREN, A. Y., TAGGART, M. J., SKILLERN, L., MACHIN, I. & BAKER, P. N. 2004. Effects of a phosphodiesterase-5 (PDE5) inhibitor on endothelium-dependent relaxation of myometrial small arteries. *Am J Obstet Gynecol*, 190, 1283-90.
- WAREING, M., O'HARA, M., SEGHIER, F., BAKER, P. N. & TAGGART, M. J. 2005b. The involvement of Rho-associated kinases in agonist-dependent contractions of human maternal and placental arteries at term gestation. *Am J Obstet Gynecol*, 193, 815-24.
- WARNER, T. D., MITCHELL, J. A., SHENG, H. & MURAD, F. 1994. Effects of cyclic GMP on smooth muscle relaxation. *Adv Pharmacol*, 26, 171-94.
- WEBER, L. P., VAN LIEROP, J. E. & WALSH, M. P. 1999. Ca²⁺-independent phosphorylation of myosin in rat caudal artery and chicken gizzard myofilaments. *J Physiol*, 516 (Pt 3), 805-24.
- WEBER, S., BERNHARD, D., LUKOWSKI, R., WEINMEISTER, P., WORNER, R., WEGENER, J. W., VALTCHEVA, N., FEIL, S., SCHLOSSMANN, J., HOFMANN, F. & FEIL, R. 2007. Rescue of cGMP kinase I knockout mice by smooth muscle specific expression of either isozyme. *Circ Res*, 101, 1096-103.
- WEINER, C. P., KNOWLES, R. G. & MONCADA, S. 1994. Induction of nitric oxide synthases early in pregnancy. *Am J Obstet Gynecol*, 171, 838-43.
- WETZKA, B., NUSING, R., CHARNOCK-JONES, D. S., SCHAFER, W., ZAHRADNIK, H. P. & SMITH, S. K. 1997. Cyclooxygenase-1 and -2 in human placenta and placental bed after normal and pre-eclamptic pregnancies. *Hum Reprod*, 12, 2313-20.
- WHITE, R. E., LEE, A. B., SHCHERBATKO, A. D., LINCOLN, T. M., SCHONBRUNN, A. & ARMSTRONG, D. L. 1993. Potassium channel stimulation by natriuretic peptides through cGMP-dependent dephosphorylation. *Nature*, 361, 263-6.
- WILCOX, M., GARDOSI, J., MONGELLI, M., RAY, C. & JOHNSON, I. 1993. Birth weight from pregnancies dated by ultrasonography in a multicultural British population. *BMJ*, 307, 588-91.
- WILSON, B. J., WATSON, M. S., PRESCOTT, G. J., SUNDERLAND, S., CAMPBELL, D. M., HANNAFORD, P. & SMITH, W. C. 2003. Hypertensive diseases of pregnancy and risk of hypertension and stroke in later life: results from cohort study. *BMJ*, 326, 845.
- WILSON, D. P., SUSNJAR, M., KISS, E., SUTHERLAND, C. & WALSH, M. P. 2005a. Thromboxane A₂-induced contraction of rat caudal arterial smooth muscle involves activation of Ca²⁺ entry and Ca²⁺ sensitization: Rho-associated kinase-mediated phosphorylation of MYPT1 at Thr-855, but not Thr-697. *Biochem J*, 389, 763-74.
- WILSON, D. P., SUTHERLAND, C., BORMAN, M. A., DENG, J. T., MACDONALD, J. A. & WALSH, M. P. 2005b. Integrin-linked kinase is responsible for Ca²⁺-independent myosin diphosphorylation and contraction of vascular smooth muscle. *Biochem J*, 392, 641-8.
- WIMALASUNDERA, R. C., THOM, S. A., REGAN, L. & HUGHES, A. D. 2005. Effects of vasoactive agents on intracellular calcium and force in myometrial

- and subcutaneous resistance arteries isolated from preeclamptic, pregnant, and nonpregnant woman. *Am J Obstet Gynecol*, 192, 625-32.
- WISDOM, S. J., WILSON, R., MCKILLOP, J. H. & WALKER, J. J. 1991. Antioxidant systems in normal pregnancy and in pregnancy-induced hypertension. *Am J Obstet Gynecol*, 165, 1701-4.
- WOLFE, L., CORBIN, J. D. & FRANCIS, S. H. 1989a. Characterization of a novel isozyme of cGMP-dependent protein kinase from bovine aorta. *J Biol Chem*, 264, 7734-41.
- WOLFE, L., FRANCIS, S. H. & CORBIN, J. D. 1989b. Properties of a cGMP-dependent monomeric protein kinase from bovine aorta. *J Biol Chem*, 264, 4157-62.
- WOODSOME, T. P., ETO, M., EVERETT, A., BRAUTIGAN, D. L. & KITAZAWA, T. 2001. Expression of CPI-17 and myosin phosphatase correlates with Ca(2+) sensitivity of protein kinase C-induced contraction in rabbit smooth muscle. *J Physiol*, 535, 553-64.
- WOOLDRIDGE, A. A., MACDONALD, J. A., ERDODI, F., MA, C., BORMAN, M. A., HARTSHORNE, D. J. & HAYSTEAD, T. A. 2004. Smooth muscle phosphatase is regulated in vivo by exclusion of phosphorylation of threonine 696 of MYPT1 by phosphorylation of Serine 695 in response to cyclic nucleotides. *J Biol Chem*, 279, 34496-504.
- WU, X., HAYSTEAD, T. A., NAKAMOTO, R. K., SOMLYO, A. V. & SOMLYO, A. P. 1998. Acceleration of myosin light chain dephosphorylation and relaxation of smooth muscle by telokin. Synergism with cyclic nucleotide-activated kinase. *J Biol Chem*, 273, 11362-9.
- WU, X., SOMLYO, A. V. & SOMLYO, A. P. 1996. Cyclic GMP-dependent stimulation reverses G-protein-coupled inhibition of smooth muscle myosin light chain phosphate. *Biochem Biophys Res Commun*, 220, 658-63.
- XIA, C., BAO, Z., YUE, C., SANBORN, B. M. & LIU, M. 2001. Phosphorylation and regulation of G-protein-activated phospholipase C-beta 3 by cGMP-dependent protein kinases. *J Biol Chem*, 276, 19770-7.
- YAMAMOTO, Y., OLSON, D. M., VAN BENNEKOM, M., BRINDLEY, D. N. & HEMMINGS, D. G. 2010. Increased expression of enzymes for sphingosine 1-phosphate turnover and signaling in human decidua during late pregnancy. *Biol Reprod*, 82, 628-35.
- YOSHII, A., IIZUKA, K., DOBASHI, K., HORIE, T., HARADA, T., NAKAZAWA, T. & MORI, M. 1999. Relaxation of contracted rabbit tracheal and human bronchial smooth muscle by Y-27632 through inhibition of Ca²⁺ sensitization. *Am J Respir Cell Mol Biol*, 20, 1190-200.
- YOUNG, T. 1805. An Essay on the Cohesion of Fluids. *Philos Trans R Soc Lond B Biol Sci*, 95, 65-97.
- YU, J. T. & LOPEZ BERNAL, A. 1998. The cytoskeleton of human myometrial cells. *J Reprod Fertil*, 112, 185-98.
- ZHANG, D. X., BORBOUSE, L., GEBREMEDHIN, D., MENDOZA, S. A., ZINKEVICH, N. S., LI, R. & GUTTERMAN, D. D. 2012. H₂O₂-induced dilation in human coronary arterioles: role of protein kinase G dimerization and large-conductance Ca²⁺-activated K⁺ channel activation. *Circ Res*, 110, 471-80.
- ZHANG, X. 2001. Effects of Nitrovasodilators on the Human Fetal-Placental Circulation In Vitro. *Placenta*, 22, 337-346.
- ZHANG, X. Q., KWEK, K., READ, M. A., DONOGHUE, J. F. & WALTERS, W. A. 2001. Effects of nitrovasodilators on the human fetal-placental circulation in vitro. *Placenta*, 22, 337-46.

ZUCCHI, R., RONCA-TESTONI, S., YU, G., GALBANI, P., RONCA, G. & MARIANI, M. 1994. Effect of ischemia and reperfusion on cardiac ryanodine receptors--sarcoplasmic reticulum Ca²⁺ channels. *Circ Res*, 74, 271-80.